THE UNIVERSITY OF HULL

Role of Hypoxia-Induced ADAM 10 in Colorectal Cancer Progression

being a Thesis submitted for the Degree of Doctor of Philosophy

in the University of Hull

by

Anna Elizabeth Todd, BSc, MSc

April 2016

Contents

Declaration

I declare that this work has not been previously submitted as an exercise for a degree at this or any other university.

Unless otherwise stated, this thesis is the sole work of the author, who gives permission for the library to lend or copy this work upon request.

Anna Todd

April 2016

Summary

Colorectal cancer (CRC) is one of the most prevalent cancers worldwide and is the second deadliest form of cancer within the UK. The majority of CRC arises sporadically, as a result of epigenetic alterations transforming normal epithelium to malignant adenocarcinoma. CRC is highly metastatic and as a solid state tumour possesses regions of hypoxia, which promote metastasis. There is evidence for the involvement of the A Disintegrin And Metalloproteinase (ADAM) family in cancer progression and the hypoxic tumour microenvironment, however ADAM 10 is one of the least characterised members in the context of hypoxia-mediated cancer progression. ADAM 10 is strongly implicated in the regulation of normal colon biology, with an ADAM 10 knockout mouse model displaying embryonic lethality. Therefore, ADAM 10 is a key target of CRC research, to determine what effect hypoxia has on ADAM 10 and what implications this may have in the context of CRC progression.

In this study, CRC cell lines were examined to characterise the effects of severe hypoxia on ADAM 10. Exposure to severe hypoxia induced an alteration to ADAM 10 expression at both protein and transcript levels, with a previously un-reported doublet band seen for mature ADAM 10 at protein level. The doublet is believed to be a hypoxia-mediated post-translational modification, potentially through alterations in ADAM 10 glycosylation. No effects of either severe hypoxia or ADAM 10 knockdown were seen on CRC cellular migration. However, a downregulation in cellular viability was observed in HCT116 cells after ADAM 10 knockdown, independently of hypoxia, indicating a role of ADAM 10 in the regulation of CRC cell viability. Attempts to elucidate the underlying mechanisms behind this revealed a role for ADAM 10 in the regulation of *c-MYC* and *CCND1* expression in HCT116 cells, however no effect on cell cycle progression was observed after ADAM 10 knockdown. This study has identified an important role for ADAM 10, independently of hypoxia, in the regulation of CRC viability, which may promote the progression and metastasis of CRC.

Acknowledgements

I would like to thank my supervisors Dr Isabel Pires and Professor John Greenman for their knowledge and guidance throughout my PhD, as without them this research would not have been possible. I am especially grateful to Isabel for being there every step of the way and for all the help and encouragement she has offered on a daily basis.

I would like to thank the University of Hull for my PhD scholarship, and the opportunity to undertake this research.

Thank you to the staff members and students within the University of Hull cancer group, for their input and advice throughout the duration of this project. A special thank you must go to Becky, Flore-Anne and Hannah for keeping me sane throughout the last three years. We have gone through every step of this process together and have forged a great friendship as a result, which has made my PhD all the more enjoyable. A big thank you to Ellie, for her technical support, mycoplasma testing and great friendship throughout the last three years. Thank you to Brittany Wingham for her help with the FACS sample processing and analysis; and to Kevin Welham for the mass spec service he provided.

Last but not least I would like to thank my family and friends for their constant support and encouragement throughout the last three years, especially my Mum and Dad who have been behind me the whole time and offered encouragement and motivation throughout the tough patches. A very special thank you to Nathan, who has been by my side every step of the way and has believed in me, even when I didn't believe in myself.

Dedication

I dedicate this thesis to Nathan – I couldn’t have done it without you!

List of Figures

List of Tables

Abbreviations

ADAM	A disintegrin and metalloproteinase
APC	Adenomatous polyposis coli
APP	Amyloid precursor protein
APS	Ammonium persulphate
ARD1	ADP-ribosylation factor domain protein 1
B2M	β-2 Microglobulin
BCA	Bicinchoninic acid
bp	Base pair
BrdU	Bromodeoxyuridine
BSA	Bovine serum albumin
BTC	Betacellulin
CBP	c-AMP-response element-binding protein
cDNA	Complimentary DNA
CCICs	Colon cancer-initiating cells
CCLE	Cancer cell line encyclopaedia
CDK	Cyclin-dependent kinase
CHARM	Compact Hough and radial map
Cip	CDK interacting protein
CK1α	Casein kinase 1α
CKI	Cyclin kinase inhibitors
CRAPome	Contaminant repository for affinity purification-ome
CRC	Colorectal cancer
CREBBP	c-AMP-response element-binding protein gene
CSL	CBF-1/Suppressor of hairless/LAG1
CTNNB1	β-Catenin
DBZ	Dibenzazepine

DEPC	Diethylpyrocarbonate
DLL-1	Delta-like ligand 1
DLL-3	Delta-like ligand 3
DLL-4	Delta-like ligand 4
ECIS	Electric cell-substrate impedance sensing
ECL	Enhanced chemiluminescence
ECM	Extracellular matrix
EDTA	Ethylenediaminetetraacetic acid
EGF	Epidermal growth factor
EGFR	Epidermal growth factor receptor
ELISA	Enzyme-linked immunosorbent assay
EMT	Epithelial-mesenchymal transition
EP300	E1A binding protein p300
ERK	Extracellular signal-related kinase
ESI	Electrospray ionisation
ESI-MS	Electrospray ionisation mass spectrometry
FAP	Familial adenomatous polyposis
FBS	Foetal bovine serum
FOBT	Faecal occult blood testing
GAB1	GRB2-assocaiated binding protein 1
GI	Gastrointestinal
GRB2	Growth factor receptor bound protein 2
GRP	Gastrin-releasing peptide
GSK3	Glycogen synthase kinase 3
GTP	Guanosine triphosphate
HB-EGF	Heparin-binding EGF-like growth factor
Hes	Hairy enhancer of split
Hey	Hairy enhancer of split related with YRPW motif

Hsp-90	Heat shock protein 90
HIF	Hypoxia-inducible factor
HIF-1	Hypoxia inducible factor 1
HIF-1α	Hypoxia inducible factor α
HIF-1β	Hypoxia inducible factor β
HIF-2	Hypoxia inducible factor 2
HPLC	High performance liquid chromatography
HRE	Hypoxia response element
HRP	Horse radish peroxidise
ICD	Intracellular domain
INK4	Inhibitors of CDK4
IP	Immunoprecipitation
JAG1	Jagged-1
JAG2	Jagged-2
JAK	Janus kinase
Kip	Kinase inhibiting protein
KRAS	Kirsten rat sarcoma
LC-MS	Liquid chromatography mass spectrometry
L1	L1 cell adhesion molecule
Lef	Lymphoid enhancer factor
LRP	Low-density lipoprotein receptor-related protein
mAb	Monoclonal antibody
MALDI-MS	Matrix-assisted laser desorption/ionization mass spectrometry
MALDI-TOF	Matrix-assisted laser desorption/ionization time of flight
MEK	Mitogen-activated protein kinase kinase
MICA	Major histocompatability complex class I chain-related gene A
MMP	Matrix metalloproteinase
NICD	Notch intracellular domain

NTC	No template control
pAb	Polyclonal antibody
PARP	Poly ADP-ribose polymerase
PAS	Periodic acid-Schiff
PBS	Phosphate buffered saline
PC7	Pro-protein convertase 7
PDK1	Phosphoinositide-dependent kinase 1
pEGFR	Phosphorylated epidermal growth factor receptor
pERK	Phosphorylated extracellular single-related kinase
pGAB1	Phosphorylated GRB2-associated binding protein
PHD	Prolyl hydroxylase domain
PI	Propidium iodide
PI3K	Phosphoinositide 3-kinase
PLOD	procollagen-lysine, 2-oxoglutarate 5-disoygenase
PLOD1	procollagen-lysine, 2-oxoglutarate 5-disoygenase 1
PLOD 2	procollagen-lysine, 2-oxoglutarate 5-disoygenase 2
PMA	Phorbol-12-myristate-13-acetate
PNGase F	*N*-Glycosidase F
pO_2	Oxygen partial pressure
PS	Phosphatidylserine
pSTAT5	Phosphorylated signal transducer and activator of transcription 5
PTB	Phosphotyrosine binding
PTEN	Phosphatase and tensin homolog
PTK7	Protein tyrosine kinase 7
PTMs	Post-translational modifications
PVDF	Polyvinylidene fluoride
qPCR	Quantitative polymerase chain reaction
Raf	Rapidly accelerated fibrosarcoma

Ras	Rat sarcoma
RB	Retinoblastoma
RER	Rough endoplasmic reticulum
RPM	Revolutions per minute
RTK	Receptor tyrosine kinase
STDEV	Standard deviation
SDS	Sodium dodecyl sulphate
SDS-PAGE	Sodium dodecyl sulphate polyacrylamide gel electrophoresis
SEM	Standard error mean
siRNA	Silent interfering RNA
SMI	Small molecule inhibitor
SNP	Single nuclear polymorphism
SOS	Son of sevenless
STAT	Signal transducer and activator of transcription
STAT3	Signal transducer and activator of transcription 3
TACE	Tumour necrosis factor α converting enzyme
TBS	Tris buffered saline
TBST	Tris buffered saline – tween
TCF	T-cell factor
TEMED	Tetramethylethylenediamine
TNM	Tumour, node, metastasis
TOF	Time of flight
TGF-α	Transforming growth factor α
TGF-β	Transforming growth factor β
TNFs	Tumour necrosis factors
TNF-R1	Tumour necrosis factor receptor 1
TNF-α	Tumour necrosis factor α
TP53	Tumour protein 53

TUNEL	Terminal deoxynucleotidyl transferase-dUTP nick end labelling
UTR	Untranslated region
VEGF	Vascular endothelial growth factor
VHL	Von Hippel-Lindau
ZEB	Zinc finger E-box binding homeobox

Units

bp	Base pairs
°C	Degrees Celsius
cm	centimetre
g	grams
x *g*	acceleration due to gravity
h	hour
kDa	kiloDalton
kg	kilogram
L	litre
mg	milligram
min	minute
ml	millilitre
mM	milimolar
mm	millimetre
µg	microgram
µl	microlitre
µM	micromolar
µm	micrometer
nm	nanometre
nM	nanomolar
s	seconds
U	units
v/v	volume per volume
w/v	weight per volume

Chapter 1 : Introduction

1.1 Cancer

Cancer is one of the most prevalent diseases affecting society worldwide and is a key target of medical research across the world. With hundreds of different types of cancer affecting millions of people every year, one of the main focuses of cancer research is on increasing the existing knowledge of tumour development and the subsequent development of improved diagnostics and therapeutics to help combat the disease (Hanahan and Weinberg, 2000). The mechanisms behind tumourigenesis vary greatly amongst the different types of cancer, and for the main part remain unknown. However the complexity of the origins of cancer poses numerous questions to be addressed when attempting to identify these underlying mechanisms (Hanahan and Weinberg, 2000). In 2000 Hanahan and Weinberg suggested that there are six main alterations in the physiology of cells that lead to the development of tumours. These are sustained angiogenesis, resisting cell death, evading growth suppressors, tissue invasion and metastasis, self-sufficiency in growth signals and replicative immortality (Hanahan and Weinberg, 2000). In 2011, the hallmarks were revisited and updated, to include two further hallmarks which encompass progress within the field, as seen in **Figure 1.1**.The authors implicated these eight acquired capabilities of cells in the development of the vast majority of cancer types, although they acknowledged that the sequences of events leading to tumour development will vary (Hanahan and Weinberg, 2000, Hanahan and Weinberg, 2011). The hallmarks of cancer, as they became known, have subsequently become key topics on which cancer research focuses, trying to understand how these acquisitions arise and how they can be exploited for therapeutic targeting.

1.2 Colorectal Cancer

Colorectal cancer (CRC) is the fourth most common cancer in the UK and is defined as

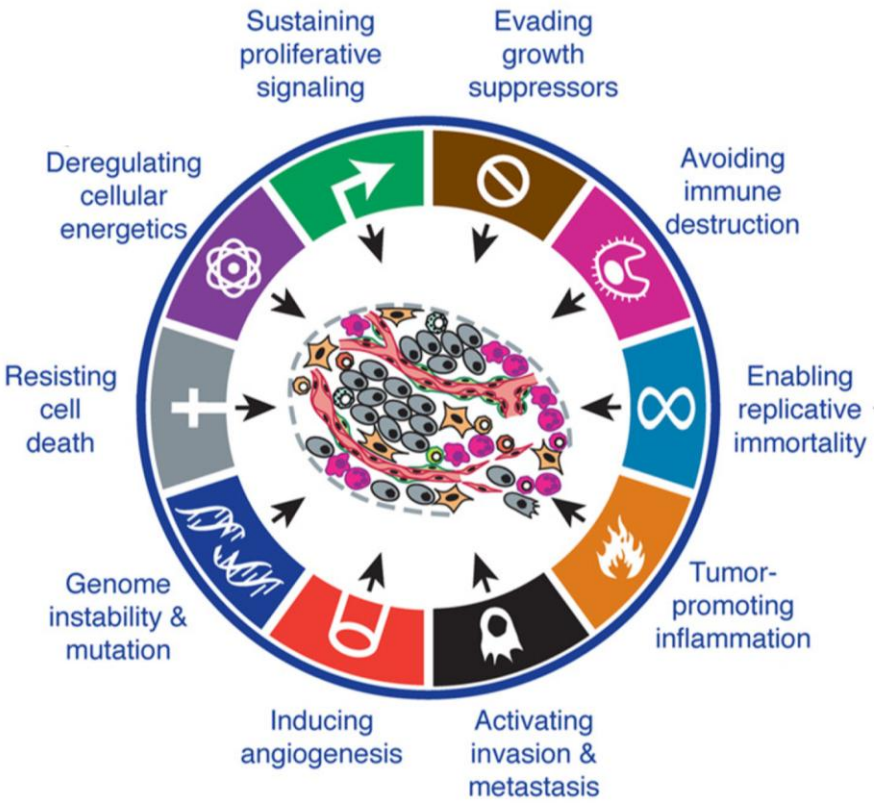

Figure 1.1: The Hallmarks of Cancer

There are eight hallmarks of cancer defined by Hanahan and Weinberg (2011), plus two additional characteristics which are believed to promote the onset of cancer (genome instability and tumour-promoting inflammation). Originally developed in 2000, the hallmarks encompass characteristics that cells will acquire some of or all of during their transformation to malignancy. Figure adapted from Hanahan and Weinberg (2011).

carcinogenesis of the colon and rectum (Ballinger and Anggiansah, 2007, Ferlay et al., 2015). Approximately 40 000 patients are diagnosed with the disease on an annual basis, accounting for 12% of all cancer diagnosed per annum within the UK (Massat et al., 2013). CRC is the second deadliest type of cancer within the UK, with over 16 000 people dying from the disease in 2012. This, combined with the fact that CRC has increased in incidence by 14% since the late-1970s, means that CRC has increasingly become a focus for research (NICE, 2011, Brenner et al., 2014).

1.2.1 Risk Factors

A number of risk factors have been associated with the development of CRC including age, sex, lifestyles choices and family history. Age is an important factor to consider, as over 90% of CRC cases are in the over 50s, with 43% of cases being in the over 75s, however the disease can affect people of all ages (Ballinger and Anggiansah, 2007). Although CRC is known to affect both men and women, there is a slight increased risk of CRC development in the male population, particularly those within the target age range. The predicted risk of developing CRC in males is 1 in 14, whereas in females it is 1 in 19 (Cunningham et al., 2010, Ferlay et al., 2015). Environmental factors such as diet and lifestyle choices are known to strongly increase the risk of CRC, with 54% of CRC being as a direct result of patient lifestyle. Such factors include smoking (12% of CRC), alcohol consumption (8%), obesity (13%) and red meat/processed food consumption (21%) (Parkin et al., 2011, Parkin and Boyd, 2011, Magalhaes et al., 2012). As lifestyles choices such as those listed above are avoidable it's deemed that 54% of CRC is actually preventable through avoidance of such environmental exposures. Such environmental factors are more prevalent in developed countries, resulting in an increase in incidence of CRC, compared to lesser-developed regions (Ballinger and Anggiansah, 2007, Holleczek et al., 2015). Family history is also an important risk factor in the consideration of CRC development, albeit only a small

number of cases arise from such genetic links (Brenner et al., 2014). A ‘strong’ family history can be indicative of an increased risk of CRC and is defined as one first degree family member diagnosed at under 45 years old or two first degree relatives diagnosed at any age (Ballinger and Anggiansah, 2007, Jasperson et al., 2010, Brenner et al., 2014).

1.2.2 Aetiology

The majority (95%) of CRC tumours are adenocarcinomas, originating from transformed glandular cells within the bowel lining. However, other forms are known, albeit considerably rarer including squamous cell carcinomas which originate from within the skin like cells of the bowel lining (Cunningham et al., 2010). Typically, CRC is highly metastatic and is known to primarily metastasise to the liver due to the close proximity of the two, however metastases in the lungs are also common (Brenner et al., 2014).

Whilst the majority of CRC development is sporadic (approximately 95%), 5% of cases arise from pre-disposing genetic conditions such as Lynch syndrome and familial adenomatous polyposis (FAP) (Jasperson et al., 2010, Brenner et al., 2014). Lynch syndrome is the most common hereditary link to CRC, and occurs in roughly 1 in 300 people with CRC (Cunningham et al., 2010). It arises through the inheritable mutation of one of four DNA mismatch repair (MMR) genes, *MSH2*, *PMS2*, *MSH6* or *MLH1*, with the majority of sufferers being identified through a strong family history (Moller et al., 2015, Cunningham et al., 2010). Not only does Lynch syndrome pre-dispose patients to CRC, it also increases their risk of developing a range of other gastrointestinal (GI) or gynaecological cancers (Jasperson et al., 2010). Predominantly, the onset of CRC in Lynch syndrome sufferers is early in comparison to the onset of sporadic CRC, with an average age of approximately 45 years, and it is known that

accelerated carcinogenesis occurs from adenomas compared to that of the general CRC population (Cunningham et al., 2010, Moller et al., 2015). FAP is caused by mutations within the adenomatous polyposis coli (*APC*) gene which subsequently results in the formation of numerous adenomas (polyps) within the colon and rectum. These polyps can be found in patients as young as 10 and extremely prevalent throughout the bowel; they are also highly likely to become cancerous over time. As such, it is normal for FAP patients to have their colons removed by the age of 25 to prevent the high-risk development of CRC (Jasperson et al., 2010, Lynch et al., 2016).

Sporadic CRC develops as a result of epigenetic changes that drive the transformation of normal epithelium, leading to the formation of adenomatous polyps (non-FAP patients), which subsequently progress to invasive CRC (Ballinger and Anggiansah, 2007, Lao and Grady, 2011). There are known to be thousands of epigenetic alterations that promote the development of CRC and efforts to characterise these have already led to the development of targeted therapies for CRC treatment. Epigenetic alterations identified within CRC include histone modification, DNA methylation and non-coding RNAs and are responsible for the alteration of gene expression without DNA sequence modification (Lao and Grady, 2011, Vaiopoulos et al., 2014). DNA methylation through hyper- or hypo-methylation sees the alteration of the transcriptional silencing of genes, and almost all CRC tumours exhibit atypically methylated genes. DNA methylation is linked to the early formation of CRC, rather than the latter, metastatic stages (Lao and Grady, 2011). Histone modifications typically present as acetylation or methylation in CRC and affect the transcriptional regulation capacity by altering DNA accessibility. Furthermore, microRNA have been shown to be related to the transcriptional regulation of gene expression within CRC, with aberration of microRNA present in a large proportion of CRC tumours, which results in upregulated gene expression (Vaiopoulos et al., 2014). The epigenetic alteration of genes within CRC results in altered signalling

pathways, which promote CRC progression. One of the main affected pathways within CRC is epidermal growth factor receptor (EGFR) signalling, with EGFR found to be overexpressed in the majority of tumours (60-80%) (Banck and Grothey, 2009, Li et al., 2011, Tan and Du, 2012, Hong et al., 2015, Pabla et al., 2015, Kocoglu et al., 2016). Two of the main pathways attenuated as a result of upregulated EGFR in CRC are the Ras-Raf-MAPK and PI3K-PTEN-AKT (Tol et al., 2010, Lupini et al., 2015, Kocoglu et al., 2016). Kirsten rat sarcoma (KRAS) mutations are prevalent in CRC, occurring in 35-45% of CRC cases, and being associated with poorer prognosis in patients (Tan and Du, 2012, Phipps et al., 2013, Lemieux et al., 2015). In *KRAS* mutation cases the GTPase activity of KRAS is impaired, resulting in an accumulation of KRAS protein and a 'switched-on' guanosine triphosphate (GTP)-bound state, which activates downstream signalling pathways mediating proliferation (Tan and Du, 2012, Phipps et al., 2013).

The traditional selective sweep model of tumour development has recently been disputed in the context of CRC. The selective sweep model proposes that genetic natural selection occurs as a result of reduced variability in neighbouring loci to a mutation (Smith and Haigh, 1974, Depaulis et al., 1999, Kim and Maruki, 2011). The mutation induces increased fitness (reproductive success) of the carrier and subsequently such alleles are then favoured over others (Smith and Haigh, 1974, Depaulis et al., 1999, Kim and Maruki, 2011). The more recently proposed Big Bang model of tumour growth disputes this. Sottoriva et al. (2015) suggest that after tumours are established selective sweep events are rare due to spatial and dynamic constraints. Instead, it is proposed that tumours establish as a result of single expansion, wherein this results in increased intra-tumour heterogeneity and mixed, non-selective sub-clonal populations (Sottoriva et al., 2015). Results indicate that the variegated tumour cell population predominantly consists of both clonal and sub-clonal alterations. Sub-clonal

alterations are continuously occurring throughout tumour growth, however only early-stage alterations will prevail in the final tumour (Sottoriva et al., 2015). Late-stage sub-clonal alterations will be rare and undetectable in the tumour, however these may present a mechanism of resistance to therapeutics. Such knowledge indicates that regardless of fitness of sub-clonal alterations it is the timing of their occurrence that is key to their establishment within the tumour. Results from analysis of CRC tumours strongly support the proposed Big Bang model, as opposed to the traditional selective sweep model (Sottoriva et al., 2015).

1.2.3 Diagnosis

Early diagnosis is key to successful treatment of CRC, however as symptoms are somewhat generalised and subtle, this often results in patients not seeking medical advice and subsequently, late diagnosis (Ballinger and Anggiansah, 2007). Symptoms of CRC include bleeding from the back passage or blood in faeces; a change in bowel habits and straining upon passing faeces. Further symptoms include pain in the abdomen or rectum and the presence of a lump within these regions, weight loss and extreme tiredness (Ballinger and Anggiansah, 2007). Diagnosis of CRC is typically achieved through use of sigmoidoscopy and/or colonoscopy, which allows the doctors to examine the rectum and colon. Biopsies of any suspect areas will be taken during this process and sent away for histological analysis (Cunningham et al., 2010, Brenner et al., 2014). If positive for CRC then further investigations will be undertaken, in the form of CT or MRI scans, which will allow the CRC to be staged according to the tumour, node, metastasis (TNM) system, which ranges from stage 0 (carcinoma in situ) to stage 4 bowel cancer (established metastases), with tumour severity increasing in correlation with stage (Ballinger and Anggiansah, 2007, Cunningham et al., 2010). In 2006 a screening programme was implemented in England, which screens people between the ages of 60 and 74 for bowel cancer through the use of Faecal Occult Blood Testing

(FOBT) (Cunningham et al., 2010, Brenner et al., 2014). FOBT detects trace amounts of blood within faeces, which can be indicative of CRC and warrants further investigation. In early 2015, a bowel scope screening programme was developed and is being rolled out across the UK, which will involve one-off screening of the over 55s for polyps, and is expected to be fully national by late 2016 (Ballinger and Anggiansah, 2007, Cunningham et al., 2010, Brenner et al., 2014).

1.2.4 Treatment and Survival

Treatment for early stage CRC is typically through surgical intervention, with adjuvant chemotherapy in the form of oxaliplatin and fluorouracil. Late stage CRC is normally highly metastatic and therefore the focus shifts from curative to control of the cancer, with varied options due to individual patients requirements (Brenner et al., 2014). Palliative chemotherapy and radiotherapy will be employed to try and shrink the tumour and metastases, and surgical interventions such as bowel and liver re-section are also undertaken, if in the patient's best interests (Cunningham et al., 2010, Pabla et al., 2015).

Overexpression of EGFR in CRC has led to the development of targeted therapies, which prevent the upregulation of EGFR (Ciardiello and Tortora, 2008, Cripps et al., 2010, Tol et al., 2010, Nishimura et al., 2015, Sato et al., 2015). Such therapies include monoclonal antibodies such as cetuximab, erlotinib and panitumumab, which prevent binding of ligands to EGFR and subsequently prevent the receptor dimerization and downstream signalling activation (Tol et al., 2010, Lupini et al., 2015, Kocoglu et al., 2016, Ciardiello and Tortora, 2008). A variety of EGFR inhibitors have also been designed, which also prevent the downstream effects of EGFR upregulation. Success rates of such therapies vary greatly due to individual tumour heterogeneity. For example *KRAS* mutations, which occur in approximately 30% of CRC tumours, are less

susceptible to EGFR attenuation through therapeutic intervention (Tan and Du, 2012, Lupini et al., 2015, Kocoglu et al., 2016).

Survival rates from CRC have increased by over 50% within the last 40 years, and currently 59% of people with CRC will live for 5 years post-diagnosis, and 57% will survive 10 years of disease (Ferlay et al., 2015, Holleczek et al., 2015). When broken down into colon and rectum cancer individually it was found that 52% of colon cancer and 54% of rectum patients will have a 5 year survival (Holleczek et al., 2015). Factors affecting survival rates include age, with research showing that survival decreases in correlation with increasing age, in both colon and rectum cancer (Holleczek et al., 2015). The stage at which CRC is diagnosed also greatly impacts the survival rates of the disease, with early stage CRC exhibiting a much higher (90%) 5 year survival rate than that of CRC diagnosed at advanced stages (10%) (Ballinger and Anggiansah, 2007, Holleczek et al., 2015).

1.3 Cellular Proliferation in Cancer

Dysregulation of cellular proliferation is a key event in the establishment and subsequent progression of cancer. It is defined as one of the hallmarks of cancer, and is probably the most fundamental characteristic of cancer cells (Hanahan and Weinberg, 2000, Hanahan and Weinberg, 2011). Normal tissues have extensive regulatory mechanisms in place for the control of cellular proliferation, including cell cycle check points, and the ability to overcome these mechanisms is vital to cancer development (Hanahan and Weinberg, 2011). Carcinogenesis which sees the development of sustained cellular proliferation is associated with a phenotypic change in cells. Typically, normal cells enter a proliferative state when activated by appropriate signals and expire when their lifespan is reached. However, cancerous cells acquire a different phenotype, which is achieved through alterations in a variety of areas encompassing

cellular metabolism, cell cycle regulation, autophagy and the tumour microenvironment (Evan and Vousden, 2001, Feitelson et al., 2015). By acquiring such a phenotype cancer cells become in charge of their own proliferative capabilities and subsequently sustained proliferation is achieved (Hanahan and Weinberg, 2011). One of the main regulatory mechanisms that are altered in cancer cells is mitogenic signalling, that is known to move cells from a quiescent state to an active state. These growth signals are received by cell surface receptors and trigger signalling pathways that favour proliferation and prevent activation of apoptosis (Dhillon et al., 2007, Hanahan and Weinberg, 2011, Feitelson et al., 2015). Promotion of autophagy is also known to contribute to sustained proliferative capacity within cancer cells. In normal cells, autophagy is present to maintain healthy homeostasis through the removal and elimination of damaged factors within cells (Mathew et al., 2007, Yang et al., 2011, Thorburn et al., 2014, White, 2015). As such, autophagy is widely acknowledged to be a mechanism for tumour suppression under normal homeostatic conditions (Mathew et al., 2007, Yang et al., 2011). However, during carcinogenesis the basal levels of autophagy become increased, thus resulting in a pro-survival state of autophagy (Thorburn et al., 2014, White, 2015). The attenuated levels of autophagy in cancer cells are attributed to the increased internal metabolic stress, which in conjunction with downregulation of apoptosis, allows for the sustained cellular proliferation seen in cancer (Mathew et al., 2007, Yang et al., 2011). Whilst there are numerous factors that contribute to sustained cellular proliferation in cancer, one of the most important is the dysregulation of signalling pathways. Various cellular pathways are known to be altered during carcinogenesis which leads to the upregulation of cellular proliferation. Such pathways include Wnt/β-Catenin, Notch and PI3K/AKT /mTOR, amongst others, alterations in such pathways are well reported within various cancer types, including CRC, and will be covered in further detail below (**Section 1.9**) (Rocks et al., 2008b, Vidal et al., 2011, Minder et al., 2012, Przemyslaw

et al., 2013, Danielsen et al., 2015, Feitelson et al., 2015, Feng et al., 2015, Huynh et al., 2015, Li et al., 2015a, Yang et al., 2015). Evasion of growth suppressors is also reputed to contribute to the promotion of sustained cellular proliferation under carcinogenesis. By evading signals designed to inhibit growth under normal circumstances, cancer cells are able to continue proliferating, thus promoting cancer progression. Tumour suppressors are typical examples of growth suppressors that must be evaded under carcinogenesis. Two main tumour suppressors that are linked to control of proliferation are retinoblastoma-associated (RB) and TP53 proteins (Hanahan and Weinberg, 2011). RB protein is responsible for determining whether cells should progress through the cell cycle in response to both intracellular and extracellular signals, whereas TP53 can halt cell cycle progression in response to intracellular signals and stresses (Hanahan and Weinberg, 2011). The cell cycle control of cellular proliferation will be discussed in more detail below.

1.3.1 Cell Cycle Regulation in Cancer

Under normal, non-cancerous conditions the cell cycle checkpoints are maintained by cyclins and cyclin-dependent kinases (CDKs) (Feitelson et al., 2015, Santo et al., 2015). Aberrant CDK expression is reported in many cancer types, which promotes the progression of mutated/damaged cells through the cell cycle. There are three major cell cycle checkpoints: G1/S which prevents damaged cells from progressing into S phase and is regulated by D-type cyclins and CDK 4/6; Intra-S phase which detects damage missed in G1/S and is mediated by CDK2 and Cyclin E/A and finally G2/M which controls mitotic division and is mediated by CDK1 and Cyclin B (Santo et al., 2015). If no cellular damage is detected at any checkpoint then cells progress uninterrupted, however, if damage is detected then cells are arrested. In order for cells to progress if no damage is detected cyclin-dependent kinase inhibitors (CKIs) must be present at each stage. In G1/S phase inhibitors of CDK 4/6 are members of the inhibitors of CDK4

(INK4) family and encompass p16, p15, p18 and p19 and these undergo competitive binding with Cyclin D, and thus inhibit cell cycle arrest (Feitelson et al., 2015, Santo et al., 2015). Cyclin D and CDK 4/6 are also responsible for the phosphorylation of RB protein, which prevents its activation of downstream genes that promote the advancement to S phase, by inhibiting this the cell cycle cannot proceed. Inhibitors within the intra-S phase include p21, p27 and p57, which are members of the CDK interacting protein/kinase inhibitory protein (Cip/Kip) family and are responsible for regulating the activity of Cyclin E and A. An illustrative diagram of the cell cycle and its checkpoints can be seen in **Figure 1.2**.

The dysregulation of cellular proliferation in cancer has been shown to be associated with aberrant CDK and cyclin expression, which are widely reported to be upregulated in many cancer types. Conversely, CKIs are known to be downregulated, thus leading to aberrant cell cycle regulation (Feitelson et al., 2015, Santo et al., 2015)The majority of alterations in cancer occur within the CDK 4/6 Cyclin D genes and their regulators (Santo et al., 2015). It has been shown that Cyclin D1 was upregulated in cervical cancer tissue and cells, and that by preventing this upregulation cellular proliferation was decreased (Li et al., 2015c). Furthermore, silencing Cyclin D1 in prostate cancer cells resulted in cell cycle arrest at G1 and subsequent reduction in proliferative capacity (Marampon et al., 2015). Notably, downregulation of Cyclin D1 results in decreased cell proliferation in colorectal cancer cells and caused cellular arrest (Tsukahara et al., 2015, Al-Qasem et al., 2016). Furthermore in colorectal cancer, both Cyclin A and D were found to be overexpressed, and correlated with poor survival (Bahnassy et al., 2004, Li et al., 2014b). Upregulated expression of CDK 4/6 is also reported within cancer cells, and as a result several therapeutic inhibitors of CDK 4/6 have been developed (Vora et al., 2014, DeMichele et al., 2015, VanArsdale et al., 2015). Furthermore, inhibition of CDK 4/6 shows reduced cellular viability and

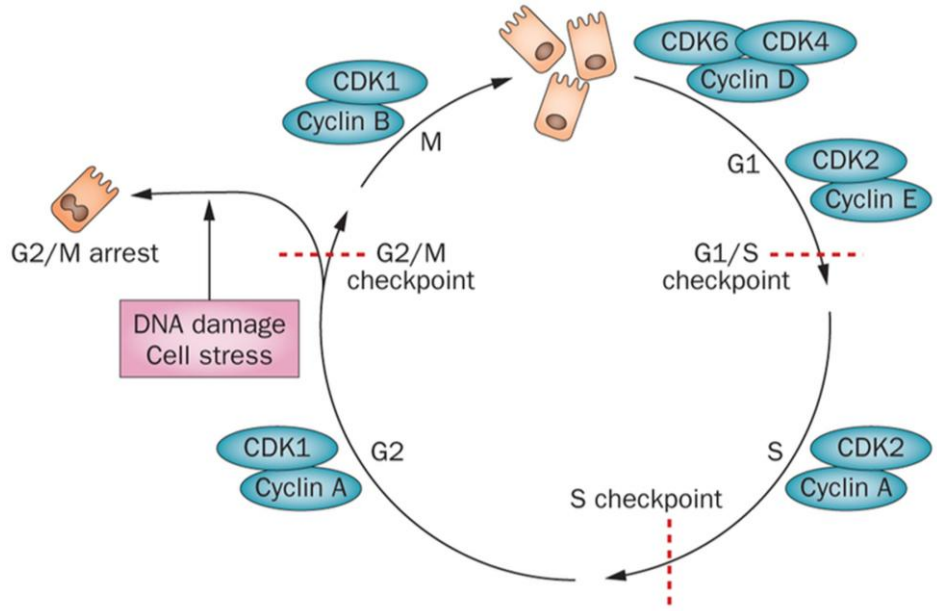

Figure 1.2: The Cell Cycle and its Checkpoints

Diagram illustrating the phases of the cell cycle along with the kinases and cyclins involved in its regulation. Proliferating cells progress through the cell cycle, and under normal, non-cancerous conditions they progress through the checkpoints without hindrance. Upon detection of DNA damage or cellular irregularities cell checkpoints are enforced and cell cycle arrest occurs. Cancerous cells acquire mechanisms allowing them to evade or override the checkpoints, thus allowing their un-interrupted progression through the cell cycle. Image adapted from Ferenbach and Bonventre (2015).

proliferation, resulting in cell cycle arrest, thus confirming the role of CDK 4/6 in driving the aberrant proliferation seen in cancer (Fry et al., 2004, Finn et al., 2009, Rivadeneira et al., 2010, Logan et al., 2013, Lv et al., 2015).

1.4 Tumour Microenvironment

The tumour microenvironment is complex, and its components include several different cell types that are believed to contribute to the development and metastasis of cancer, as well as physical (such as low oxygen availability or hypoxia), and chemical (such as low pH or acidosis, extracellular matrix) components (Lorusso and Ruegg, 2008). Since the identification of the six hallmarks of cancer in 2000, the tumour microenvironment has been identified as a key contributor to the development of cancer and, as such, must be considered when attempting to understand the traits leading to the development of cancer (Hanahan and Weinberg, 2011). This emerging trend has led to a focus on tumour microenvironment research, including the diverse cell types and signalling mechanisms, their interaction with the malignant cells and their surrounding environment which results in cancer development (Hanahan and Weinberg, 2011).

The tumour microenvironment is composed of numerous different cell types that all contribute, under normal circumstances, to regulating localised tissue (Lorusso and Ruegg, 2008). These include endothelial cells, fibroblasts, smooth muscle cells, and numerous immune cells (Lorusso and Ruegg, 2008). Together these cells participate in the regulation of normal stroma, whereas in neoplastic conditions these regulatory mechanisms become altered (Lorusso and Ruegg, 2008). It is thought that the development of cancer is due to a multi-component approach from the microenvironment, including numerous cells, signalling mechanisms and pathways (Hanahan and Weinberg, 2011). In non-cancerous tissues, interaction between cells from differing tissue environments is prevented by the presence of extracellular matrix

(ECM) and its components and signalling mechanisms (Liotta and Kohn, 2001). Under neoplastic conditions, malignant cells use the host tissue microenvironment to drive their progression, including the recruitment of vasculature and stroma. Furthermore, the activation of the local environment drives the proliferation and invasive potential of cancer cells (Liotta and Kohn, 2001). Malignant cells continually inflict insult on the host tissue and environment which causes the promotion of tumour growth and progression by the host microenvironment (Lorusso and Ruegg, 2008). The basement membrane of the host environment is the first barrier to be breached in the establishment of cancer and once this has occurred the ECM is altered to allow metastasis (Liotta and Kohn, 2001).

The cross talk between the various cells of the tumour microenvironment and their signalling mechanisms results in the metastatic and invasive nature of tumour cells (Mbeunkui and Johann, 2009, Mathias et al., 2013). The majority of the stromal/microenvironment cells have the capability to contribute to the remodelling of the ECM, which is crucial for tumour progression and metastasis, and are believed to contribute as such through the secretion of growth factors, cytokines and proteins (Mathias et al., 2013). The signals originating from the tumour microenvironment also activate various transcription factors that are responsible for inducing genes associated with cancer progression. The range of genes and molecules induced by cellular cross-talk within the microenvironment is vast and includes VEGF (vascular endothelial growth factor), TGF-β (transforming growth factor β), TNF-α (tumour necrosis factor α), inflammatory mediators, immunosuppressors and extracellular matrix degrading proteases (Cammarota et al., 2010, Peddareddigari et al., 2010). Other factors contributing to the progression include enzymes such as matrix metalloproteinases (MMPs) and A Disintegrin And Metalloproteinases (ADAM) factors, which play a role in proteolytic processing and subsequent ECM degradation (Mathias et al., 2013). The

degradation of the extracellular matrix leads to the breakdown of normal tissue boundaries that prevent metastatic cells from progressing. Therefore, by manipulating the host tissue microenvironment, metastatic cells can significantly alter and breach the ECM, thus resulting in the barrier being removed and the progression of the neoplastic cells (Liotta and Kohn, 2001). Enzymatic cascades are strongly implicated in the breakdown of the ECM, triggered by the activation of various proteinases such as MMPs, leading to the degradation of ECM structural proteins.

1.5 Tumour Hypoxia

It is widely believed that the occurrence of regions of hypoxia, or low oxygen, within the tumour microenvironment exacerbates the metastatic nature of cells (Kunz and Ibrahim, 2003). Hypoxia occurs as a result of insufficient oxygen supply and irregular vasculature and is prevalent amongst solid-state tumours due to the nature of their microenvironment. In rapidly growing tumours the blood vessels form quickly and abnormally creating a non-uniform vasculature with a range of diffusion distances throughout the tumour (Rademakers et al., 2008). The abnormalities in the vasculature of tumours limit their ability to oxygenate all the cells present within the tumour and the majority of the oxygen supplied is consumed within the first 70-150 μm from the blood vessels thus creating hypoxic regions (Olive et al., 1992, Dewhirst, 1998, Rademakers et al., 2008, Bennewith and Dedhar, 2011). The degree of hypoxia within tumours varies greatly depending on tumour type and characteristics, but typically range from approximately 1-50% of the tumour mass (Bennewith and Dedhar, 2011). **Figure 1.3** illustrates the gradient of hypoxia in tumour tissue, increasing in conjunction with the distance from blood vessels. Hypoxia can be classified into chronic, acute and anaemic hypoxia, associated to its origins and duration. In acute hypoxia tissues are exposed to low oxygen concentrations for a short amount of time, whilst in chronic hypoxia the

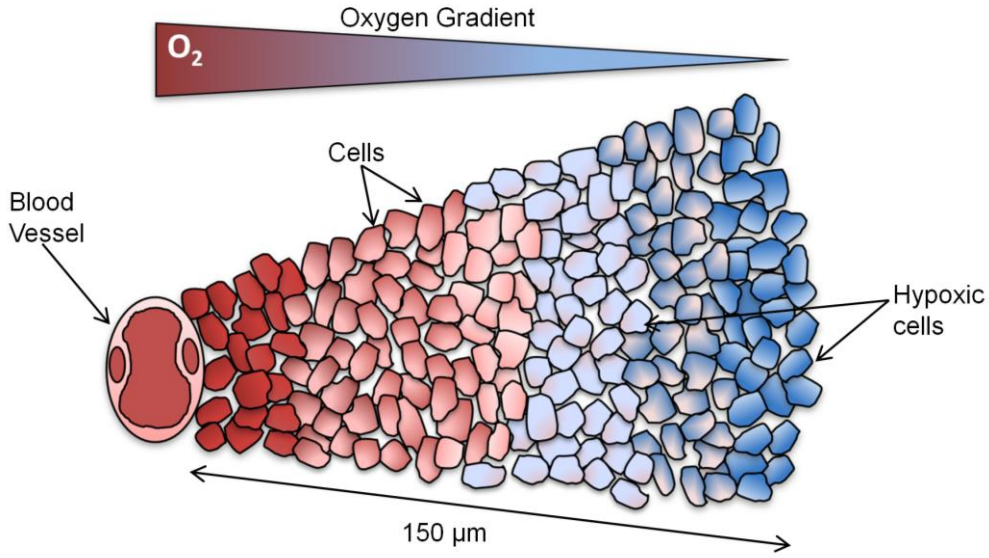

Figure 1.3: Schematic Diagram Illustrating Tumour Hypoxia

Irregular vasculature development during tumour formation results in hypoxic regions within solid state tumours. Typically the blood oxygen is consumed within 70-150 µm from the vasculature. As the oxygen tension within the cells decreases, the resistance to therapeutics increases conversely. Image kindly provided by Dr Isabel Pires (originally adapted from Brown and Giaccia (1998)) and adapted.

low-oxygen exposure is prolonged (Vaupel and Harrison, 2004). Finally, anaemia-associated hypoxia arises as a result of low oxygen transport in the blood as a consequence of therapeutic intervention or from the tumour itself (Vaupel and Harrison, 2004, Rademakers et al., 2008).

The oxygen tension limits in a tissue classified as hypoxia are strongly disputed, due to variation in 'normal' O_2 levels between tissue types (Ivanovic, 2009). Hypoxia in cells is therefore classified as lower than the oxygen levels of normal, non-malignant cells, typically $\leq$2% O_2 (Bertout et al., 2008, Hancock et al., 2015). Experimentally it has been shown that in malignant tissue the levels of oxygen are lower than those measured in normal tissue, but that the levels vary greatly amongst tissue types (Brown and Wilson, 2004). For example, in prostate cancer the pO_2 levels were shown to be 2.4 mm Hg in malignant tissue compared to 30 mm Hg in non-cancerous surrounding tissue, similarly altered levels have also been reported in breast, lung, cervical and pancreatic cancer (Koong et al., 2000, Movsas et al., 2001, Vaupel et al., 2002, Nordsmark et al., 2003). The vast majority of cells cannot survive for long in hypoxic environments, however malignant cells are better adapted to this environment and can survive for longer than non-cancerous cells under these conditions. This ability is somewhat advantageous to the acquisition of a metastatic phenotype. Hypoxia induces a plethora of alterations in cellular signalling, the best characterised being the transcriptional activation of genes that promote angiogenesis, cell proliferation, invasion and metastasis (Ke and Costa, 2006, Mandl et al., 2013). The key transcription factor responsible for this up regulation is HIF-1 (hypoxia inducible factor 1) and HIF-2. HIF α and β subunits play a key role in the activation of the HIF pathway (**Figure 1.4**) and the promotion of cell survival under hypoxic conditions. The HIFα subunit is degraded by the proteasome under normoxic conditions via the VHL (Von Hippel-Lindau), E3

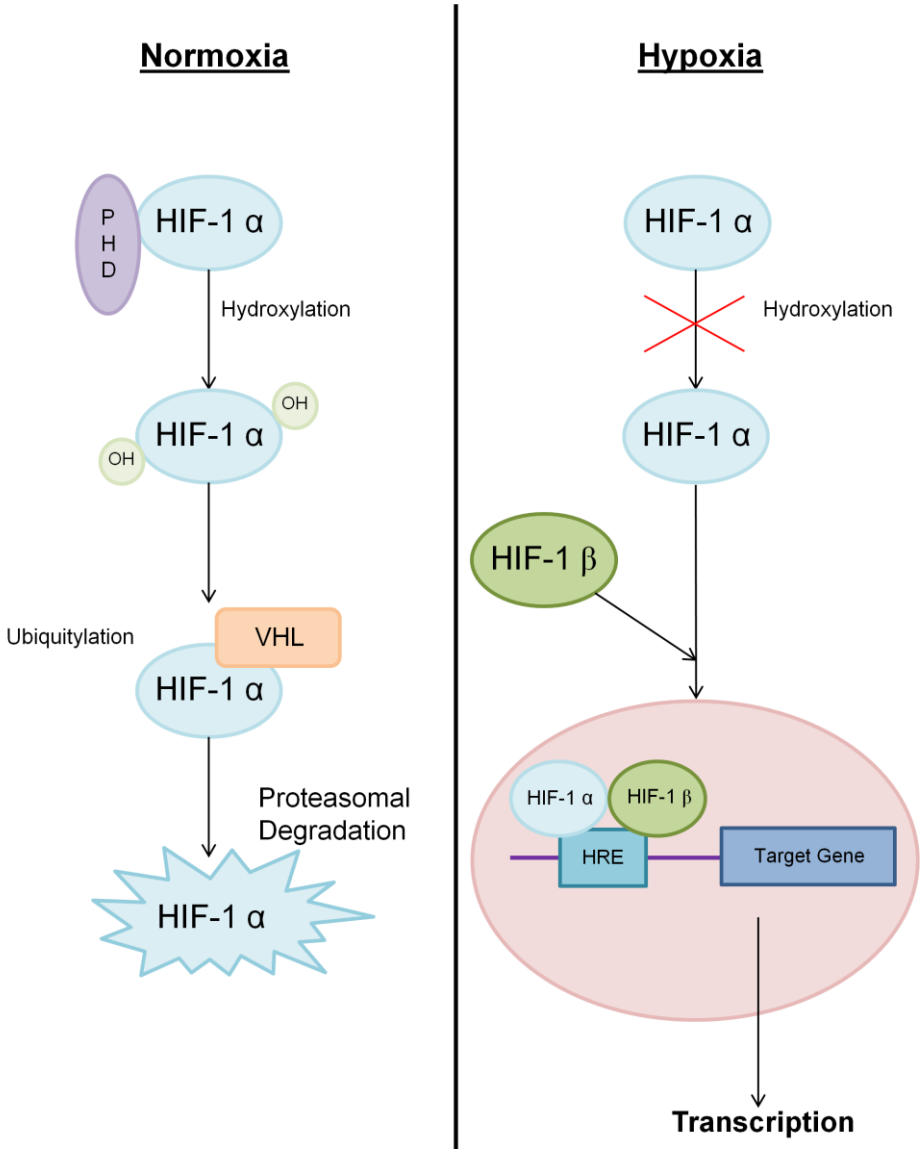

Figure 1.4: HIF Signalling in Tumour Hypoxia

Under normoxic conditions the HIF-1α subunit is hydroxylated by prolyl hydroxylase domain (PHD) proteins after which it is ubiquitylated by Von Hippel-Lindau (VHL) protein and targeted for proteasomal degradation. Under hypoxic conditions the hydroxylation of HIF-1α is prevented and as a result HIF-1α translocates to the nucleus where it dimerises with HIF-1β, binds to the hypoxia-response element (HRE) in target genes and regulates transcriptional activation.

ligase complex, a tumour suppressor, whereas under hypoxic conditions its degradation is prevented through inhibition of HIFα hydroxylation (Mandl et al., 2013). HIF-1α then translocates to the nucleus where it dimerises with HIF-1β and induces gene transcription (Mandl et al., 2013). The HIF-1 pathway has numerous target genes including VEGF, which promotes angiogenesis, transforming growth factor-α (TGF-α), which promotes cell proliferation and survival, and many others that promote mechanisms such as glucose metabolism, apoptosis evasion and erythropoiesis (Ke and Costa, 2006). It is the activation of such genes that leads to the survival and increased tumourigenic potential of hypoxic cancer cells, including increased metastatic proneness.

Hypoxia is also known to influence cellular proliferation in cancer cells, and such effects are well documented within the literature, albeit somewhat conflicting. Previously, an upregulation in prostate cancer cellular proliferation has been reported after exposure to hypoxia (1% O_2; 24-48 hours) (Tang et al., 2015). Additionally, in lung cancer similar upregulations in cell proliferation have been described, with results showing a significant increase after a short hypoxic exposure (1% O_2; 4 hours) (Liang et al., 2015). Contrastingly to the study by Tang et al. (2015), Ma et al. (2011) reported that exposure to hypoxia had no effect on cellular proliferation in prostate cancer cells (1% O_2; 12-48 hours). Conflicting reports have also described a downregulation of cellular proliferation in response to hypoxic exposure (Zhu et al., 2010, Yu and Hales, 2011, Westwood et al., 2014). In ovarian cancer it was reported that in some cell lines cellular proliferation was decreased after prolonged hypoxic exposure (1% O_2; 72 hours) (Zhu et al., 2010). Importantly, in CRC cells it was previously shown that there was a significant downregulation of proliferation after exposure to hypoxia *in vitro* (Westwood et al., 2014). However, when examined *in vivo* CRC derived xenografts were found to be unaffected by prolonged hypoxic exposure (10% O_2, 21 days)

(Westwood et al., 2014). In xenograft models of lung cancer proliferation was reported to be decreased after chronic hypoxic exposure (10% O_2; 14 days) (Yu and Hales, 2011). The conflicting nature of existing research suggests that the effect of hypoxia on cellular proliferation is dependent upon the exposure conditions and cell type. Furthermore, evidence indicates that hypoxic modulation of cellular proliferation is a complex system, encompassing a variety of signalling pathways that differ amongst cancer types.

It is widely acknowledged that the hypoxic microenvironment sees in increase in growth factors and their receptors, which in turn activates downstream signalling mechanisms through the EGFR cascade. Furthermore, the Warburg effect, which sees the shift to glycolytic metabolism under hypoxic conditions, promotes cell proliferation through increased ATP production (Feitelson et al., 2015). It has also been shown that autophagy is increased within the hypoxic microenvironment (Papandreou et al., 2008, Chen et al., 2009, Hu et al., 2012, Li et al., 2015b). Notably, exposure to severe hypoxia (0.02% O_2) has been shown to induce S phase arrest in CRC cell lines, which induced p53 stabilisation and subsequent phosphorylation (Hammond et al., 2002, Hammond et al., 2003, Pires et al., 2010). Importantly, this induction is independent of DNA damage, and following re-oxygenation, replication restarts (Hammond et al., 2002, Pires et al., 2010). Furthermore, deregulation of cellular proliferation has also been attributed to alteration in c-MYC and cyclin-D1 expression (Yang et al., 2006, Dang, 2012, Miller et al., 2012, Boudjadi et al., 2015, Lynch et al., 2015, Wahlstrom and Henriksson, 2015).

1.6 Metastasis

Various mechanisms have been attributed to increased survival, tumourigenesis and metastatic potential of tumour cells under hypoxic conditions. Deregulation of normal tissue homeostasis occurs in cancer, and this is exacerbated in hypoxic conditions,

which subsequently allows a greater metastatic potential of the invading cells (Catalano et al., 2013). Metastasis is initiated by the tumour cells by acquiring a motile-phenotype through epithelial-mesenchymal transition (EMT) and the loss of epithelial characteristics (Catalano et al., 2013). Loss of key elements such as E-Cadherin, a widely recognised tumour suppressor gene, as well as the acquisition of more mesenchymal characteristics, such as increased N-Cadherin and Vimentin expression is the first step for tumour cells in acquiring metastatic potential (Pecina-Slaus, 2003, Medici et al., 2006a, Catalano et al., 2013). E-Cadherin is repressed by transcription factors upregulated under hypoxic conditions (Medici et al., 2006a). The loss of factors such as E-Cadherin which promote cell-cell adhesion allows the tumour cells to acquire a more motile mesenchymal phenotype and thus initiate the invasion of cancer cells (Vleminckx et al., 1991, Medici et al., 2006a).

Such transitions are promoted more heavily under hypoxic conditions due to the activation of the HIF pathway and the subsequent activation of signalling cascades such as the EGFR (Epidermal Growth Factor Receptor) and TGF-β (Transforming Growth Factor - β) pathways (Kannan et al., 2013). The activation of the HIF pathway can lead to alterations in the expression of proteins such as Caveolin-1, which is downregulated in cancers (Kannan et al., 2013). This event subsequently activates the EGFR signalling cascade which promotes the transcription of factors that repress E-Cadherin, thus promoting EMT (Kannan et al., 2013). After EMT, tumour cells possess the ability to move in an invasive manner and thus begin to degrade the basement membrane localised to their origin. The invading tumour cells release factors that degrade the basement membrane, such as metalloproteinases, and deregulate its remodelling process (Lu and Kang, 2010). The deregulation of collagen type IV, leads to a reduction in its levels in many cancer types, including CRC, and this is widely hypothesised to be a critical factor in the breaching of the basement membrane by metastatic cancer cells

(Tanjore and Kalluri, 2006). As the structural backbone of the basement membrane, a reduction or dysregulation allows cancer cells to invade the ECM and disseminate (Lu and Kang, 2010, Tanjore and Kalluri, 2006). Once the cells have invaded the ECM they invade localised blood vessels (intravasion), allowing them to enter the circulation and disseminate to other areas away from the point of origin (extravasion), where they establish metastatic tumour sites (Lu and Kang, 2010). The effect of tumour hypoxia on cancer metastasis is a key research target due to evidence implicating these regions in driving the metastatic progression of tumours. **Figure 1.5** illustrates the metastatic progression of cancer.

1.7 ADAMs Family

Proteolytic processing has been implicated in the progression of cancer and one such mechanism involves a group of metalloproteinases known as the ADAMs family. The A Disintegrin And Metalloproteinase (ADAMs) family are a group of multidomain transmembrane proteins that have various roles and subsequently effect a variety of cellular processes such as adhesion, proliferation, migration and signalling (Edwards et al., 2008). The main identified role for the ADAMs family proteins is an involvement in membrane remodelling and protein processing through the activation of growth factors and cytokines and the shedding of extracellular domains of receptors for growth factors (Duffy et al., 2011). Many studies have implicated a number of ADAMs family substrates in cancer development and the following sections will examine such a role.

1.7.1 ADAMs Background

The ADAMs family is composed of numerous members, with twenty-one having been identified within the human genome (Murphy, 2008, Reiss and Saftig, 2009). The ADAMs family belong to the metzincins super family, which also includes the class III

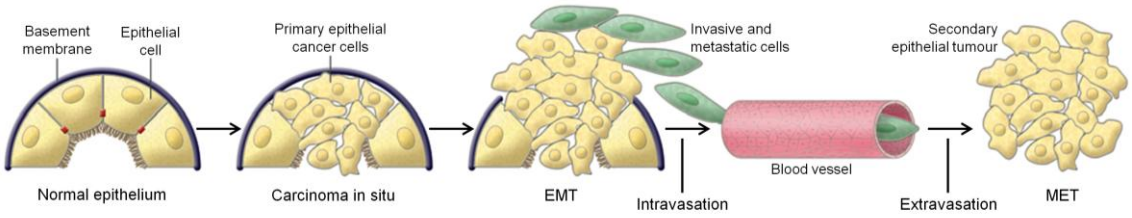

Figure 1.5: Metastatic Progression of Cancer

Diagram illustrating the progression of cancer from cells in situ to distant metastases, encompassing the phenotypical changes during EMT. Metastatic cancer progression is initiated by cells undergoing EMT, which promotes a more mobile and invasive nature. The basement membrane is degraded, thus allowing the movement of cancer cells to vasculature. Subsequently, dissemination of the cancer cells occurs through the vascular system, allowing the formation of distant metastases. EMT – epithelial to mesenchymal transition; MET – mesenchymal-epithelial transition. Image adapted from Kalluri and Weinberg (2009).

snake venom metalloproteases, and are categorised within the adamlysin subfamily (Anders et al., 2001, Klein and Bischoff, 2011). ADAMs proteins are typically 70-90 kDa in size in their mature form however they are primarily secreted as precursors, approximately 20 kDa bigger, due to the presence of their prodomain which is removed upon maturation (Anders et al., 2001, Tousseyn et al., 2006).

1.7.2 ADAMs Structure

Each member of the metalloproteinase family shares a typical, generalised structure that contains eight different domains, with each one possessing different functional activity. The domains identified within the generalised ADAMs structure include the following: signal domain, pro domain, metalloproteinase domain, disintegrin binding domain, cysteine rich domain, epidermal-growth factor (EGF) like domain, transmembrane domain and finally intracellular C-terminal cytoplasmic domain (Duffy et al., 2011, Edwards et al., 2008) (**Figure 1.6**). There is slight deviation between the structure of membrane bound ADAMs and the secreted form, as detailed in **Figure 1.6**. The secreted form has the same generalised structure as the membrane bound form however it lacks the transmembrane domain and the cytoplasmic domain (Tousseyn et al., 2006). The ectodomain shed form of the ADAMs is initially formed as the membrane bound variety however it is then sliced directly above the transmembrane domain. This sees the release of the remainder of the structure whilst the transmembrane stub remains membrane bound, as seen in **Figure 1.6** (Tousseyn et al., 2006).

The signal domain on the ADAMs family is responsible for directing the proteins to the correct secretory pathway and is attached to the prodomain (Edwards et al., 2008). The prodomain present in the precursor form of ADAMs proteins is within the N-terminal and during maturation is cleaved by proprotein convertases in the trans-Golgi-network

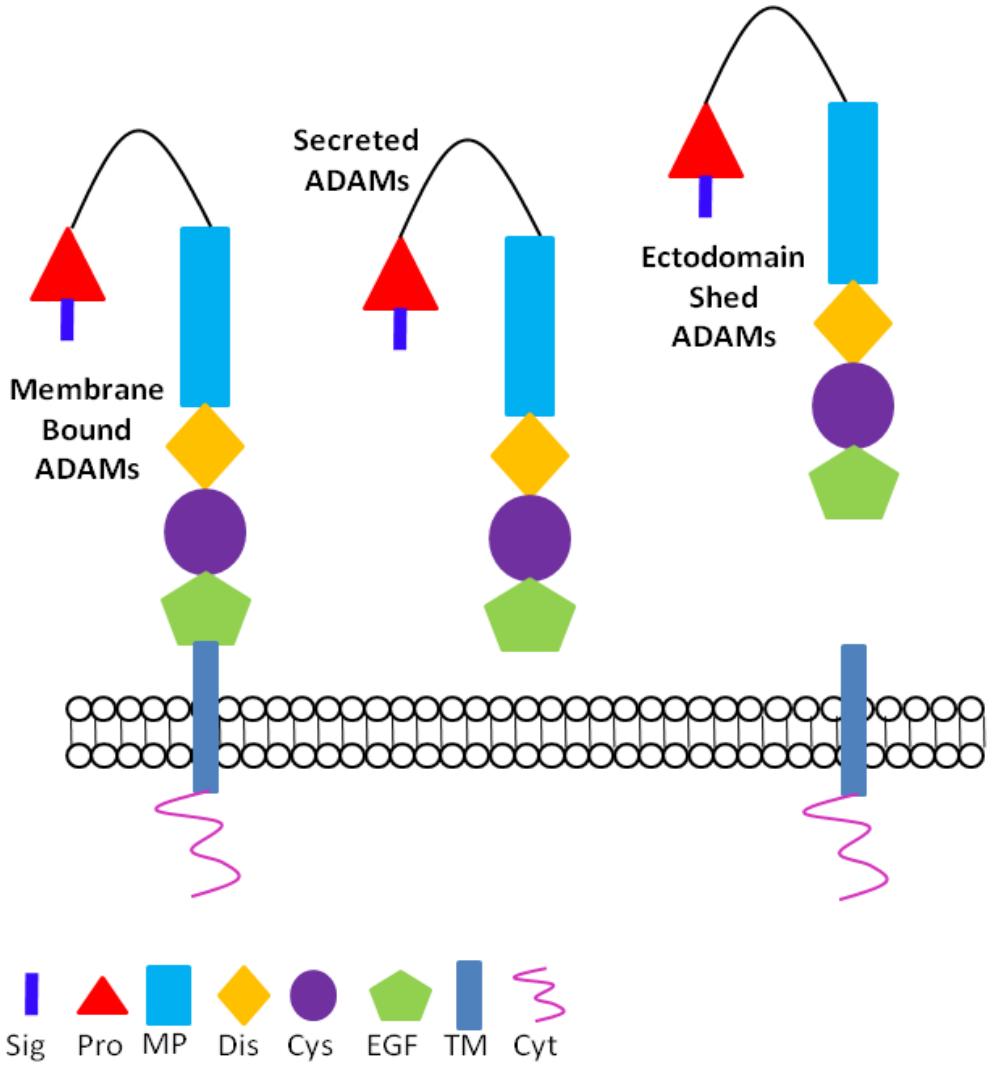

Figure 1.6: Schematic Diagram Illustrating the Generalised Structure of the ADAMs Family

Both membrane bound and secreted forms are illustrated. Each member typically has a signal domain (Sig), a prodomain (Pro), a metalloprotease domain (MP), a disintegrin domain (Dis), a cysteine rich domain (Cys) and an EGF-like domain (EGF). The variation in structure comes in the membrane bound and secreted versions. The membrane bound ADAMs have a transmembrane domain (TM) and a cytoplasmic tail (Cyt) whereas the secreted ADAMs lack these elements, unless created by ectodomain shedding.

(Anders et al., 2001, Tousseyn et al., 2006). This cleavage is a common characteristic amongst metzincins and is illustrated in **Figure 1.7** (Anders et al., 2001). The generation of the ADAMs proteins as inactive forms prevents protein degradation by premature enzymatic activity and facilitates correct protein folding (Anders et al., 2001). There have been seven pro-protein convertases identified in mammals, two of which have been shown to act on the ADAMs family by cutting at a recognised sequence within the C-terminal of the prodomain (Anders et al., 2001, Reiss and Saftig, 2009). Pro-protein convertases such as pro-protein convertase 7 (PC7) or furin cleave pro-domains from ADAMs family members through recognition of the RXXR cleavage site between the pro-domain and the metalloproteinase domain (Anders et al., 2001, Rocks et al., 2008b). Cleavage by pro-protein convertases occurs within the secretory pathway, typically within the Trans-Golgi network and the removal of the prodomain is crucial for the activation of some ADAMs family members. Furin is a serine endoprotease and is localised within the Trans-Golgi network. Here it auto-removes its own inhibitory pro-domain, thus allowing it to function as a protease and mediate the removal of pro-domains from proteins such as ADAMs family members (Thomas, 2002). Furin also mediates a role in the regulation of protein folding (Anders et al., 2001, Thomas, 2002). PC7, a lesser studied pro-protein convertase, also functions as an endoprotease, however its localisation is believed to be primarily within the endoplasmic reticulum and at the cell surface. Some localisation is also seen in the Trans-golgi network, with results indicating that PC7 localisation is somewhat cell type specific (Rousselet et al., 2011).

ADAMs members pro-domains act as inhibitors of the protease and this has been demonstrated in both ADAM 10 and 17, which have been shown to remain catalytically inactive without prodomain removal (Schlondorff et al., 2000, Anders et al., 2001). The recognition of the cleavage site by pro-protein convertases cleaves the pro-domain form

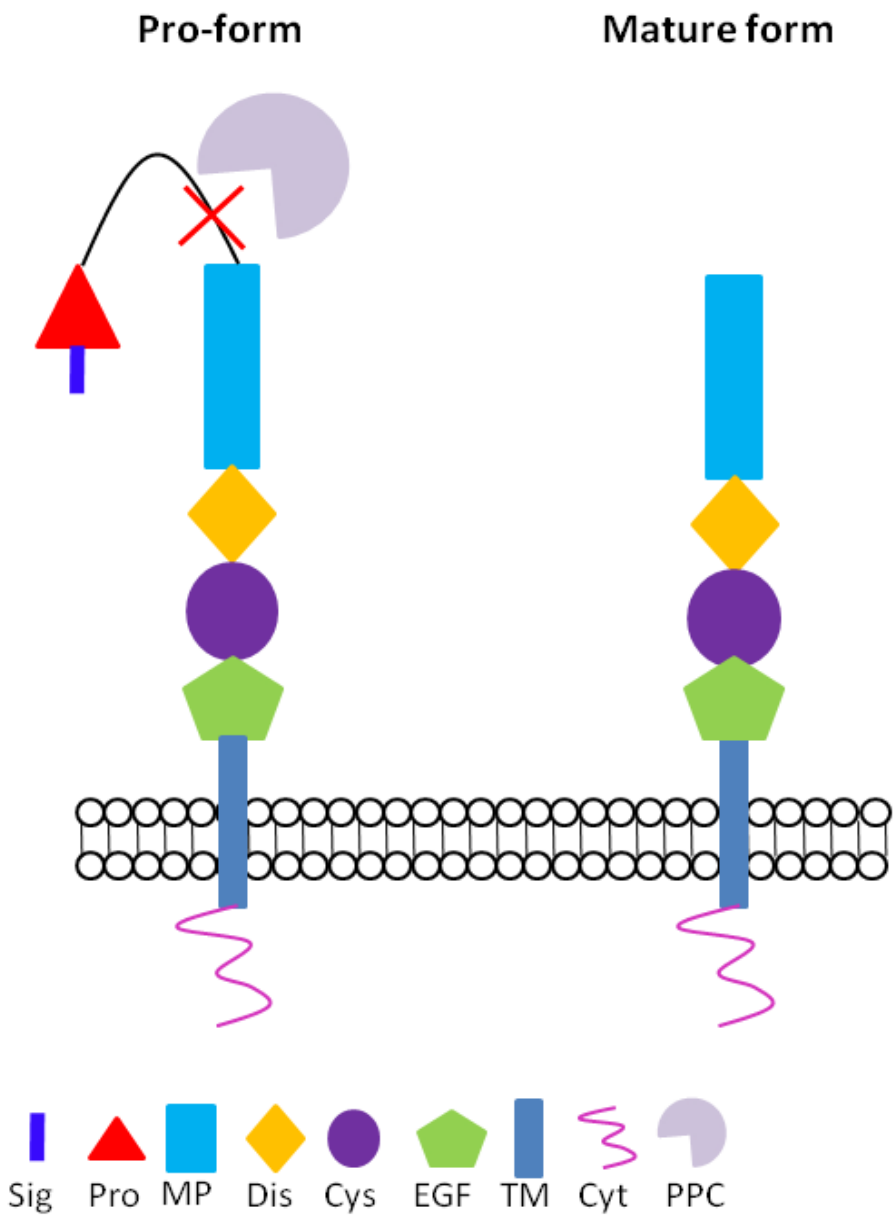

Figure 1.7: Schematic Diagram Illustrating the Cleavage of the Prodomain During the Maturation of the ADAM Protein

The pro-domain is cleaved by proprotein convertases (PPC), such as furin, within the Trans-Golgi network. The ADAMs protein is subsequently in its mature form and active form and is capable of exerting its sheddase activity within cells.

ADAMs members and initiates a cysteine switch. In their inactive form, with attached pro-domain ADAMs members possess a highly conserved cysteine residue that inhibits the zinc atom within the active site (Milla et al., 2006, Moss et al., 2007, Edwards et al., 2008). Upon cleavage by pro-protein convertases this inhibitory mechanism is reverted, thus allowing ADAMs members to become catalytically active. It is believed that pro-protein convertases are also responsible for mediating the pro-domain removal of secreted and ectodomain shed ADAMs members, prior to the occurrence of their secretion/shedding.

The metalloprotease domain of the ADAMs family is attached to the C-terminal of the prodomain and is crucial for the functional action of the ADAMs. Not all members of the ADAMs family possess the required zinc-binding motif that allows the processing of the ADAMs protein substrates (Reiss and Saftig, 2009). Within the zinc binding motif there are three histidine residues along with a methionine-turn within the helix of the active site and members of the ADAMs family must possess the consensus sequence (HEXGHXXGXXHD) in order to become catalytically active, currently thirteen of identified ADAMs family members do (Reiss and Saftig, 2009). Adjacent to the metalloprotease domain is the disintegrin domain and this is responsible for adhesion to various integrins which mediates cell-cell adhesion (Tousseyn et al., 2006). This section contains a fourteen amino acid sequence called the disintegrin loop that is crucial in mediating the interactions between integrins and ADAMs family members (Edwards et al., 2008). Together with the subsequent cysteine rich domain it is also involved in the regulation of the activity of the ADAMs. Notably, previous research has revealed that neither ADAM 10 nor ADAM 17 possess an EGF-like domain, thus making them different to other ADAMs members (Janes et al., 2005). The transmembrane domain is responsible for the anchorage of the ADAMs to the membrane for the membrane bound forms and is absent in the secreted version. This domain is at the N-terminal of the

cytoplasmic tail that varies in length between ADAMs and is believed to be functional in cellular signalling mechanisms (Edwards et al., 2008).

1.7.3 ADAMs in Cancer

The role of ADAMs in cancer has been widely investigated and there is strong evidence that a selection of the ADAMs family of proteins do in fact play a role in the development and progression of cancer. Although several aspects of the mechanism by which these ADAMs family members contribute to the cancer development remains unknown there is strong evidence that supports the hypothesis that the ADAMs family are instrumental in the initiation of the metastatic nature of cancer cells.

ADAM 17 is one of the better characterised family members in the field of cancer and has been strongly implicated in the progression of various types of cancer, with evidence for its role in tumour hypoxia also well documented (Edwards et al., 2008). ADAM 17, also known as tumour necrosis factor-α converting enzyme (TACE), has been shown to be involved in the shedding of a number of different but pathologically relevant substrates including TNF-α and epidermal growth factor receptor (EGFR) ligands (Blanchot-Jossic et al., 2005, Richards et al., 2012). Numerous studies have reported an upregulation of ADAM 17 in various cancer types, including but not limited to, colorectal, head and neck, gastric, lung, ovarian and breast (Blanchot-Jossic et al., 2005, Kornfeld et al., 2011, Richards et al., 2012, Pan et al., 2012, Benson et al., 2014). Numerous studies have reported that this upregulation is directly correlated to tumour grade, which is in contrast to one study in colon cancer which determined that there was no such correlation (Blanchot-Jossic et al., 2005, Kornfeld et al., 2011, Pan et al., 2012). Based on this correlation it is hypothesised that ADAM 17 could be used as a potential prognostic marker in a variety of different cancer types (Kornfeld et al., 2011, Pan et al., 2012, Benson et al., 2014).

It has been shown that ADAM 17 upregulation is particularly prevalent in tissue with an invasive phenotype, further linking ADAM 17 to the development of a metastatic phenotype and subsequent tumour progression (Kornfeld et al., 2011). Numerous studies have also demonstrated that the upregulation of ADAM 17 is strongly linked to increased cellular proliferation, which is a key element that becomes deregulated in cancer (McGowan et al., 2007, Merchant et al., 2008, Göőz et al., 2009). It has been shown that ADAM 17 inhibition, leads to a decrease in cellular proliferation, thus implicating ADAM 17 in mediating proliferative activities (Göőz et al., 2009).

Due to the highly metastatic nature of hypoxic tumour cells and the knowledge that ADAM 17 is believed to play a role in driving the metastasis of various cancers, research has shifted towards investigating the implications of a hypoxic environment on ADAM 17 and its subsequent effects on cancer cells. Many studies have identified that ADAM 17 is expressed at significantly higher levels under hypoxic conditions at both protein and transcript level compared to normoxic counterparts in both breast and brain cancer (Charbonneau et al., 2007, Zheng et al., 2007, Rzymski et al., 2012). It has also been shown that the proteolytic activity of ADAM 17 is upregulated in hypoxic conditions, leading to an increased shedding of substrates such as TNF-α (Charbonneau et al., 2007, Rzymski et al., 2012). Furthermore, decrease of hypoxia-induced ADAM 17 protein levels upon re-oxygenation has reinforced the idea of low-oxygen dependent ADAM 17 upregulation (Rzymski et al., 2012).

1.8 ADAM 10

ADAM 10 is a catalytically active member of the ADAMs family, which has been implicated in the development of cancer, although at a lesser extent than some other members of the ADAMs family (Edwards et al., 2008, Parkin and Harris, 2009, Reiss and Saftig, 2009). ADAM 10 contains the catalytic protease domain that is required to

act as a functional metalloproteinase and therefore is involved in the cleavage of cell surface proteins (Parkin and Harris, 2009, Duffy et al., 2011). Human ADAM 10 is primarily synthesised as a precursor of 748 amino acids in length which undergoes maturation to become the transmembrane glycoprotein that is typical of the ADAMs family (Tousseyn et al., 2006, Parkin and Harris, 2009). It has been shown that pro-domain removal, by PC7 and furin, is required for ADAM 10 maturation and subsequent activation of its proteolytic activity (Anders et al., 2001, Moss et al., 2007). The mechanism by which the ADAM 10 prodomain inhibits its proteolytic activity differs to other members of the ADAMs family, which typically require a cysteine residue for the inhibition (Milla et al., 2006, Moss et al., 2007, Edwards et al., 2008). Importantly, ADAM 10 does not possess an EGF-like domain, which is typical of other family members (Janes et al., 2005) ADAM 10 has been shown to be involved in the shedding of various types of cell surface proteins (seen in **Table 1.1** below), triggering signalling mechanisms and subsequently influencing cellular properties such as adhesion, migration and signalling (Parkin and Harris, 2009).

Table 1.1: Known ADAM 10 Substrates (adapted from Edwards et al. (2008))

ADAM 10 Substrate	References
Amyloid precursor protein (APP)	Fahrenholz et al. (2000)
Delta-like ligand 1 (DLL-1)	Six et al. (2003)
Epidermal growth factor (EGF)	Sahin et al. (2004)
Pro-betacellulin	Sahin et al. (2004); Sanderson et al. (2005)
TNF-α	Lunn et al. (1997); Mężyk-Kopeć et al. (2009)
Heregulin	Ebbing et al. (2016)
E-Cadherin	Maretzky et al. (2005); Maretzky et al. (2008)
N-Cadherin	Reiss et al. (2005)
Notch	Hartmann et al. (2002); van Tetering et al. (2009)
ErbB-2	Liu et al. (2006)
CD44	Nagano et al. (2004); Anderegg et al. (2009); Pan et al. (2012)
RANKL	Hikita et al. (2006)

Collagen XVII	Franzke et al. (2009)
c-Met	Kopitz et al. (2007)
L1	Pan et al. (2012)
Fas-ligand (FasL)	Kirkin et al. (2007); Schulte et al. (2007)

1.8.1 ADAM 10 in Cancer

The implication of ADAM 10 in cancer progression is less characterised in comparison to some of the better studied ADAM family members such as ADAM 17. The results of various studies have provided a somewhat conflicting view of the role of ADAM 10 in cancer development and progression, dependent on context and cancer type. ADAM 10 has been found to be upregulated in numerous cancer types including: gastric, head and neck, prostate, breast and oral (McCulloch et al., 2004, Xu et al., 2010, Wang et al., 2011a, Bulstrode et al., 2012, Jones et al., 2013, Mullooly et al., 2015). Several immunohistochemical studies have shown that increased staining for ADAM 10 is present in tumour tissue samples, with intensity of staining correlating to higher tumour histological grade, as well as metastatic status (Arima et al., 2007, Xu et al., 2010, Wang et al., 2011a). Studies have identified that ADAM 10 is significantly upregulated at both protein and mRNA level when directly compared to non-cancerous counterparts (Xu et al., 2010, Wang et al., 2011a, Jones et al., 2013). However, some conflicting studies have provided evidence for non-altered expression of ADAM 10 in cancerous conditions (McCulloch et al., 2004, Lendeckel et al., 2005). Such findings indicate that the role of ADAM 10 in the development of cancer may vary between cancer types.

Interestingly, the subcellular localisation of ADAM 10 can be altered in cancer. Specifically, it has been shown that ADAM 10 translocates form the plasma membrane to the nucleus (McCulloch et al., 2004, Arima et al., 2007, Wang et al., 2011a). Specifically, McCulloch et al. (2004) reported that, in benign prostate tissue, the majority of ADAM 10 staining was found on the cell surface whereas in cancerous

prostate tissue samples the majority of ADAM 10 staining was nuclear, with cell surface staining visibly diminished. Similar findings in prostate cancer by Arima et al. (2007) identified that, after translocation, ADAM 10 binds to the androgen receptor in the nucleus. The authors hypothesised that this causes ADAM 10 to act like a transcription factor, transactivating several genes key for cancer cell proliferation (Arima et al., 2007). Studies such as those by Arima et al. (2007) and Wang et al. (2011a) indicated that the translocation of ADAM 10 directly correlated with the grade and prognostic value in both prostate and gastric cancer, thus further implicating ADAM 10 in cancer progression.

Alteration of ADAM 10 expression in cancer strongly implicates it in the development of the disease, with further evidence provided from research showing its involvement in the metastatic progression. Various studies have demonstrated that the knockdown of ADAM 10 reduces such metastatic characteristics (Xu et al., 2010, Jones et al., 2013). Xu and colleagues showed that, when ADAM 10 was knocked down in highly metastatic cells, their proliferation and migration was significantly reduced (Xu et al., 2010). Similar results were reported by Maretzky et al. (2005), Jones et al. (2013), and (Mullooly et al., 2015). In oral cancer, it was reported that silencing of ADAM 10 resulted in reduced migration and invasion of cells (Jones et al., 2013). Additionally, in breast cancer ADAM 10 was associated with higher grade samples, and cells were found to migrate less after ADAM 10 knockdown (Mullooly et al., 2015). These findings, amongst others, further implicate ADAM 10 in the progression of various cancers and make it a strong target for future research.

1.8.2 ADAM 10 and Hypoxia

Evidence for the involvement of ADAM 10 in hypoxia-mediated tumour development and progression is extremely limited and somewhat conflicting (Webster et al., 2002,

Marshall et al., 2006, Barsoum et al., 2011). One key study by Barsoum et al. (2011) showed that ADAM 10 expression was significantly upregulated in hypoxic conditions (0.5% O_2) in breast and prostate cancer. It was shown that there was a link between HIF-1α and ADAM 10, as when HIF-1α was knocked down ADAM 10 upregulation was absent (Barsoum et al., 2011). It was also shown that ADAM 10 may play a role in the evasion of the innate immune system under hypoxic conditions through the regulation of MHC class I chain-related molecule A (MICA). Under hypoxic conditions MICA is inhibited via shedding action and it has been shown that ADAM 10 regulates this, as when ADAM 10 was down-regulated the decrease/inhibition of MICA was absent, thus allowing the ADAM 10 knockdown cells to be targeted by the innate immune response (Barsoum et al., 2011). This study strongly implicates ADAM 10 in the hypoxia-mediated tumourigenesis and highlights a link between HIF-1α and ADAM 10. Interestingly, both Webster et al. (2002) and Marshall et al. (2006) observed that in neuroblastoma, under hypoxic conditions (2.5% O_2) ADAM 10 expression was decreased, with both the pro-form and mature form being affected. The fact that there are only a few studies on ADAM 10's role in hypoxia mediated tumour progression and that they are conflicting of one another highlights the need for further research into ADAM 10 in hypoxia.

1.8.3 ADAM 10 Post-Translational Modifications (PTMs)

PTMs are known to mediate protein diversity and subsequently affect a variety of aspects of cellular functionality including protein structure and stability, signal transduction and cellular interactions (Wang et al., 2014, Duan and Walther, 2015). Previous research has revealed that ADAMs family members are modified by post-translational events such as glycosylation and phosphorylation (Maretzky et al., 2008, Gooz, 2010). One of the main PTMs affecting ADAMs family members is the removal of the pro-domain by pro-protein convertases (as discussed in **Section 1.7.2**). In the case

of ADAM 10, the pro-domain, has been shown to inhibit the proteolytic activity of the protein (Anders et al., 2001, Moss et al., 2007). Only upon removal of the pro-domain does the metalloproteinase domain becomes active, allowing for proteolytic activity, thus making pro-domain removal a crucial PTM of ADAM 10 (Anders et al., 2001, Moss et al., 2007). The removal of the ADAM 10 pro-domain is catalysed by either pro-protein convertase 7 (PC7) or furin, however it has been shown that in furin-negative cells prodomain cleavage is still seen, indicating that furin is not essential for pro-domain removal (Anders et al., 2001).

Further types of PTMs affecting the ADAMs family include glycosylation and phosphorylation (Izumi et al., 1998, Suzuki et al., 2000, Diaz-Rodriguez et al., 2002, Zhang et al., 2006, Escrevente et al., 2008, Yin and Yu, 2009, Gooz, 2010). Glycosylation is one of the most common post-translational modifications to affect proteins, and in the context of cancer biology, deregulated protein glycosylation is a key characteristic of the disease and thus understanding such processes is important (Zhang et al., 2014b, Pinho and Reis, 2015, Stowell et al., 2015). Glycosylation of proteins can greatly alter their structure, stability and conformation (Shirato et al., 2011, Roth et al., 2012, Tian and Zhang, 2013). Protein glycosylation in cancer is acknowledged as a key promoter of cancer progression through alterations in cellular growth, survival, metastatic phenotype and signalling (Freire-de-Lima, 2014, Zhang et al., 2014b, Pinho and Reis, 2015, Stowell et al., 2015). Phosphorylation of proteins is also known to be central to cancer biology and tumour progression (Reimand et al., 2013). As one of the most studied PTMs, phosphorylation is involved in nearly all cellular processes, including mediating cellular signalling and the activity of many proteins, with dysregulations widely reported in cancer (Cohen, 2002, Radivojac et al., 2008, Humphrey et al., 2015, Lim, 2005).

PTMs of ADAM 10 have been revealed in the form of *N*-linked glycosylation, with mutated models showing a role of *N*-glycosylation in protein folding and activation, maintenance of enzymatic activity and protection from protease degradation (Escrevente et al., 2008). It was shown that ADAM 10 possesses four *N*-linked glycosylation sites, three of which are located within the active, metalloproteinase domain and the final one within the disintegrin domain (Escrevente et al., 2008). The residues at which the *N*-linked glycosylation was identified are 267, 278, 439 and 551 respectively. The study determined that all four sites were occupied within mature ADAM 10, suggesting that glycosylation of the protein has occurred upon maturity. Furthermore, it was shown that mutation of residue 278 resulted in accumulation within the endoplasmic reticulum, indicating that it is retained in its precursor form and thereby implicating it in protein folding (Escrevente et al., 2008). Importantly, it was shown that *N*-linked glycosylation was required for ADAM 10 proteolytic activity, and that mutation of residue 439 increased the susceptibility of ADAM 10 protease action, which may allow for protease mediated degradation (Escrevente et al., 2008).

A further PTM that affects ADAM 10 is its ectodomain cleavage by other ADAMs members, primarily ADAM 9 and ADAM 15 (Parkin and Harris, 2009, Tousseyn et al., 2009). It was reported that ADAM 10 could be identified within the conditioned media from neuroblastoma cell lines, and that treatment with an ADAMs inhibitor prevents this presence (Parkin and Harris, 2009). Furthermore, ADAM 9 was identified as a mediator of ADAM 10 ectodomain cleavage, as increased presence of ADAM 10 in conditioned media was observed after ADAM 9 overexpression (Parkin and Harris, 2009). Similar findings were reported by Tousseyn et al. (2009) in murine fibroblasts, however, ADAM 15 was also identified as a mediator of ADAM 10 ectodomain cleavage. Notably, ADAM 10 was shown to retain its proteolytic activity after undergoing ectodomain cleavage (Tousseyn et al., 2009). Furthermore, it was also

shown that ADAM 10 undergoes a further PTM, through γ-secretase mediated cleavage of the intracellular domain (ICD) (Tousseyn et al., 2009). The released ICD of ADAM 10 was then observed to undergo nuclear translocation, which is believed to mediate gene activation (Tousseyn et al., 2009).

ADAM 17, the most closely related ADAMs member to ADAM 10, has been shown to possess six *N*-linked glycosylation sites, three within the metalloproteinase domain, two within the disintegrin domain then the final site is within the cysteine-rich domain. Furthermore, it has been shown that there are a further three *N*-glycosylation sites within the pro-domain region of the protein (Gooz, 2010). However, despite this knowledge, little is known about how this glycosylation impacts on ADAM 17 activity. ADAM 17 has also been shown to undergo phosphorylation by a variety of molecules including extracellular signal-related kinase (ERK), phosphoinositide-dependent kinase 1 (PDK1) and gastrin-releasing peptide (GRP) (Diaz-Rodriguez et al., 2002, Zhang et al., 2006, Yin and Yu, 2009).

1.8.3.1 Proteomic Methodologies in Analysis of PTMs

Mass Spectrometry techniques can be used to identify post-translational modifications, including those known to affect the ADAMs family, such as glycosylation and phosphorylation (Aebersold and Mann, 2003, Escrevente et al., 2008, Chen and Pramanik, 2009, Yates et al., 2009, Yin and Yu, 2009). Such methods include glycoproteomics to identify glycosylation and phosphoproteomics for the identification of phosphorylation (Aebersold and Mann, 2003, Anderegg et al., 2009, Chen et al., 2009, Yates et al., 2009). Several biochemical techniques are available for the characterisation of glycosylation including the use of glycosylation inhibitors such as tunacimycin or endoglycosidases such as PNGase F (Escrevente et al., 2008, Wojtowicz et al., 2012). Glycoprotein analysis can be undertaken in a number of ways including

staining, enzymatic protocols and affinity-based separation. Staining of glycoproteins can be undertaken after separation by SDS-PAGE, and are typically reliant upon the periodic acid-Schiff (PAS) and the production of a fluorescent signal (Roth et al., 2012). Affinity-based protocols are more specific in nature and see the use of immobilised lectins for glycan binding. Glycan specificity varies amongst lectins, and thus can be used to identify the type of glycosylation present (Tian and Zhang, 2013, Zhang et al., 2014b). For example Concanavalin A affinity purification is typically used for *N*-linked glycosylation binding (Roth et al., 2012, Tian and Zhang, 2013). Enzymatic-based glycan removal can also help with characterisation of glycosylation, as specific glycans are cleaved by different enzymes. PNGase F is glycosidase responsible for removal of *N*-linked glycans, and is more generic than Endo H for example, which is known to cleave high-mannose *N*-glycans (Escrevente et al., 2008). By exploiting the varying specificities of the enzymes the type of glycosylation on a protein can be identified. Additionally, inhibition of glycosylation can also lead to identification of glycan type. Tunicamycin, one example of a glycosylation inhibitor, blocks the biosynthesis of *N*-glycans, thus preventing their binding to proteins (de Freitas Junior et al., 2011, Wojtowicz et al., 2012). By inhibiting such processes knowledge can be gained regarding the type of glycans affecting proteins.

Glycoproteomic analysis can also be undertaken by MS methodologies and these are aimed at identifying the location of glycosylation on the protein, the structure and identification of the various glycans and finally the point to which they bind the protein. Quantifiable data regarding the extent of protein glycosylation can also be gathered (Sagi et al., 2005, Anderegg et al., 2009, Pasing et al., 2012, Zhang et al., 2014b).

1.9 ADAMs and Regulation of Signalling Pathways in Cancer

1.9.1 Cell Proliferation

Cellular proliferation is reported to be dysregulated in the vast majority of cancer types, and ADAMs family members have been implicated in regulatory roles of cellular proliferation in cancer (Edwards et al., 2008). Their upregulation in many cancer types has been reported to result in increased cellular proliferation. Indeed, ADAM 12 has been shown to be involved in cell proliferation in bladder, lung and breast cancer (Frohlich et al., 2006, Rocks et al., 2008a, Roy and Moses, 2012, Shao et al., 2014). In small cell lung cancer it was identified that cellular proliferation was reduced after ADAM 12 silencing, and conversely was enhanced upon ADAM 12 overexpression (Shao et al., 2014). Furthermore, ADAM 12 was shown to mediate bronchial epithelial cell proliferation, with ADAM 12 overexpressed cells displaying an increased proliferative phenotype (Rocks et al., 2008a). Similarly, overexpression of ADAM 12 in breast cancer cells was shown to promote proliferation (Roy and Moses, 2012).

ADAM 17 has been implicated in regulating cellular proliferation within breast, lung, liver, prostate and glioma (Lin et al., 2012, Zheng et al., 2012, McGowan et al., 2013, Liu et al., 2014, Lv et al., 2014). In prostate cancer overexpression of ADAM 17 was identified to increase PC-3 proliferation, as assessed by a variety of methods including CCK-8 assay and BrdU analysis (Lin et al., 2012). Notably, overexpression of ADAM 17 also mediated G1-S phase transition. Such findings were reversed in DU145 cells with ADAM 17 knockdown (Lin et al., 2012). In lung cancer it was shown that ADAM 17 silencing significantly reduced cellular proliferation *in vitro* and tumour growth was impaired *in vivo* (Lv et al., 2014). Similarly, in glioma, ADAM 17 overexpression was identified to promote cellular proliferation *in vitro*, whereas ADAM 17 silencing resulted in significant decrease. *In vivo* ADAM 17 overexpression increased tumour

growth and ADAM 17 silencing conversely reduced tumour volume (Zheng et al., 2012). Furthermore, McGowan et al. (2013) showed a significant correlation between inhibition of ADAM 17 and reduced cell proliferation in triple-negative breast cancer cell lines.

ADAM 10 has also been implicated in the regulation of cellular proliferation, albeit less research has been undertaken in this area. It has been shown that ADAM 10 is linked to cell proliferation in bladder, tongue and liver cancer (Yuan et al., 2013, Fu et al., 2014, Liu et al., 2015b, Shao et al., 2015). In hepatocellular carcinoma ADAM 10 silencing reduced the proliferation and clonogenic capacity of HepG2 cells (Yuan et al., 2013). Such results were corroborated by Liu et al. (2015b), who also demonstrated that ADAM 10 silencing reduced HepG2 proliferation *in vitro*. Additionally, *in vivo* ADAM 10 silencing corresponded to reduced tumour growth (Liu et al., 2015b). Similarly, ADAM 10 silencing also resulted in reduced cellular proliferation in both bladder cancer and tongue carcinoma (Fu et al., 2014, Shao et al., 2015).

1.9.2 EGFR Signalling Cascade

The EGFR signalling cascade is one of the most prominent linked to cancer development and is known to mediate the proliferation, migration, survival and differentiation of cancer cells (Gee and Knowlden, 2003, Blobel, 2005, Normanno et al., 2006, Seshacharyulu et al., 2012). EGFRs are part of the receptor tyrosine kinase (RTK) family, which encompasses the ErbB proteins, of which EGFR is one (ErbB-1; HER1). Other family members include ErbB-2 (HER2), ErbB-3 (HER3) and ErbB-4 (HER4). All EGFR/ErbB family member proteins are transmembrane bound with a ligand-binding extracellular region (Normanno et al., 2006, Seshacharyulu et al., 2012). ErbB receptors are activated by a number of ligands, including transforming growth factor alpha (TGF-α), epidermal growth factor (EGF), betacellulin (BTC), and heparin-binding

EGF-like growth factor (HB-EGF) (Borrell-Pages et al., 2003, Gee and Knowlden, 2003, Blobel, 2005, Kataoka, 2009, Maretzky et al., 2011). Upon activation by extracellular ligand binding, the receptors undergo dimerization which leads to phosphorylation within the cytoplasmic tail, subsequently, proteins containing Src homology 2 and phosphotyrosine binding (PTB) sites are recruited (Normanno et al., 2006, Seshacharyulu et al., 2012). Subsequently, intracellular signalling pathways are activated, including Ras-Raf-MEK-ERK and PI3K-AKT pathways. An illustrative diagram of EGFR signalling, including downstream pathways and molecules included can be seen in **Figure 1.8**.

The phosphoinositide 3-kinase (PI3K) pathway containing AKT is a major signalling pathway implicated in cancer progression, of which AKT is the main effector, and promotes cellular proliferation and survival (Engelman, 2009). As such, aberrant, increased expression of AKT is reported in numerous cancer types, including lung, breast, prostate, colorectal and ovarian cancer (Cheng et al., 1992, Page et al., 2000, Brognard et al., 2001, Roy et al., 2002, Setia et al., 2014, Liu et al., 2015c). Furthermore, altered expression of AKT has been linked to increased cellular proliferation and survival, as shown through modulation of AKT expression by targeted therapies. Downregulation or inhibition of AKT has been shown to reduce the proliferative capacity of cancer cells (Festuccia et al., 2008, Holland et al., 2015, Mu et al., 2015, Zheng et al., 2015). Notably, it has previously been shown that modulation of AKT expression can increase sensitivity of cancer cells to other therapeutics (Shin et al., 2010, Puglisi et al., 2014, Mehta et al., 2015).

The Ras-Raf-MEK-ERK signalling pathway is also activated by ligand binding to ErbB receptors, and consists of a number of signalling molecules including rapidly accelerated fibrosarcoma (Raf), mitogen-activated protein kinase kinase (MEK) and

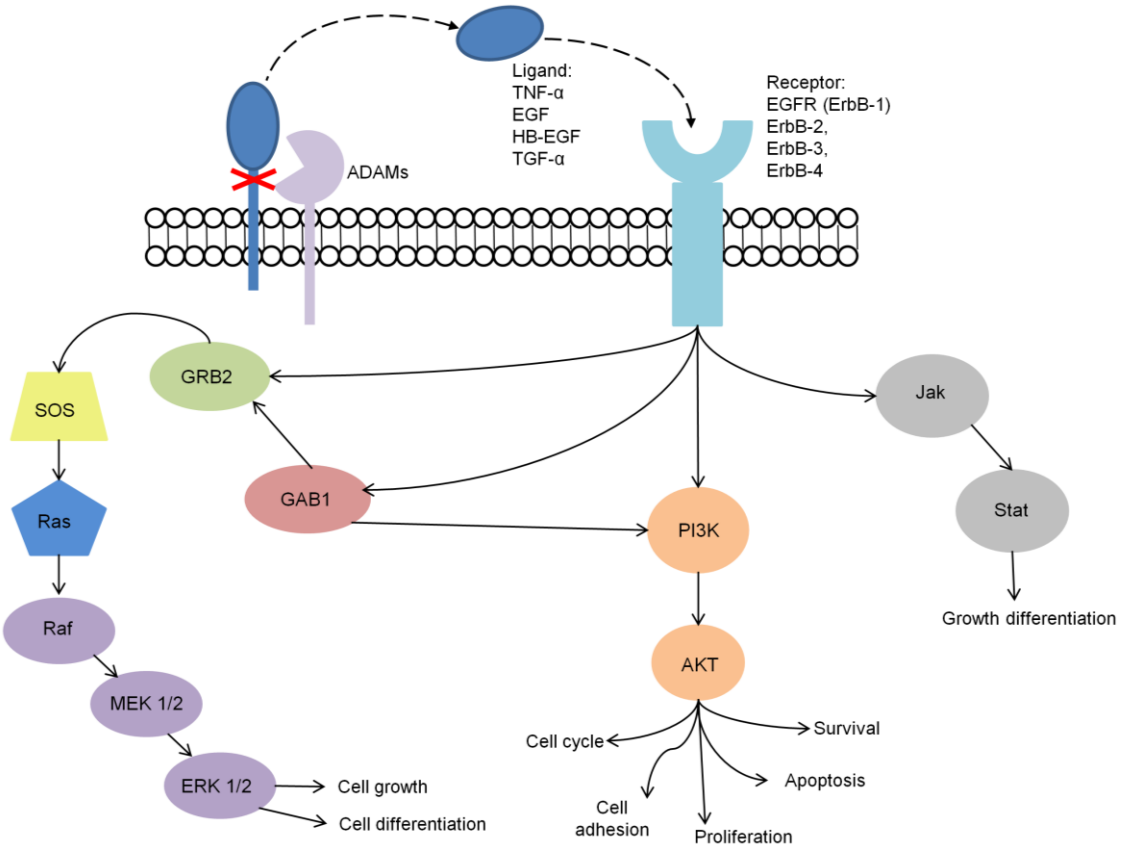

Figure 1.8: EGFR Signalling Cascade

The EGFR signalling cascade is extremely complex in nature and encompasses numerous downstream signalling pathways including Ras-Raf-MEK-ERK and PI3K-AKT. Activation of the EGFR cascade is through binding of ligands to ErbB receptors, which in turn activates a number of downstream pathways which promote cellular proliferation, survival and differentiation. A number of the ligands known to activate EGFR signalling are shed from the cell surface by members of the ADAMs family, including ADAM 10 and ADAM 17. Dysregulation of EGFR signalling is widely reported in a number of cancer types, and thus has become a key target for research and therapeutic development.

extracellular signal-regulated kinase (ERK) (McCubrey et al., 2007, Roberts and Der, 2007). Ras is one the of the main downstream effectors of the EGFR signalling pathway, and one member of the Ras family, KRAS, is known to be mutated within CRC, resulting in dysregulated cellular proliferation (Roberts and Der, 2007, Phipps et al., 2013). Raf is the substrate to Ras and once it is activated it phosphorylates MEK, which subsequently phosphorylates and activates ERK (Fang and Richardson, 2005). Activation of ERK results in the downstream targeting of transcription factors involved in cellular proliferation (Fang and Richardson, 2005). Upregulated expression of downstream target ERK 1/2 is reported in cancer, and research has shown that downregulation of ERK, typically through MEK inhibition, leads to a reduction in cellular proliferation (Wiesenauer et al., 2004, Lefloch et al., 2008, Joseph et al., 2010, Doldo et al., 2015, Shao et al., 2015, Kress et al., 2010).

Research has implicated ADAMs family members in the EGFR signalling cascade, as they are known sheddases of various EGFR ligands including: TNF-α (Tumour Necrosis Factor- α), TGF-α (Transforming Growth Factor- α), EGF (Epidermal Growth Factor), HB-EGF (Heparin Binding EGF-like Growth Factor) and TNF-R1 (Tumour Necrosis Factor Receptor 1) (Borrell-Pages et al., 2003, Gee and Knowlden, 2003, Sahin et al., 2004, Blobel, 2005, Kataoka, 2009, Maretzky et al., 2011). The shedding of such ligands releases them from the membrane, where they activate the ErbB receptors and trigger the signalling cascade. Previous research has strongly implicated ADAM 17 activity in the activation of EGFR signalling. Studies have demonstrated that ADAM 17 is responsible for the cleavage of TNF-α, with knockdown of the gene resulting in reduced TNF-α mature form present within cells (Black et al., 1997, Moss et al., 1997). Furthermore, overexpression of ADAM 17 showed an increased in TNF-α processing (Moss et al., 1997). ADAM 17 has also been shown to be involved in the processing of TGF-α, HB-EGF, betacellulin, epiregulin and amphiregulin (Peschon et al., 1998,

Sunnarborg et al., 2002, Borrell-Pages et al., 2003, Sahin et al., 2004, Maretzky et al., 2011) ADAM 17-deficient keratinocytes displayed reduced soluble TGF-α in comparison to wild-type counterparts. Similar results were identified in ADAM 17 deficient fibroblasts, with less TGF-α processing seen compared to wild-type comparatives (Peschon et al., 1998). Furthermore, overexpression of ADAM 17 results in increased TGF-α, amphiregulin and HB-EGF cleavage, however ADAM 17 showed a greater affinity for TGF-α cleavage compared to other molecules (Sunnarborg et al., 2002). Notably, it has been shown that inhibition of ADAM 17 processing results in the membrane bound TGF-α interacting with, but not activating, EGFR receptors (Borrell-Pages et al., 2003). ADAM 10 has been lesser studied within the context of EGFR ligand cleavage, however it has been shown that ADAM 10 is involved in the cleavage of TNF-α, EGF and betacellulin (Lunn et al., 1997, Sahin et al., 2004, Sanderson et al., 2005, Mężyk-Kopeć et al., 2009, Armanious et al., 2011, Maretzky et al., 2015). Notably, it was identified that in murine embryonic fibroblasts ADAM 10 was not responsible for the cleavage of HB-EGF, amphiregulin or epiregulin (Sahin et al., 2004). The role of ADAM 10 in TNF-α cleavage was confirmed by the observation that TNF-α cleavage was significantly reduced in ADAM 10 silenced fibroblasts and Jeko-1 cells (Lunn et al., 1997, Mężyk-Kopeć et al., 2009, Armanious et al., 2011). Similarly, it was shown that overexpression of ADAM 10 resulted in increased betacellulin cleavage, whereas when inactivated ADAM 10 was overexpressed there was a decrease (Sanderson et al., 2005).

Based on evidence that knockdown or inhibition of ADAMs family member's results in decreased cellular proliferation and induction of cell cycle arrest, it is feasible that this is a result of decreased EGFR ligand shedding. For example, upon ADAM 17 silencing levels of phosphorylated AKT and ERK were downregulated in glioblastoma cells, and resulted in decreased migration and invasion capabilities (Chen et al., 2013). Similarly,

in inducible ADAM 10 knockout cells, ADAM 17 was shown to mediate the levels of phosphorylated ERK, which were reduced upon ADAM 10 knockdown, with the proliferative capacity of the cells also impaired (Maretzky et al., 2011). It was reported that ADAM 17 mediated proliferation and cellular viability in breast cancer and upon ADAM 17 silencing these were reduced, along with TGF-α cleavage and phosphor-EGFR and phosphor-AKT levels (Zheng et al., 2009). ADAM 10 has also been implicated in the control of cancer progression through activation of the EGFR pathway. In hepatocellular carcinoma it was shown that silencing of ADAM 10 resulted in reduced cellular proliferation, migration and invasion *in vitro* and *in vivo* it was shown that tumour growth was significantly impaired (Liu et al., 2015b). Furthermore, phosphorylation of both PI3K and AKT was reduced upon ADAM 10 silencing (Liu et al., 2015b). In addition, a correlation was identified between ADAM 10 and EGFR expression. In ADAM 10 silenced cells EGFR expression was found to be reduced, as was the proliferation, migration and invasion potential of tongue cancer cells (Shao et al., 2015). Conversely, in non-small cell lung cancer cells it was shown that whilst ADAM 10 knockdown did affect cellular migration and invasion, no effects were seen on the levels of phosphorylated ERK 1/2 (Guo et al., 2012).

Hypoxia is known to influence the expression of ADAMs members and upregulation of downstream EGFR effectors have also been reported. As previously described in **Section 1.8.1** it has been shown that ADAM 10 mediates proliferation and migration, and as a known sheddase of EGFR ligands it's feasible that such actions may be through EGFR signalling activation. ADAM 17 on the other hand, has been somewhat characterised within the remit of hypoxia. For example, in glioma it was found that ADAM 17 was responsible for the hypoxia-mediated increase in invasiveness, and that it played a role in the phosphorylation of EGFR and AKT (Zheng et al., 2007). Both ADAM 17 and the invasiveness of U87 cells were upregulated under hypoxic

conditions, and the invasive potential of cells was reduced upon ADAM 10 silencing. Furthermore, hypoxia mediated an increase in the expression of EGFR and AKT phosphorylation, however these increases were reduced after ADAM 17 knockdown (Zheng et al., 2007). Notably, it has also been shown that EGFR targeted therapies result in a reduction of hypoxic related genes and proteins, along with reduced hypoxic CRC tumour volume post treatment (Greening et al., 2015). Furthermore, EGFR antagonist treatment can reduce the hypoxia-mediated angiogenesis response within tumours (Lee and Wu, 2015, Wang et al., 2015b, Wang et al., 2015c).

1.9.3 Notch Signalling Pathway

Notch signalling is strongly implicated in promoting cancer progression and various associated characteristics, including proliferation, differentiation, migration and invasion. Dysregulated Notch signalling has been identified in a number of cancer types, including colorectal; breast; lung and prostate cancer (Shou et al., 2001, Bolos et al., 2013, Dai et al., 2014, Hassan et al., 2014, Yuan et al., 2015c). There are five Notch ligands: delta-like ligand 1, 3 and 4 (DLL-1; DLL-3, DLL-4) and Jagged-1 and 2 (JAG1, JAG2), which are responsible for the activation of Notch receptors, and subsequently Notch signalling (Sethi and Kang, 2011, Yuan et al., 2015b). There are four Notch receptors available for ligand binding, Notch 1-4, and such binding occurs on the cell membrane. Notch receptors are single-pass, transmembrane proteins and are primarily conserved within the ER and Golgi apparatus, as a pre-cursor form (Vinson et al., 2015). Here, it undergoes fucosylation by *O-fucosyltransferase* in the ER before being glycosylated within the Golgi and cleaved by Furin to produce a heterodimer. The receptor is then transported to and assembled on the cell surface membrane, upon which it is available for ligand binding (Vinson et al., 2015). Ligand-receptor interaction occurs, upon which the ligand begins to be retracted via endocytosis back into the signalling cell. This reveals a hidden cleavage site on the Notch receptor which is then

cleaved by ADAMs family members, primarily ADAM 10 or ADAM 17, resulting in the release of the extracellular part of Notch (Sethi and Kang, 2011, Vinson et al., 2015, Yuan et al., 2015b). Subsequently, the remainder of the Notch receptor undergoes a further cleavage by γ-secretase, at the point at which the intracellular region meets the cell membrane. The Notch intracellular domain (NICD) is then released and translocates to the nucleus, upon which it binds to the transcription factor CBF-1/Suppressor of hairless/LAG1 (CSL) (Vinson et al., 2015). CSL becomes active upon binding and thus acts as a transcriptional activator of Notch target genes, including members of the Hes (Hairy/Enhancer of Split) and Hey (Hairy/Enhancer of Split related with YRPW motif) families, Cyclin D1, c-MYC, p21 and Slug (Yuan et al., 2015b). Notch target genes have been implicated in a range of characteristics of cancer progression, including the regulation of cellular proliferation and EMT. An illustrative diagram encompassing the various stages of Notch signalling can be seen in **Figure 1.9**. Impairment of Notch signalling has been shown to result in reduced migration, invasion and cellular proliferation in various cancer types including colorectal, lung and breast (Sikandar et al., 2010, Bolos et al., 2013, Suman et al., 2013, Dai et al., 2014). In breast cancer it was shown that downregulation of Notch signalling impaired both cellular viability and EMT characteristics such as migration and invasion (Bolos et al., 2013, Suman et al., 2013). In colorectal cancer it was shown that knockdown of Notch ligand, JAG1, resulted in decreased cellular proliferation and induced cell cycle arrest. Furthermore, Notch target genes were also downregulated, including Cyclin D1 and c-MYC and cells displayed reduced migration and invasion capacities (Dai et al., 2014). Additionally, such results translated *in vivo*, where it was shown that xenograft proliferation was impaired and cells were less metastatic (Dai et al., 2014). Conflictingly, in small cell lung cancer it has been shown that Notch1 silencing resulted in increased EMT characteristics such as cellular adhesion and invasion (Hassan et al., 2014).

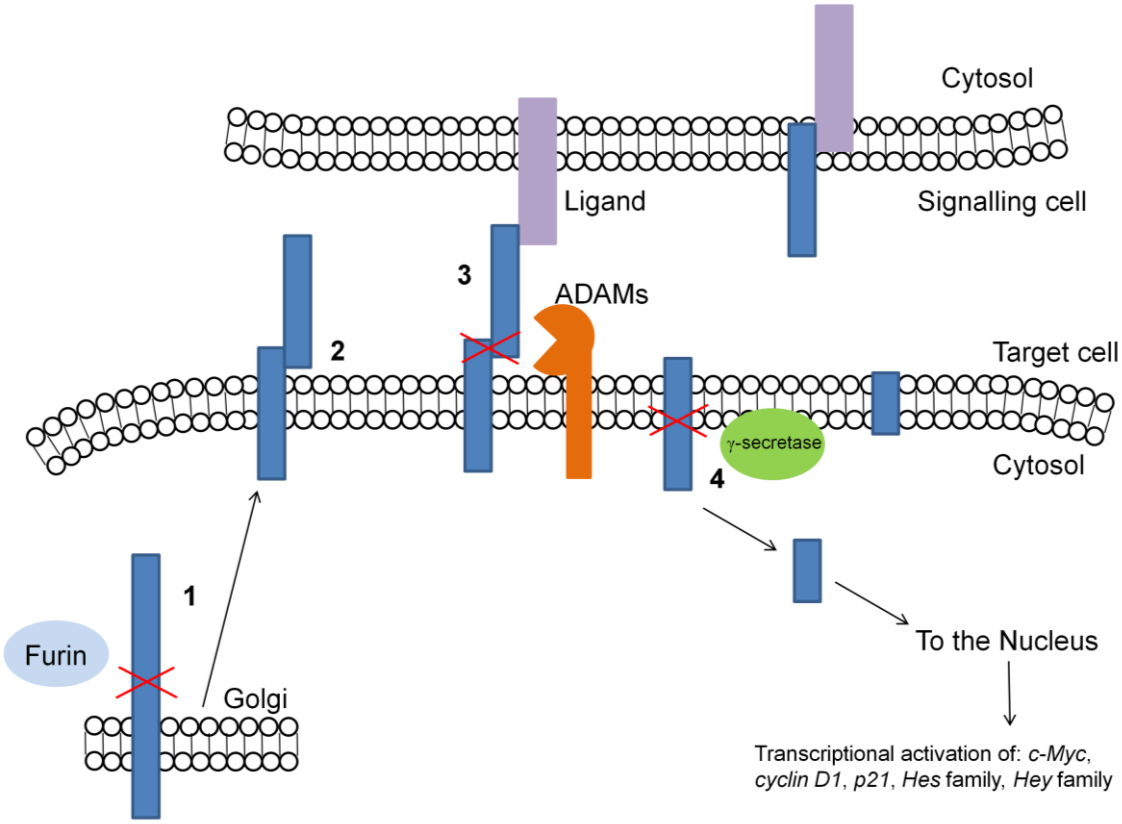

Figure 1.9: Notch Signalling Pathway

Schematic diagram illustrating the Notch signalling pathway, and the role of ADAMs in mediating Notch cleavage. Primary cleavage of Notch takes place in the Golgi apparatus by Furin (1) before Notch is expressed on the cell surface as a heterodimer (2). Notch then binds to a ligand, including delta-like ligand or Jagged, on a neighbouring cell. Upon binding the ligand begins to be retracted into the cell via endocytosis, thus revealing a cleavage site on the Notch receptor. ADAMs family members then cleave Notch and release the extracellular domain (3). A further cleavage of Notch is then mediated by γ-secretase which released the intracellular part (4). This then translocates to the nucleus where it is involved in the transcriptional activation of genes known to promote cellular proliferation and EMT.

ADAMs family members are heavily involved in the regulation of Notch signalling, due to their role in mediating the cleavage of Notch receptors after activation. ADAM 10 and ADAM 17 in particular are known to mediate this cleavage (Hartmann et al., 2002, Bozkulak and Weinmaster, 2009, van Tetering et al., 2009, Guo et al., 2013).

Previous research has shown that ADAM 10 is crucial for successful Notch signalling, with one study showing that without ADAM 10 expression murine embryonic development was impaired, with no viable embryos past day 9 (Hartmann et al., 2002). Furthermore, embryonic development was significantly impaired, with many growth defects present. Notably, expression of *Notch1* remained unchanged in ADAM 10 deficient embryos, however aberration of other genes was reported (Hartmann et al., 2002). Additionally, it was shown by van Tetering et al. (2009) that Notch signalling was not impaired by knockout of ADAM 17, nor other members of the ADAMs family, including ADAM 9, 12 and 15. Importantly, it was shown that ADAM 10 knockdown inhibited Notch cleavage and subsequent signalling (van Tetering et al., 2009). Follow up research to this indicated that the use of ADAM 10 or ADAM 17 in Notch signalling is selective dependent upon activation circumstances (Bozkulak and Weinmaster, 2009). It was shown that ADAM 10, and not ADAM 17, is required for cleavage of Notch1 activated by ligand binding, however it was also shown that ADAM 17 participated in ligand-independent Notch signalling (Bozkulak and Weinmaster, 2009). Furthermore, ADAM 10 has been shown to be a sheddase for DLL1, a known Notch ligand (Six et al., 2003). Further evidence for the role of ADAM 10 in Notch signalling is seen after the modulation of ADAM 10 expression, in various cell types. In non-small cell lung cancer is was found that *in vivo* ADAM 10 expression positively correlated with that of Notch1, and that higher expression levels were exhibited in metastatic tissue (Guo et al., 2012). Furthermore, it was identified that ADAM 10 knockdown impaired the cleavage of NICD of Notch1 and that subsequently a reduced migratory and invasive phenotype

in vitro was exhibited (Guo et al., 2012). Additionally, ADAM 10 knockout mouse brains displayed significantly decreased expression of Notch target genes, including *Hes1*, *Hes5*, *Hey1* and *Hey2* (Jorissen et al., 2010, Zhuang et al., 2015).

It has also been shown that there is a link between tumour hypoxia and the activation of Notch signalling (Chen et al., 2007, Ishida et al., 2013, Yu et al., 2013, Villa et al., 2014). In lung cancer it was identified that Notch1 and its downstream target genes, *Hes1*, *Hey1* and *Hey2*, were significantly upregulated after exposure to hypoxia (1% O_2). Similarly in oral carcinoma, Notch receptor and ligand expression, along with Notch target genes, were significantly upregulated after exposure to hypoxia (1% O_2). Additionally, it was also shown that hypoxic exposure induced EMT, with reduced E-Cadherin expression and increased cellular migration and invasion (Ishida et al., 2013). In the case of hepatocellular carcinoma it was also shown that hypoxic exposure resulted in an increased migratory and invasive phenotype. Furthermore, the expression of Notch1 and Hes1 were upregulated, at both protein and transcript level, after hypoxic exposure (Yu et al., 2013). Notch1 knockdown cells displayed a less aggressive phenotype, with reduced cellular migration and invasion (Yu et al., 2013).

1.9.4 Epithelial-Mesenchymal Transition

EMT is a complex biological process that cells undergo, encompassing a variety of molecules, which results in a switch from an epithelial state to a mesenchymal phenotype (Kalluri and Weinberg, 2009). Such phenotypical changes are identified as being instrumental in enhancing the invasiveness and migratory potential of cancer cells, which subsequently promotes metastasis (Kalluri and Weinberg, 2009, Yilmaz and Christofori, 2009, Hanahan and Weinberg, 2011, Cao et al., 2015). Typically cells possess an epithelial phenotype with close cell-cell contact and apical-basal polarity, which allows for cell-cell communication, and expression of epithelial proteins such as

E-Cadherin . Upon activation of EMT one of the primary alterations is the loss of cellular adhesion and cell-cell junctions (Medici et al., 2006b, Medici et al., 2008, Yilmaz and Christofori, 2009, Huang et al., 2012). These are deconstructed and proteins, such as E-Cadherin, occludin and claudin, are degraded (Kalluri and Weinberg, 2009, Lamouille et al., 2014). Transcriptional downregulation of E-Cadherin is regulated by increased expression of transcription factors such as Slug, Snail and zinc finger E-box binding homeobox (ZEB) 1 and 2 (Spaderna et al., 2008, Zhang et al., 2015b). The loss of E-Cadherin is crucial to the development of EMT, and downregulated expression is found across a variety of cancer types including prostate (Umbas et al., 1992, Rubin et al., 2001); gastric (Joo et al., 2002, Almeida et al., 2010); breast (Kowalski et al., 2003, Shargh et al., 2014); colorectal (Dorudi et al., 1993, Kroepil et al., 2013) and liver cancer (Wei et al., 2002, Chen et al., 2014). As a result of E-Cadherin degradation β-Catenin can no longer interact and therefore is typically stabilised (via Wnt signalling, as discussed in **Section 1.9.5**). After loss of cell-cell contact, apical-basal polarity is lost, under normal circumstances cells maintain such polarity through contact through their basal surface with the basement membrane. During EMT this contact is lost through the repression of polarity associated proteins and the loss of E-Cadherin mediated adhesion (Lamouille et al., 2014). Cytoskeletal alterations are also seen, which promote the motility of the changing cells, including the formation of actin-rich lamelilipodia and filopodia. Such extensions facilitate basement membrane degradation and subsequent metastasis (Yilmaz and Christofori, 2009, Lamouille et al., 2014). Alongside the loss of epithelial markers, such as E-Cadherin, EMT sees the gain of mesenchymal markers such as N-Cadherin, Vimentin, Slug, Snail and β-Catenin (Medici et al., 2008, Kalluri and Weinberg, 2009, Lamouille et al., 2014, Zhang et al., 2015b). A representative diagram illustrating the phenotypical changes of EMT can be seen in **Figure 1.10**. A vast range of signalling pathways are known to

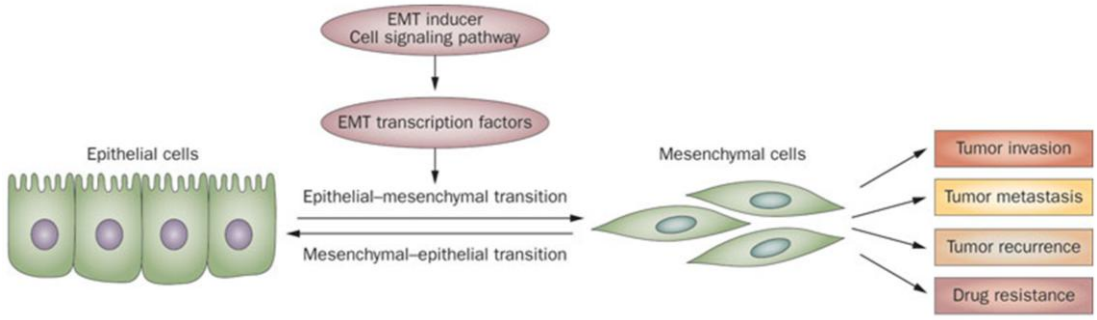

Figure 1.10: Epithelial-Mesenchymal Transition

EMT sees the switch of cells from a epithelial phenotype to a mesenchymal one. In a normal epithelial state cells are tightly adhered and possess an organised arrangement. As such they are relatively non-motile and stable. However, induction of EMT sees the loss of E-Cadherin, along with other epithelial markers, which is progressive and correlates to the gain of mesenchymal markers such as N-Cadherin and Vimentin. The loss of cell-cell contact and polarity, along with formation of cytoskeleton projections allows a more migratory phenotype to be gained, and as such cells are more aggressive and invasive in nature. Image adapted from Wang et al. (2011b).

activate EMT and its downstream effectors, including EGFR, Wnt and Notch signalling cascades (Yilmaz and Christofori, 2009). ADAMs family members have previously been implicated in promoting EMT within cancer, with numerous studies showing downregulation of ADAM 10 led to a less invasive phenotype. In the case of tongue carcinoma it was shown that ADAM 10 silencing resulted in reduced migration and invasion of cells. Furthermore, it was identified that E-Cadherin levels increased post-ADAM 10 silencing, thus implicating ADAM 10 in mediating the suppression of E-Cadherin (Shao et al., 2015). ADAM 10 has previously been shown to mediate the cleavage of E-Cadherin in keratinocytes, which influenced the migratory capacity of the cells. ADAM 10 overexpression saw increased cellular migration, and ADAM 10 inhibition saw increased cellular adhesion and E-Cadherin expression (Maretzky et al., 2005). Additionally, it was shown in non-small cell lung cancer that ADAM 10 activated the Notch1 signalling pathway, which mediated a more migratory and invasive phenotype (Guo et al., 2012). Furthermore, silencing of ADAM 10, both *in vitro* and *in vivo*, reduced cellular migration and invasion (Liu et al., 2015b). Similar effects of ADAM 10 silencing on migration in nasopharyngeal carcinoma have also been reported *in vitro* (You et al., 2015).

Tumour hypoxia has also been attributed to promotion of EMT, with research indicating that hypoxic exposure exerts an invasive phenotype on cells (Higgins et al., 2007, Cannito et al., 2008, Zhang et al., 2013b, Gammon and Mackenzie, 2015, Zhang et al., 2015b). In hepatocellular carcinoma hypoxia was found to induce EMT, through modulation of EMT-related genes, including E-Cadherin, N-Cadherin and Vimentin (Zhang et al., 2013b). Morphological alterations supporting a more mesenchymal phenotype were also identified after hypoxic exposure, along with an increase in cellular migration and invasion (Zhang et al., 2013b). Furthermore, in CRC overexpression of HIF-1α resulted in a downregulation of E-Cadherin, alongside an

upregulation of N-Cadherin and Vimentin. Additionally, it was found that there was an increase in cellular migration which *in vivo* translated to an increase in metastasis (Zhang et al., 2015b). Similar results have also been observed in breast cancer, with hypoxic exposure resulting in increased cellular migration and invasion (Chen et al., 2010). E-Cadherin expression was also reduced, along with upregulation of mesenchymal markers such as Slug and Snail. In this study it was identified that hypoxia mediated EMT through Notch signalling (Chen et al., 2010).

1.9.5 Wnt/β-Catenin Pathway

The Wnt/β-Catenin pathway is primarily responsible for mediating signalling involved in embryonic cellular development, including axis development and stem cell development and proliferation (MacDonald et al., 2009, Niehrs, 2012). Wnts are a group of cysteine-rich proteins that are ligands for a variety of receptors and subsequently activate downstream signalling. Such receptors include Frizzled, protein tyrosine kinase 7 (PTK7) and low-density lipoprotein receptor-related protein (LRP), amongst others (Niehrs, 2012). Upon receptor activation two pathways are activated and are classified as either β-Catenin-dependent or β-Catenin-independent. The combination between Wnt ligand and receptor denotes which pathway is activated (MacDonald et al., 2009, Niehrs, 2012). Under non-stimulatory circumstances, glycogen synthase kinase 3 (GSK3) phosphorylates β-Catenin and subsequently targets it for degradation, through interaction with a complex consisting of APC, Axin and casein kinase 1α (CK1α) (Niehrs, 2012). However, upon activation by Wnt binding, β-Catenin becomes stabilised and translocates to the nucleus where it binds to transcription factors such as T-cell factor (TCF) and lymphoid enhancer factor (Lef), that mediate the transcription of genes involved in cellular differentiation and proliferation (Mazumdar et al., 2010, Niehrs, 2012, Varela-Nallar et al., 2014). β-Catenin-independent signalling encompasses a number of pathways that do not use β-Catenin, and are involved in cell

polarity, neurodegeneration and inflammation. Wnt/β-Catenin signalling is reported to be aberrant in a number of cancer types, including but not limited to, breast, liver, gastric and ovarian, and is often associated with a more invasive phenotype (Tien et al., 2005, Nunez et al., 2011, Cai and Zhu, 2012, Yoshioka et al., 2012, Bodnar et al., 2014, Gedaly et al., 2014, Jang et al., 2015a, Jang et al., 2015b, Xu et al., 2015). Dysregulation of the Wnt/β-Catenin pathway is prevalent within sporadic colorectal cancer. A number of epigenetic mutations present within CRC have been linked to aberrant Wnt/β-Catenin signalling including *KRAS* and APC (Herbst et al., 2014, Lemieux et al., 2015). The tumour suppressor APC is part of the β-Catenin degradation complex within Wnt signalling and this gene has been shown to be downregulated within CRC, particularly in the case of FAP patients. The mutation of APC allows for β-Catenin to become stabilised and thus activate downstream signalling (Herbst et al., 2014, Lemieux et al., 2015). Furthermore, it has been shown that *KRAS* signalling activation within CRC subsequently activates Wnt/β-Catenin signalling and promotes EMT. Upon KRAS or MEK activation through mutation EMT was induced in CRC cells, with typical E-Cadherin downregulation present (Lemieux et al., 2015). Additionally, it was found that oncogenic *KRAS* signalling triggered β-Catenin activation through low density lipoprotein receptor-related protein 6 (LRP6), and that downstream transcriptional activity of β-Catenin was dependent upon MEK signalling (Lemieux et al., 2015). Due to the complex nature of Wnt/β-Catenin signalling, it is one of the most difficult pathways to inhibit, thus making it hard to therapeutically target (Gedaly et al., 2014).

One of the main links of β-Catenin expression in cancer is to regulation of EMT, which, as discussed in **Section 1.9.4**, drives metastasis through cellular migration and invasion. (Valenta et al., 2012). Wnt/β-Catenin signalling is known to activate a number of targets genes that mediate E-Cadherin expression. Such targets include Twist, Slug and Snail,

which are strongly attributed to driving EMT. Little research has been undertaken into the role of ADAMs family members mediating Wnt/β-Catenin signalling, however it is known that members, including ADAM 10, can mediate the cleavage of E-Cadherin (Maretzky et al., 2005, Maretzky et al., 2008). It was shown that ADAM 10 was responsible for the cleavage of E-Cadherin, which promoted cellular migration and invasion and activation of the β-Catenin target gene Cyclin D1 (Maretzky et al., 2005). Notably, ADAM 10 has previously been identified as a target gene of β-Catenin, along with oncogenes Cyclin D1 and c-MYC (Herbst et al., 2014). Hypoxia has been linked to Wnt/β-Catenin signalling, with research showing that HIF-1α modulates Wnt/β-Catenin signalling (Mazumdar et al., 2010, Zhang et al., 2013c, Varela-Nallar et al., 2014, Liu et al., 2015a). Reports of effect of hypoxia on Wnt/β-Catenin signalling are somewhat conflicting, with research showing that hypoxia can inhibit the signalling pathway through competitive binding with HIF-1α (Lim et al., 2008). It was shown that HIF-1α binds to ADP-ribosylation factor domain protein 1 (ARD1) which prevents the acetylation based activation of β-Catenin, and furthermore, HIF-1α was shown to bind to TCF, which prevented downstream transcriptional activation of target genes (Kaidi et al., 2007, Lim et al., 2008). Conflictingly, hypoxia has been shown to regulate stem cell growth and EMT through Wnt/β-Catenin signalling (Mazumdar et al., 2010, Zhang et al., 2013c, Varela-Nallar et al., 2014, Liu et al., 2015a). In the context of EMT and invasive potential, a correlation between HIF-1α and β-Catenin expression was identified in hepatocellular carcinoma cells. Notably, a decrease in Wnt signalling activity was identified after hypoxic exposure, however, β-Catenin expression remained unchanged, and after prolonged exposure upregulated (Zhang et al., 2013c). Furthermore, it was found the HIF-1α directly interacts with β-Catenin, and that cells with β-Catenin knockdown display a less invasive and EMT-typical phenotype (Zhang et al., 2013c, Liu et al., 2015a).

1.10 ADAMs as Therapeutic Targets in Cancer

The evidence showing involvement of ADAMs family members in cancer progression is strong and therefore focus has turned to targeting them for therapeutic purposes. ADAMs members, including ADAM 10 and ADAM 17 have been shown to mediate the shedding of ligands which activate various cancer associated signalling pathways and promote a tumourigenic phenotype, as discussed above (Edwards et al., 2008, Murphy, 2008, Duffy et al., 2011). Furthermore, hypoxia has been shown to upregulate the expression of ADAMs members in cancer. As such, a number of ADAMs inhibitors have been developed for therapeutic use, albeit with limited success thus far (Duffy et al., 2011). The main mechanism of action of anti-ADAMs therapies is to inhibit proteolytic activity, thus preventing activation of downstream signalling pathways (Duffy et al., 2011). Two of the most investigated ADAM 10 and ADAM 17 inhibitors are INCB3619 and INCB7839, which have shown success *in vitro* (Zhou et al., 2006, Fridman et al., 2007, Witters et al., 2008). It was observed that treatment with INCB3619 prevented ADAM 10 and ADAM 17 mediated cleavage of numerous ErbB ligands, including Heregulin, TGF-α, HB-EGF and EGF, in non-small cell lung cancer (Zhou et al., 2006). Results showed that INCB3619 induced apoptosis, impaired EGFR signalling, and in xenograft models, tumour growth was significantly impaired (Zhou et al., 2006). Importantly, INCB3619 was observed to increase sensitivity to EGFR tyrosine kinase inhibitor gefitinib (Zhou et al., 2006). Similar results were also reported by Fridman et al. (2007), and xenograft models, of head and neck cancer, were shown to have impaired tumour growth. Furthermore, combination of either INCB3619 or INCB7839 with a lapatinib-like EGFR inhibitor impaired breast cancer cell or xenograft growth, respectively (Witters et al., 2008). Early clinical trials of INCB7389 indicate that it is fairly well tolerated, with a 50% response rate in HER2-positive breast cancer when used in conjunction with trastuzumab (Duffy et al., 2011). More recently, a

monoclonal antibody targeting the ADAM 17 cysteine rich domain has been shown to reduce cellular proliferation and migration/invasion of triple-negative breast cancer cells (Caiazza et al., 2015). ADAM 10 specific inhibitor, GI254023X, has shown positive anti-migratory effects in keratinocytes and both ovarian and breast cancer (Maretzky et al., 2005, Gooden et al., 2014, Mullooly et al., 2015). Research has shown that ADAM 10 ectodomain can be shed by ADAM 9 and ADAM 15, however further research is required to determine the relevance of this in terms of the retention of proteolytic activity after ectodomain shedding, as current research is somewhat conflicting (Parkin and Harris, 2009, Tousseyn et al., 2009). If ADAM 10 proteolytic activity is retained after ectodomain shedding then this may enhance substrate cleavage and subsequent activation of cancer associated signalling pathways. If the implications of ADAM 10 ectodomain shedding are determined to be physiologically relevant in ADAM 10 mediated cancer progression, then it is feasible that through multi-approach inhibition of ADAM 10 and ADAM 9/ADAM 15 the role of ADAM 10 in cancer progression could be limited.

1.11 ADAMs in Gastrointestinal and CRC Signalling

In terms of gastrointestinal biology, ADAM 10 and ADAM 17 are the two most studied members of the ADAMs family, as a number of ADAMs mediated pathways are involved in homeostasis of the intestinal environment (Jones et al., 2016). Notch and Wnt signalling pathways are heavily involved in intestinal homeostasis, particularly in cellular proliferation and differentiation during intestine development (Jones et al., 2016). Both ADAM 10 and 17 have been implicated in Notch and Wnt signalling, as described above (**Section 1.9.3** and **Section 1.9.5**, respectively). Intestinal stem cells heavily utilise Notch signalling for regulation of function, proliferation and differentiation (Zeki et al., 2011, Carulli et al., 2015). ADAM 10 is expressed in all cells

within the intestinal tract and research has shown that it is profusely expressed on the basolateral surfaces of intestinal epithelial cells (Jones et al., 2016). The crucial role of ADAM 10 in mediating Notch signalling is essential for intestinal development, with research reporting that knockout of ADAM 10 is embryonic lethal, at day 9.5, which corresponds with mouse gut formation (Hartmann et al., 2002, Tsai et al., 2014, Jones et al., 2016). Phenotypically, ADAM 10 knockout mice embryos displayed a number of defects which are associated with lack of Notch signalling. Embryos were observably smaller in size, with the caudal body region being particularly underdeveloped (Hartmann et al., 2002). Cardiac development was also severely impaired, with underdevelopment prevalent throughout ADAM 10 deficient mice. Wild-type counterparts displayed folded heart phenotypes, with individual compartments visible, whereas ADAM 10 knockout mice presented linearly arranged cardiac compartments within an extremely enlarged pericardial sac (Hartmann et al., 2002). Importantly, at day 9.5 embryos were still viable in terms of detectable heartbeats, however, past this stage no viable ADAM 10 deficient embryos were detects. Irregularities within the neural tube were also identifiable within ADAM 10 knockout embryos (Hartmann et al., 2002). Severe disruption to somitogenesis, a process heavily regulated by Notch signalling, was also evident throughout, with irregularities in lineation and size of somites (Hartmann et al., 2002).

An alternative loss of function ADAM 10 mouse model demonstrated that no ADAM 10-deficient mice survived beyond 1 day post-natal. Using tamoxifen inducible ADAM 10-deficiency the loss of ADAM 10 in adult mouse intestines was examined, which showed morbidity within 7-9 days post tamoxifen treatment (Tsai et al., 2014). Histological analysis of both newborn and adult intestines showed increased goblet cell numbers and reduced cellular burden within the epithelium as a result of decreased cellular viability. Increases in differentiation of secretory cells was also evident

throughout both immature and adult mouse intestines, indicating a role for ADAM 10 in regulating cell fate (Tsai et al., 2014). In this model, ADAM 10-deficiency resulted in a reduction in the Notch target gene *Hes1*, whilst neither Notch receptors nor ligands were affected (Tsai et al., 2014). Notch signalling has previously been implicated in CRC progression, with previous research showing Notch signalling was crucial for the evasion of apoptosis in colon cancer-initiating cells (CCICs) (Sikandar et al., 2010, Gopalakrishnan et al., 2014, Fender et al., 2015). Similarly, a significant increase of Notch in CRC cells has been shown to result in increased EMT as a result of signalling activation (Fender et al., 2015).

Alongside Notch signalling ADAM 10 is known to activate other signalling pathways involved in intestinal regulation through its sheddase of ligands such as EGF and E-Cadherin (Jones et al., 2016). In CRC, ADAM 10 expression and its downstream signalling pathways become aberrant and promote cellular proliferation and tumourigenesis, particularly via Notch, EGFR and Wnt signalling pathways (Jones et al., 2016). Whilst altered ADAMs related signalling has been identified in CRC, little research has shown a direct involvement of ADAM 10, thus making this a target for future research. However, it has been observed that upregulation of ADAM 10 expression correlates with a higher stage in CRC, thus implicating it in promoting a tumourigenic phenotype (Knösel et al., 2005, Gavert et al., 2007).

1.12 Project Rationale

CRC is one of the most prevalent cancers worldwide and is highly metastatic. Solid tumours, such as CRC, are known to possess hypoxic regions, which promote metastasis. Evidence for the role of the ADAMs family in cancer progression is strong, and research has implicated them in the hypoxia-driven tumour microenvironment. However, ADAM 10 remains relatively uncharacterised in the context of hypoxia-mediated cancer progression, thus making it a target of research. There is evidence for the role of ADAMs, especially ADAM 10, in normal colon biology. Indeed, ADAM 10-knockout mouse models display embryonic lethality at 9.5 days, with an array of deformities present. Therefore, understanding the role of ADAM 10 in the CRC hypoxic tumour microenvironment could provide crucial information regarding CRC progression and become a potential therapeutic target. This thesis aims to characterise ADAM 10 in the context of hypoxia-mediated CRC progression and elucidate mechanisms by which ADAM 10 may be contributing to the progressive nature of CRC.

1.12.1 Project Hypothesis

Hypoxia-induced ADAM 10 expression and activity mediates the progression of CRC through promotion of cellular migration and proliferation.

1.12.2 Project Aims and Objectives

- Determine the effects of exposure to severe hypoxia on ADAM 10 expression within CRC cell lines (**Chapter 3**)
- Elucidate the implications of hypoxia-mediated ADAM 10 on CRC tumourigenic phenotypes (**Chapter 4**)
- Identify the effects of hypoxia-mediated ADAM 10 on cellular signalling pathways linked to CRC progression (**Chapter 5**)

Chapter 2 : Materials and Methods

2.1 Materials and Methods

Unless otherwise stated all material and methods were obtained from Fisher Scientific UK Ltd (Loughborough, UK).

2.2 Cell Lines

HCT116, HT29 and RKO colorectal cancer cell lines were used throughout the experiments. HCT116 cells are from a carcinoma origin and were isolated from a male patient with malignant colon carcinoma. HT29 cells originate from the primary tumour of a 44 year old female with colon adenocarcinoma and present a well differentiated phenotype. RKO cells are a poorly differentiated cell line that is of colon carcinoma origin. All cell lines were purchased from ATCC, Middlesex, UK or ECACC, Salisbury, UK.

2.3 Cell Culture

HCT116, HT29 and RKO cells were grown in T75 flasks (Greiner Bio-One, Stonehouse, UK) containing Dulbecco's Modified Eagle's Medium (DMEM; High Glucose; Lonza, Basel, Switzerland) supplemented with 10% Foetal Bovine Serum (FBS; Gibco, Loughborough, UK) and 1 % sodium pyruvate (GE Healthcare, Buckinghamshire, UK) in a humidified incubator (Nuaire IR Direct Heat CO_2 Incubator (Triple Red, Buckinghamshire, UK)) at 37 °C in 5% CO_2. Faster BH-EN 2004 Laminar flow hoods (Faster S.r.l, Ferrara, Italy) and aseptic techniques were employed for cell culture work. All equipment and cell culture reagents were sterilised with 70% ethanol prior to use within the laminar flow hoods. All reagents were stored at 4°C and heated to 37°C prior to use.

2.4 Cell Subculture

Cell passaging was undertaken at 70-80% confluency, in order to keep exponential growth. Spent media was discarded and cells were rinsed in 1X Phosphate Buffered Saline (PBS) (GE Healthcare, Buckinghamshire, UK) then detached using trypsin-EDTA (GE Healthcare, Buckinghamshire, UK). Cells were re-suspended in growth medium before being passaged to the desired ratio (1:3-1:12). Passage numbers were recorded to track the number of passages undertaken.

2.5 Preparation of Frozen Cell Stocks

Cells were routinely frozen and stored in liquid nitrogen to maintain low passage stocks of all cell lines. Confluent (~80-90%) T75 cm^2 flasks were rinsed in 1X PBS and cells trypsinised. Trypsin was then inactivated with complete media prior to being centrifuged at 300 x *g* for 5 minutes. Supernatant was then removed prior to cells being re-suspended in 1X PBS, before being spun at 300 x *g* for 5 minutes. Supernatant was discarded and cells re-suspended, gradually, in 1.5 ml freeze mix (90% FBS, 10% diemthyl sulphoxide (DMSO)). The freeze mix/cell suspension was then aliquoted into cryovials (1:3, 500 µl/vial) and labelled. Cells were then stored at -80°C in a Nalgene Mr Frosty overnight, prior to being transferred to liquid nitrogen for long term storage.

2.6 Reconstitution of Frozen Cell Stocks

Frozen cells were removed from liquid nitrogen and thawed rapidly by hand before being transferred into complete medium and spun at 300 x *g* for 5 minutes. Supernatant was then discarded and cells re-suspended in complete medium and transferred to a T25 cm^2 cell culture flask.

2.7 Viable Cell Count

Viable cell number in a cell suspension was determined prior to seeding for experiments using the Trypan-blue exclusion method, which identifies non-viable cells through blue staining. Cells were washed with PBS and detached using trypsin before being re-suspended in growth medium. Cells were then centrifuged at 300 x *g* for 5 minutes. The supernatant was then removed and the cells re-suspended in growth media. A 1:1 dilution of cells with 0.4% Trypan Blue solution (Gibco, Loughborough, UK) was prepared, and cells were counted using a Neubauer Improved Haemocytometer (Marienfeld Superior, Lauda-Königshofen, Germany). Cells were counted by microscopy (Olympus CKX41 x 10 magnification) and cells in the four large corners of the haemocytometer grid were counted. Viable cells were determined by the exclusion of trypan blue, therefore non-viable, blue cells were excluded from cell counts. Cells were then seeded according to the experiments specifications.

2.8 Mycoplasma Testing

Cell lines were regularly tested (~ every 3 months) for mycoplasma contamination using EZ-PCR Mycoplasma Test kit (Geneflow, Staffordshire, UK). All mycoplasma testing was undertaken by Ellie Beeby, Laboratory Technician. 1 ml cell culture supernatant was removed from the flask and centrifuged at 250 x *g* briefly to exclude cell debris. Supernatant was then transferred and re-spun at 21 000 x *g* for 10 minutes to pellet mycoplasma. Supernatant was then discarded and pellet re-suspended in 35 µl buffer solution added to each sample. Samples were mixed thoroughly and heated at 95 °C for 3 minutes. 2.5 µl of each sample was then prepared for PCR using reagents provided (17.5 µl H_2O; 5 µl reaction mix) before being amplified using Techne TC-3000 thermal cycler. PCR products were then separated by gel electrophoresis, alongside positive control sample (2% agarose gel, 100V for 20 minutes) before being imaged using

ChemiDoc XRS+ system (Bio-Rad, Hertfordshire, UK). Banding was then compared to positive control for positive identification of mycoplasma contamination.

2.9 Hypoxic Treatment

Cells were seeded into dishes according to specific experimental conditions, and media was refreshed prior to hypoxic exposure. Cells were then placed in a H35 Hypoxystation (Don Whitley Scientific, Shipley, UK). This instrument allows for an accurate control and regulation of several micro environmental conditions, such as temperature (37 °C), humidity (75%), CO_2 (5%) and variable O_2 conditions. Prior to an experiment, the hypoxia chamber was programmed to the desired O_2 concentration and allowed to stabilise before the cells were placed into the hypoxic environment. Oxygen tensions used in this thesis ranged from 0.5% to 0.1% O_2. Cells were harvested within the chamber up to the point of lysis. Incubation in a conventional humidified incubator at 5% CO_2 was used as a normoxic (tissue culture conditions) control (20% O_2).

2.10 siRNA Transfection

Cells underwent a viable cell count (section 2.3) and were then seeded into 6 well plates (Greiner Bio-One, Stonehouse, UK) at a density of 200 000 cells/well. Cells were left to adhere overnight before transfection. Cells were then transfected with 25 nM siRNA using DharmaFECT I (Thermo Scientific, Loughborough, UK) transfection reagent as per manufacturer's instructions (details of siRNA oligos can be found in **Table 2.1**). In brief, siRNA oligos (Thermo Scientific, Loughborough, UK) were first diluted from the stock concentration (100 µM) with sterile DEPC water to 2 µM. The 2 µM siRNA was then mixed with an equal volume of serum-free media, whilst DharmaFECT was mixed with serum-free media (1:70). Both of these solutions were then incubated for 5 minutes at room temperature. The siRNA and DharmaFECT mixes were then combined and incubated for a further 20-30 minutes at room temperature. Existing growth medium in

the desired wells was then removed before being replaced with fresh growth medium mixed with the siRNA solution. siRNA was used to target ADAM 10 (siADAM 10) and a non-targeting control siRNA (siNT) was used in each experiment. Approximately 10 hours post-transfection the media was removed from the wells and the cells washed with 1X PBS. The cells were then trypsinised and re-suspended in growth media before being transferred into 6cm dishes (Greiner Bio-One, Stonehouse, UK) for the specific experimental procedures.

Table 2.1: siRNA used for ADAM 10 Knockdown Experiments

siRNA	Target	Manufacturer	Final Concentration	Target Sequence
siADAM 10	ADAM 10	siGENOME SMARTpool (ThermoScientific, UK) Ref: M-004503-02-0005	25 nM	5' GCUAAUGGCUGGAUUUAUU 3' 5' GGACAAACUUAACAACAAU 3' 5' CCCAAAGUCUCUCACAUUA 3' 5' GCAAGGGAAGGAAUAUGUA 3'
siNT	Non-Targeting	siGENOME SMARTpool (ThermoScientific, UK) Ref: D-001210-02-20	25 nM	Non-Targeting siRNA #2

2.11 Cell Lysis and Protein Extraction

Cells were plated into 10 cm cell culture dishes and left to adhere overnight before being placed into normoxia or hypoxia. At the time of lysis the media was removed from the dishes and the cells washed with 1X PBS. The cells were then detached from the dish surface into 1X PBS using a cell scraper, before being spun at 21000 x *g* for 2 minutes to pellet the cells. The supernatant was then removed before the cells were re-suspended in 150 µl lysis buffer (20 mM Tris-HCl pH 7.4; 150 mM NaCl; 0.5% Triton X-100; 0.1% Sodium dodecyl sulphate (SDS); 1 mM Ethylenediaminetetraacetic acid (EDTA); 1x PhosStop phosphatase inhibitor cocktail (Roche, Sussex, UK) and 1x cOmplete ULTRA EDTA-free protease inhibitor cocktail (Roche, Sussex, UK), as

described in Kornfeld et al. (2011). The cells incubated on ice for approximately 45 minutes to allow for complete lysis, before being centrifuged at 21000 x *g* for 15 minutes at 4°C. The supernatant was then transferred to a fresh micro-centrifuge tube before being stored at -20 °C ready for quantification.

2.12 Protein Quantification

The protein content of whole cell lysates was quantified using the BCA protein assay (Expedeon, Cambridgeshire, UK) in a 96 well plate format. Samples were diluted 1:20 with lysis buffer and 10 µl sample was pipetted into a 96 well plate format. 260 µl of working reagent (A:B; 50:1) was added before shaking the plate gently and incubating at 37 °C for 30 minutes. Samples were quantified against known BSA standards (0-2000 µg/ml). Absorbances were read at 595 nm on a Biotek Absorbance Microplate Reader (North Star Scientific, Leeds, UK).

2.13 Protein De-Glycosylation

Protein lysates were combined with 10% v/v glycobuffer and Milli-Q H_2O before the addition of 10% v/v PNGase F (New England Biolabs, Hitchin, UK) as per manufacturer's instructions. Samples were then incubated at 37°C for 24 hours before the addition of a reducing sample buffer (3.3% w/v SDS, 6 M urea, 17 mM Tris-HCl pH 7.5, 0.07 M β-mercaptoethanol, 0.01% w/v bromophenol blue). Samples were then heated to 100°C for 5 minutes to ensure complete protein denaturation.

2.14 γ-Secretase Inhibition

2.5 x 10^5 cells were seeded into 6 well plates and left to adhere overnight. Cells were either pre-treated for 6 hours with 100 nM and 500 nM Dibenzazepine (DBZ) (Tocris Bioscience, Bristol, UK) or treated at prior to hypoxic exposure. Cells were then placed

in either normoxia or hypoxia (0.5% O_2) for 24 hours before samples were lysed and protein extracted, as above.

2.15 SDS-PAGE

SDS-Polyacrylamide gels (7.5 or 10%) were prepared using a 7.5 or 10% resolving gel mix (1.5 M Tris-HCl pH 8.8, 30% Acrylamide, 10% (w/v) SDS, 10% (w/v) Ammonium persulphate (APS), 10% Tetramethylethylenediamine (TEMED)) in the appropriate volumes. The gel was then pipetted into the Mini-PROTEAN casting system (Bio-Rad, Hertfordshire, UK). A thin layer of Milli-Q H_2O was then pipetted over the top of the gel to dissipate bubbles and ensure a flat gel. The gel was then left to polymerise. Once set the H_2O was removed and the stacking gel (H_2O, 0.5 M Tris-HCl pH 6.8, 30% (w/v) Acrylamide, 10% (w/v) SDS, 10% (w/v) APS and 10% TEMED) in the appropriate volumes mixed and pipetted on top of the resolving gel. Spacing combs were then placed into the casting system and the gels left to polymerise. Protein samples were prepared prior to usage. Each sample was prepared to contain 30 µg protein using lysis buffer as a diluent with a reducing sample buffer added (3.3% w/v SDS, 6 M urea, 17 mM Tris-HCl pH 7.5, 0.07 M β-mercaptoethanol, 0.01% w/v bromophenol blue). Protein samples were then heated to 100°C for 5 minutes to ensure complete protein denaturation.

2.16 Western Blotting

Polyacrylamide gels were assembled into the Mini-PROTEAN tank (Bio-Rad, Hertfordshire, UK) and the combs removed. The inner reservoir and wells were then flooded with 1X running buffer (1:10 dilution 10X (30.20 g/L Tris, 144 g/L Glycine, 1% w/v SDS)) prior to the remainder of the tank being filled to the specified level. The protein samples were then loaded into the wells slowly alongside a BLUeye PreStained Protein Ladder as a molecular weight marker (Geneflow, Staffordshire, UK) which

allows for identification of proteins via molecular weight. Samples were separated by molecular weight by electrophoresis at 100V for approximately 1.5 hours. When the dye front reached the bottom of the gel the electrophoresis was stopped. A Polyvinylidene fluoride (PVDF) membrane was cut to size prior to usage and then activated in methanol for a few seconds before being left to equilibrate in 1X blotting buffer (1:10 dilution of 10X blotting buffer (30.20 g/L Tris, 144 g/L Glycine, 20% v/v methanol)). The blotting cassette was assembled for the Mini Trans-Blot system (Bio-Rad, Hertfordshire, UK), which was filled with blotting buffer. An ice pack was placed in the tank to minimise the heat produced by the blotting process. The buffer was also stirred during the blotting process to ensure continuous buffer mixing. The transfer was done at 100V for 1.5 hours, allowing the complete transfer of the proteins to the PVDF membrane. The membrane was incubated for 1 hour at room temperature using blocking buffer: 5% milk-TBST (5% w/v non-fat milk, 1X Tris buffered saline – tween (TBST) (1:10 dilution of 10X (88 g/L NaCl, 24 g/L Tris, 0.1% v/v Tween 20)). After blocking the membrane was washed in TBST for 3 x 5 minutes. Primary antibodies (detailed in **Table 2.2**) were diluted in 1% w/v milk-TBST or 5% BSA (Bovine Serum Albumin)-TBST at appropriate dilutions (see **Table 2.2**). The membrane was incubated with the primary antibody overnight at 4°C, whilst rolling. After incubation, the primary antibody was removed before the membrane was washed for 3 x 10 minutes in TBST whilst shaking. The HRP (horse radish peroxidise)-conjugated secondary antibody (details in **Table 2.2**) was diluted in 1% w/v milk-TBST and was added to the membrane for 1 hour at room temperature and incubated whilst shaking. The membrane was then washed for a further 3 x 10 minutes in TBST as before. The membrane was incubated with an enhanced chemiluminescence (ECL) Clarity chemiluminescence reagent (Bio-Rad, Hertfordshire, UK) in order to allow for specific band detection, as per manufacturer's instructions. The signal generated was imaged using the ChemiDoc

XRS+ system (Bio-Rad, Hertfordshire, UK). Densitometric analysis of band intensity was performed using the ImageLab Software (Bio-Rad, Hertfordshire, UK). Band intensity values were normalised to β-actin band intensity for the corresponding lane.

Table 2.2: Antibodies Used Within this Project
Table detailing the range of antibodies used for Western Blotting within this research, both primary and secondary antibodies included.

Target	Source	Reference	Origin	Dilution
β-Actin	Santa Cruz	Sc-69879	Mouse mAb	1:10 000 in 1% milk-TBST
ADAM 10	Abcam	Ab1997	Rabbit pAb	1:1000 in 1% milk-TBST
β-Catenin	Cell Signalling	8480	Rabbit mAb	1:1000 in 5% BSA-TBST
E-Cadherin	Santa Cruz	Sc-8426	Mouse mAb	1:1000 in 1% milk-TBST
c-MYC	Cell Signalling	13987	Rabbit mAb	1:1000 in 5% BSA-TBST
Cyclin D1	Cell Signalling	2978	Rabbit mAb	1:1000 in 5% BSA-TBST
Slug	Cell Signalling	9585	Rabbit mAb	1:1000 in 1% milk-TBST
Snail	Cell Signalling	3879	Rabbit mAb	1:1000 in 1% milk-TBST
p21	Cell Signalling	2946	Mouse mAb	1:2000 in 1% milk-TBST
pAKT	Cell Signalling	4060	Rabbit mAb	1:1000 in 5% BSA-TBST
pEGFR	Cell Signalling	3777	Rabbit mAb	1:1000 in 5% BSA-TBST
pERK 1/2	Cell Signalling	4370	Rabbit mAb	1:1000 in 5% BSA-TBST
pGAB1	Cell Signalling	3233	Rabbit mAb	1:1000 in 5% BSA-TBST
pStat5	Cell Signalling	4322	Rabbit mAb	1:1000 in 5% BSA-TBST
Rabbit HRP	Dako	P 0448	Goat pAb	1:2000 in 1% milk-TBST
Mouse HRP	Dako	P 0161	Rabbit pAb	1:2000 in 1% milk-TBST

2.17 Immunoprecipitation

Immunoprecipitation is utilised for the purification of proteins from whole cell lysates and sees the use of an antibody targeting the desired protein immobilised to a solid support such as magnetic beads or agarose beads.

Cells were plated into 15 cm cell culture plates and left to adhere overnight before being placed into normoxia or hypoxia for the specified time. At the time of lysis the media was removed from the dishes and the cells washed twice with 1X ice cold PBS. The cells were then detached from the dish surface into 1X PBS using a cell scraper, before being spun at 21000 x *g* for 2 minutes to pellet the cells. The supernatant was then removed before the cells were re-suspended in 500 µl of lysis buffer (20 mM Tris-HCl

pH 7.4; 150 mM NaCl; 0.5% Triton X-100; 0.1% SDS; 1 mM EDTA; 1x PhosStop phosphatase inhibitor cocktail (Roche, Hertfordshire, UK), 1x cOmplete ULTRA EDTA-free protease inhibitor cocktail (Roche, Hertfordshire, UK), as described in Kornfeld et al. (2011). Lysates were allowed to lyse completely at 4°C for 20 minutes whilst being rotated, before being centrifuged at 21000 x *g* at 4°C for 20 minutes to collect clarified lysate. Input samples were taken at this stage for each condition. 50 µl Protein A Dynabeads (Invitrogen, Loughborough, UK) were washed 3 x in lysis buffer on ice. Beads were then incubated with 2 µg of antibody for 30 minutes at 4°C whilst rotating to allow complete antibody conjugation. Beads were then washed 1 x with lysis buffer, as before. Clarified cell lysates were then added to the antibody conjugated beads. The lysate and bead slurry was then incubated for 4 hours at 4°C whilst rotating. After incubation, the supernatant was removed as the beads washed 3 x in lysis buffer on ice, as before. After removal of the final wash, the beads were re-suspended in 2X Laemmli buffer (65.8 mM Tris-HCl, pH 6.8, 2.1% SDS, 26.3% (w/v) glycerol, 0.01% bromophenol blue (Bio-Rad, Hertfordshire, UK)) diluted in lysis buffer, before heating for 5 minutes at 100°C. Samples were then stored at -20°C.

2.18 Coomassie Protein Stain

Samples were run by SDS-PAGE then stained for protein with Coomassie Blue solution (50% v/v MeOH, 10% v/v Acetic acid, 0.1% w/v Coomassie Brilliant Blue-R250 (Fisher, UK)). Gels were stained for 1 hour at room temperature whilst gently shaking, before being de-stained in a destain solution (40% v/v MeOH, 10% v/v Acetic Acid) until protein bands were visible. Gels were then stored in MilliQ water before being imaged using the ChemiDoc XRS+ system (Bio-Rad, Hertfordshire, UK).

2.19 MALDI-MS

MALDI-MS (Matrix Assisted Laser Desorption/Ionisation-Mass Spectrometry) is a mass spectrometry based technique, which separates proteins and analyses them to allow for positive identification according to peptide sequence and molecular weight.

Samples for MALDI-MS analysis were run by SDS-PAGE on 7.5% polyacrylamide gels before being stained for protein using Coomassie Blue. Bands of interest were then excised from the stained gel using a scalpel, before being placed into eppendorf tubes and sent for MALDI-MS analysis at the University of York proteomics facility, as per the protocol provided by the facility. In brief, gel pieces were washed twice with 50% v/v acetonitrile containing 25 mM ammonium bicarbonate. A further wash with 50% v/v acetonitrile was undertaken before drying in a vacuum concentrator for 20 minutes. Porcine trypsin (Promega, Hampshire, UK) in 50 mM acetic acid, diluted five-fold with 25 mM ammonium bicarbonate (final trypsin concentration 0.02 μg/μl) was added to the gel pieces, with enough 25 mM ammonium bicarbonate to cover the pieces before incubating overnight at 37 °C. 1 μl of sample was applied to MALDI target plate followed by equal volume of 5 mg/ml 4-hydroxy-α-cyano-cinnamic (Sigma Aldrich, Dorset, UK) in 50% v/v acetonitrile with 0.1% v/v trifluoroacetic acid. MALDI analysis was undertaken using a Bruker Ultraflex III (Bruker UK Ltd, Coventry, UK) across a spectra of 800-5000 *m/z*. Calibration was against a 6 peptide mix with a signal-to-noise (S/N) threshold of set to 2. Samples with a S/N greater than 30 were selected for MS/MS fragmentation with Bruker flexAnalysis software 3.3 (Bruker UK Ltd, Coventry, UK) used to perform processing and peak generation. Data was compared to Mascot database (Matrix Science Ltd, London, UK) through the Bruker ProteinScape 2.1 interface (Bruker, Coventry, UK). Data was compared against the human subset of

the UniProt database and filtered to accept peptides with an expect score of 0.05 or lower.

2.20 LC-MS

LC-MS (Liquid chromatography mass spectrometry) is also a mass spectrometry based principle, which sees the separation of proteins by liquid chromatography prior to mass spectrometry analysis, allowing for protein identification.

Samples for LC-MS analysis were run by SDS-PAGE on 7.5% polyacrylamide gels (as detailed in Section 2.15). Gels were then stained using Coomassie Blue before the bands of interest were excised from the gel. Bands were then cut into small, approximately 1 mm^2 pieces and placed into an eppendorf tube. Samples were then prepared for LC-MS analysis using a Trypsin Profile In-Gel Digestion kit (Sigma Aldrich, Dorset, UK). Gel pieces were incubated with Destaining solution at 37 °C for 30 minutes twice before being dehydrated in a SpeedVac (Thermo Scientific, Loughborough, UK) at 45 °C for 30 minutes. 20 µl Trypsin Solution (1 mM HCl; 20 µg/ml trypsin; 40 mM ammonium bicarbonate and 9% v/v acetonitrile) was added to the pieces in conjunction with 50 µl Trypsin Reaction Buffer (40 mM ammonium bicarbonate and 9% v/v acetonitrile) and incubated for 4 hours at 37 °C. The trypsin digest was then separated from the gel pieces and then analysed by LC-MS by Dr Kevin Welham in the Department of Chemistry at the University of Hull. In brief, a liquid chromatography Thermo Dionex Ultimate 3000 nanoLC system was used with samples maintained at 8 °C in a refrigerated sample tray throughout the experiment. A Thermo Scientific Acclaim PepMap 100 75 µm x 250 mm NanoViper column was used at 40 °C for a total run time of 70 minutes. Samples and blanks were injected in volumes of 5 µl, with solvent blanks run between each pair of sample injections. MS analysis was undertaken using a Bruker Impact qQTOF MSMS in autoMSMS mode with a threshold of 500 counts per 3 second

cycle. The captive ion source used in positive ion mode. Peptide scan range was from 50 to 2200 daltons. All data was processed using Bruker ProteinScape 3.1 software with protein identification by MASCOT 2.1. For detailed settings of LC-MS analysis see **Appendix 1**.

2.21 Refining of LC-MS Data

Potential contaminants of the LC-MS samples were identified using the CRAPome (Contaminant Repository for Affinity Purification) database (Mellacheruvu et al., 2013). The repository details known contaminants of immunoprecipitation and affinity purification and the LC-MS data was compared to the 411 affinity purification studies to determine whether any contaminants were present. A threshold of 10% was set, which determined any proteins present in ≤ 10% of studies within the repository were true protein hits. Proteins identified ≥ 10% of studies were determined to be contaminants.

2.22 Glycoprotein Affinity Purification using Concanavalin A

Concanavalin A based affinity purification utilises Concanavalin A lectins bound to sepharose resin beads, which bind sugar residues on glycoproteins and subsequently purify these glycoproteins for further analysis.

Cells were plated into 10 cm dishes and lysed in 200 µl as per protein extraction procedure, detailed above (Section 2.11). Input samples were taken after lysis and frozen until required. Concanavalin agarose beads (Sigma Aldrich, Dorset, UK) were washed twice in ice cold lysis buffer. 60 µl of washed beads were added to the cell lysates (FLAG agarose beads were used for control) and incubated at 4°C for 2 hours whilst rotating. After incubation samples were spun at 2000 x *g* at 4°C for 2 minutes, supernatant was then removed. Beads were then washed 3 x in 500 µl ice cold lysis

buffer. After last wash the supernatant was discarded. Beads were resuspended in 2X sample buffer (0.0625 M Tris-HCl pH 6.8, 20% v/v glycerol, 5% w/v SDS, 0.05% w/v bromophenol blue, 5% v/v β-mercaptoethanol) diluted in lysis buffer, before heating samples for 5 minutes at 100°C. Samples were then stored at -20°C.

2.23 mRNA Extraction

Cells were plated into 6 cm dishes and mRNA extraction was carried out using the Bio-Rad Aurum Total RNA kit (Bio-Rad, Hertfordshire, UK) after hypoxic exposure. Cells were rinsed with 1X PBS before being lysed with 350 µl provided lysis solution. Cells were harvested and re-suspended to ensure complete lysis. 350 µl 70% ethanol was then added to the samples and re-suspended thoroughly. Samples were then transferred to RNA binding columns and centrifuged at 21000 x *g* for 30 seconds. The flow through was discarded and 700 µl low stringency wash solution was added to the columns, prior to spinning at 21000 x *g* for 30 seconds. Flow through was then discarded and 15:1 mix of DNAse 1 dilution solution and DNAse 1 added to the columns and incubated at room temperature for 15 minutes. 700 µl high stringency wash solution was then added to the columns and centrifuged at 21000 x *g* for 30 seconds. Flow through was discarded before 700 µl low stringency wash solution was added to columns and centrifuged at 21000 x *g* for 1 minute, then a further 2 minutes after discarding flow through. 80 µl elution solution was then added to columns before centrifuging at 21000 x *g* for 2 minutes to elute RNA. Extracted mRNA was then stored at -80°C.

2.24 mRNA Quantification

mRNA samples were quantified using the NanoDrop 1000 Spectrophotometer (Thermo Fisher Scientific, Loughborough, UK). The loading platform was cleaned prior to use with H_2O before being blanked with elution solution (from Bio-Rad Aurum Total RNA

kit (Bio-Rad, Hertfordshire, UK)). 2 µl each sample was loaded onto platform and RNA concentration measured in ng/ml.

2.25 cDNA Synthesis

Reverse transcription was undertaken using a RevertAid H Minus First Strand cDNA Synthesis Kit (Thermo Fisher Scientific, Loughborough, UK). 1 µg of extracted total RNA was combined with 1 µl oligo $(dT)_{18}$ primers and 12 µl H_2O before being combined with 8 µl reaction mix (4 µl 5X Reaction Buffer; 1 µl Ribolock RNase Inhibitor (20 u/µl); 2 µl 10 mM dNTP mix and 1 µl RevertAid Minus M-MuLV Reverse Transcriptase (200 u/µl)). The reaction was performed in a Bio-Rad C1000 Thermal Cycler (Bio-Rad, Hertfordshire, UK), using the following cycling conditions: heated for 60 minutes at 42°C followed by heating at 70°C for 5 minutes to terminate the reaction. Synthesised cDNA was then stored at -20°C until required for qPCR analysis.

2.26 Real Time quantitative PCR Analysis

Real Time quantitative PCR (RT-qPCR) was undertaken using SYBR Green technology. QuantiFAST SYBR Green master mix and QuantiTECT pre-designed primer assays (both from Qiagen, Manchester, UK) were used, and reactions were performed in a StepOnePlus Real Time PCR machine (Applied Biosystems, Loughborough, UK). (Details of all QuantiTECT primer assays used can be found in **Table 2.3**). The qPCR reaction was setup as follows, using the cycling protocol noted in **Table 2.4**. cDNA samples were diluted 1:5 with sterile Diethylpyrocarbonate (DEPC) water. A master mix solution was prepared containing SYBR Green (1:2, v/v) QuantiTECT primer assays (1:10, v/v), diluted in sterile DEPC water. The diluted cDNA samples were added to a 96-well plate, with sterile DEPC water used for the no template control NTC wells, to give a final concentration of 1:10 (v/v). Triplicate wells

were prepared for each sample and primer assay, with triplicate of NTC for each primer assay. B-2 microglobulin (*B2M*) was used as the housekeeping gene within all experiments and all results were normalised to *B2M* levels.

Table 2.3: QuantiTECT Primer Assays used for qPCR

Target	Catalogue Number	Length of Amplicon
ADAM 10	QT00032641	87 bp
SLC2A1 (GLUT-1)	QT00068957	77 bp
B2M	QT00088935	98 bp

Table 2.4: Sigma Custom Primers used for qPCR

Target Gene	Sequence	Amplicon length	Reference
Notch1 – F	TACTCCTCGCCTGTGGACAA	128bp	Chen et al. (2007)
Notch1 – R	CAGTCGGAGACGTTGGAATG	128bp	
Hes1 – F	TCAACACGACACCGGATAAA	150bp	Chen et al. (2007)
Hes1 – R	CCGCCAGCTATCTTTCTTCA	150bp	
Hes5 – F	TCAGCCCCAAAGAGAAAAAC	232bp	Chen et al. (2007)
Hes5 – R	TAGTCCTGGTGCAGGCTCTT	232bp	
Hey1 – F	TGGATCACCTGAAAATGCTG	200bp	Chen et al. (2007)
Hey1 – R	TTGTTGAGATGCGAAACCAG	200bp	
Hey2 – F	GTACCTGAGCTCCGTGGAAG	241bp	Chen et al. (2007)
Hey2 – R	AGTTGTGGAGAGGCGACAAG	241bp	
c-MYC – F	GGCTCCTGGCAAAAGGTCA	119bp	Dai et al. (2014)
c-MYC – R	CTGCGTAGTTGTGCTGATGT	119bp	
CCND1 (CyclinD1) – F	CTCCTGTGCTGCGAAGTGG	204bp	Self-designed
CCND1 (CyclinD1) – R	CTTCTGTTCCTCGCAGACCTCC	204bp	

Table 2.5: Cycling Protocol for qPCR

Initial Denaturation	Denaturation	Annealing/Extension	Melt Curve		
95°C 5min 1x	95°C 10 sec	60°C 3 sec	95°C 15 sec	60°C 1 min	95°C 15 sec
	x 35 Cycles		+ 0.3°C per step		

2.27 Scratch Assay

Scratch assays allow for the assessment of cellular migration through cell monolayer wounding and observation to determine migratory distance over a specified period of time.

2.27.1. GI254023X Treatment

2 x 10^5 – 2 x10^6 cells were seeded into 6 well plates and left to adhere overnight. Cells were then treated with 1 μM and 5 μM GI254023X (Tocris Bioscience, Bristol, UK) in media for 6 hours. The media was then removed and the confluent monolayer of cells scratched 3 times using a P200 tip. Cells were then washed once with 1X PBS and media containing 0.5% FBS added to the wells. A horizontal line, perpendicular to the scratches, was then drawn onto the under surface of the well. Images were then obtained of the point at which the line intercepted the scratches, using Axio Vert.A1 inverted microscope and ZEN 2012 software, using the 5X objective (Carl Zeiss, Cambridge, UK). Cells were then placed in either normoxia or hypoxia (0.5% O_2) for 16 hours before being re-imaged. Scratches were then measured by hand.

2.27.2. siRNA Transfection

Cells were transfected as above (Section 2.10). The confluent monolayer of cells was scratched 3 times with a P200 tip. Cells were then washed once with 1X PBS, before 0.5% FBS media was added to the wells. A line, perpendicular to the scratches, was then drawn on the underneath of the wells and the scratches imaged using Axio Vert.A1 inverted microscope and ZEN 2012 software, using the 5X objective (Carl Zeiss, Cambridge, UK). Cells were then incubated for 16 hours in

either normoxia or hypoxia (0.5% O_2) before being re-imaged. Scratches were measured by hand.

2.28 MTS Assay

MTS (3-(4,5-dimethylthiazol-2-yl)-5-(3-carboxymethoxyphenyl)-2-(4-sulfophenyl)-2H-tetrazolium) assays measure cellular viability through the metabolic reduction of tetrazolium salts to formazan. This colorimetric based assay assumes that that formazan reduction will be proportional to the exponentially growing, viable cells in the sample.

2.28.1. GI254023X Treatment

5000 cells/well were seeded into 96 well plates (Greiner Bio-One, Stonehouse, UK) and left to adhere overnight. Cells were then treated with a range of GI254023X concentrations, 0.2 μM – 135 μM, with DMSO as the vehicle control, with a final volume per well of 100 μl. Cells were then placed into either normoxia or hypoxia (0.5% O_2) for 16 hours. 20 μl (3-(4,5-dimethylthiazol-2-yl)-5-(3-carboxymethoxyphenyl)-2-(4-sulfophenyl)-2H-tetrazolium) (MTS) reagent (Promega, Hampshire, UK) was added per well and incubated at 37 °C for 2 hours. Absorbance was then read at 490 nm on a Biotek Absorbance Microplate Reader (North Star Scientific, Leeds, UK).

2.28.2. siRNA Transfection (16h timepoint)

200 000 cells/well were seeded into 6 well plates for transfection (Section 2.10). Cells then underwent a viable cell count and 5000 cells/well were re-seeded into 96 well plates, in a final volume of 100 μl/well. Cells were then left to adhere for approximately 8 hours before being placed in either normoxia or hypoxia (0.5% O_2) for 16 hours. 20 μl of MTS reagent was then added to each well and incubated for 2 hours at 37°C. Absorbance was then read at 490 nm.

2.28.3. siRNA Transfection (24-72h timepoints)

200 000 cells/well were seeded for transfection (Section 2.10). Cells then underwent a viable cell count before 3000 cells/well were re-seeded into 96 well plates, in a final volume of 100 µl/well. Cells were then left to adhere overnight before being placed in either normoxia or hypoxia (0.5% O_2) for 24, 48 or 72 hours. The outer wells of each plate were filled with 200 µl PBS to minimise evaporation of media. After specified time of incubation 20 µl of MTS reagent was added to each well and incubated at 37°C for 2 hours. Absorbance was then read at 490 nm.

2.29 Clonogenic Survival Assay

Clonogenic assays assess the capability of cells to form colonies and undergo unlimited replication. The premise of clonogenic assays is that if a cell possesses reproductive capability then it is likely to be an actively proliferating cell.

The appropriate plating density and period of incubation to obtain approximately 200 colonies was determined for each cell line. Specifically, 250 cells/well (HCT116) or 500 cells/well (HT29) were seeded into a well of a 6 well plate, with 6 wells seeded/condition. Cells were left to adhere overnight before being placed in normoxic or hypoxic (0.5% O_2) conditions for 24 hours. Cells were then transferred to a dedicated humidified incubator at 37 °C and 5% CO_2, and left for 7-10 days to allow macroscopic colony formation (colonies comprised of more than 50 cells). Once colonies reached the desired size, media was carefully removed from the wells, and carefully washed with 1X PBS. Colonies were then fixed and stained with crystal violet (0.1% w/v crystal violet; 70% v/v methanol and 30% v/v H_2O) for 1 hour. Excess crystal violet solution was then removed and plates carefully washed in distilled water before being left to air dry. Colonies were then counted using a GelCount™ (Oxford Optronics, Oxfordshire, UK). CHARM (compact Hough and radial map) algorithm settings were determined for

each cell line. Plating efficiency was calculated as the average number of colonies divided by the number of cells seeded. The surviving fraction was calculated as the average number of colonies divided by the plating efficiency of the control, multiplied by the seeding density.

2.30 Cell Cycle Analysis

Propidium iodide (PI) staining allows for assessment of cell cycle as PI is a fluorescent dye which binds to DNA and its fluorescence emission, as assessed by flow cytometry, is proportional to the amount of DNA within a cell. Different cell cycle stages of proliferating cells display different DNA content, thus allowing for cell cycle analysis.

200 000 cells/well (HCT116) were seeded for transfection (Section 2.10) before being placed in either normoxia or hypoxia (0.5% O_2) for 24 hours. Media was then collected and cells washed 1X in PBS before being trypsinised and re-suspended in collected media. Cells were then centrifuged at 500 x *g* for 5 minutes before being re-suspended in 1X ice cold PBS. Cells were then centrifuged at 500 x *g* for 5 minutes before -20°C 70% ethanol was added slowly to fix the cells. Cells were then stored at -20°C until ready to proceed with staining. Cells were then centrifuged for 5 minutes at 500 x *g* before being re-suspended with 1X ice cold PBS. A cell strainer was then used to produce a single-cell suspension before cells were centrifuged at 500*g* for 5 minutes. Cells were then re-suspended in 1X PBS; 5 μg/ml propidium iodide (PI; Sigma Aldrich, Dorset, UK); 10 μg/ml RNase A. PI staining was then measured and analysed using a FACSCalibur (BD Biosciences, Oxford, UK).

2.31 ADAM 10 Activity Assay

ADAMs family members are known sheddases and Peptide A and B (detailed below) can be used to assess ADAMs activity through emission of a fluorescent signal upon their cleavage by ADAMs family members.

2.31.1 GI254023X or GM6001 Treatment

5000 cells/well (HCT116) were seeded into 96 well plate format (fluorescent compatible plates) and left to adhere overnight. Cells were then treated with 5 μM or 10 μM GI254023X or GM6001 (Tocris Bioscience, Bristol, UK), in DMEM, with DMSO used as vehicle control, for 6 hours before being placed into normoxia or hypoxia (0.5% O_2) for 16 hours. Media was removed and fresh drug treatment in combination with 20 μM MOCAc-Lys-Pro-Leu-Gly-Leu-Dap(Dnp)-Ala-Arg-NH_2 (Peptide A; Peptides International, Kentucky, USA) or Ala-Gln-Ala-Val-Arg-Ser-Ser-Ser-Arg-Dap(Dnp)-NH_2 (Peptide B; Peptides International, Kentucky, USA) in DMEM was added to cells. Cells were then incubated for 1 hour at 37 °C in the dark before fluorescence was measured at excitation 328 nm, emission 393 nm (Peptide A) or excitation 320 nm, emission 420 nm (Peptide B) using a Tecan i-control infinite 200 plate reader.

2.31.2 siRNA Transfection

200 000 cells/well (HCT116) were seeded for transfection (Section 2.10) before undergoing a viable cell count (Section 2.5) and 5000 cells/well were seeded into a 96 well plate (opaque black – fluorescence compatible). Cells were then left to adhere for 8 hours before being placed into normoxia or hypoxia (0.5% O_2) for 16 hours. 20 μM Peptide A or Peptide B was then added to each well, in DMEM, and incubated in darkness for 1 hour at 37°C. Fluorescence was then measured at excitation 328 nm,

emission 393 nm (Peptide A) or excitation 320 nm, emission 420 nm (Peptide B) using a Tecan i-control infinite 200 plate reader.

2.32 Statistical Analysis

Experiments were replicated three times, unless otherwise stated, and appropriate statistical analysis undertaken to determine any significance in observable differences. Student *t*-tests were used to compare two groups and ANOVAs were undertaken to compare three or more groups with one another. Types of test undertaken for each experiment can be identified within the appropriate figure legend. The standard deviations (STDEV) and standard error mean (SEM) were calculated and displayed in graphs as error bars, as indicated within figure legends. All graphs were generated and statistical analysis undertaken using Graphpad Prism 6 software (Graphpad, California, USA).

Chapter 3 : Characterisation of ADAM 10 in Hypoxia in Colorectal Cancer

3.1 Introduction

3.1.1 ADAMs and hypoxia

ADAM 10 is one of the lesser-studied members of the ADAMs family, particularly in the context of cancer, as discussed in **Section 1.8.1** (Edwards et al., 2008, Reiss and Saftig, 2009, Mullooly et al., 2015). In particular, not many studies have evaluated the effects of hypoxia on ADAM 10 expression and function. Previous research is somewhat conflicting, suggesting that the effects of hypoxia on ADAM 10 are cancer type specific (Webster et al., 2002, Marshall et al., 2006, Barsoum et al., 2011) (**Section 1.8.2**). Specifically, exposure to hypoxia (2.5% O_2) has been shown to decrease the expression of ADAM 10 in neuroblastoma (Webster et al., 2002, Marshall et al., 2006). On the other hand, in prostate and breast cancer, exposure to severe hypoxia (0.5% O_2) was shown to result in the upregulation of ADAM 10 expression (Barsoum et al., 2011). However, other members of the ADAMs family have been more widely characterised in the hypoxic tumour microenvironment and are known to be altered under hypoxic conditions (Zheng et al., 2007, Rzymski et al., 2012, Wang et al., 2013).

3.1.2 Regulation of ADAM10 Activity and Stability by Post-translational Modifications

ADAM 10 is known to undergo a variety of PTMs including pro-domain removal for activation of its catalytic activity (**Section 1.8.3**) (Anders et al., 2001, Peiretti et al., 2003, Leonard et al., 2005, Moss et al., 2007). Furthermore, ADAM 10 is known to have four potential N-linked glycosylation sites, within the mature form of the protein, with three of the sites residing within the active, metalloproteinase domain (Escrevente et al., 2008). Research in the context of ADAM 10 PTMs has also shown the ectodomain cleavage of ADAM 10 by other ADAMs family members and the removal of ADAM 10 cytoplasmic tail by γ-secretase.

3.1.3 Proteomic Methodologies in Protein and PTM Identification

Mass spectrometry (MS) has long been established as a key technique for the identification of proteins and their post-translational modifications (Aebersold and Mann, 2003). The many advantages of mass spectrometry see it emerging as the method of choice for protein characterisation within the proteomic field (Aebersold and Mann, 2003, Susnea et al., 2013, Schlage and auf dem Keller, 2015). Such advantages include high sensitivity, accuracy, small sample size and rapid analysis. Mass spectrometry methodologies rely on the ionisation of samples, with the various methodologies ionising the samples in differing ways (Aebersold and Mann, 2003, Gonnet et al., 2003, Susnea et al., 2013). Matrix-assisted laser desorption ionisation mass spectrometry (MALDI-MS) allows for analysis of proteins through sample ionisation and subsequent separation according to their mass (Yates et al., 2009, Susnea et al., 2013). Liquid chromatography mass spectrometry (LC-MS) demonstrates a higher levels of sensitivity than MALDI-MS and is capable of analysing more complex protein mixes, and therefore is emerging as a more popular method for protein characterisation (Chen and Pramanik, 2009, Karpievitch et al., 2010). Glycoproteomics sees the study of glycosylation-based alterations to proteins and several biochemical techniques can be used for this purpose (**Section 1.8.3.1**). Such methodologies include PNGase F for glycan removal, inhibition of glycosylation through usage of tunicamycin and Concanavalin A for affinity based purification of *N*-linked glycosylated proteins (Escrevente et al., 2008, Wojtowicz et al., 2012, Roth et al., 2012, Tian and Zhang, 2013). More detailed glycoproteomic analysis can also be undertaken through MS based approaches, which aim to identify the location of glycosylation on the protein, the structure and identify the various glycans and the point to which they bind the protein (Sagi et al., 2005, Anderegg et al., 2009, Pasing et al., 2012, Zhang et al., 2014b).

3.1.4 Rationale, Aims and Objectives of this Chapter

It is established that ADAM 10 is altered within CRC, however there is limited research characterising the role that ADAM 10 plays within the hypoxic tumour microenvironment. Previous studies have reported conflicting results in terms of ADAM 10 expression within tumour hypoxia, suggesting expression patterns and the role of ADAM 10 may be cancer specific. This chapter aims to identify the effects severe hypoxia has upon the expression of ADAM 10 in CRC cell line models.

The experimental work within this chapter was designed to test the hypothesis 'Exposure to severe hypoxia will increase ADAM 10 expression in CRC cell lines' and subsequently address the following questions:

- Does exposure to severe hypoxia result in alterations in expression of ADAM 10 at both protein and transcript levels in CRC cell line models?
- Is hypoxia responsible for mediating the formation of the ADAM 10 mature form doublet band?
- Is the formation of the doublet band as a result of a hypoxia-mediated post-translational modification, and if so, what type of post-translational modification is ADAM 10 undergoing?

3.2 Methods

3.2.1 Western Blotting

CRC cell lines were exposed to hypoxia for a range of time point (**Section 2.9**) lysed and protein extracted (**Section 2.11**) and quantified (**Section 2.12**). 30 μg of protein lysates were separated by SDS-PAGE (**Section 2.15**) and then protein expression analysed by Western Blotting (**Section 2.16**). A polyclonal anti-ADAM 10 antibody was used for detection of ADAM 10 protein expression, and β-Actin was used as the loading control, as per dilutions specified in **Table 2.2**, to which all values were normalised.

3.2.2 qPCR

CRC cell lines were exposed to hypoxia (**Section 2.9**) for a range of time points and mRNA extracted (**Section 2.23**). mRNA was then quantified (**Section 2.24**) and 1 μg of extracted RNA underwent cDNA synthesis (**Section 2.25**). qPCR was then undertaken, as described in **Section 2.26**. QuantiTECT primer assays (as described in **Table 2.3**) were used for detection of *ADAM 10* expression. *SLC2A1* expression was analysed to serve as a control for a hypoxic environment and *B2M* expression was used as the housekeeping control, to which all results were normalised. qPCR was carried out as per the cycling protocol in **Table 2.5**.

3.2.3 ADAM 10 Immunoprecipitation

HT29 cells were exposed to normoxia or hypoxia (**Section 2.9**) before undergoing immunoprecipitation (**Section 2.17**) for purification of ADAM 10. An anti-ADAM 10 antibody (as detailed in **Table 2.2**) was used at a concentration of 2 μg. Samples were then separated by SDS-PAGE (**Section 2.15**) and then either stained with Coomassie

Blue (**Section 2.18**) or ADAM 10 expression analysed by Western Blotting (**Section 2.16**) with an anti-ADAM 10 antibody used as specified in **Table 2.2**.

3.2.4 MALDI-MS

HT29 cells were exposed to normoxia or hypoxia (**Section 2.9**) and underwent ADAM 10 immunoprecipitation (as above; **Section 2.17**). Proteins were then separated by SDS-PAGE (**Section 2.15**) and total protein content stained with Coomassie Blue (**Section 2.18**) before undergoing MALDI-MS analysis (**Section 2.19**).

3.2.5 LC-MS

HT29 cells were exposed to either normoxia or hypoxia (**Section 2.9**) and underwent ADAM 10 immunoprecipitation (as above; **Section 2.17**). Proteins were then separated by SDS-PAGE (**Section 2.15**) and total protein content stained with Coomassie Blue (**Section 2.18**) before undergoing LC-MS analysis (**Section 2.20**). The LC-MS data was then refined using the CRAPome database (**Section 2.21**).

3.2.6 γ-Secretase Inhibition

HCT116 cells were treated with 100 nM or 500 nM DBZ for inhibition of γ-secretase (**Section 2.14**) before being exposed to normoxia or hypoxia for 16 hours (**Section 2.9**). Cells were then lysed and protein extracted (**Section 2.11**) and quantified (**Section 2.12**). 30 μg of protein lysates were separated by SDS-PAGE (**Section 2.15**) and ADAM 10 protein expression analysed by Western Blotting (**Section 2.16**), using an anti-ADAM 10 antibody. β-Actin was used as the loading control, to which all values were normalised. All antibodies were used as per dilutions specified in **Table 2.2**.

3.2.7 Concanavalin A Pull Down

CRC cell lines were exposed to either normoxia or hypoxia (**Section 2.9**) and lysed (**Section 2.11**) before undergoing glycoprotein affinity purification using Concanavalin A (**Section 2.22**). Samples were then separated by SDS-PAGE (**Section 2.15**) and ADAM 10 protein expression analysed by Western Blotting (**Section 2.16**). An anti-ADAM 10 antibody was used as specified in **Table 2.2**.

3.2.8 Protein De-Glycosylation

HCT116 cells were exposed to normoxia or hypoxia (**Section 2.9**) and lysed (**Section 2.11**). Samples were then quantified (**Section 2.12**) and 30 μg of each protein lysate treated with PNGase F, as detailed in **Section 2.13**. Experimental controls were implemented including whole cell lysate with normal ADAMs lysis buffer (**Section 2.11**); whole cell lysate with H_2O and glycobuffer, both +/ 24 hours at 37 °C. All samples were then separated by SDS-PAGE (**Section 2.15**) and ADAM 10 protein expression analysed by Western Blotting (**Section 2.16**) using an ADAM 10 antibody as detailed in **Table 2.2**.

3.3 Results

3.3.1 Characterisation of the Effects of Hypoxia on ADAM 10 Expression

In order to determine the effects of hypoxia on ADAM 10 expression, colorectal cancer cell line models were exposed to two different oxygen tensions (0.5% or 0.1% O_2) for a range of time points and the protein and transcript expression patterns of ADAM 10 analysed by Western Blot and qPCR, respectively.

3.3.1.1 ADAM 10 is Expressed across a Panel of CRC Cell Lines and is Induced by Hypoxia

Western blotting was used to identify any alterations in ADAM 10 expression at protein level, after exposure to severe hypoxia. Densitometry was subsequently carried out on the blots, **Figure 3.1** and **Figure 3.2** depict the expression of ADAM 10 in HCT116 colorectal cancer cells after exposure to 0.5% O_2 and 0.1% O_2 respectively, for a range of time points. It can be observed that, whilst there is no clear alteration in expression levels of what has been identified as the pro-form of ADAM 10 (80 kDa), there are visible alterations in the levels and nature of the mature form of ADAM 10 (65 kDa). After 2 hours in both severe hypoxia oxygen tensions, an apparent doublet band was visible in the mature form of ADAM 10, and remained present for the duration of the hypoxic exposure (**Figures 3.1 A** and **3.2 A**). Despite clearly observable alterations in the banding pattern of mature ADAM 10, when analysed by densitometry this did not correspond to a statistically significant increase. Limitations of densitometry analysis in the context of the aforementioned results can be seen in **Figure 3.3**. Individual experimental repeats of ADAM 10 expression in HCT116 cells after exposure to 0.5% O_2. all showed the same pattern of expression, with little or no alteration in pro-form levels but clear alterations in the expression of mature form ADAM 10 were visible

A)

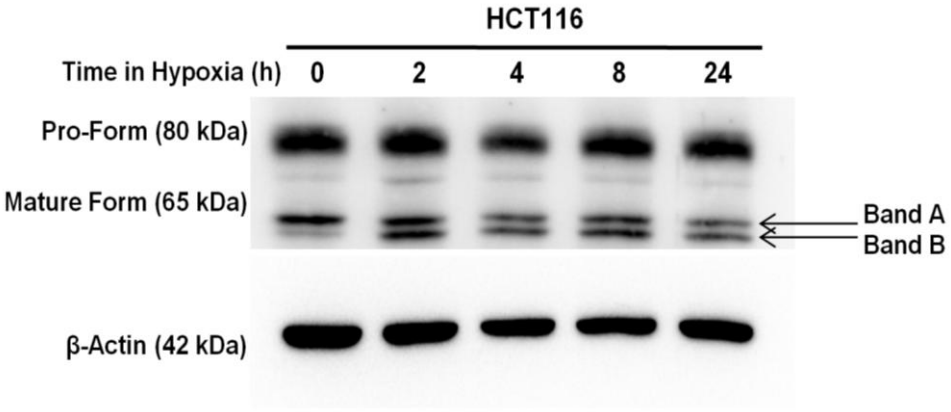

B)

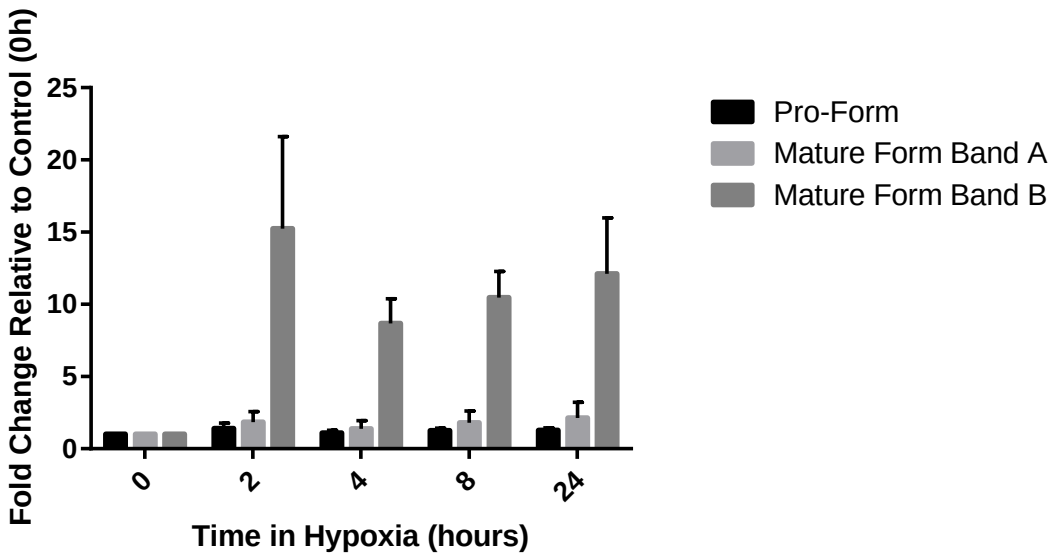

Figure 3.1: Expression of ADAM 10 in Severe Hypoxia (0.5% O_2) in HCT116 Cells

A - HCT116 cells were exposed to hypoxia (0.5% O_2) for a range of time points. Cells were lysed, 30 μg of each protein sample were separated by SDS-PAGE and expression of ADAM 10 protein was analysed by Western Blotting. The mature form of ADAM 10 is visible as a doublet, comprised of higher (Band A) and lower (Band B) molecular weight bands. β-Actin was used as a loading control. Blots shown are representative of three independent experiments.

B - Densitometry analysis of band intensity for the pro-form and mature form of ADAM 10 was carried out using Image Lab software. All values were normalised to the loading control. Results are expressed as fold change relative to the 0h control of n=3 experiments. Error bars represent +/- SEM. Statistical analysis by one way ANOVA, with Dunnett's post-hoc correction. All results deemed non-significant.

A)

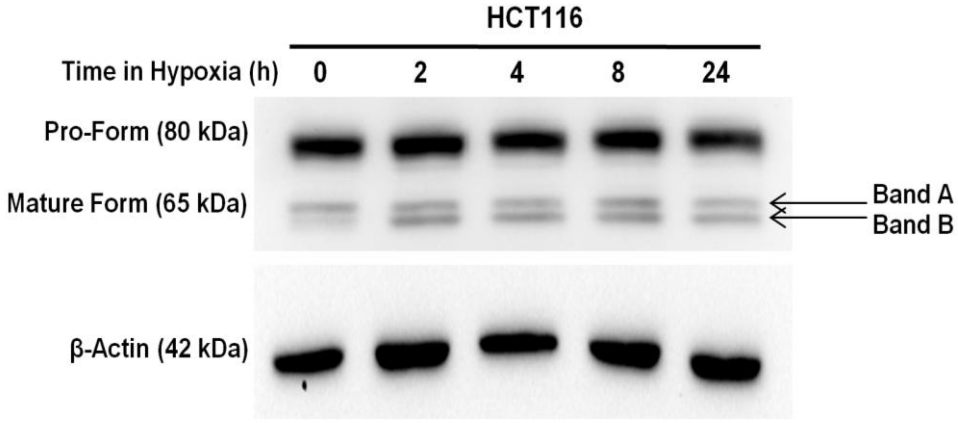

B)

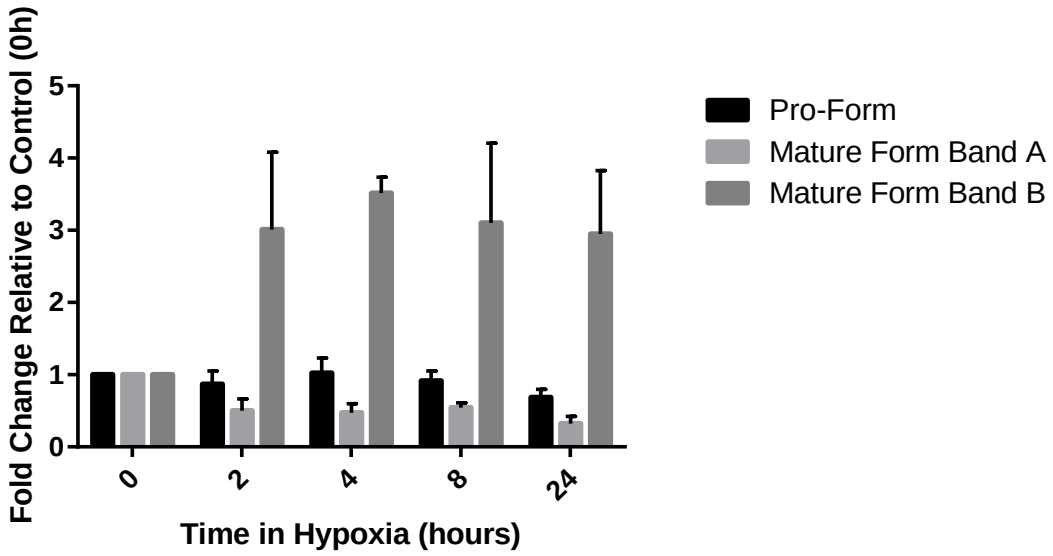

Figure 3.2: Expression of ADAM 10 in Severe Hypoxia (0.1% O_2) in HCT116 Cells

A - HCT116 cells were exposed to hypoxia (0.1% O_2) for a range of time points. Cells were lysed, 30 µg of each protein sample were separated by SDS-PAGE and expression of ADAM 10 protein was analysed by Western Blotting. The mature form of ADAM 10 is visible as a doublet, comprised of higher (Band A) and lower (Band B) molecular weight bands. β-Actin was used as a loading control. Blots shown are representative of three independent experiments.

B - Densitometry analysis of band intensity for the pro-form and mature form of ADAM 10 was carried out using Image Lab software. All values were normalised to the loading control. Results are expressed as fold change relative to the 0h control of n=3 experiments. Error bars represent +/- SEM. Statistical analysis by one way ANOVA, with Dunnett's post-hoc correction. All results deemed non-significant.

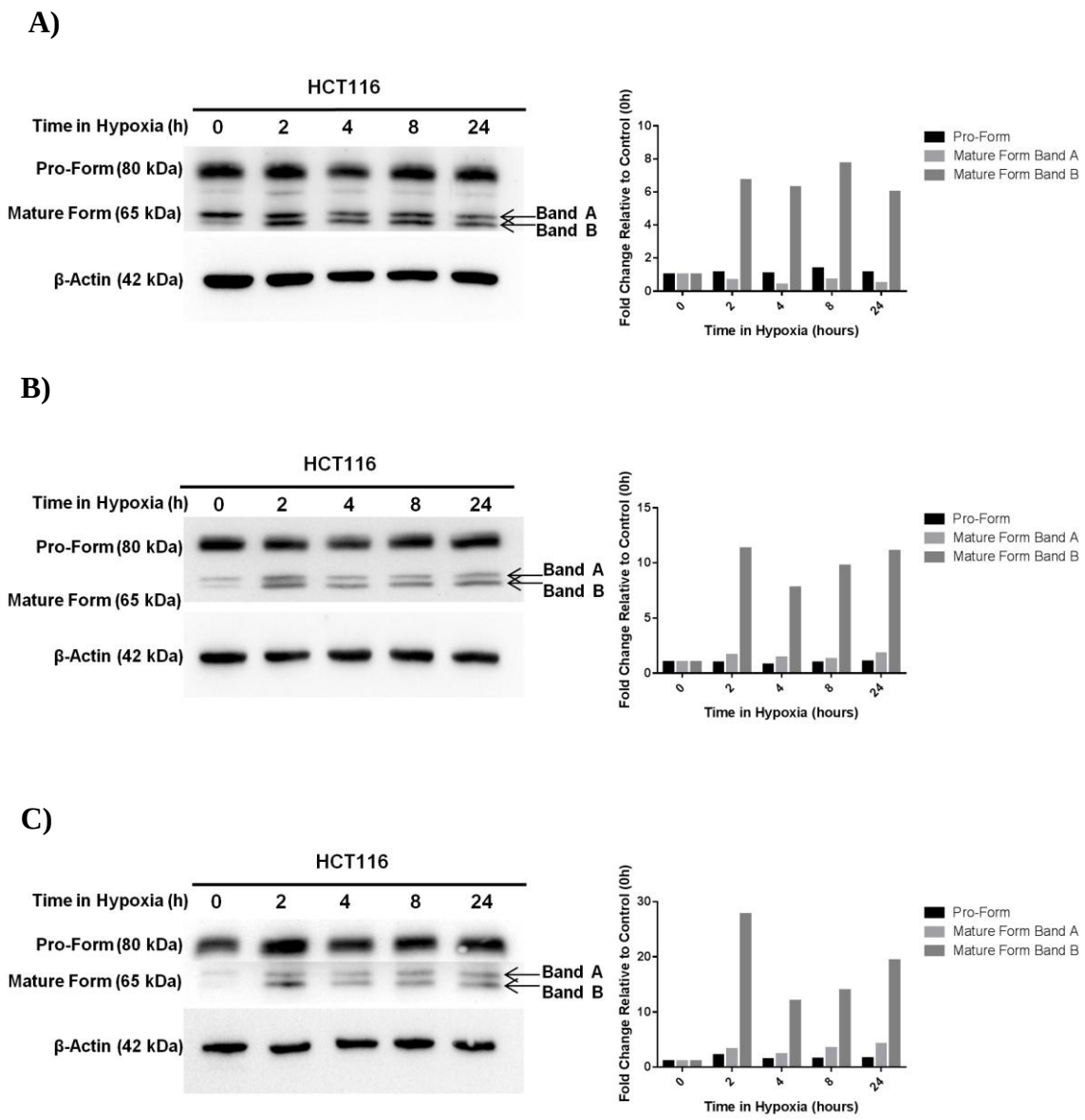

Figure 3.3: Comparative Figure Illustrating Individual Repeats for HCT116 Cells after Exposure to Severe Hypoxia

Blots shown represent the three independent experiment repeats (A, B & C) to illustrate the deviation in densitometry analysis between them.

HCT116 cells were exposed to hypoxia (0.5% O_2) for a range of time points. Cells were lysed, 30 µg of each protein sample were separated by SDS-PAGE and expression of ADAM 10 protein was analysed by Western Blotting. The mature form of ADAM10 is visible as a doublet, comprised of higher (Band A) and lower (Band B) molecular weight bands. β-Actin was used as a loading control.

Densitometry analysis of band intensity for the pro-form and mature form of ADAM 10 was carried out using Image Lab Software. All values were normalised to the loading control. Results expressed as fold change relative to the 0h control.

(**Figure 3.3**). It can be consistently observed that, a faint doublet band is present at the 0 hours time point (normoxic control), which intensifies after exposure to severe hypoxia. Band B of the doublet is repeatedly clearly increased during the hypoxic exposure. However, when quantitatively analysed by densitometry, due to the varying levels of quantification among experimental repeats, no significance is present.

Expression of ADAM 10 in HT29 colorectal cancer cells after exposure to 0.5% O_2 and 0.1% O_2 can be observed in **Figure 3.4** and **Figure 3.5** respectively. Western blot banding patterns indicate an increase in both the pro and mature forms of ADAM 10, with a doublet band visible for mature ADAM 10 after hypoxic exposure, similar to that observed for HCT116 (**Figures 3.1 A** and **3.2 A**). However, when quantitatively analysed by densitometry no statistical significance was found for changes of either pro or mature forms of ADAM 10 upon exposure to hypoxia. No clear increases in ADAM 10 pro-form protein were observed for RKO cells after exposure 0.5% O_2 and 0.1% O_2 (**Figure 3.6** and **Figure 3.7** respectively). However, as with HCT116 and HT29 cells, a doublet form of mature ADAM 10 was visible, with increases after exposure to hypoxia. However, any visible increases did not correlate to significant upregulation in protein levels when quantitatively analysed. Whilst non-significant in nature, it is clearly observable from these data that even a short exposure of CRC cells to severe hypoxia (0.1% - 0.5% O_2) lead to a resolution of mature ADAM 10 into a doublet band.

3.3.1.2 *ADAM 10* is Induced by Hypoxia at Transcript Level

In order to assess any contribution of transcriptional changes to the alterations in ADAM 10 protein expression, *ADAM 10* mRNA levels were assessed by qPCR. **Figure 3.8** depicts the expression of *ADAM 10* after exposure to severe hypoxia in HCT116 cells. Little alteration is seen in the expression of *ADAM 10* after exposure to either

A)

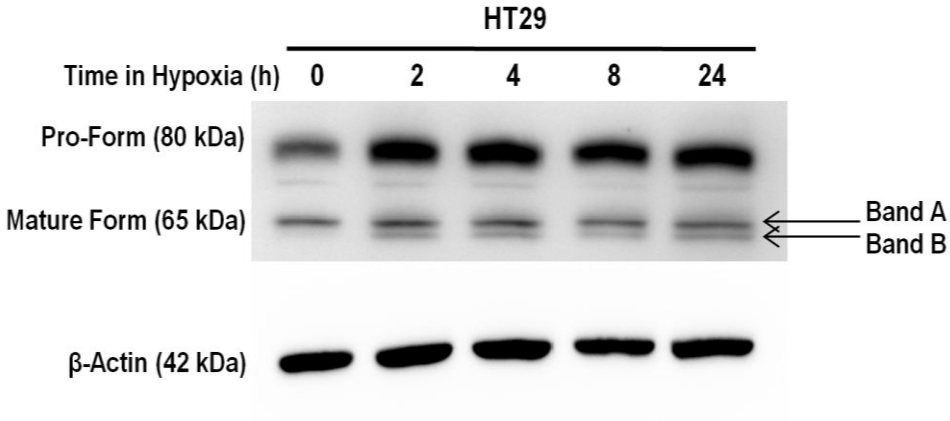

B)

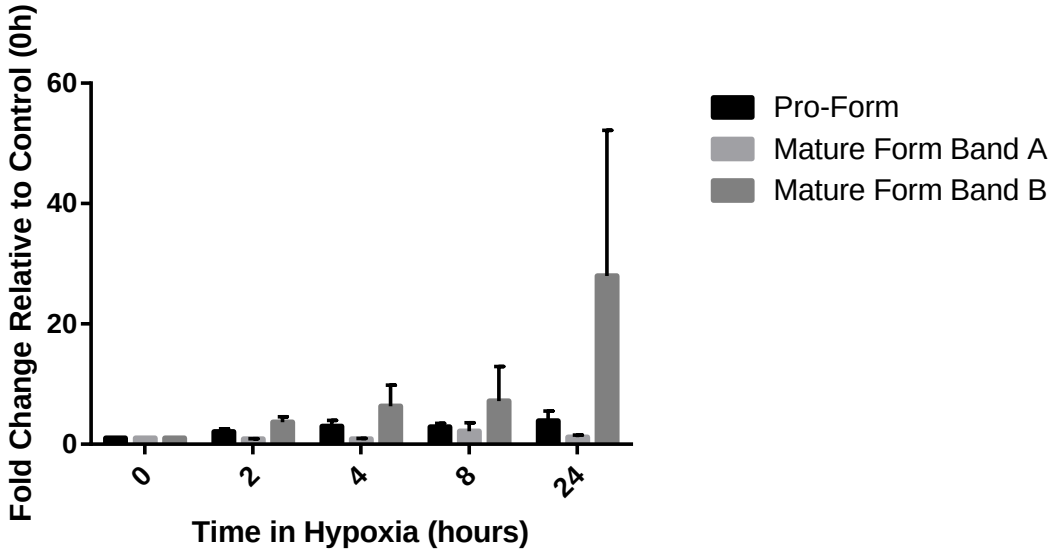

Figure 3.4: Expression of ADAM 10 in Severe Hypoxia (0.5% o_2) in HT29 Cells

A – HT29 cells were exposed to hypoxia (0.5% O_2) for a range of time points. Cells were lysed, 30 μg of each protein sample were separated by SDS-PAGE and expression of ADAM 10 protein was analysed by Western Blotting. The mature form of ADAM 10 is visible as a doublet, comprised of higher (Band A) and lower (Band B) molecular weight bands. β-Actin was used as a loading control. Blots shown are representative of three independent experiments.

B - Densitometry analysis of band intensity for the pro-form and mature form of ADAM 10 was carried out using Image Lab software. All values were normalised to the loading control. Results are expressed as fold change relative to the 0h control of n=3 experiments. Error bars represent +/- SEM. Statistical analysis by one way ANOVA, with Dunnett's post-hoc correction. All results deemed non-significant.

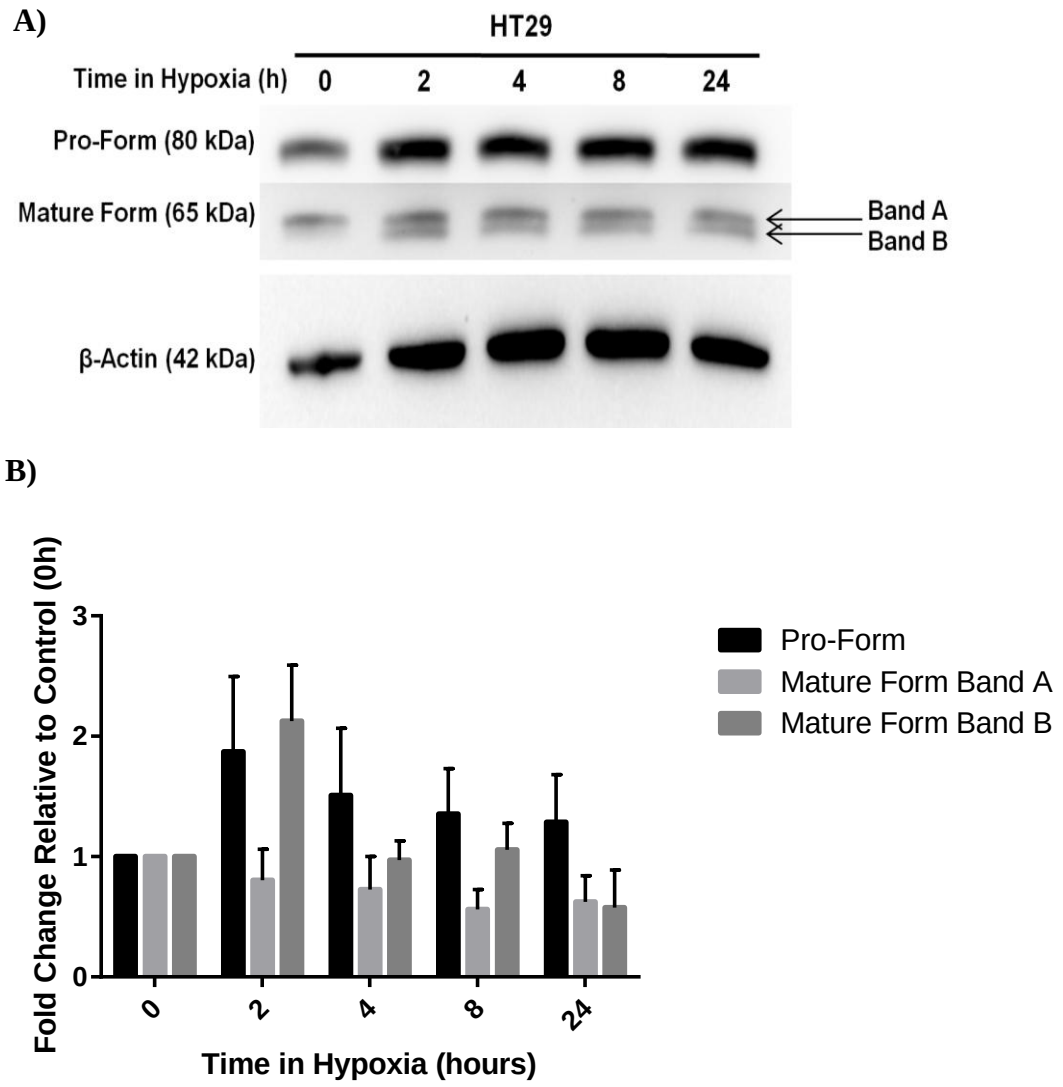

Figure 3.5: Expression of ADAM 10 in Severe Hypoxia (0.1% O_2) in HT29 Cells

A – HT29 cells were exposed to hypoxia (0.1% O_2) for a range of time points. Cells were lysed, 30 µg of each protein sample were separated by SDS-PAGE and expression of ADAM 10 protein was analysed by Western Blotting. The mature form of ADAM 10 is visible as a doublet, comprised of higher (Band A) and lower (Band B) molecular weight bands. β-Actin was used as a loading control. Blots shown are representative of three independent experiments.

B - Densitometry analysis of band intensity for the pro-form and mature form of ADAM 10 was carried out using Image Lab software. All values were normalised to the loading control. Results are expressed as fold change relative to the 0h control of n=3 experiments. Error bars represent +/- SEM. Statistical analysis by one way ANOVA, with Dunnett's post-hoc correction. All results deemed non-significant.

A)

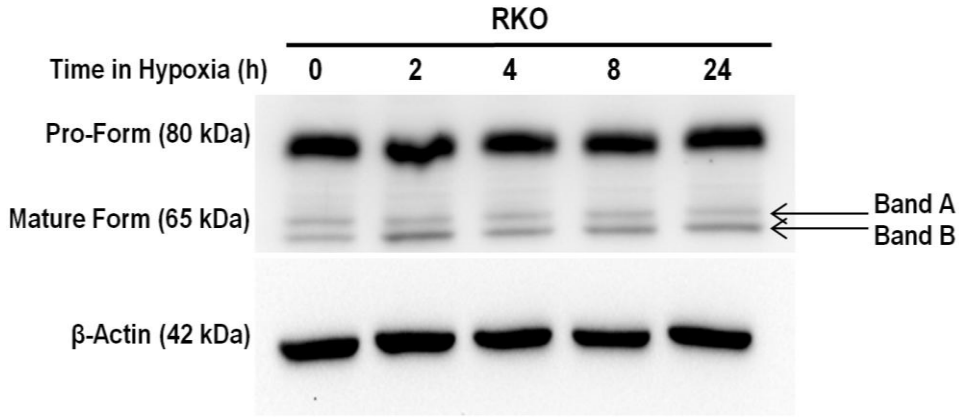

B)

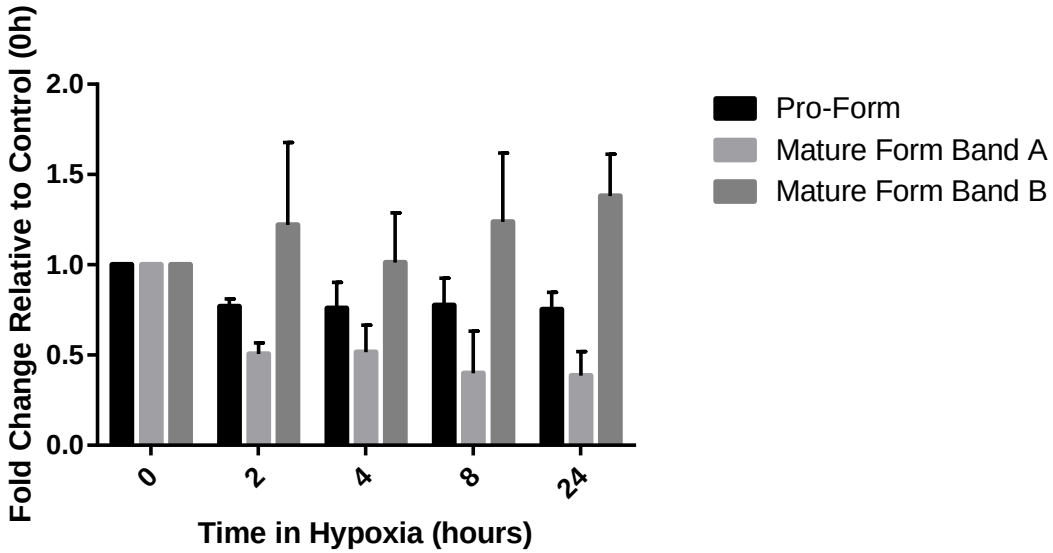

Figure 3.6: Expression of ADAM 10 in Severe Hypoxia (0.5% O_2) in RKO Cells

A – RKO cells were exposed to hypoxia (0.5% O_2) for a range of time points. Cells were lysed, 30 µg of each protein sample were separated by SDS-PAGE and expression of ADAM 10 protein was analysed by Western Blotting. The mature form of ADAM 10 is visible as a doublet, comprised of higher (Band A) and lower (Band B) molecular weight bands. β-Actin was used as a loading control. Blots shown are representative of three independent experiments.

B - Densitometry analysis of band intensity for the pro-form and mature form of ADAM 10 was carried out using Image Lab software. All values were normalised to the loading control. Results are expressed as fold change relative to the 0h control of n=3 experiments. Error bars represent +/- SEM. Statistical analysis by one way ANOVA, with Dunnett's post-hoc correction. All results deemed non-significant.

A)

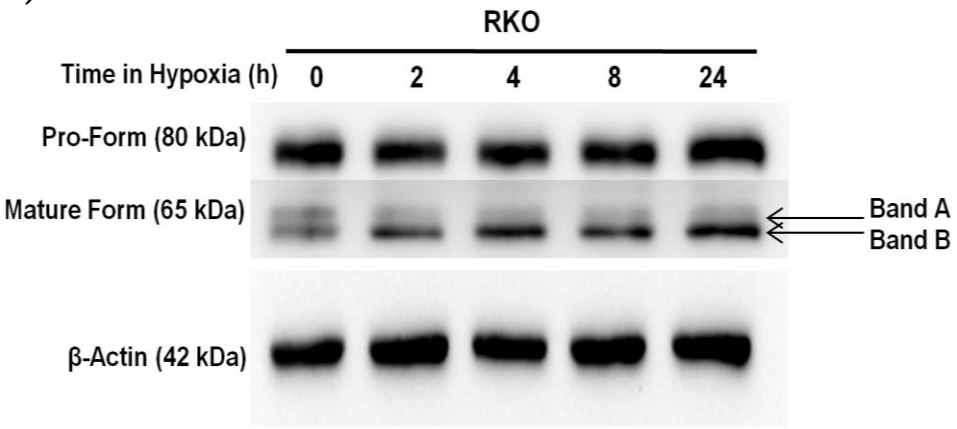

B)

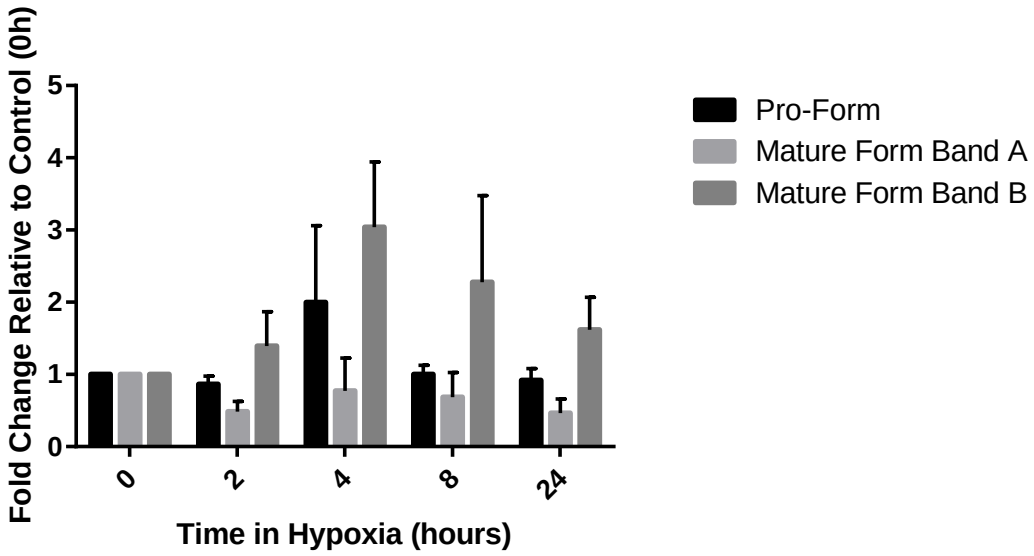

Figure 3.7: Expression of ADAM 10 in Severe Hypoxia (0.1% O_2) in RKO Cells

A – RKO cells were exposed to hypoxia (0.1% O_2) for a range of time points. Cells were lysed, 30 µg of each protein sample were separated by SDS-PAGE and expression of ADAM 10 protein was analysed by Western Blotting. The mature form of ADAM 10 is visible as a doublet, comprised of higher (Band A) and lower (Band B) molecular weight bands. β-Actin was used as a loading control. Blots shown are representative of three independent experiments.

B - Densitometry analysis of band intensity for the pro-form and mature form of ADAM 10 was carried out using Image Lab software. All values were normalised to the loading control. Results are expressed as fold change relative to the 0h control of n=3 experiments. Error bars represent +/- SEM. Statistical analysis by one way ANOVA, with Dunnett's post-hoc correction. All results deemed non-significant.

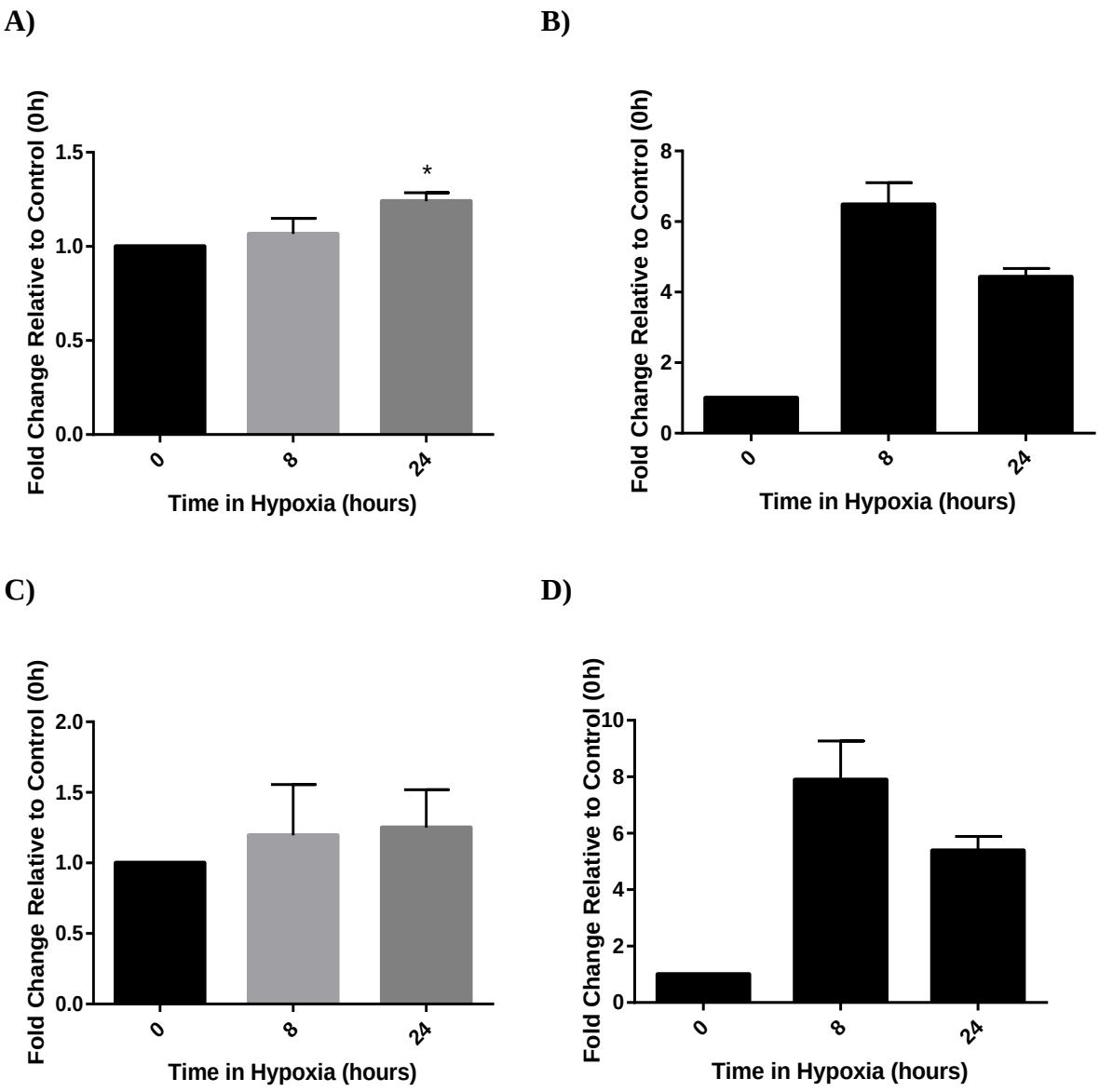

Figure 3.8: Expression of *ADAM 10* in severe hypoxia in HCT116 cells

HCT116 cells were exposed to hypoxia 0.5% O_2 (A & B) or 0.1% O_2 (C & D) for a range of time points. mRNA was extracted (as described in Section 2.23), and *ADAM 10* (A & C) or *SLC2A1* (B & D) expression analysed by qPCR (as described in Section 2.26). All results are normalised to the housekeeping gene, *B2M*. *SLC2A1* expression used as a control for confirmation of hypoxic induction. Results are expressed as fold change relative to the 0 h control (normoxia). A & C) n=3 experiments; Error bars represent +/- SEM; Statistical analysis by one way ANOVA, with Tukey's post-hoc correction. * $p<0.05$. B & D) n=2 experiments; Error bars represent +/- STDEV.

0.5% O_2 or 0.1% O_2, however a statistically significant, albeit small increase (1.24 ± 0.1-fold), was observed after 24 hours in 0.5% O_2.

3.3.1.3 *ADAM 10* is Induced by Hypoxia at Transcript Level

In order to assess any contribution of transcriptional changes to the alterations in ADAM 10 protein expression, *ADAM 10* mRNA levels were assessed by qPCR. **Figure 3.8** depicts the expression of *ADAM 10* after exposure to severe hypoxia in HCT116 cells. Little alteration is seen in the expression of *ADAM 10* after exposure to either 0.5% O_2 or 0.1% O_2, however a statistically significant, albeit small increase (1.24 ± 0.1-fold), was observed after 24 hours in 0.5% O_2. Similarly, little or no increase is seen for HT29 cells exposed to either 0.5% O_2 or 0.1% O_2 (**Figure 3.9**). However, a small (1.18 ± 0.1-fold) but significant increase is observed after 24 hours in hypoxia (0.5% O_2). RKO cells show a similar trend after hypoxic exposure (0.5% O_2; and 0.1% O_2;) but with no significance seen (1.72 ± 0.3-fold change) (**Figure 3.10**). In all cell lines the trends indicating a small increase in *ADAM 10* expression are consistent across both oxygen tensions examined (0.5% O_2 and 0.1% O_2). These data indicate that *ADAM 10* is not a canonical hypoxia-inducible gene in CRC. Analysis of *SLC2A1* expression shows increases after 8 and 24 hours in both 0.5% and 0.1% O_2, thus confirming presence of hypoxia.

3.3.2 ADAM 10 is Identified by Mass Spectrometry

Mass-spectrometry analysis was undertaken to confirm the identity of the mature form ADAM 10 doublet described earlier in this chapter. **Figure 3.11** depicts the Coomassie stained SDS-PAGE gel separation of the HT29 ADAM 10 immunoprecipitation (IP) samples, in preparation for the mass-spectrometric analysis. HT29 cells were selected due to their complete lack of doublet band in normoxic ADAM 10, in comparison to

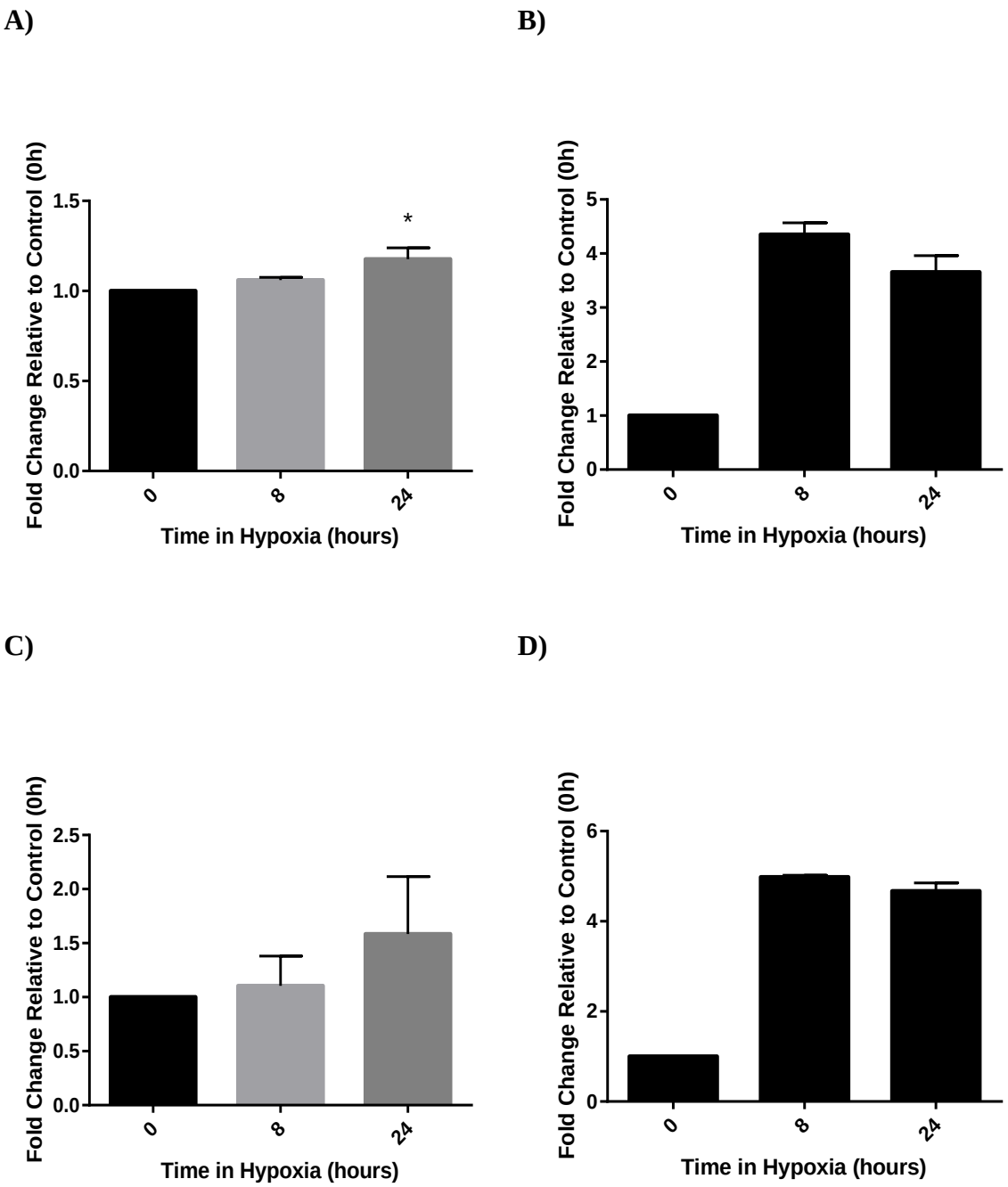

Figure 3.9: Expression of *ADAM 10* in severe hypoxia in HT29 cells

HT29 cells were exposed to hypoxia 0.5% O_2 (A & B) or 0.1% O_2 (C & D) for a range of time points. mRNA was extracted (as described in Section 2.23), and *ADAM 10* (A & C) or *SLC2A1* (B & D) expression analysed by qPCR (as described in Section 2.26). All results are normalised to the housekeeping gene, *B2M*. *SLC2A1* expression used as a control for confirmation of hypoxic induction. Results are expressed as fold change relative to the 0 h control (normoxia). A & C) n=3 experiments; Error bars represent +/- SEM; Statistical analysis by one way ANOVA, with Tukey's post-hoc correction. * $p<0.05$. B & D) n=2 experiments; Error bars represent +/- STDEV.

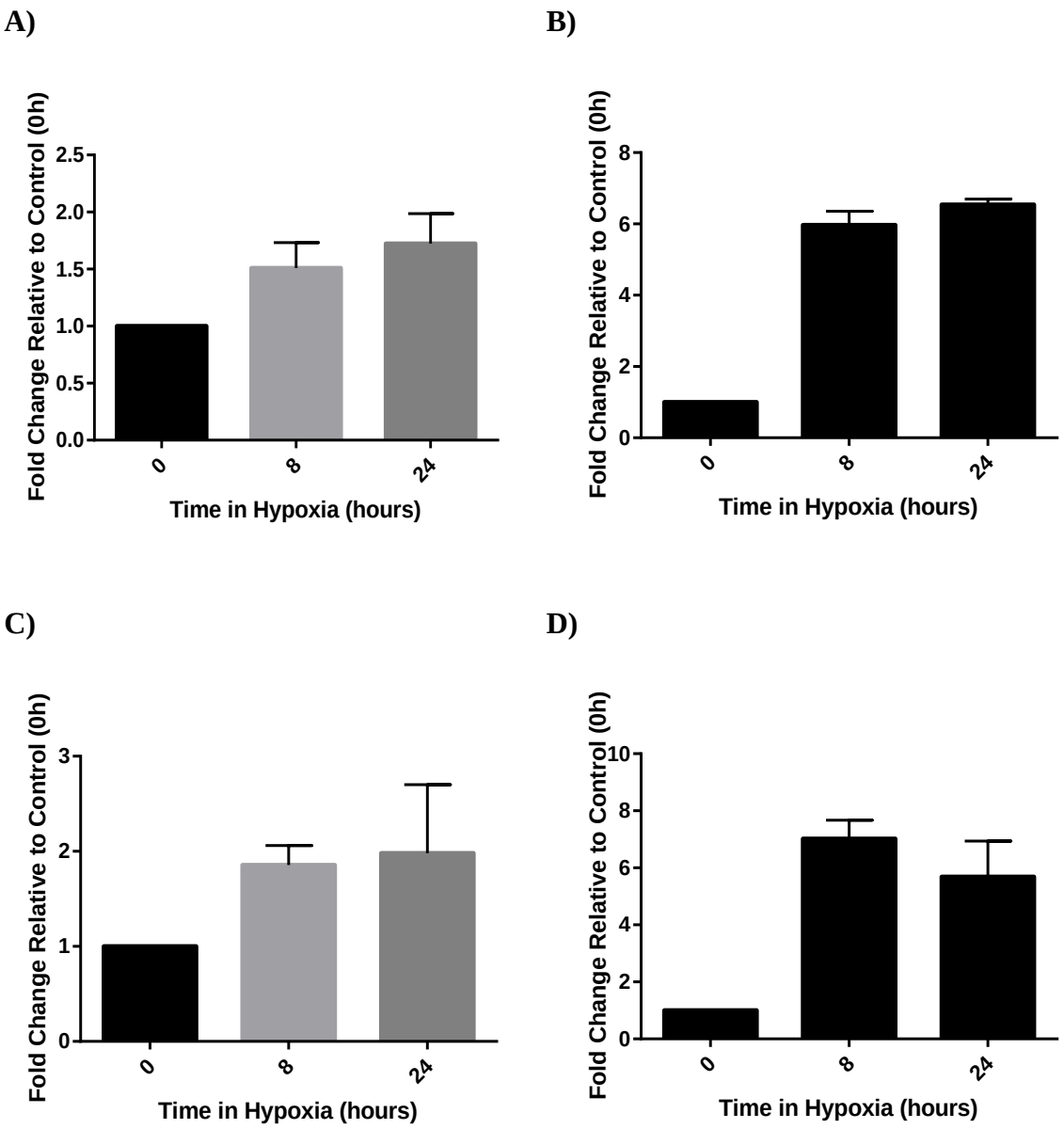

Figure 3.10: Expression of *ADAM 10* in severe hypoxia in RKO cells

RKO cells were exposed to hypoxia 0.5% O_2 (A & B) or 0.1% O_2 (C & D) for a range of time points. mRNA was extracted (as described in Section 2.23), and *ADAM 10* (A & C) or *SLC2A1* (B & D) expression analysed by qPCR (as described in Section 2.26). All results are normalised to the housekeeping gene, *B2M*. *SLC2A1* expression used as a control for confirmation of hypoxic induction. Results are expressed as fold change relative to the 0 h control (normoxia). A & C) n=3 experiments; Error bars represent +/- SEM; Statistical analysis by one way ANOVA, with Tukey's post-hoc correction. * $p<0.05$. B & D) n=2 experiments; Error bars represent +/- STDEV.

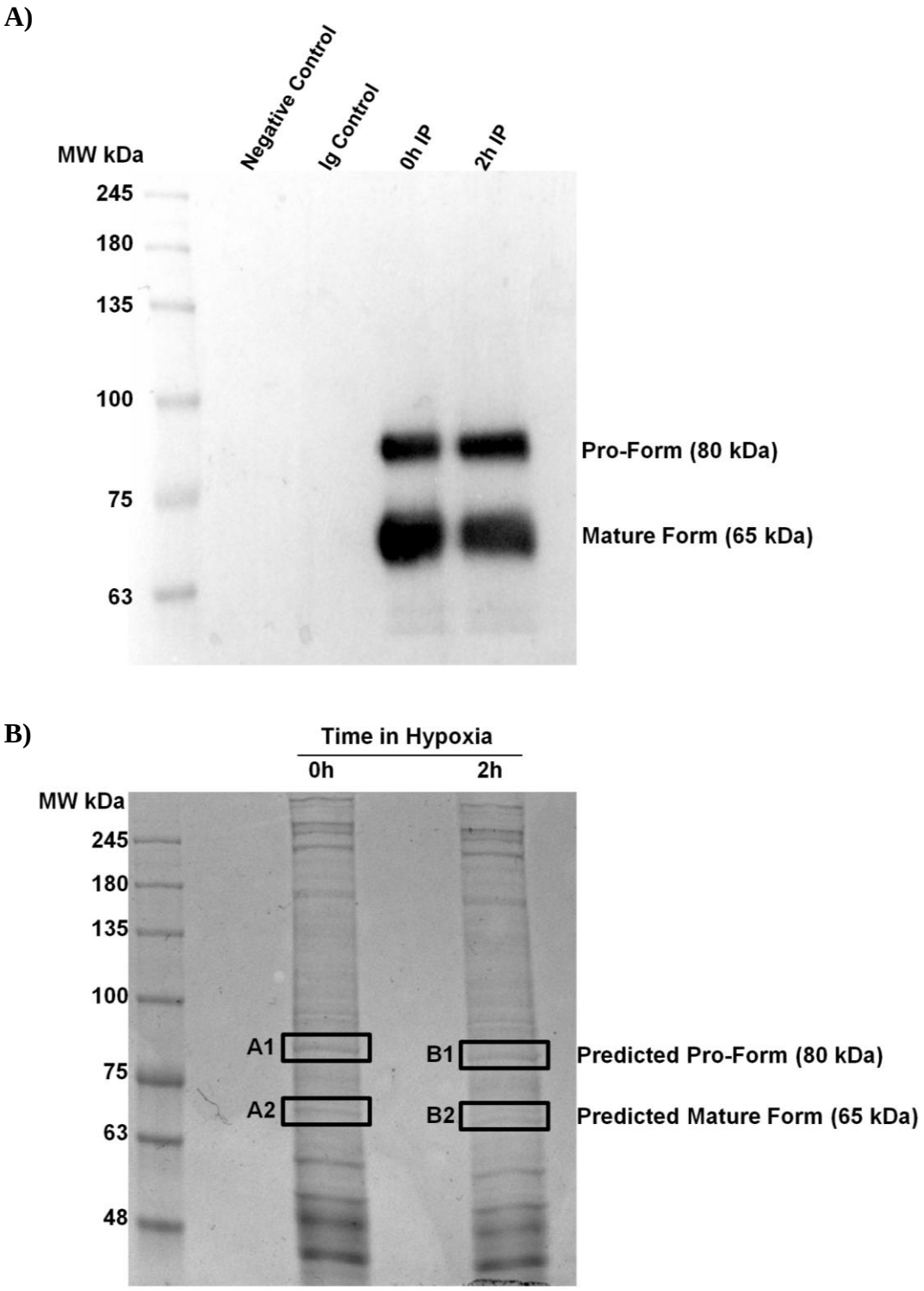

Figure 3.11: Visualisation of MS Sample Location

HT29 cells were exposed to severe hypoxia (0.5% O_2) for 2 hours before being lysed and undergoing ADAM 10 immunoprecipitation. Samples were then separated by SDS-PAGE and underwent either Western Blotting for ADAM 10 protein (A) or were stained with Coomassie Blue (B). After confirming success of ADAM 10 pull down via Western Blot (A) gel bands in the locations of ADAM 10 pro-form and mature form were cut and sent for MALDI-MS or LC-MS analysis.

HCT116 and RKO cells that have faint doublet expression. The locations of the excised bands sent for MALDI-MS analysis can be observed within **Figure 3.11**, where faint bands, expected to be the pro-form and mature form of ADAM 10, can be seen within the excised regions. The bands cut out and sent for analyses are identified by A1, A2, B1 and B2. These correspond to the predicted molecular weight regions of both the pro (~80kDa) and mature (~60kDa) forms of ADAM 10. A1 or A2 bands were excised from the normoxic sample, whereas B1 or B2 bands were taken from the hypoxia exposed sample. Initially, MALDI-MS analysis was carried out on excised SDS-PAGE bands by the Proteomics and Analytical Biochemistry Laboratory, University of York. However, the only peptide hits obtained were for known IP contaminants (such as Heat shock protein 90 and Heat shock cognate 71), which indicates that a more sensitive approach needed to be utilised. LC-MS was therefore utilised next, as it is a more sensitive analytical methodology. Immunoprecipitation of ADAM 10 was undertaken, followed by separation by SDS-PAGE, band excision, processing and analysis (as for the MALDI-MS). Peptides belonging to ADAM 10 protein were identified through MASCOT database analysis and then mapped to the ADAM 10 amino acid sequence (**Figure 3.12**) to identify which domain they originate from within the ADAM 10 protein.

ADAM 10 peptides were successfully identified by LC-MS, and mapped onto the domains within the ADAM 10 protein to which they belong (**Table 3.1** - **Table 3.4**). **Table 3.1** - **Table 3.4** were compiled from two intra-experimental LC-MS repeats. As peptides identified within each run were the same, albeit varying in numbers, the results were amalgamated into one. **Table 3.1** shows the peptides identified within the normoxic (0h) pro-form band. It can be observed that peptides originating from the pro-domain of the ADAM 10 protein are present. Such peptides are also present in

A)

```
  1 mvllrvlill lswaagmggq ygnplnkyir hyeglsynvd slhqkhqrak ravshedqfl
 61 rldfhahgrh fnlrmkrdts lfsdefkvet snkvldydts hiytghiyge egsfshgsvi
121 dgrfegfiqt rggtfyvepa eryikdrtlp fhsviyhedd inyphkygpq ggcadhsvfe
181 rmrkyqmtgv eevtqipqee haangpellr kkrttsaekn tcqlyiqtdh lffkyygtre
241 aviaqisshv kaidtiyqtt dfsgirnisf mvkririntt adekdptnpf rfpnigvekf
301 lelnseqnhd dyclayvftd rdfddgvlgl awvgapsgss ggicekskly sdgkkkslnt
361 giitvqnygs hvppkvshit fahevghnfg sphdsgtect pgesknlgqk engnyimyar
421 atsgdklnnn kfslcsirni sqvlekkrnn cfvesgqpic gngmveqgee cdcgysdqck
481 deccfdanqp egrkcklkpg kqcspsqgpc ctaqcafksk sekcrddsdc aregicngft
541 alcpasdpkp nftdcnrhtq vcingqcags icekygleec tcassdgkdd kelchvccmk
601 kmdpstcast gsvqwsrhfs grtitlqpgs pcndfrgycd vfmrcrlvda dgplarlkka
661 ifspelyeni aewivahwwa vllmgialim lmagfikics vhtpssnpkl pppkplpgtl
721 krrrppqpiq qpqrqrpres yqmghmrr
```

B)

Domain	Amino Acid Location	No of Amino Acids
Signal	1-18	18
Pro	19-213	195
Metalloproteinase	214-455	242
Disintegrin	456-551	96
Cysteine Rich	552-672	121
Transmembrane	673-696	24
Cytoplasmic	697-748	52

C)

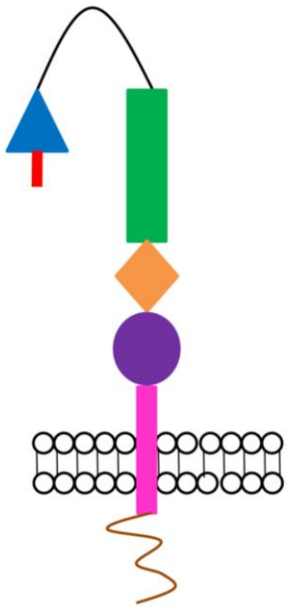

Figure 3.12: ADAM 10 Protein Sequence and Domain Location

A) Amino acid sequence for ADAM 10, colour coded to denote the domains of the ADAM 10 protein.

B) Table detailing the amino acid locations for each domain and the amount of amino acids present within each

C) Schematic diagram of the ADAM 10 structure, including the different domains, colour coded to correspond to the amino acid sequence above

Table 3.1: ADAM 10 Peptides as Identified by LC-MS for 0h Pro-Form (80 kDa band)

Peptide Sequence	Amino Acid Location	Domain Location
HYEGLSYNVDSLHQK	31-45	Pro
DTSLFSDEFKVETSNK	78-93	Pro
EAVIAQISSHVK	240-251	Metalloproteinase
AIDTIYQTTDFSGIR	252-266	Metalloproteinase
AIDTIYQTTDFSGIR	252-266	Metalloproteinase
NISFMVK	267-273	Metalloproteinase
ENGNYIMYAR	411-420	Metalloproteinase
ENGNYIMYAR	411-420	Metalloproteinase
ENGNYIMYAR	411-420	Metalloproteinase
LVDADGPLAR	647-656	Cysteine Rich
LVDADGPLAR	647-656	Cysteine Rich
LPPPKPLPGTLK	710-721	Cytoplasmic

Table 3.2: ADAM 10 Peptides as Identified by LC-MS for 0h Mature Form (65 kDa band)

Peptide Sequence	Amino Acid Location	Domain Location
EAVIAQISSHVK	240-251	Metalloproteinase
EAVIAQISSHVK	240-251	Metalloproteinase
AIDTIYQTTDFSGIR	252-266	Metalloproteinase
AIDTIYQTTDFSGIR	252-266	Metalloproteinase
NISFMVK	267-273	Metalloproteinase
FPNIGVEK	292-299	Metalloproteinase
FPNIGVEK	292-299	Metalloproteinase
SLNTGIITVQNYGSHVPPK	357-375	Metalloproteinase
ENGNYIMYAR	411-420	Metalloproteinase
ENGNYIMYAR	411-420	Metalloproteinase
ENGNYIMYAR	411-420	Metalloproteinase
ENGNYIMYAR	411-420	Metalloproteinase
LVDADGPLAR	647-656	Cysteine Rich
LVDADGPLAR	647-656	Cysteine Rich
LPPPKPLPGTLK	710-721	Cytoplasmic
LPPPKPLPGTLKR	710-722	Cytoplasmic
RRPPQPIQQPQR	723-734	Cytoplasmic
ESYQMGHMR	739-747	Cytoplasmic

Table 3.3: ADAM 10 Peptides as Identified by LC-MS for 2h Pro-Form (80 kDa band)

Peptide Sequence	Amino Acid Location	Domain Location
HYEGLSYNVDSLHQK	31-45	Pro
LDFHAHGR	62-69	Pro
FEGFIQTR	124-131	Pro
EAVIAQISSHVK	240-251	Metalloproteinase
EAVIAQISSHVK	240-251	Metalloproteinase
AIDTIYQTTDFSGIR	252-266	Metalloproteinase
AIDTIYQTTDFSGIR	252-266	Metalloproteinase
NISFMVK	267-273	Metalloproteinase
FPNIGVEK	292-299	Metalloproteinase
SLNTGIITVQNYGSHVPPK	357-375	Metalloproteinase
ENGNYIMYAR	411-420	Metalloproteinase
ENGNYIMYAR	411-420	Metalloproteinase

LVDADGPLAR	647-656	Cysteine Rich
LVDADGPLAR	647-656	Cysteine Rich
LPPPKPLPGTLK	710-721	Cytoplasmic

Table 3.4: ADAM 10 Peptides as Identified by LC-MS for 2h Mature Form (65 kDa band)

Peptide Sequence	Amino Acid Location	Domain Location
GGTFYVEPAER	132-142	Pro
EAVIAQISSHVK	240-251	Metalloproteinase
EAVIAQISSHVK	240-251	Metalloproteinase
AIDTIYQTTDFSGIR	252-266	Metalloproteinase
AIDTIYQTTDFSGIR	252-266	Metalloproteinase
FPNIGVEK	292-299	Metalloproteinase
FPNIGVEK	292-299	Metalloproteinase
SLNTGIITVQNYGSHVPPK	357-375	Metalloproteinase
ENGNYIMYAR	411-420	Metalloproteinase
ENGNYIMYAR	411-420	Metalloproteinase
LVDADGPLAR	647-656	Cysteine Rich
LVDADGPLAR	647-656	Cysteine Rich

Table 3.3, which details peptides found within the 2h hypoxic pro-form sample. There was only one pro-domain peptide present within the two mature form samples (**Table 3.2** & **Table 3.4**). The majority of peptides identified within all analysed samples originate from the metalloproteinase domain, with peptides from the cysteine rich and cytoplasmic domains also being identified. Some peptides identified were identical to those found within other analysed samples and some were detected more than once within the same sample. A number of other protein peptides were also identified alongside the ADAM 10 peptides. As contaminants were observed in the MALDI-MS analysis, the obtained datasets were analysed using the CRAPome database, to eliminate known contaminants of protein immunoprecipitation. After this analysis, a list of non-contaminant proteins was compiled (**Appendix 1**).

3.3.3 Characterisation of ADAM 10 Doublet Banding Pattern

Attempts to characterise potential alterations to ADAM 10 expression in hypoxic conditions identified the occurrence of a potential hypoxia-associated doublet form of ADAM 10 (**Section 3.3.1.1**). Alongside the direct protein ID, via the proteomic analysis

(**Section 3.3.2**), potential post-translational modifications, such as cleavage and glycosylation, which are known to affect ADAM 10, were investigated. First, the cleavage of ADAM 10 by γ-secretase was analysed using specific inhibitor DBZ. Furthermore, the glycosylation status of ADAM 10 in the CRC cell lines in normoxia and hypoxia was also analysed.

3.3.3.1 γ-secretase Inhibition does not Prevent ADAM 10 Doublet Formation

In order to determine whether exposure to severe hypoxia exerts a γ-secretase mediated cleavage of mature ADAM 10, HCT116 cells were treated with 100 nM or 500 nM DBZ, a known inhibitor of γ-secretase. ADAM 10 protein expression was then analysed by Western Blotting (**Figure 3.13**). As observed previously, the doublet form of mature ADAM 10 was clearly identifiable in hypoxic samples, with only a single band visible in the normoxic samples (**Figure 3.13**). Treatment with γ-secretase inhibitor, DBZ, did not prevent ADAM 10 doublet band formation under hypoxic conditions. The mature ADAM 10 doublet band was still present after treatment with both DBZ concentrations in hypoxia (**Figure 3.13**). Neither of the two DBZ treatment regimes had an effect on doublet formation either. These data indicated that it is unlikely that the hypoxic doublet formation is associated with a cleavage of mature ADAM 10 by γ-secretase in low oxygen conditions.

3.3.3.2 ADAM 10 Glycosylation is Altered under Hypoxic Conditions in CRC Cells

In order to evaluate if the doublet observed for hypoxic mature ADAM 10 is the result of glycosylation, Concanavalin A affinity purification pull-downs were performed for all cell lines in normoxic and hypoxic conditions (2 hours exposure at 0.5% O_2). As it can be observed in **Figure 3.14 - Figure 3.16**, input samples for all three cell lines, display the ADAM 10 banding pattern described earlier in this chapter, with both pro-

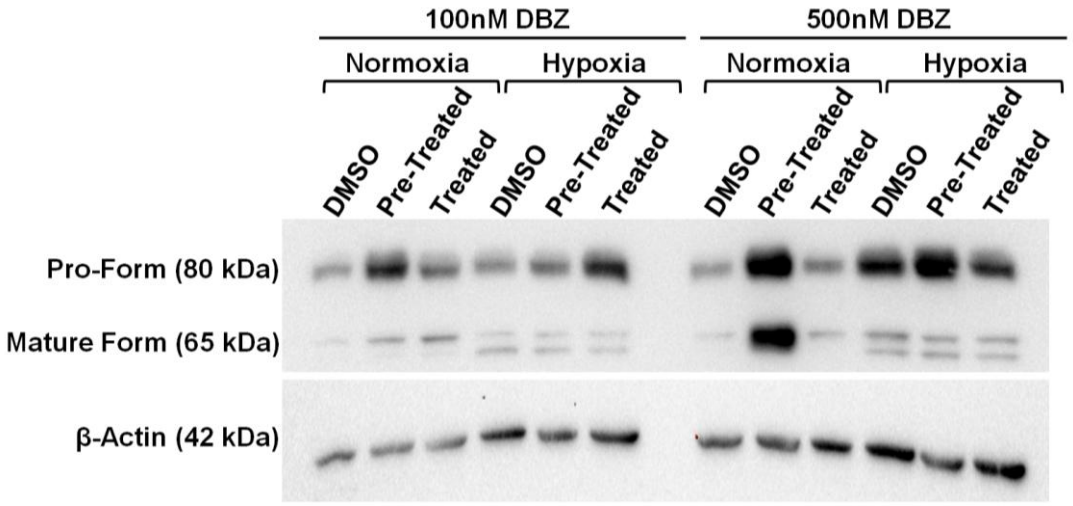

Figure 3.13: Effect of γ-secretase Inhibition on ADAM 10 Doublet Formation in HCT116 cells

HCT116 cells were treated with 100 nM or 500 nM DBZ before being exposed to severe hypoxia (0.5% O_2). Pre-treatment cells were treated for 6 hours prior to hypoxic exposure (as described in Section 2.14). Cells were lysed, 30 μg of each protein samples were separated by SDS-PAGE and expression of ADAM 10 protein analysed by Western Blotting. HCT116 cells were treated with DMSO as the vehicle control and β-Actin was used as a loading control. Blot is representative of two individual experiments.

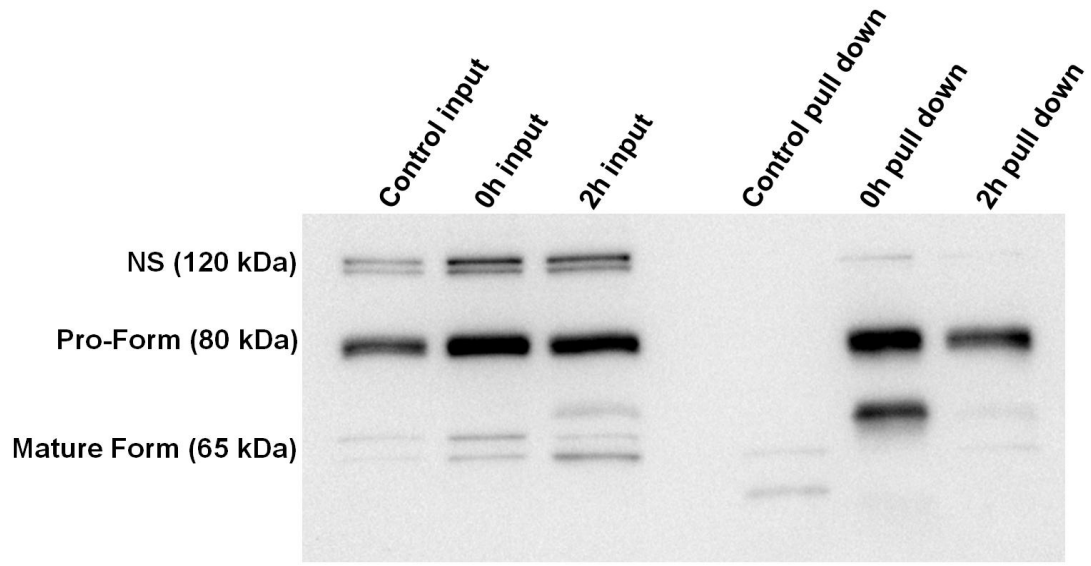

Figure 3.14: Expression of *N*-glycosylated ADAM 10 in HCT116 Cells

HCT116 cells were exposed to severe hypoxia (0.5% O_2) for 2 hours and lysed, before undergoing Concanavalin A pull down (as described in Section 2.21). Whole cell lysates (inputs collected prior to pull down) were separated by SDS-PAGE and ADAM 10 protein expression was analysed by Western Blotting. Normoxic control (0h) and FLAG agarose beads used for negative control. Blot is representative of three individual repeat experiments. NS denotes non-significant bands.

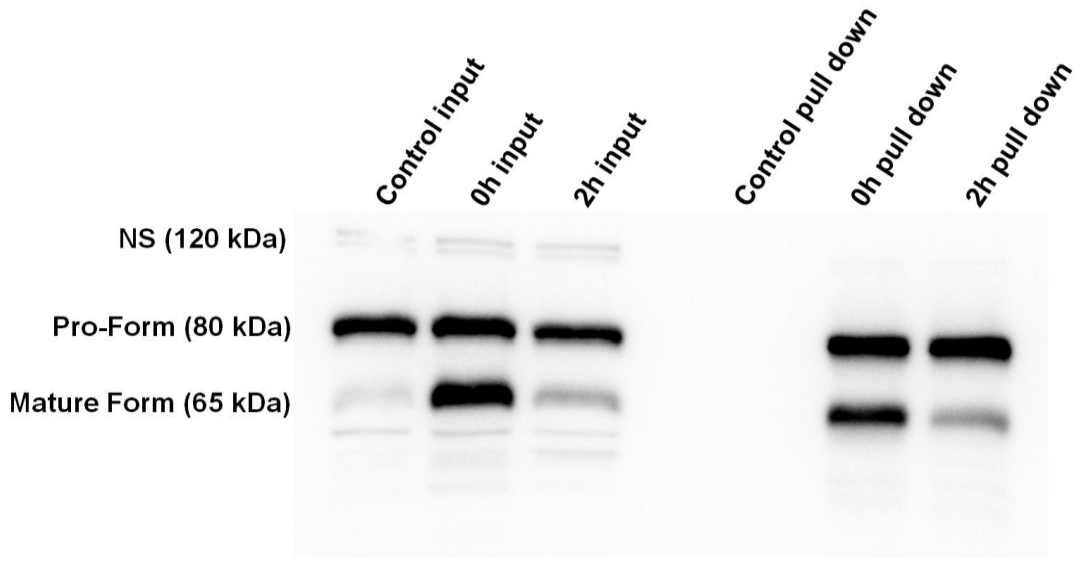

Figure 3.15: Expression of *N*-glycosylated ADAM 10 in HT29 Cells

HT29 cells were exposed to severe hypoxia (0.5% O_2) for 2 hours and lysed, before undergoing Concanavalin A pull down (as described in Section 2.21). Whole cell lysates (inputs collected prior to pull down) were separated by SDS-PAGE and ADAM 10 protein expression was analysed by Western Blotting. Normoxic control (0h) and FLAG agarose beads used for negative control. Blot is representative of three individual repeat experiments. NS denotes non-significant bands.

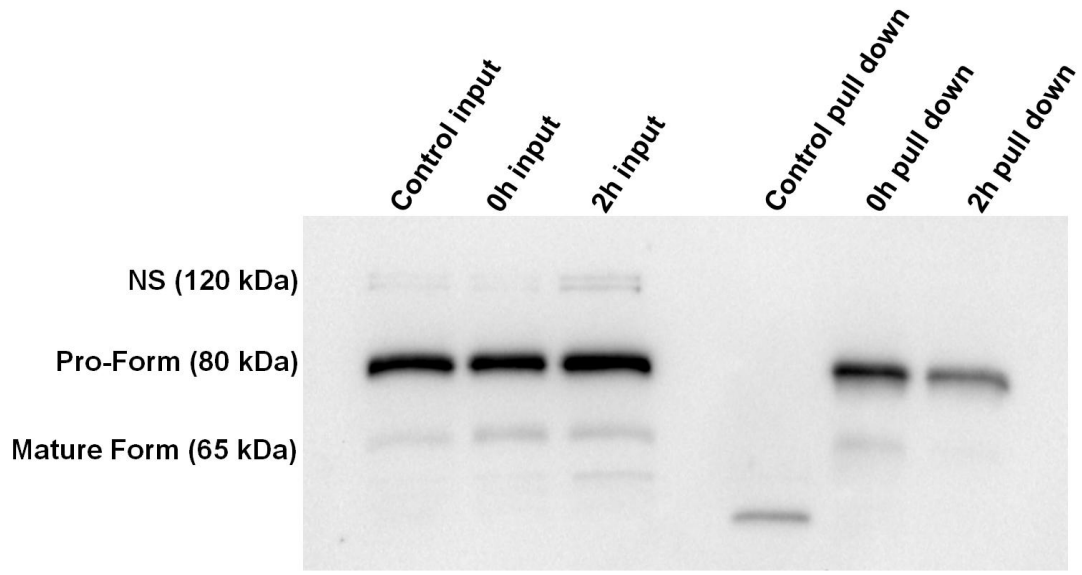

Figure 3.16: Expression of *N*-glycosylated ADAM 10 in RKO Cells

RKO cells were exposed to severe hypoxia (0.5% O_2) for 2 hours and lysed before undergoing Concanavalin A pull down (as described in Section 2.21). Whole cell lysates (inputs collected prior to pull down) were separated by SDS-PAGE and ADAM 10 protein expression was analysed by Western Blotting. Normoxic control (0h) and FLAG agarose beads used for negative control. Blot is representative of three individual repeat experiments. NS denotes non-significant bands.

form and mature form visible, including the doublet mature form band. Importantly, ADAM 10 was identified as one of the proteins pulled down using Concanavalin A (**Figure 3.14** - **Figure 3.16**). Specifically, in the normoxic samples, bands for the molecular weight corresponding to both the pro- and mature form of ADAM 10 could be detected. However, after a 2 hour hypoxic exposure, the intensity of the band at the molecular weight corresponding to the mature form of ADAM 10 was reduced (**Figure 3.14 - Figure 3.16**). There was no observable reduction of the pro-form of ADAM 10 in the Concanavalin A samples in HT29 cells (**Figure 3.15**), whereas in both HCT116 and RKO cells (**Figure 3.14** & **Figure 3.16**, respectively) a reduction in pro-form ADAM 10 was observed under hypoxic conditions. These data indicate that, both the pro and mature form of ADAM 10 appear to be glycosylated in normoxic samples, there is a clear and robust reduction in the glycosylated form of the mature ADAM 10 form in hypoxic conditions.

In order to further evaluate the nature of this glycosylation, whole cell lysates prepared from HCT116 cells exposed to normoxic and hypoxic (0.5% O_2) conditions were treated with a known de-glycosylating enzyme, PNGase. In **Figure 3.17**, it can be observed that PNGase F treatment results in a downward shift of the pro-form of ADAM 10, of approximately 5 kDa. This is consistent between both normoxia and hypoxia. The mature form remains largely unaffected by PNGase F treatment, with no observable downwards shift (**Figure 3.17**), however a potential slight decrease is observable in mature form levels, making the doublet band less visible, in both normoxia and hypoxia. Incubation at 37°C also has a slight effect on ADAM 10, particularly the pro-form. In the incubated control samples the pro-form undergoes a slight downward shift, albeit not to the extent of PNGase F treatment (**Figure 3.17**).

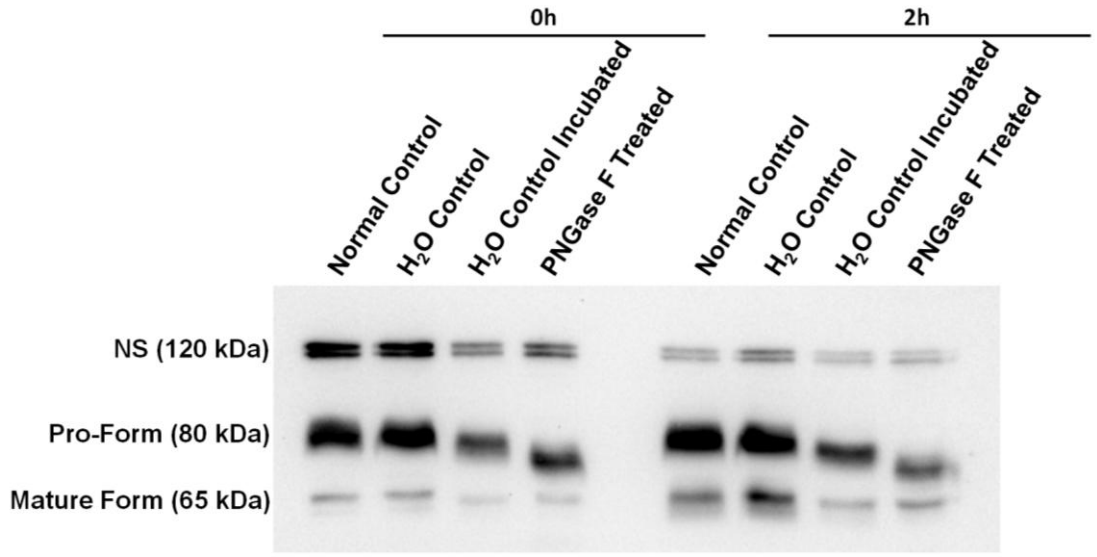

Figure 3.17: ADAM 10 Expression after *N*-glycan Removal of HCT116 Whole Cell Lysates

HCT116 cells were exposed to normoxia or severe hypoxia (0.5% O_2) for 2 hours and lysed before undergoing PNGase F treatment. 30 μg of each protein lysate was treated with PNGase F treatment for 24 hours at 37°C (as described in Section 2.21). Experimental controls included whole cell lysates containing lysis buffer, protein lysate with water and glycobuffer +/- 24 hours at 37 °C. All samples were then separated by SDS-PAGE and ADAM 10 protein expression examined by Western Blotting. Blot is representative of three independent repeat experiments. NS denotes non-specific bands.

3.4 Discussion

Research into the role of ADAM 10 in hypoxia-mediated cancer progression is lacking, with only three prior investigations into the effects of hypoxia on ADAM 10 (Webster et al., 2002, Marshall et al., 2006, Barsoum et al., 2011). As such, this study aimed to characterise the role of this protein in hypoxia-mediated CRC progression. Specifically, this chapter aimed to investigate whether exposure to severe hypoxia (0.5% or 0.1% O_2) resulted in alterations in ADAM 10 expression at either protein or transcript level.

Analysis of ADAM 10 at protein level identified an upregulation in the expression of the mature, active form of the protein. Importantly, a hypoxia-mediated doublet band was identified for mature ADAM 10, after a short exposure of 2 hours in hypoxia, which remained for the duration of the time course. Examination of *ADAM 10* at transcript level identified small but significant upregulations after hypoxic exposure. Furthermore, ADAM 10 was identified by LC-MS, however biochemical attempts to characterise the nature of the ADAM 10 doublet were unsuccessful.

0.5% and 0.1% oxygen tensions were selected for these experiments based on previous induction of ADAMs members at these levels, albeit in different cancer types. Barsoum et al. (2011) showed induction of ADAM 10 in 0.5% O_2 in both prostate and breast cancer, and Rzymski et al. (2012) identified that in HCT116 cells levels of ADAM 17 were considerably higher when exposed to 0.1% than 1% O_2. Therefore, this study aimed to identity whether ADAM 10 expression was altered by severe hypoxia, and whether severity of the hypoxic exposure influenced ADAM 10 expression. Induction of ADAM 10 expression after exposure to 0.1% O_2 was found to be at a lesser extent than the induction seen at 0.5% O_2. It is feasible that such differences between oxygen tensions are simply as a result of the large variations in generated densitometry values. This is supported by the lack of visual alteration in banding intensity between the two

oxygen tensions. However, it is possible that it is indicative of altered ADAM 10 biology under more severe oxygen tensions and could be a target for further investigation. Time scales for examination of ADAM 10 expression at protein and transcript level were selected based on the knowledge that whilst transcriptome changes take place prior to protein level alterations, other factors can influence the protein level quicker than transcriptome-mediated protein alterations would be evident (Walsh et al., 2005). Such factors include PTMs which can rapidly modify a protein to exert control over its functionality in terms of its structure, processing and involvement in cellular signalling processes (Wang et al., 2014, Duan and Walther, 2015).

No prior studies on the effects of hypoxia on ADAM 10 in CRC have been identified and what few studies exist in other cancer types present a conflicting view. In prostate and breast cancer an upregulation in ADAM 10 at both protein and transcript level was reported, after exposure to severe hypoxia (24 hours; 0.5% O_2), which is in agreement with the findings presented here (Barsoum et al., 2011). However, in neuroblastoma it has previously been shown that ADAM 10 is downregulated at both protein and mRNA levels after prolonged hypoxic exposure (24 and 48 hours; 2.5% O_2) (Webster et al., 2002, Marshall et al., 2006). The differences in previous results would indicate that alterations to the expression of ADAM 10 under hypoxic conditions may be cancer type specific and/or dependent upon the severity of the hypoxic exposure. Previous research has shown a hypoxia-mediated upregulation of ADAM 17, ADAM 10's closest family member, in a number of cancer types (Szalad et al., 2009, Rzymski et al., 2012, Wang et al., 2013). Szalad et al. (2009) showed that after exposure to hypoxia (<1% O_2) ADAM 17 was upregulated at both protein and transcript level in glioma. Rzymski et al. (2012) reported similar upregulations in glioma, ovarian, breast, and importantly, colorectal cancer. Thus, indicating that a hypoxia-mediated upregulation of ADAMs members is prevalent within cancer. In the context of CRC such upregulations have been linked to

poor prognosis within patients, thus implicating *ADAM 10* in mediating CRC progression (Knösel et al., 2005).

One limitation of these experiments is the lack of confirmation of a hypoxic environment at protein level. Whilst *SLC2A1* expression was used as the positive control at transcript level, steps should have been taken to also confirm this at protein level through blotting for HIF-1α expression. Both HIF-1α and *SLC2A1* (the gene encoding for GLUT1 (glucose transporter 1)) are induced by hypoxia (Behrooz and Ismail-Beigi, 1997, Ouiddir et al., 1999, Zhang et al., 1999, Ke and Costa, 2006, Nagaraju et al., 2015). Attempts were undertaken to probe for HIF-1α, however due to the delicate nature of the lysis buffer used to extract ADAMs proteins and the intra-nuclear localisation of HIF-1α, it was not possible to detect HIF-1α within the samples. Further clarification was attempted using more stringent lysis buffers, which confirmed induction of HIF-1α expression, however this was not undertaken alongside other experiments within this and latter chapters, and as such is a limitation of this study. A further limitation of this study is the use of densitometry to quantitatively analyse Western Blots. Densitometry typically analyses the differences in signal from the chemiluminescence applied to the Western Blots prior to imaging (Taylor et al., 2013, Taylor and Posch, 2014). Generated figures are corrected to account for any background signal and normalised to a housekeeping control. However, the methodology is widely recognised to have limitations, including poor reproducibility of quantitative values between experimental repeats (Gassmann et al., 2009, Taylor et al., 2013, Taylor and Posch, 2014). As documented in this chapter, clear visual alterations in banding patterns may not translate to significant results when quantitatively analysed due to the large degree of variability between values from experimental repeats (Gassmann et al., 2009, Taylor et al., 2013, Taylor and Posch, 2014).

Attempts to identify the nature of the ADAM 10 doublet band were unsuccessful, however detection of ADAM 10 within samples was confirmed by LC-MS analysis. Western Blotting confirmed that ADAM 10 was successfully pulled down by IP, however, there is more mature form ADAM 10 present after IP than is endogenously expressed in the cells, whilst the pro-form remains unaffected. It is possible that it is due to conformational alteration to the protein structure (Keskin, 2007). In standard SDS-PAGE the antibody is interacting with separated, denatured ADAM 10 proteins, whereas during the IP process the antibody is interacting with the ADAM 10 proteins in their native form. It is possible that the structural conformation of the protein in its native form is more conducive to antibody binding than in its denatured form (Braden and Poljak, 1995, Davies and Cohen, 1996, Keskin, 2007). Alternatively, the antibody used during ADAM 10 IP is more concentrated than that used for Western Blotting so it's possible that there is more opportunity for mature form binding as the concentration is high enough to eliminate saturation by ADAM 10 pro-form (Reverberi and Reverberi, 2007).

The majority of detected ADAM 10 peptides corresponded to the metalloproteinase domain, the largest and catalytically active part of ADAM 10 (Rosendahl et al., 1997, Prinzen et al., 2005, Moss et al., 2007). Pro-domain peptides were identified within pro-form samples but were primarily absent in mature form samples, which corresponds to the knowledge that this domain is cleaved upon maturation of the protein, for activation of the catalytic activity (Anders et al., 2001, Moss et al., 2007). ADAM 10 was identified to be present after CRAPome analysis in all samples (**Appendix 1**), thus strengthening the identification of ADAM 10 within the samples, as the possibility of it being a contaminant was eliminated (Mellacheruvu et al., 2013). Further, more detailed analysis of proteins within the IP samples could be undertaken by electrospray ionisation (ESI) coupled with MS (ESI-MS). ESI-MS is another important methodology

capable of highly sensitive protein identification, and both structural and quantitative protein analysis (Loo, 2000, Ho et al., 2003). Such methodology would be suitable for detection of lower abundant peptides within samples, that may not be detected by less sensitive methodologies, such as MALDI-MS or LC-MS. Absence of protein peptides within samples is not definitively indicative of their absence, it may be that a more sensitive approach, such as ESI-MS, is required (Loo, 2000, Ho et al., 2003). Despite the identification of ADAM 10 within IP samples further investigation is required to definitively identify the doublet band as mature ADAM 10. One methodology that could be employed for such purposes is the overexpression of ADAM 10 to identify increased intensity in doublet banding, thus identifying the doublet band as mature ADAM 10.

It was hypothesised that the doublet band seen for mature ADAM 10 was the result of a hypoxia-mediated post-translational modification or processing of the protein. As such, various biochemical methodologies were utilised to try and identify the modification behind the doublet band. Members of the ADAMs family are known to be susceptible to post-translational modifications including phosphorylation and glycosylation (Escrevente et al., 2008, Yin and Yu, 2009, Marcello et al., 2010, Schwarz et al., 2013). Indeed, it is a post-translational modification, mediated by pro-protein convertases, that is responsible for the cleavage of the pro-form and subsequent activation of ADAM 10 (Anders et al., 2001, Moss et al., 2007, Le Gall et al., 2010).

Preliminary experiments investigated re-oxygenation of HCT116 cells, however after 8 hours hypoxic exposure and 16 hour re-oxygenation in normoxia the ADAM 10 doublet band was still visible, albeit possibly reduced. (**Appendix 1**). As such, this is indicative that a non-reversible modification to mature ADAM 10 under hypoxic conditions is responsible for the doublet band formation (Walsh et al., 2005). Previous research has shown the cleavage of the intracellular region of ADAM 10 by γ-secretase (Parkin and

Harris, 2009, Tousseyn et al., 2009). Therefore, it was hypothesised that ADAM 10 doublet formation may be as a result of a hypoxia-mediated cleavage of ADAM 10 by γ-secretase, which plays a role in Notch signalling alongside ADAM 10 (Bozkulak and Weinmaster, 2009, Christian, 2012, Guo et al., 2013). However, the doublet band was not resolved upon γ-secretase inhibition, thus rejecting this hypothesis. Two γ-secretase treatment schedules were used, pre-treated for 6 hours prior to hypoxic exposure and treated immediately prior to hypoxic exposure. As ADAM 10 doublet formation occurs after as little as two hours in hypoxia it was important to ensure efficient γ-secretase inhibition was achieved at the point of hypoxic exposure. It would be expected that the pre-treatment set up would exhibit greater γ-secretase inhibition due to longer exposure to DBZ. Previous studies have also used a 6 hour pre-treatment regime, which indicated a sufficient length of treatment prior to undertaking experiments (Groth et al., 2010). However, a limitation of this experiment is the lack of confirmation of successful γ-secretase inhibition. As such, it cannot be determined which treatment type resulted in most efficient γ-secretase inhibition. Whilst DBZ concentrations were selected based on previous usage within the literature (Groth et al., 2010), due to lack of controls for confirmation of γ-secretase inhibition, it cannot be confirmed that the concentrations selected were sufficient to inhibit γ-secretase activity in this experiment. To confirm successful γ-secretase inhibition Western Blotting for NICD should be undertaken, and only when confirmation of inhibition is achieved can γ-secretase be ruled out of mediating the ADAM 10 doublet.

Furthermore, it is known that ADAM 10 can undergo ectodomain shedding by other ADAMs members, and this should be another focus for future investigation (Parkin and Harris, 2009, Tousseyn et al., 2009). Importantly, Tousseyn et al. (2009) showed a doublet banding pattern for the remaining C-terminal fragment, after ectodomain shedding of ADAM 10, albeit at a much lower molecular weight (~10 kDa) compared

to that shown in this study. However, it is possible that hypoxia is mediating some form of cleavage of ADAM 10, such as partial ectodomain shedding. Through the use of ADAMs 9 and 15 specific inhibitors, or generic ADAMs inhibitors, such as GM6001, shedding could be inhibited and the doublet banding pattern could be examined, with an absence suggesting ectodomain shedding may be responsible for the doublet formation. Furthermore, pro-protein convertases, such as Furin and PC7, are known to cleave the ADAM 10 pro-domain, and it is feasible that under hypoxic conditions these may exert an extra cleavage of the protein, resulting in the doublet band formation (Anders et al., 2001, Moss et al., 2007). If pro-protein convertases were responsible for cleavage of ADAM 10, resulting in doublet band formation, then the inhibition of them would prevent the doublet band from appearing.

As one of the most frequent PTMs affecting proteins, the glycosylation of ADAM 10 under hypoxic conditions was investigated (Walsh et al., 2005). It was hypothesised that the doublet band was as a result of altered glycosylation of mature ADAM 10 under hypoxic conditions. It is known that ADAM 10 possesses sites for *N*-linked glycosylation, the most common form of glycosylation, and it is known that hypoxia affects glycosylation rates (Escrevente et al., 2008, Shirato et al., 2011, Pasing et al., 2012, Zhang et al., 2014b). Furthermore, upregulated glycosylation has been reported in CRC patient samples, in comparison to healthy tissue (Nicastri et al., 2014). Notably, of the 54 upregulated glycoproteins, 9 were overexpressed in over 80% of samples examined, including two members of the PLOD (procollagen-lysine, 2-oxoglutarate 5-dioxygenase) family (PLOD1 and PLOD2) (Nicastri et al., 2014). Previous research has shown that hypoxia-mediated upregulation of HIF-1α is responsible for activation of PLOD family members, which are involved in tissue remodelling (Hofbauer et al., 2003). Notably, over 50% of identified cancer biomarkers are glycosylated proteins (Zhang et al., 2014b). Such findings strongly implicate glycosylation within cancer

progression, and indicate a role within hypoxia-mediated CRC progression. Concanavalin A affinity based purification showed a reduction in *N*-glycosylated ADAM 10 pulled down in CRC cells after exposure to hypoxia, particularly in the mature form, thus indicating that the glycosylation of ADAM 10 is indeed affected by hypoxic exposure (Roth et al., 2012, Tian and Zhang, 2013). As such, it was hypothesised that the ADAM 10 doublet may be as a result of glycan removal or decreased glycosylation under hypoxic conditions. A downward shift in molecular weight, such as that seen in the doublet band, would be consistent with removal of glycans from ADAM 10, as it is known that glycosylation itself increases the molecular weight of proteins (Bartels et al., 2011). Furthermore, a similar downward shift in the molecular weight of ADAM 10 was observed after glycan removal in ovarian cancer (Escrevente et al., 2008). However, PNGase F treatment, to remove *N*-linked glycans, showed no alteration to the doublet banding pattern of mature ADAM 10 in HCT116 cells. A downward shift was seen in the pro-form of the protein, which is consistent with previous findings by Escrevente et al. (2008). As such, it can be determined that whilst there appears to be an alteration to the glycosylation of ADAM 10 in hypoxia, the doublet band is not mediated by *N*-linked glycan removal from mature ADAM 10 under hypoxic conditions. To further confirm whether glycosylation plays any role in mediating the doublet band of mature form ADAM 10, glycoproteomic analysis could be used to analyse the proteomic differences in ADAM 10 between normoxia and hypoxia. Such studies would allow for identification of the location of glycosylation sites within the protein, the type of glycans, including structure, and to which site within the protein they bind (Sagi et al., 2005, Pasing et al., 2012, Zhang et al., 2014b). Furthermore, it would determine to what extent ADAM 10 is glycosylated under hypoxic conditions (Zhang et al., 2014b). Commonly glycoproteomics will see the use of affinity (e.g Concanavalin A) or chemical (e.g PNGase F) based separation prior to

MS (Zhang et al., 2014b). This technology could be utilised to determine specifically, in the context of glycosylation, what is altered in mature ADAM 10 under hypoxic conditions. Additionally, alternative methods for glycan removal, such as tunicamycin treatment, could be tried, which prevents the biosynthesis of *N*-glycans through inhibition of the pre-cursor (de Freitas Junior et al., 2011). Research has shown that *N*-linked glycan removal by tunicamycin reduced cellular proliferation in CRC cells (de Freitas Junior et al., 2011).

Here, the effects of hypoxia on ADAM 10 in CRC cell lines have been shown, allowing the hypothesis of 'Exposure to severe hypoxia will increase ADAM 10 expression in CRC cell lines' to be accepted. ADAMs family members have been linked to a more progressive phenotype in a variety of cancers, and their alteration under hypoxic conditions has been linked to this. As such, the hypoxia-mediated upregulation of ADAM 10 in CRC identified here may be indicative of a role in promoting the progression of CRC. Therefore, to further investigate the significance of the ADAM 10 upregulation observed here, the tumourigenic phenotypes and ADAM 10 activity will be examined in CRC cell lines.

Chapter 4 : Biological Impact of ADAM 10 in Hypoxia

4.1 Introduction

In Chapter 3 it was shown that exposure to severe hypoxia increases expression of ADAM 10 in CRC cell lines. Furthermore, a previously unidentified doublet band for mature ADAM 10 was identified, however attempts to characterise this proved unsuccessful. This chapter will investigate the tumourigenic and phenotypical effects of hypoxia-mediated ADAM 10 upregulation on CRC cell lines.

4.1.1 Cellular Proliferation and Migration in Cancer

In 2000, Hanahan and Weinberg identified six hallmarks of cancer, which encompass six key biological alterations that promote cancer development, as discussed in **Section 1.1** (Hanahan and Weinberg, 2000, Hanahan and Weinberg, 2011). Deregulated cellular proliferation is one of the most important acquired phenotypes of cancer cells (Hanahan and Weinberg, 2011, Feitelson et al., 2015). Numerous mechanisms are attributed to promoting the dysregulation of cell proliferation in CRC, and previous research has shown the involvement of multiple signalling pathways, including EGF, β-Catenin and Notch signalling, amongst others (**Sections 1.9.2 - 1.9.4**) (Rocks et al., 2008b, Przemyslaw et al., 2013, Minder et al., 2012, Huynh et al., 2015, Vidal et al., 2011, Li et al., 2015a, Yang et al., 2015, Feng et al., 2015, Danielsen et al., 2015).

Hypoxia-modulated cancer cell proliferation has been well reported, however, previous findings present a somewhat conflicting picture. Some studies reported a significant upregulation in the proliferation of a range of cancer cells after exposure to hypoxia, whereas other studies have presented a conflicting view, with decreased cellular proliferation after hypoxic exposure (**Section 1.5**) (Tang et al., 2015, Liang et al., 2015, Ma et al., 2011, Zhu et al., 2010, Yu and Hales, 2011, Westwood et al., 2014). The conflicting nature of existing research suggests that the effect of hypoxia on cellular proliferation is dependent upon the exposure conditions and cell type. Furthermore,

evidence indicates that hypoxic modulation of cellular proliferation is a complex system, encompassing a variety of signalling pathways that differ amongst cancer types.

Cell migration is another key feature in cancer progression, particularly in highly metastatic cancer types, such as CRC (Peddareddigari et al., 2010, Cao et al., 2015). In order for cancer cells to be able to migrate, they must undergo epithelial-mesenchymal transition (EMT), which sees the acquisition of a mesenchymal phenotype, leading to increased cellular migration and invasion (**Section 1.9.4**) (Kalluri and Weinberg, 2009, Lamouille et al., 2014, Cao et al., 2015). Hypoxia has previously been shown to result in increased EMT and subsequently an increase in cellular migration and invasion (Higgins et al., 2007, Cannito et al., 2008, Zhang et al., 2013b, Gammon and Mackenzie, 2015, Zhang et al., 2015b).

4.1.2 ADAMs in Cellular Proliferation and Migration

ADAMs family members have been strongly linked to promoting proliferation and metastasis within cancer (Edwards et al., 2008). ADAM 10 has also been shown to be involved in the regulation of proliferation and migration/invasion within various cancer types (**Section 1.9**) (Arima et al., 2007, Gavert et al., 2007, Armanious et al., 2011, Bulstrode et al., 2012, Jones et al., 2013, Yuan et al., 2013, Gangemi et al., 2014, Mullooly et al., 2015, Shao et al., 2015, You et al., 2015). However, despite evidence suggesting ADAM 10 plays a role in cellular proliferation and migration, no previous research has identified a link between this role and hypoxia, which is prevalent in solid state tumours, such as CRC.

4.1.3 Rationale, Aims and Objectives of this Chapter

Previous research has indicated an involvement of ADAM 10 in the regulation of both proliferation and migration in various cancer types. Based on the earlier findings that ADAM 10 is upregulated under severe hypoxia (Chapter 3), this chapter aims to identify the role of ADAM 10 on the regulation of CRC cell proliferation and migration under severely hypoxic conditions.

The experimental work within this chapter was designed to test the hypothesis 'Hypoxia-induced ADAM 10 expression will promote cellular proliferation and migration in CRC cell lines' and subsequently answer the following questions:

- Does ADAM 10 play a role in the regulation of migration of CRC cell line models, and if so does severe hypoxia exacerbate such effects?
- Is ADAM 10 involved in the regulation of CRC cell line proliferation, and what effect does severe hypoxia have on this role?
- Are any alterations in CRC cellular proliferation as a result of alterations in cell cycle control, mediated by ADAM 10?

4.2 Methods

4.2.1 Scratch Assay

CRC cell lines were either treated with ADAM 10 targeting siRNA (**Section 2.10**) or ADAM 10 inhibitor GI254023X (**Section 2.27.1**) before being exposed to hypoxia (**Section 2.9**) and utilised for a scratch assay to assess cellular migration (**Section 2.27**).

4.2.2 MTS Assay

CRC cell lines were seeded and underwent either siRNA transfection (**Sections 2.10**, **2.28.2 and 2.28.3**) or ADAM 10 inhibition using GI254023X (**Section 2.28.1**). Cells were then exposed to either normoxia or hypoxia (**Section 2.9**) for 16 – 72 hours before MTS assay was undertaken (**Section 2.28**).

4.2.3 Clonogenic Survival Assay

HCT116 and HT29 cells were seeded at a density of 250-500 cells/well and left overnight before being exposed to normoxia or hypoxia (**Section 2.9**) for 24 hours. Cells were then left for formation of colonies, before being fixed and stained with crystal violet as described in **Section 2.29**.

4.2.4 Cell Cycle Analysis

HCT116 cells underwent siRNA transfection as described in **Section 2.10** and were exposed to either normoxia or hypoxia for 24 hours (**Section 2.9**). Cells were then stained with PI for cell cycle analysis by flow cytometry (**Section 2.30**).

4.3 Results

The experiments here and in Chapter 5 required the usage of ADAM 10 targeting siRNA to knockdown ADAM 10 expression. The efficiency of knockdown was confirmed through use of Western Blotting and qPCR. **Figure 4.1** illustrates representative images of ADAM 10 expression at both protein (A) and transcript (B) level after use of ADAM 10 targeting siRNA. It can be observed that there is a clear reduction in ADAM 10 expression, at both pro- and mature form levels, after ADAM 10 knockdown. A significant knockdown was also observed when ADAM 10 expression was checked at transcript level by qPCR (**Figure 4.1, B**). This is consistent in both normoxia (20% O_2, 0.9 ± 0-fold decrease) and hypoxia (0.5% O_2, 0.88 ± 0-fold decrease).

4.3.1 Role of Hypoxia-mediated ADAM 10 in CRC Cell Migration

In order to determine the effects of hypoxia-induced ADAM 10 upregulation on CRC cellular migration, scratch assays were performed on CRC cell lines and these were then exposed to hypoxia (0.5% O_2). Scratch assays were done in conjunction with ADAM 10 targeting siRNA or ADAM 10 specific small molecule inhibitor, G1254023X, as described in **Section 2.27.1**.

4.3.1.1 CRC Cellular Migration is Unaffected by ADAM 10 Knockdown in Severe Hypoxia

Scratch assays were used to identify whether ADAM 10 knockdown had any effects on CRC cell line migration, and whether hypoxia played any role in mediating cellular migration. Images within **Figure 4.2 A** depict scratches to confluent RKO cells after ADAM 10 knockdown, before and after hypoxic or normoxic exposure. The scratches were measured to calculate percentage of closure of the scratch, as can be seen in.

A)

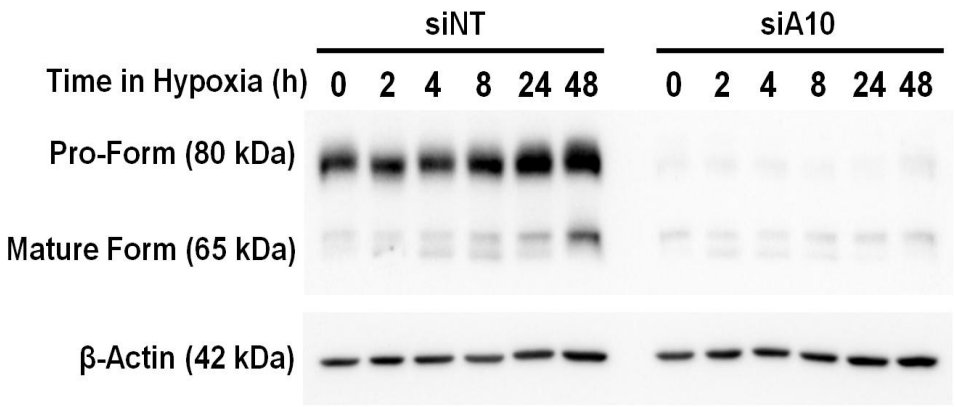

B)

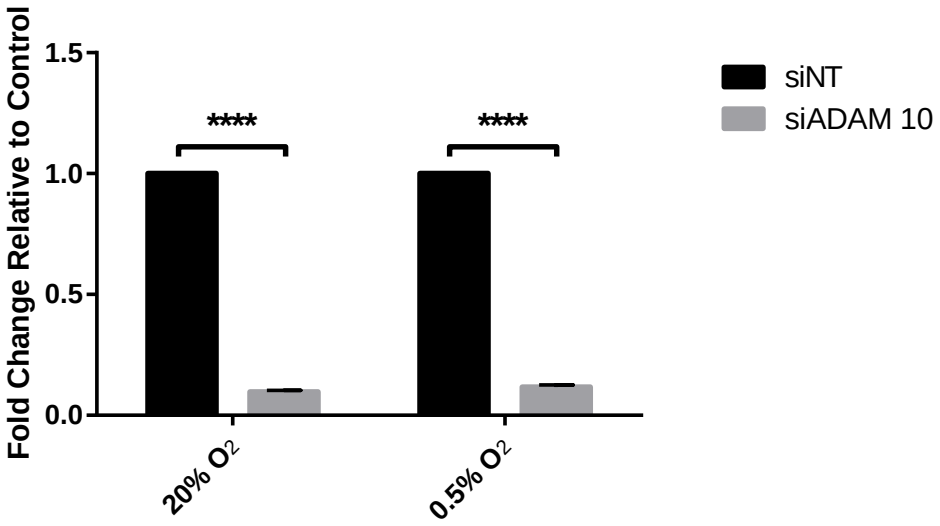

Figure 4.1: ADAM 10 Expression after ADAM 10 Knockdown by siRNA Transfection

A) HCT116 cells were transfected with ADAM 10 targeting siRNA (siADAM 10) or non-targeting siRNA (siNT) and exposed to severe hypoxia (0.5% O_2) for a range of time points. Cells were then lysed and 30 µg of each protein sample were separated by SDS-PAGE and expression of ADAM 10 protein was analysed by Western Blotting. β-Actin was used as a loading control. Blot shown is representative image of ADAM 10 knockdown at protein level.

B) HCT116 cells were transfected with ADAM 10 targeting siRNA (siADAM 10) or a non-targeting siRNA (siNT) and exposed to severe hypoxia (0.5% O_2) for 24 hours. mRNA was extracted and relative *ADAM 10* expression was determined by qPCR. All results were normalised to the housekeeping gene *B2M*. Results are expressed as fold change relative to the corresponding siNT of n=3 experiments. Error bars represent +/- SEM. Statistical analysis by two-way ANOVA with Tukey's post-hoc correction. **** = $p<0.0001$.

A)

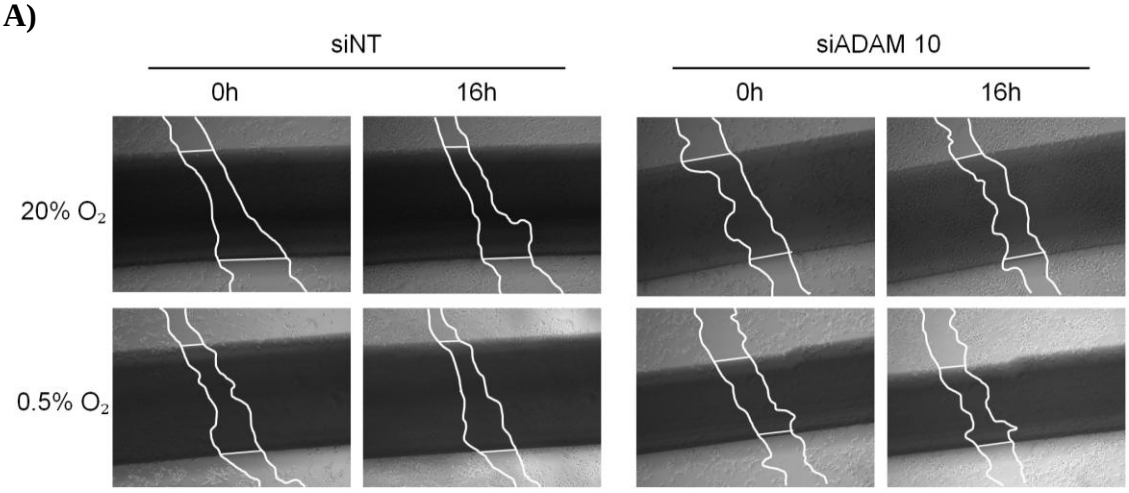

B)

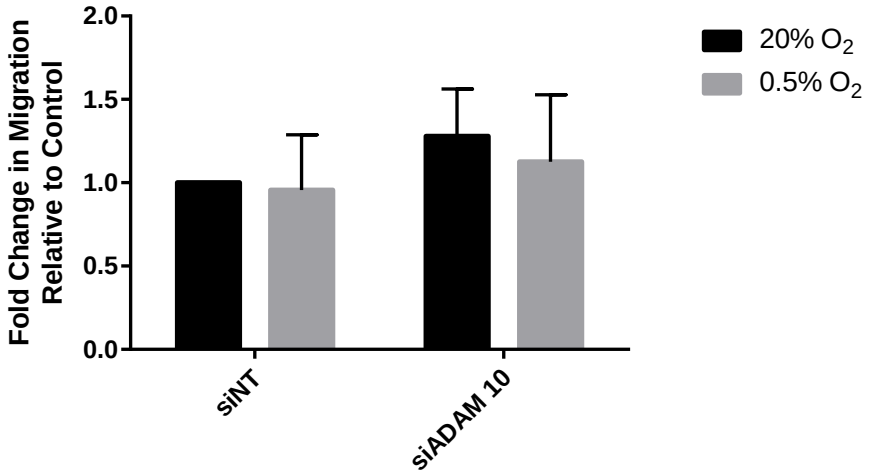

Figure 4.2: Migration of RKO Cells with ADAM 10 Knockdown in Severe Hypoxia (0.5% O_2)

A – RKO cells were transfected with ADAM 10 targeting siRNA (siADAM 10) or a non-targeting siRNA (siNT), used as a control. Once confluent the cell monolayer was scratched to create a scratch wound (Section 2.27.2). Scratches were imaged and incubated in hypoxia (0.5% O_2) or normoxia (20% O_2) for 16 hours before being re-imaged. Images representative of three intra-experimental scratches and two individual experimental repeats. Images were acquired using an Axio Vert.A1 inverted microscope and ZEN 2012 software, on a 5X objective.

B – Scratches were measured at 0 and 16 hours and migration fold change in comparison to normoxic siNT calculated. n=2; error bars represent +/- STDEV

Figure 4.2 B. Visual observation of the representative images show no closure of the scratches after 16 hours in either hypoxia (0.5% O_2) or normoxia (20% O_2). This is consistent amongst both the scrambled control cells (siNT) and the ADAM 10 knockdown cells (siADAM 10). However, a degree of variation was present amongst the inter-experimental repeats (n=2), resulting in large error bars, as seen in **Figure 4.2 B**.

4.3.1.2 CRC Cellular Migration is Unaffected by ADAM 10 Inhibition in Severe Hypoxia

Scratch assays were used to assess whether inhibition of ADAM 10 through the use of G1254023X, an ADAM 10 specific inhibitor, impacted on the migratory phenotype of CRC cell lines under severe hypoxia (0.5% O_2). RKO and HT29 cells were treated with the inhibitor for 6 hours before being scratched and exposed to either hypoxia (0.5% O_2) or normoxia (20% O_2). It can be seen (**Figure 4.3**) that neither hypoxia nor ADAM 10 inhibition has any significant effects on the migratory capabilities of RKO cells. Neither concentration of GI254023X inhibitor used has a greater degree of effect on RKO cell migration. There was a large degree of variation between the three independent experimental repeats, resulting in a large SEM and consequentially large error bars. As such, the results were deemed non-significant as per two-way ANOVA analysis with post-hoc Tukey's analysis. Similar results were seen for HT29 cells (**Figure 4.4**), where no significant differences in migration were observed in response to hypoxia or ADAM 10 inhibition. As with the RKO cells there was a large degree of inter-experimental variation which resulted in no significance amongst the results when analysed by two-way ANOVA with post-hoc Tukey's analysis.

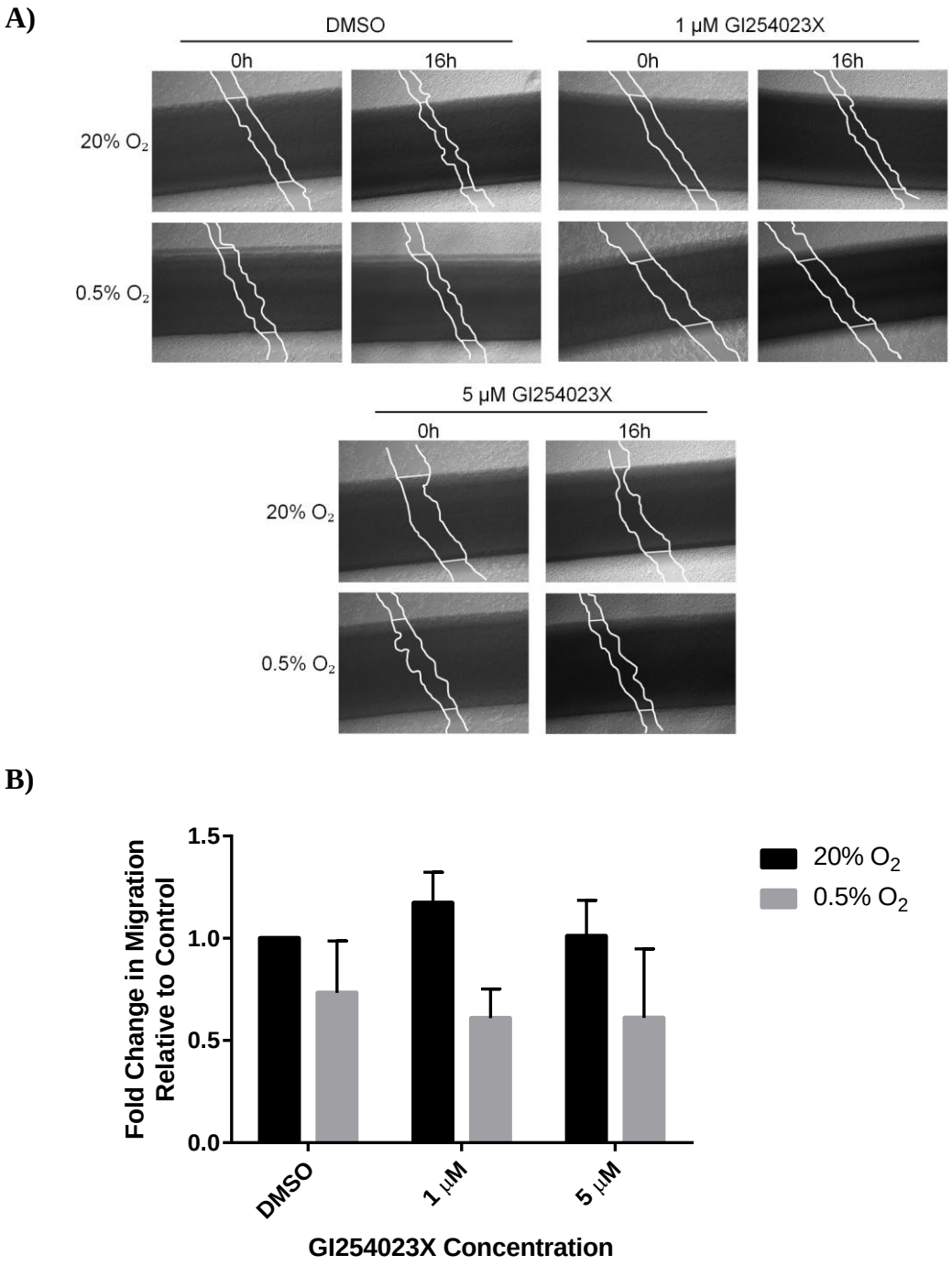

Figure 4.3: Migration of RKO Cells with ADAM 10 Inhibition in Severe Hypoxia (0.5% O_2)

A - RKO cells were treated with ADAM 10 inhibitor, G1254023X, and after 6 hours were scratched to create a wound (Section 2.27.1). Scratches were then imaged, and incubated in hypoxia (0.5% O_2) or normoxia (20% O_2) for 16 hours before being re-imaged. DMSO used as a vehicle control. Images representative of three intra-experimental scratches and three individual experimental repeats. Images were acquired using an Axio Vert.A1 inverted microscope and ZEN 2012 software, on a 5X objective.

B – Scratches were measured at 0 and 16 hours and fold change in migration in comparison to normoxic vehicle control (DMSO) calculated. n=3; error bars represent +/- SEM. All results deemed non-significant by two-way ANOVA analysis, with Tukey's post-hoc correction.

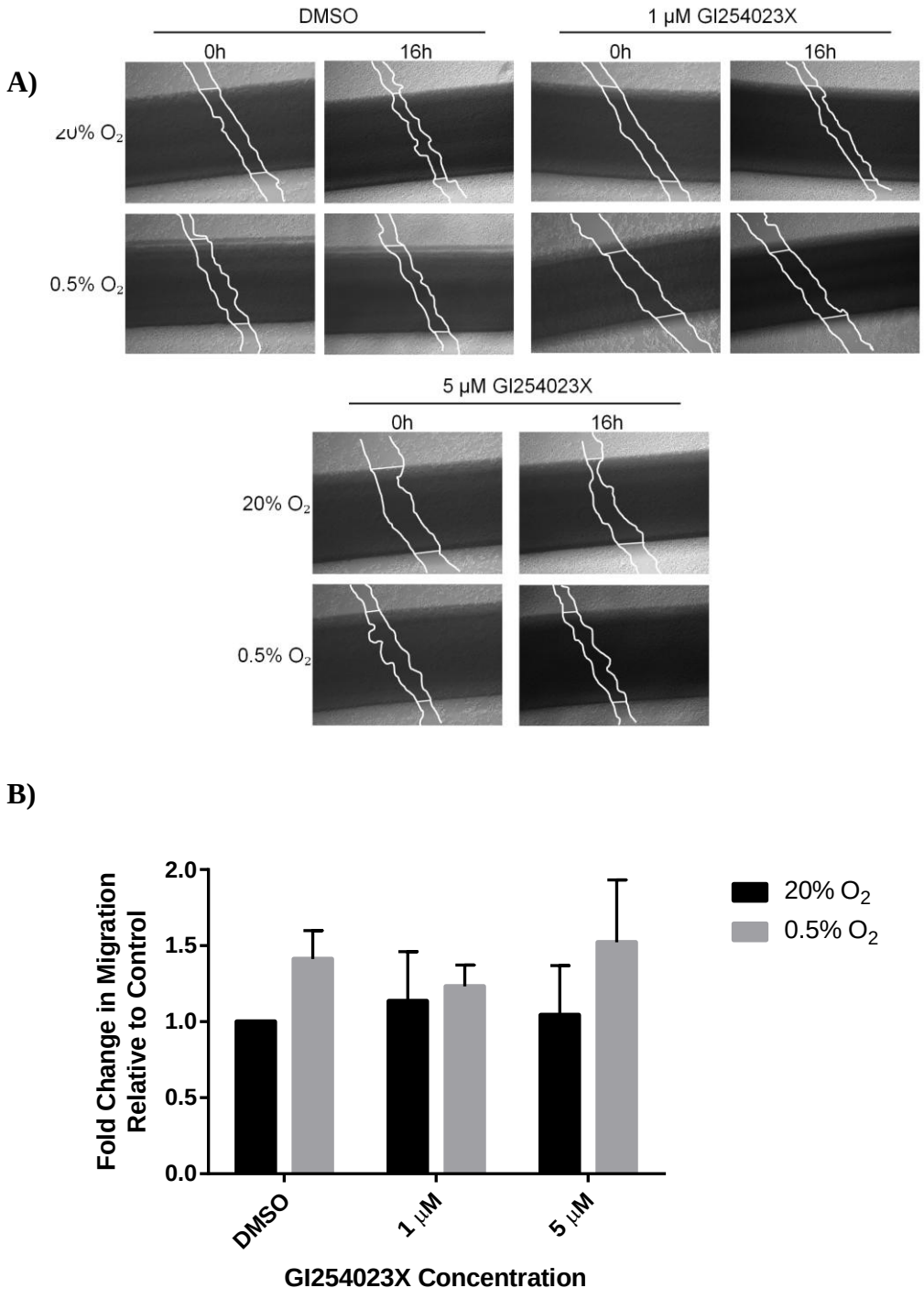

Figure 4.4: Migration of HT29 Cells with ADAM 10 Inhibition in Severe Hypoxia (0.5% O_2)

A – HT29 cells were treated with ADAM 10 inhibitor, G1254023X, and after 6 hours were scratched to create a wound (Section 2.27.1). Scratches were then imaged, and incubated in hypoxia (0.5% O_2) or normoxia (20% O_2) before being re-imaged. DMSO used as a vehicle control. Images representative of three intra-experimental scratches and three individual experimental repeats. Images were acquired using an Axio Vert.A1 inverted microscope and ZEN 2012 software, on a 5X objective.

B – Scratches were measured at 0 and 16 hours and fold change in migration in comparison to normoxic vehicle control (DMSO) calculated. n=3; error bars represent +/- SEM. All results deemed non-significant by two-way ANOVA analysis, with Tukey's post-hoc correction.

4.3.2 CRC Cellular Viability is Affected by Severe Hypoxia

To identify whether the proliferative activity of CRC cell line models was affected by severe hypoxia (0.5% O_2), CRC cell lines were exposed to hypoxia for a number of time points and their viability was measured by MTS assay, as a measure of proliferation. **Figure 4.5** shows the cellular viability of HCT116 cells after exposure to severe hypoxia for 16, 24, 48 and 72 hours (A-D respectively). Initially, exposure to severe hypoxia induced an increase in HCT116 cell viability after 16 hours (23 ± 4.4% increase, **Figure 4.5** A). However, 72 hour exposure to severe hypoxia lead to a highly significant decrease in cellular viability (**Figure 4.5** D, 38 ± 0.9% decrease, $p<0.001$). HT29 cells displayed a significant increase in viability only after 24 and 48 hours in severe hypoxia (**Figure 4.6** B (24 ± 2.9% increase) & C (20 ± 4.5% increase), $p<0.05$), but no decrease at 72 hours (**Figure 4.6** D). RKO cells showed an increase in viability after 16 hours (**Figure 4.7** A, 25 ± 5.2% increase, $p<0.05$), which was then decreased after 48 hours in severe hypoxia (**Figure 4.7** C & D, 33 ± 6.8%, $p<0.05$ and 45 ± 2.5%, $p<0.01$, respectively).

These data indicate that CRC cellular viability, as a measure of proliferation, is altered under severe hypoxia in all cell lines examined, albeit to different degrees.

4.3.2.1 CRC Cellular Viability is Decreased after ADAM 10 Knockdown

To assess the role of ADAM 10 in regulating cellular proliferation under hypoxic conditions, CRC cell lines were transfected with ADAM 10 targeting siRNA and exposed to severe hypoxia (0.5% O_2) for a range of time points, before MTS assays were undertaken. **Figure 4.8** depicts the cellular viability in HCT116 cells after ADAM 10 knockdown, in both normoxia (20% O_2) and hypoxia (0.5% O_2). After 16 hours it can be observed that there is a highly significant downregulation of cellular viability in

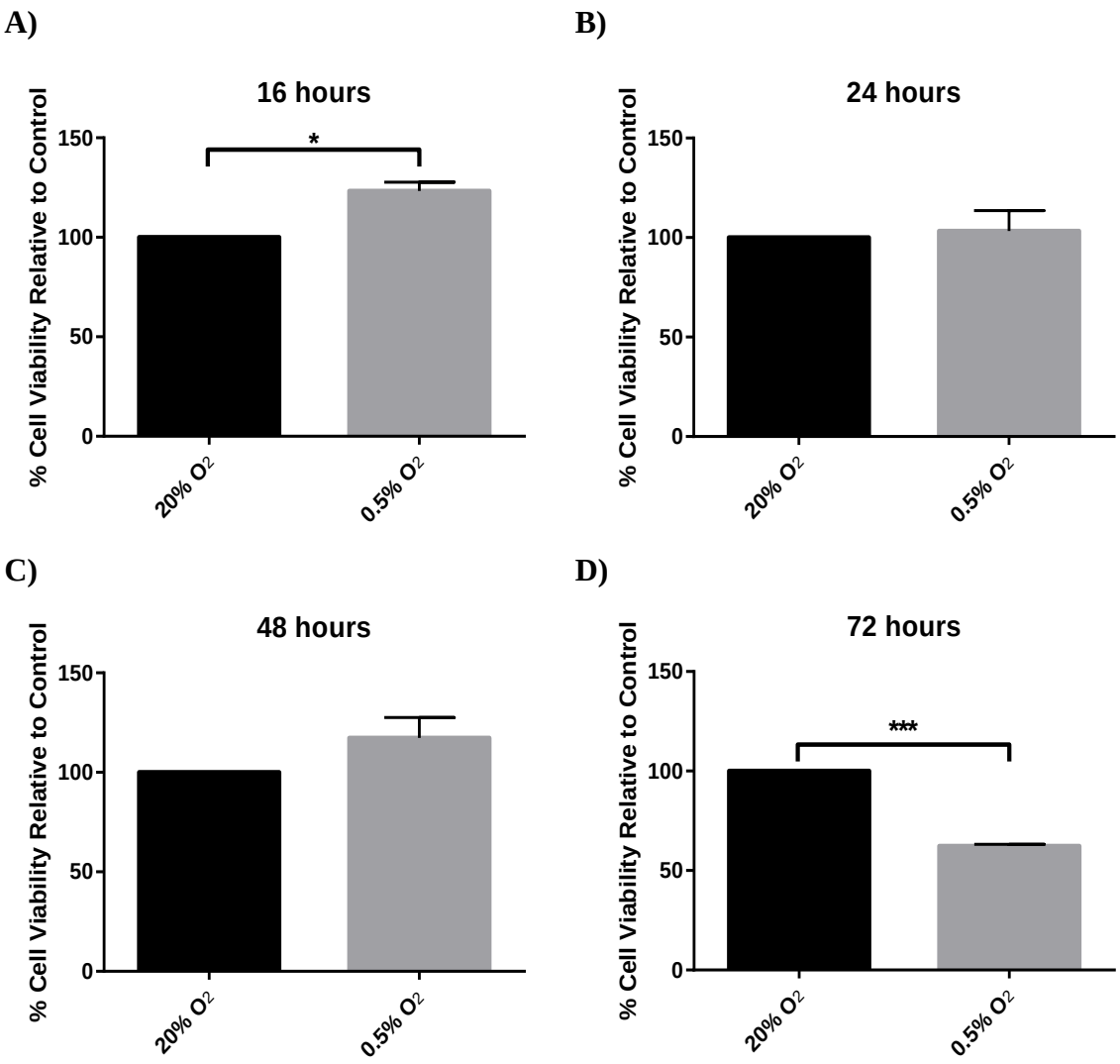

Figure 4.5: Viability of HCT116 Cells after Exposure to Severe Hypoxia (0.5% O_2)

HCT116 cells were exposed to severe hypoxia (0.5% O_2) for a range of time points (A-D). MTS assays were then carried out to determine cellular viability as a measure of proliferation. All results normalised to the normoxic (20% O_2) control and results are expressed as relative percentage change in viability of n=3 experiments. Error bars represent +/- SEM. Statistical analysis by unpaired, two-tailed T-test, with Welch's correction. * = $p<0.05$, *** = $p<0.001$.

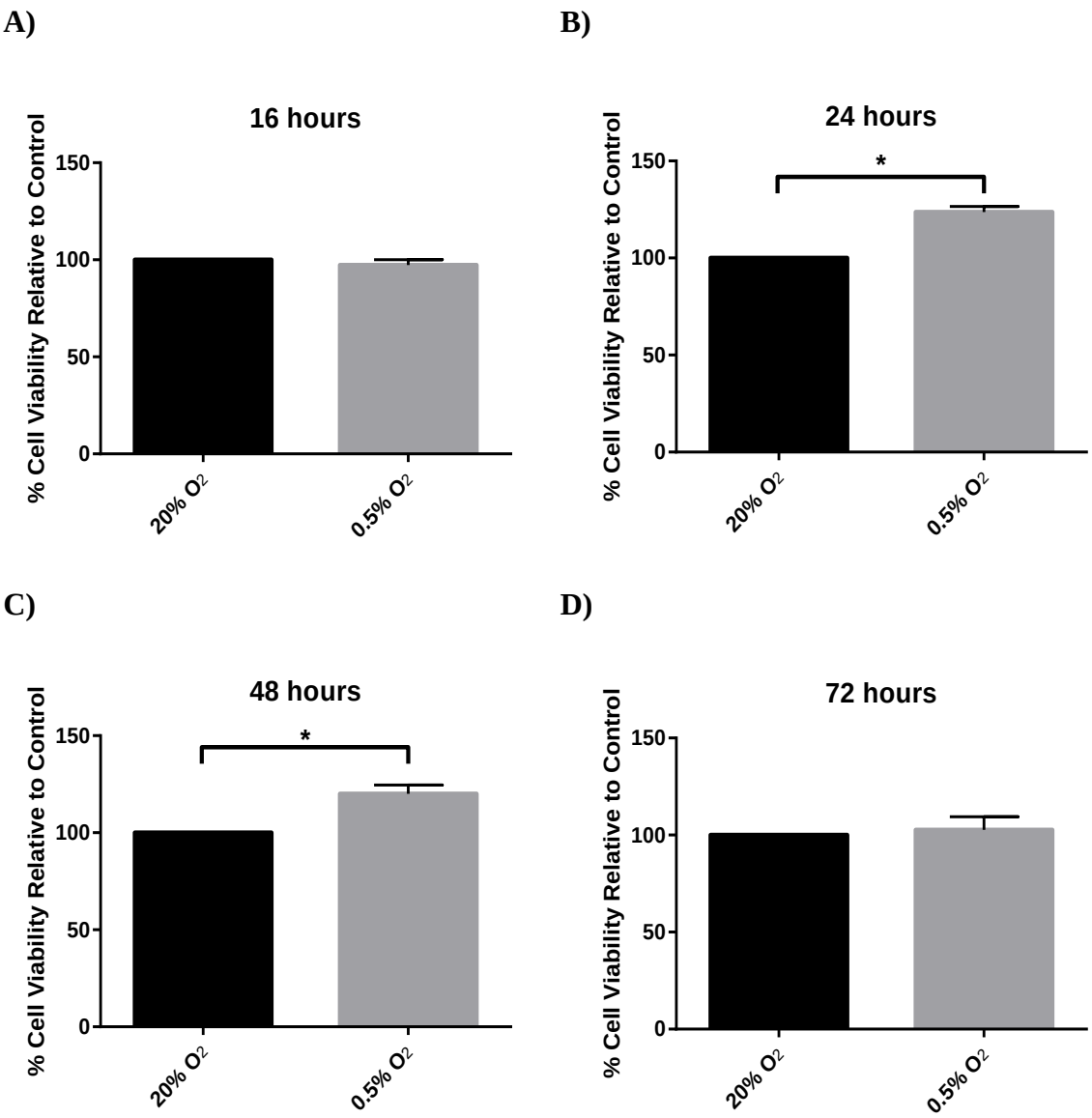

Figure 4.6: Viability of HT29 Cells after Exposure to Severe Hypoxia (0.5% O_2)

HT29 cells were exposed to severe hypoxia (0.5% O_2) for a range of time points (A-D). MTS assays were then carried out to determine cellular viability as a measure of proliferation. All results normalised to the normoxic (20% O_2) control and results are expressed as relative percentage change in viability of n=3 experiments. Error bars represent +/- SEM. Statistical analysis by unpaired, two-tailed T-test, with Welch's correction. * = $p<0.05$.

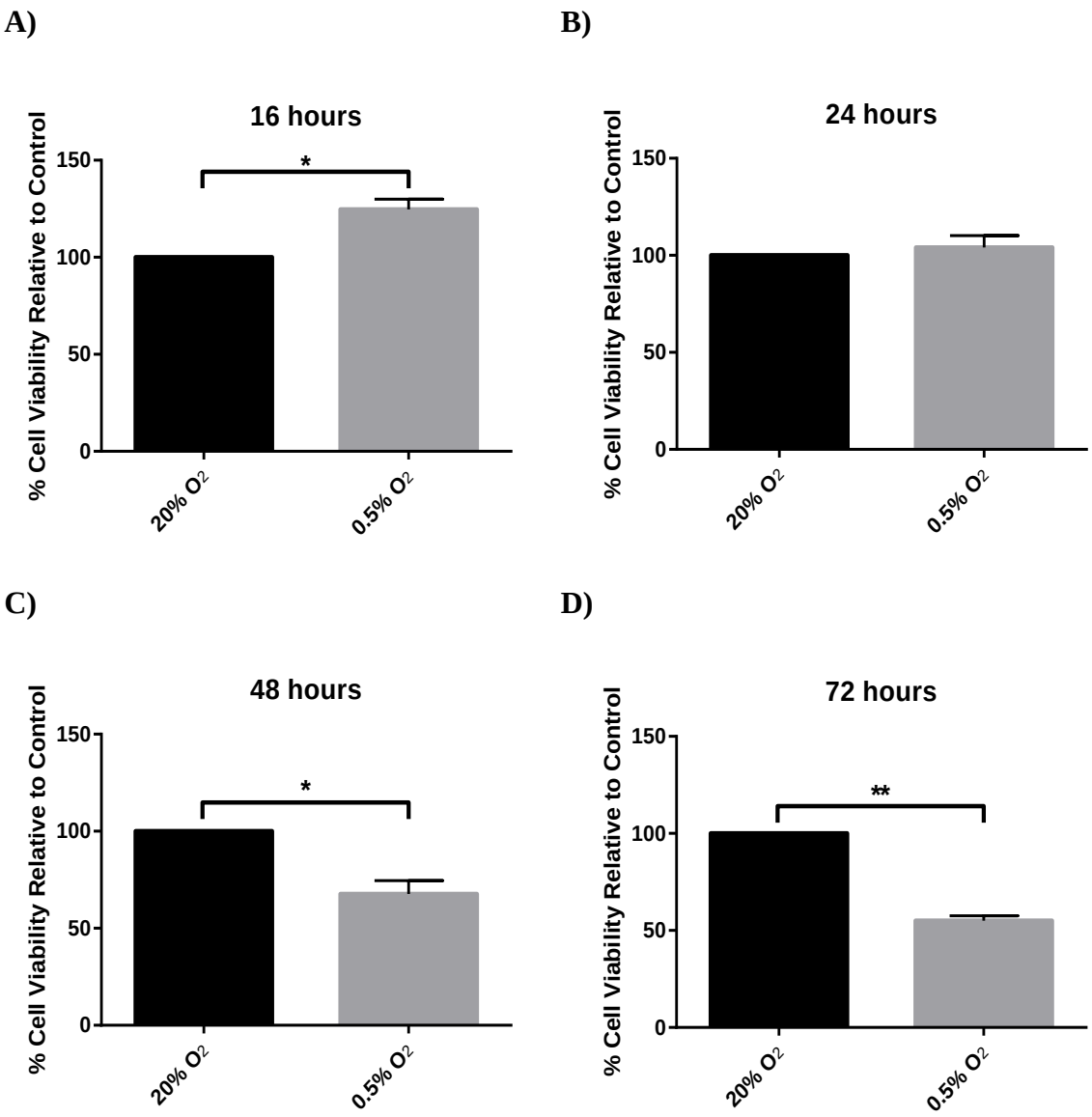

Figure 4.7: Viability of RKO Cells after Exposure to Severe Hypoxia (0.5% O_2)

RKO cells were exposed to severe hypoxia (0.5% O_2) for a range of time points (A-D). MTS assays were then carried out to determine cellular viability as a measure of proliferation. All results normalised to the normoxic (20% O_2) control and results are expressed as relative percentage change in viability of n=3 experiments. Error bars represent +/- SEM. Statistical analysis by unpaired, two-tailed T-test, with Welch's correction. * = $p<0.05$, ** = $p<0.01$.

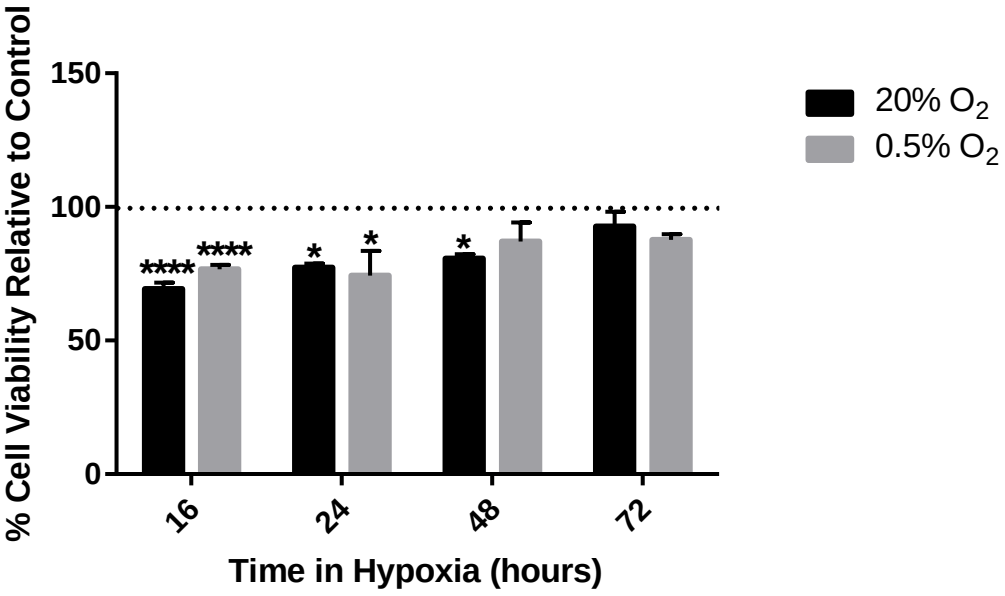

Figure 4.8: Viability of HCT116 Cells after ADAM 10 Knockdown in Severe Hypoxia (0.5% O_2)

HCT116 cells were transfected with ADAM 10 targeting siRNA (siADAM 10) or a non-targeting siRNA (siNT), used as a control. Cells were exposed to severe hypoxia (0.5% O_2) for 16 – 72 hours. MTS assays were then carried out to determine cellular viability as a measure of proliferation (Section 2.28.2 & 2.28.3). All results were normalised to the corresponding siNT control (indicated by dotted line) and results are expressed as relative percentage change in viability of n=3 experiments. Error bars represent +/- SEM. Statistical analysis by two-way ANOVA with Tukey's post-hoc correction. * = $p<0.05$, **** = $p<0.0001$.

HCT116 cells after siRNA knockdown of ADAM 10 (**Figure 4.8** A, $p<0.0001$). The decrease in viability was consistent between both normoxia and hypoxia, with a 31 ± 2.5% downregulation present in normoxia, and a 23 ± 1.4% decrease present after exposure to severe hypoxia. A significant downregulation in cellular viability can also be seen after 24 hours; which again was consistent between both normoxia (23 ± 1.5% decrease) and hypoxia (25 ± 9.1% decrease) (**Figure 4.8 B**, $p<0.05$). For longer experimental time points, ADAM 10 knockdown has a reduced effect on cellular viability, with significance only seen at 48 hours in normoxia (**Figure 4.8 B**, 20 ± 1.6% decrease; $p<0.05$). No significant differences after ADAM 10 knockdown were seen in HT29 and RKO cell lines (**Figure 4.9** & **Figure 4.10**). There were no observable differences between normoxia and hypoxia, and no difference is present amongst the time points investigated. All results were deemed non-significant by two-way ANOVA analysis.

4.3.2.2 CRC Cellular Viability is Mildly Affected by ADAM 10 Inhibition

To determine whether CRC cellular viability was affected by inhibition of ADAM 10 activity, GI254023X, an ADAM 10 inhibitor, was used. It can be observed in **Figure 4.11** that treatment of HCT116 cells with GI254023X resulted in a trend indicating upregulation of viability. This trend was consistent between both normoxia (20% O_2) and hypoxia (0.5% O_2). The data showed an increase in cellular viability after treatment with GI254023X concentrations up to 15 μM, at which point the viability decreases with increasing concentrations (up to 135 μM), back to baseline level (**Figure 4.11**). Significant differences were seen in normoxia only after treatment up to 15 μM (**Figure 4.11**). HT29 and RKO cells showed no alteration to cellular viability after GI254023X treatment (**Figure 4.12** & **Figure 4.13**).

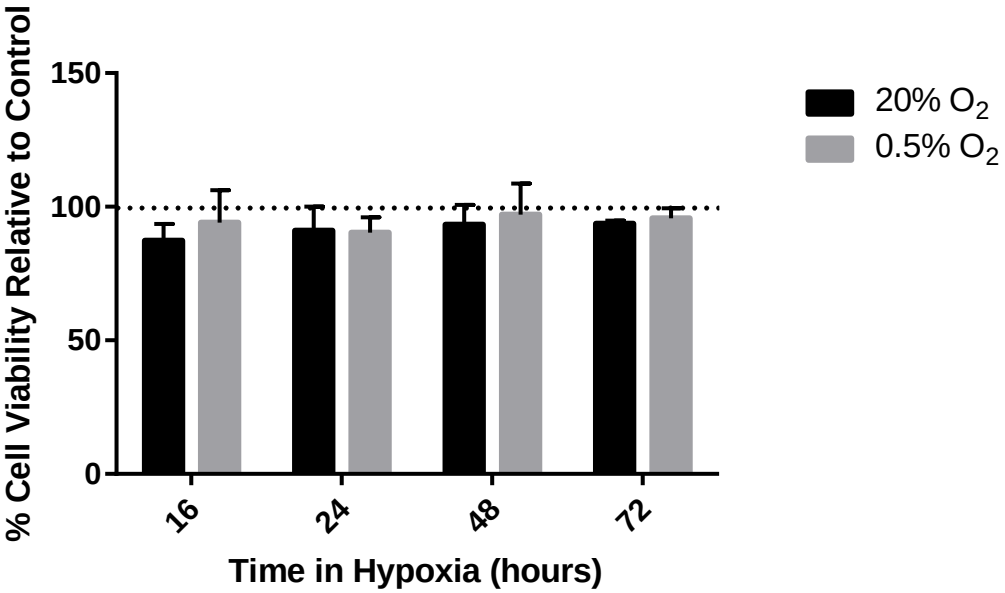

Figure 4.9: Viability of HT29 Cells after ADAM 10 Knockdown in Severe Hypoxia (0.5% O_2)

HT29 cells were transfected with ADAM 10 targeting siRNA (siADAM 10) or a non-targeting siRNA (siNT), used as a control. Cells were exposed to severe hypoxia (0.5% O_2) for 16 - 72 hours. MTS assays were then carried out to determine cellular viability as a measure of proliferation (Section 2.28.2 & 2.28.3). All results were normalised to the corresponding siNT control (indicated by dotted line) and results are expressed as relative percentage change in viability of n=3 experiments. Error bars represent +/- SEM. Statistical analysis by two-way ANOVA with Tukey's post-hoc correction. All results deemed non-significant.

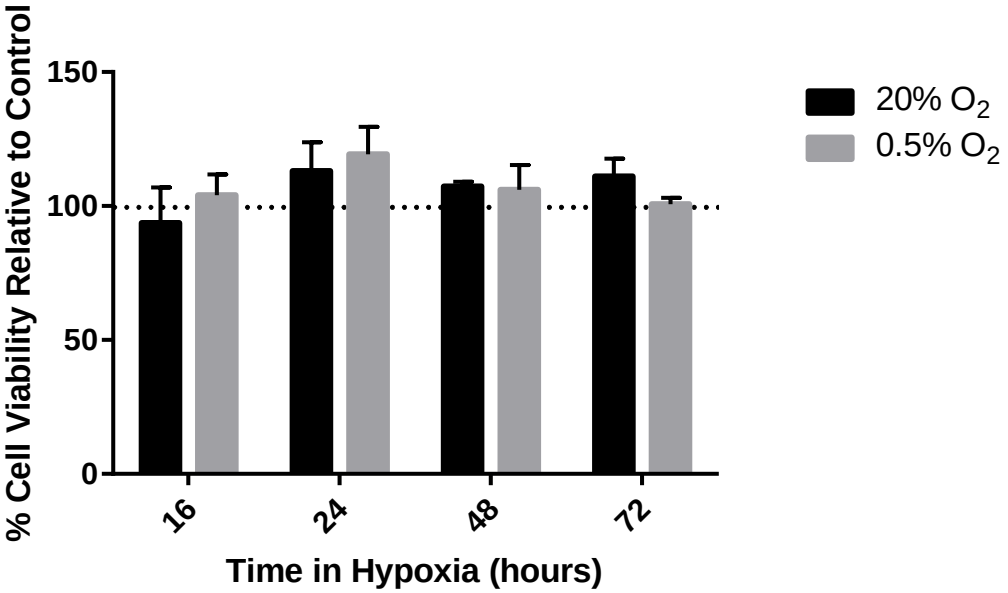

Figure 4.10: Viability of RKO Cells after ADAM 10 Knockdown in Severe Hypoxia (0.5% O_2)

RKO cells were transfected with ADAM 10 targeting siRNA (siADAM 10) or a non-targeting siRNA (siNT), used as a control. Cells were exposed to severe hypoxia (0.5% O_2) for 16 - 72 hours. MTS assays were then carried out to determine cellular viability as a measure of proliferation (Section 2.28.2 & 2.28.3). All results normalised to the corresponding siNT control (indicated by dotted line) and results are expressed as relative percentage change in viability of n=3 experiments. Error bars represent +/- SEM. Statistical analysis by two-way ANOVA with Tukey's post-hoc correction. All results deemed non-significant.

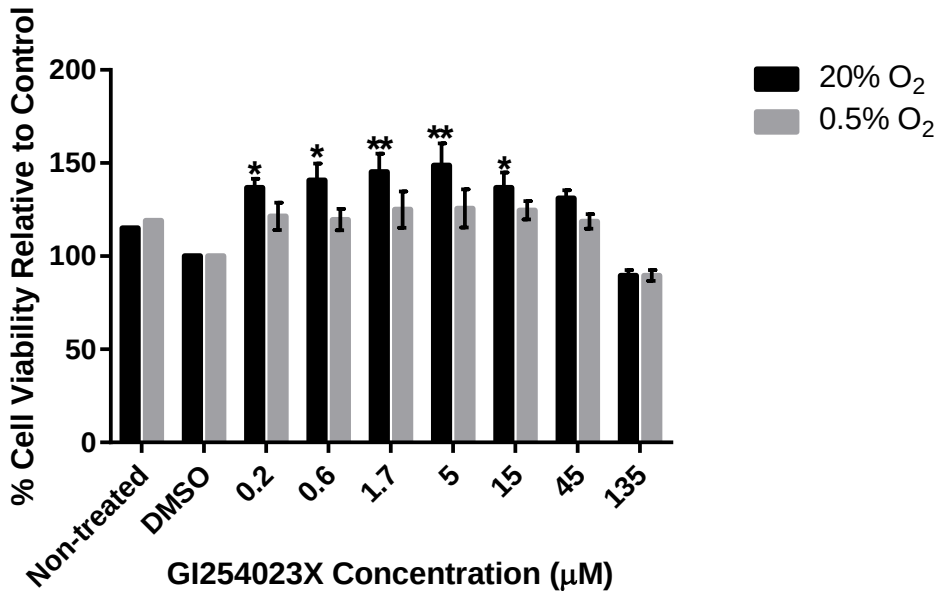

Figure 4.11: Viability of HCT116 Cells after ADAM 10 Inhibition in Severe Hypoxia (0.5% O_2)

HCT116 cells were treated with a variety of GI254023X concentrations before being exposed to severe hypoxia (0.5% O_2) or normoxia (20% O_2) for 16 hours. MTS assays were then carried out to determine cellular viability as a measure of proliferation (Section 2.28.1). DMSO was used as the vehicle control. All results were normalised to corresponding DMSO control. Results expressed as relative percentage change in viability of n=3 experiments. Non-treated control n=1 only. Error bars represent +/- SEM. Statistical analysis by two-way ANOVA with Tukey's post-hoc correction. $p<0.05$, $p<0.01$.

4.3.3 Clonogenic Survival of CRC Cells is Reduced after ADAM 10 Knockdown

To assess the impact of ADAM 10 knockdown on long term CRC cell viability clonogenic survival assays were performed (**Section 2.29**). **Figure 4.14** shows that there was a significant downregulation in the surviving fraction of HCT116 clonogenic colonies after ADAM 10 knockdown. This was consistent between both normoxia and hypoxia (**Figure 4.14**). A 28 ± 0.1% and 25 ± 0.1% decrease in surviving fractions were seen in normoxia and hypoxia, respectively, after ADAM 10 knockdown. The decreases seen at both oxygen tensions were deemed statistically significant by two-way ANOVA analysis (20% O_2: $p<0.01$; 0.5% O_2: $p<0.05$). It can be observed that HT29 cells displayed no significant reductions in surviving fractions after ADAM 10 knockdown (**Figure 4.15**). Again, this finding was consistent between both normoxia and hypoxia.

4.3.4 CRC Cell Cycle is Unaffected by ADAM 10 Knockdown

To establish the impact of ADAM 10 knockdown on the cell cycle HCT116 cells underwent cell cycle analysis by PI staining (DNA content analysis). Representative histograms indicate an upregulation in cells in sub-G1 phase after ADAM 10 knockdown, in normoxia (**Figure 4.16 A** & **B**). However, when quantitatively analysed this was found to be non-significant (**Figure 4.17**). No alterations can be observed in either G1, S of G2/M phases after ADAM 10 knockdown in normoxia (**Figure 4.16** & **Figure 4.17**). A trend indicating increased number of cells in G1 phase can be observed after ADAM 10 knockdown in hypoxia, albeit non-significant (**Figure 4.16 C** & **D**; **Figure 4.17**). It can be observed that hypoxic exposure increases the number of cells with a sub-G1 DNA content, however, when analysed by one-way ANOVA this was deemed to be non-significant (**Figure 4.16 A** & **C**; **Figure 4.17**). The error bars in **Figure 4.17** indicate a noticeable degree of variation between experimental repeats.

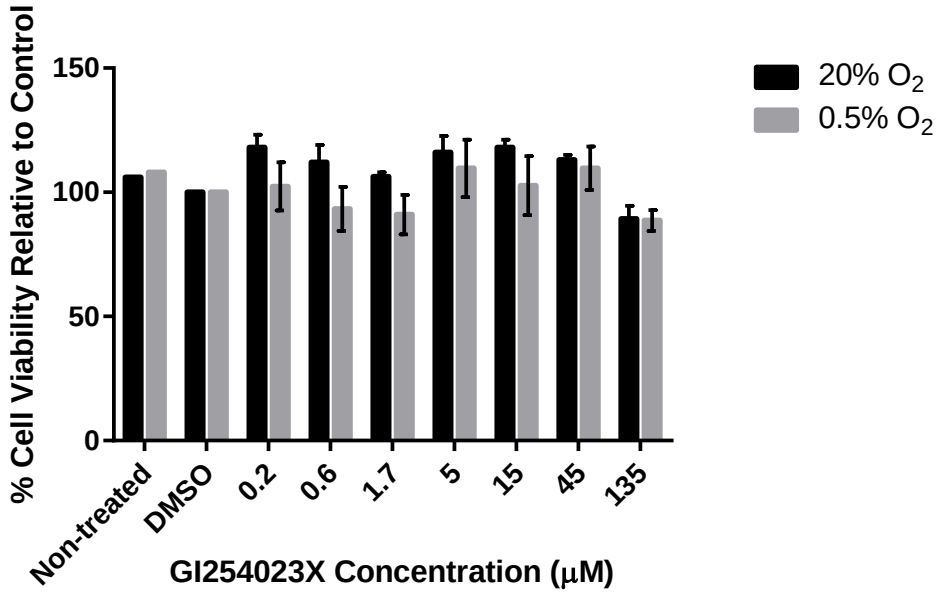

Figure 4.12: Viability of HT29 Cells after ADAM 10 Inhibition in Severe Hypoxia (0.5% O_2)

HT29 cells were treated with a variety of GI254023X concentrations before being exposed to severe hypoxia (0.5% O_2) or normoxia (20% O_2) for 16 hours. MTS assays were then carried out to determine cellular viability as a measure of proliferation (Section 2.28.1). DMSO was used as the vehicle control. All results were normalised to corresponding DMSO control. Results expressed as relative percentage change in viability of n=3 experiments. Non-treated control n=1 only. Error bars represent +/- SEM. Statistical analysis by two-way ANOVA with Tukey's post-hoc correction. All results deemed non-significant.

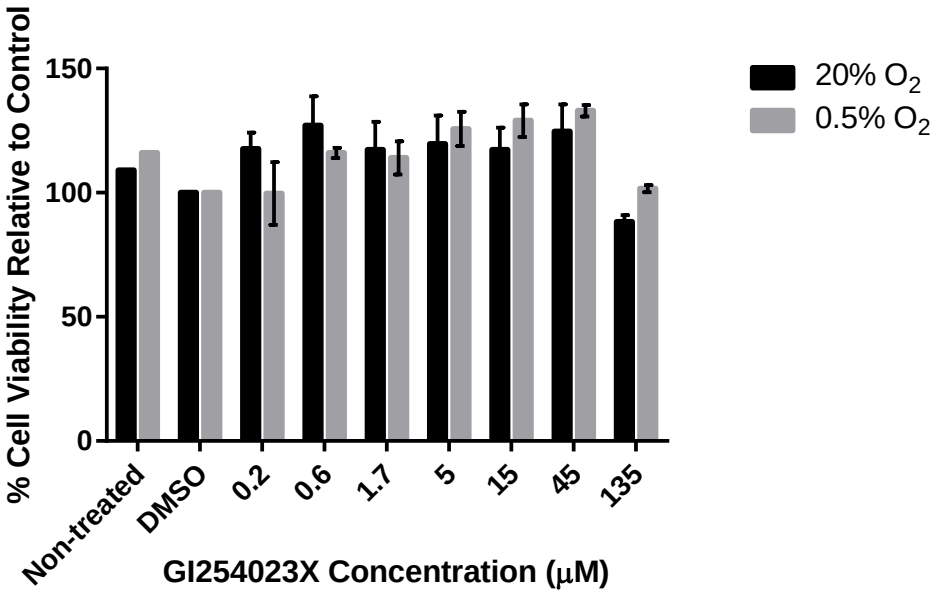

Figure 4.13: Viability of RKO Cells after ADAM 10 Inhibition in Severe Hypoxia (0.5% O_2)

RKO cells were treated with a variety of GI254023X concentrations before being exposed to severe hypoxia (0.5% O_2) or normoxia (20% O_2) for 16 hours. MTS assays were then carried out to determine cellular viability as a measure of proliferation (Section 2.28.1). DMSO was used as the vehicle control. All results were normalised to corresponding DMSO control. Results expressed as relative percentage change in viability of n=3 experiments. Non-treated control n=1 only. Error bars represent +/- SEM. Statistical analysis by two-way ANOVA with Tukey's post-hoc correction. All results deemed non-significant

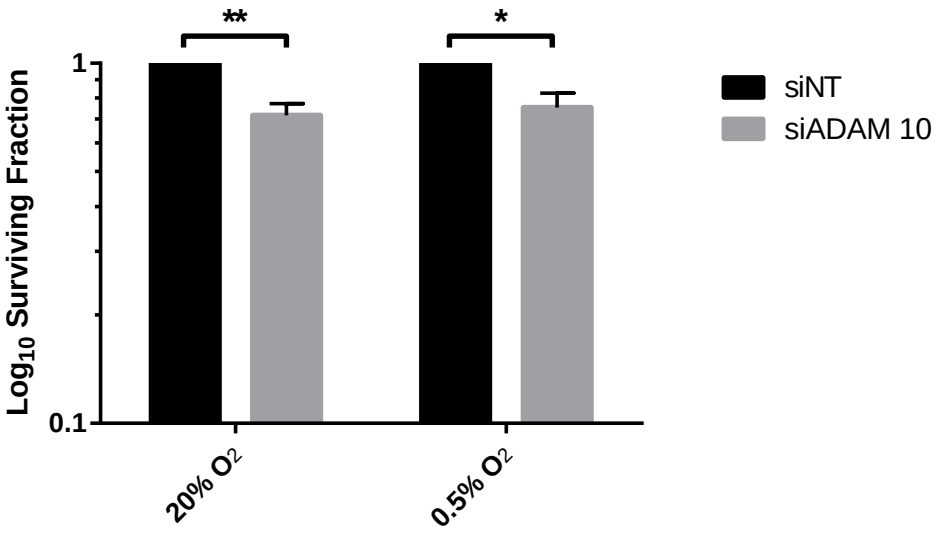

Figure 4.14: Clonogenic Survival of HCT116 Cells after ADAM 10 Knockdown in Severe Hypoxia (0.5% O_2)

HCT116 cells were transfected with ADAM 10 siRNA (siADAM 10) or a non-targeting siRNA (siNT). 250 cells were then seeded (6 wells/condition), and exposed to normoxia (20% O_2) or severe hypoxia (0.5% O_2) for 24 hours. Cells were then incubated in normoxia for 8 days to allow for colony formation. Colonies were then fixed and stained with crystal violet before being counted and surviving fraction determined (as described in Section 2.29). Scrambled siRNA (siNT) used as a control. Results expressed as fold change in surviving fraction relative to respective control (siNT). N=3 experiments, error bars represent +/- SEM. Statistical analysis by two-way ANOVA with Tukey's post-hoc correction. * = $p<0.05$, ** = $p<0.01$.

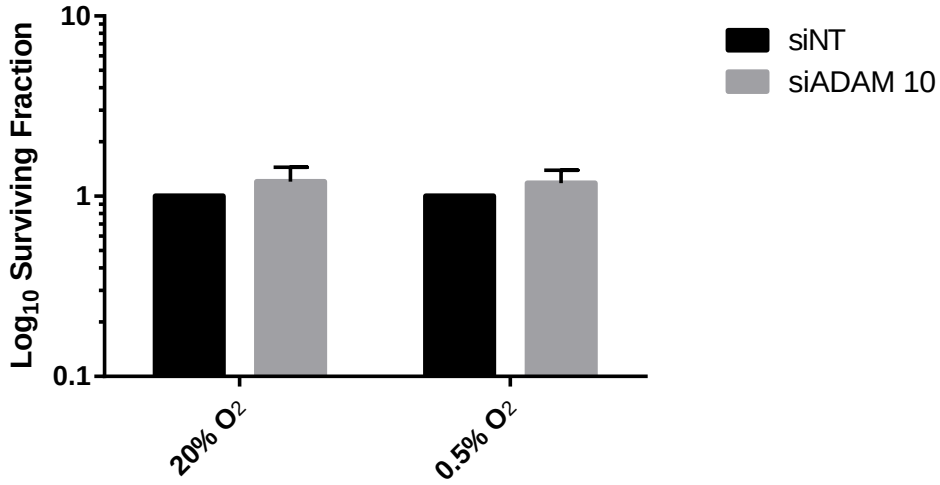

Figure 4.15: Clonogenic Survival of HT29 Cells after ADAM 10 Knockdown in Severe Hypoxia (0.5% O_2)

HT29 cells were transfected with ADAM 10 siRNA (siADAM 10) or a non-targeting siRNA (siNT). 500 cells were then seeded (6 wells/condition), and exposed to normoxia (20% O_2) or severe hypoxia (0.5% O_2) for 24 hours. Cells were then incubated in normoxia for 10 days to allow for colony formation. Colonies were then fixed and stained with crystal violet before being counted and surviving fraction determined (as described in Section 2.29). Scrambled siRNA (siNT) was used as a control. Results expressed as fold change in surviving fraction relative to respective control. N=3 experiments, error bars represent +/- SEM. Statistical analysis by two-way ANOVA with Tukey's post-hoc correction. All results deemed non-significant.

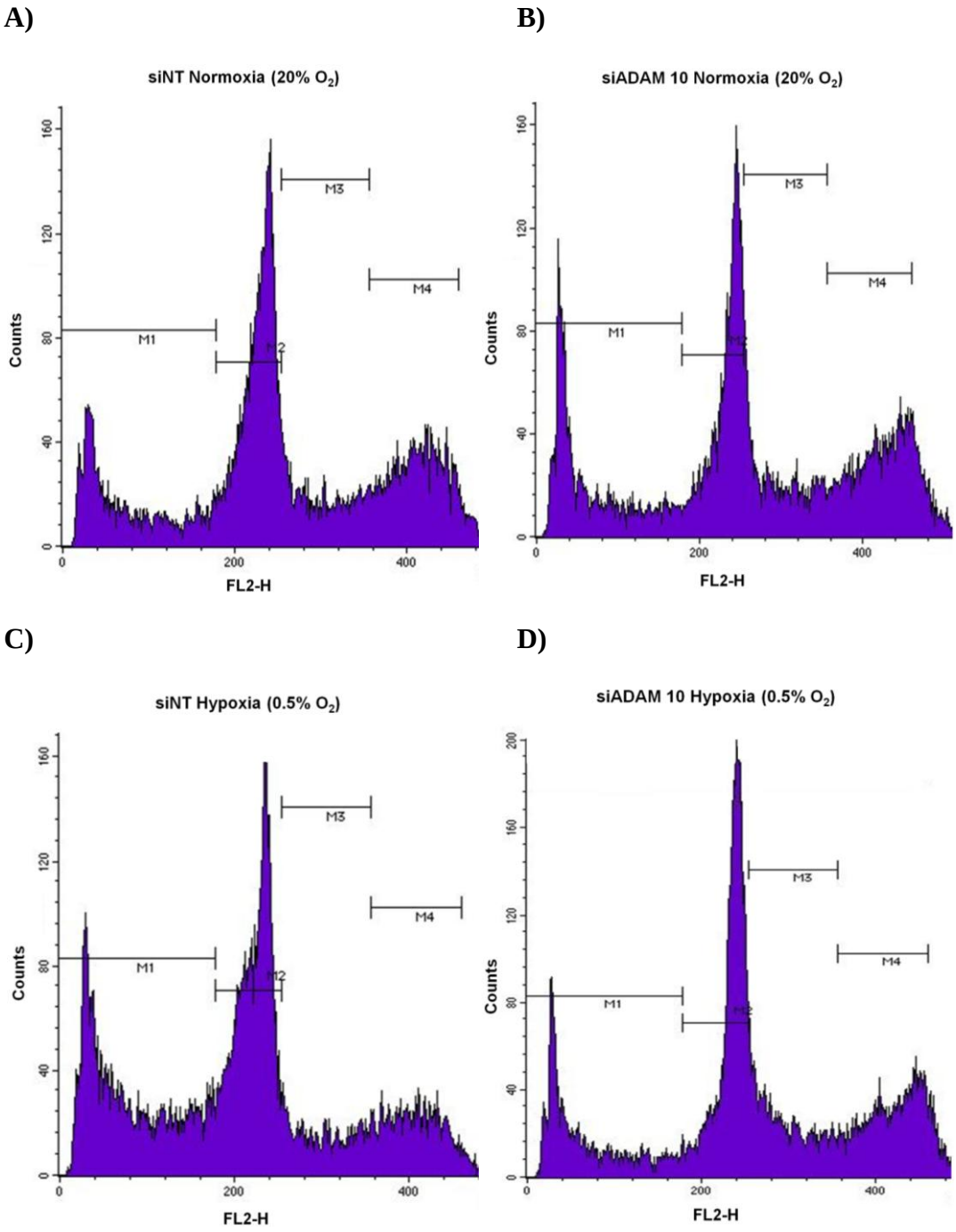

Figure 4.16: HCT116 Cell Cycle Profiles after ADAM 10 Knockdown in Severe Hypoxia

HCT116 cells were transfected with ADAM 10 siRNA (siADAM 10) or non-targeting siRNA (siNT), used as a control. Cells were then incubated in normoxia (20% O_2) or hypoxia (0.5% O_2) for 24 hours. Cells were fixed prior to staining with PI, before being analysed by flow cytometry (Section 2.30). Histograms are representative of three independent experiments. Gates represented by M1-M4 on histograms. Each gate represents different a cell cycle phase. M1 = sub-G1; M2 = G1; M3 = S and M4 = G2/M. For non-transfected and mock transfected controls see **Appendix 1**.

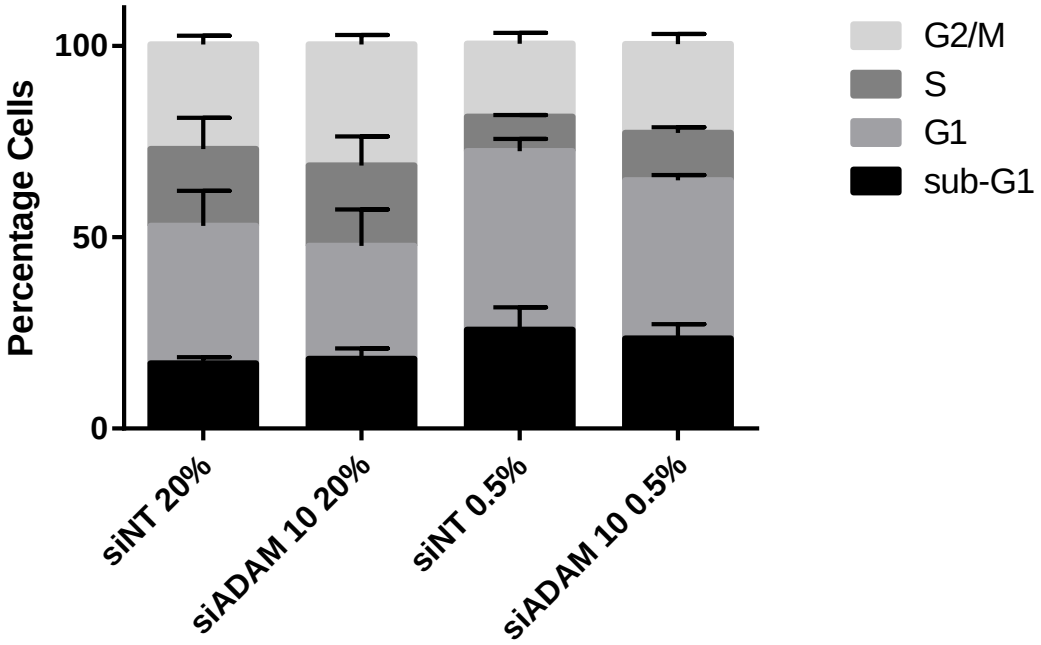

Figure 4.17: Quantitative HCT116 Cell Cycle Profiles after ADAM 10 Knockdown in Severe Hypoxia

HCT116 cells were transfected with ADAM 10 siRNA (siADAM 10) or non-targeting siRNA (siNT), used as a control. Cells were then incubated in normoxia (20% O_2) or hypoxia (0.5% O_2) for 24 hours. Cells were fixed prior to staining with PI, before being analysed by flow cytometry (Section 2.30). Cell counts for each phase were expressed as a percentage of the total count, for each of three independent experiments. n=3; error bars represent +/- SEM. Statistical analysis by one-way ANOVA, with Tukey's post-hoc correction. All results deemed non-significant by analysis.

4.4 Discussion

In the previous chapter an upregulation of ADAM 10 in CRC cell lines after exposure to hypoxia was reported. The hypoxic tumour microenvironment is known to promote metastasis and ADAMs family members have also previously been linked to the progression of cancer (Mochizuki and Okada, 2007, Edwards et al., 2008, Hongo et al., 2013, Nagaraju et al., 2015). As such, it was hypothesised that the upregulation of ADAM 10 under hypoxic conditions will promote the tumourigenic phenotype of CRC cells and mediate increased migration and proliferation.

Results showed that neither ADAM 10 knockdown or inhibition had an effect on CRC cellular migration, in either normoxia or hypoxia. An ADAM 10 mediated effect on cellular viability was identified, although this was independent of hypoxia. However, cell cycle analysis showed no alteration to the cell cycle after ADAM 10 knockdown.

GI254023X was selected for ADAM 10 inhibition due to its 100-fold specificity for ADAM 10 over ADAM 17, making it one of the most specific ADAM 10 inhibitors commercially available (Ludwig et al., 2005, Hoettecke et al., 2010, Pruessmeyer et al., 2014). Concentrations of GI254023X were used in accordance with previous reports (Maretzky et al., 2005, Pruessmeyer et al., 2014, Mullooly et al., 2015). No role of ADAM 10 in mediating cellular migration was identified, either in normoxia or hypoxia, which is in contrast to previously reported findings (Maretzky et al., 2005, Pan et al., 2012, Jones et al., 2013, Yuan et al., 2013, Fu et al., 2014, Mullooly et al., 2015, Shao et al., 2015, You et al., 2015). In bladder cancer ADAM 10 knockdown reduced cellular migration, as assessed by scratch assay (Fu et al., 2014). Similarly, in nasopharyngeal cancer, scratch assays showed that ADAM 10 silencing resulted in decreased cell migration (You et al., 2015). Fewer investigations into ADAM 10 inhibition by SMIs and cellular migration are available in the literature. However,

ADAM 10 inhibition by GI254023X has been shown to significantly reduce cell migration in breast and ovarian cancers, which is also in contrast to the data presented here (Gooden et al., 2014, Mullooly et al., 2015).

HT29 and RKO cells were two of the three CRC cell lines used throughout these experiments, and as such were examined for their migratory capacity after ADAM 10 knockdown or inhibition. A number of studies have utilised these cell lines for examination of migration previously, in the format of a scratch wound assay, and as such, based on this evidence they were selected for utilisation here (Fang et al., 2009, Kim et al., 2011, Lee et al., 2015b, Wang et al., 2015a, Yuan et al., 2015a). One limitation of this set of experiments is that it is possible neither cell line possess a particularly motile phenotype, and alternative cell lines may have been better suited for investigation into the role of ADAM 10 in CRC cell migration. One limitation of these experiments is the usage of scratch assays to assess cellular migration. Whilst it is a commonly used technique for this purpose it's not without its flaws, and as such an alternative methodology may have been more appropriate (Kramer et al., 2013). One main flaw in this technique is the poor reproducibility between experimental repeats, which was a large problem in this study, as indicated by the large SEM. However, others include the induction of a damage response from the wounded cell and the prevention of migration as a result of damage to the growth surface (Liang et al., 2007, Hulkower and Herber, 2011, Kramer et al., 2013). Alternative methodologies that may be more reproducible include the Transwell assay, the Platypus assay and electric cell-substrate impedance sensing (ECIS) assay, however these are not without their own limitations (Hulkower and Herber, 2011, Kramer et al., 2013). Previous success in measuring the effect of ADAM 10 migration has been had with Transwell assays, in a number of cancer types. These studies showed ADAM 10 knockdown resulted in decreased cellular migration in oral (Jones et al., 2013); hepatocellular (Yuan et al.,

2013); tongue (Shao et al., 2015) and breast cancer (Mullooly et al., 2015). Usage of Transwell assays would also have allowed for migration to be assessed in all three CRC cell lines in this study. Both HCT116 and HT29 cells were found to be unsuitable for scratch assays in conjunction with ADAM 10 siRNA, due to strong cell-cell adherence and low cell numbers, respectively. Therefore, by switching methodology these problems could be overcome. A further limitation of these experiments is the time scale over which migration was assessed. A number of studies that reported an ADAM 10 mediated effect examined migration over a longer time scale (Fu et al., 2014, You et al., 2015). It is feasible that the role of ADAM 10 in CRC migration was missed by examining it over a shorter time scale, therefore this should be a target for further investigation.

ADAM 10 silencing has also been shown to reduce the invasive capacity of cancer cells, a phenotype that was not examined here due to time constraints. In breast, tongue, hepatocellular, bladder and oral cancer similar findings have been reported (Mullooly et al., 2015, Shao et al., 2015, Yuan et al., 2013, Fu et al., 2014, Jones et al., 2013), respectively. It is feasible that in the case of CRC ADAM 10 may mediate an alteration in the invasive capacity of cells, whilst not affecting their migration. Therefore, the invasive phenotype of CRC cells should be investigated post-ADAM 10 knockdown through the use of Transwell invasion assays (Kramer et al., 2013).

Results showed an increase in cellular viability after exposure to severe hypoxia, which was reversed after chronic (72 hours) exposure. These results are indicative that hypoxia may affect the proliferative capabilities of CRC cells under hypoxic conditions. This is consistent with previous findings which showed that cellular viability was significantly reduced under hypoxic conditions in LoVo cells, after 48 and 72 hours (Westwood et al., 2014). However, this data contradicts previous research which has shown that both HCT116 and HT29 cells exhibited decreased proliferation after exposure to severe

hypoxia (0.1% O_2) after only 16 hour exposure (Yao et al., 2005a, Yao et al., 2005b). The downregulation observed increased in correlation to length of hypoxic exposure (Yao et al., 2005a, Yao et al., 2005b). Similarly, other studies have also reported a down regulation of CRC cell proliferation after hypoxic exposure (Westwood et al., 2014). Such differences may be accounted for due to the oxygen tensions used between this study and others. Here, 0.5% O_2 was used which is higher than that used by Yao et al., 2005a and Yao et al., 2005b (0.1% O_2), which, at nearly anoxia, may result in cell death earlier than a higher oxygen tension.

HCT116 cellular viability was significantly reduced after ADAM 10 knockdown, independently of hypoxia, with no alteration seen in HT29 or RKO cells. Such findings indicate a role of ADAM 10 in regulating the viability of HCT116 cells, which may be indicative of altered proliferation. However, results indicate that the role of ADAM 10 in CRC cell viability/proliferation is more prominent in some cell lines than others. Genetic differences between cell lines could account for such experimental variation, particularly in the context of CRC related mutations known to promote cellular proliferation. Such alterations and cell line differences will be discussed in further detail in the concluding discussion (**Section 6.1**). In line with the results shown here, previous studies have reported a role of ADAM 10 in regulating cell proliferation, in various cancer types including prostate, bladder, hepatocellular, adenoid and glioma (Maretzky et al., 2005, Arima et al., 2007, Xu et al., 2010, Bulstrode et al., 2012, Yuan et al., 2013, Fu et al., 2014, Shao et al., 2015, You et al., 2015). In hepatocellular carcinoma ADAM 10 knockdown significantly reduced cellular proliferation across 96 hours (Yuan et al., 2013). Similarly, in tongue cancer MTT analysis showed marked reduction in proliferation after ADAM 10 silencing (Shao et al., 2015). Furthermore, in bladder cancer similar results were seen post-ADAM 10 knockdown, albeit across a longer time frame (5 days) (Fu et al., 2014). Long-term reduction (up to 8 days) in proliferation after

ADAM 10 knockdown was also reported in adenoid cystic carcinoma (Xu et al., 2010). Such results indicate that the impact of ADAM 10 silencing on cellular proliferation may vary in length amongst cancer types. Previous studies have linked ADAM 10 to the progression of CRC, albeit no direct investigations into proliferation have been undertaken (Knösel et al., 2005, Gavert et al., 2007). Knösel et al. (2005) showed that *ADAM 10* expression correlated to more advanced disease and a higher tumour staging. Furthermore, ADAM 10 overexpression in CRC cells was shown to mediate liver metastasis *in vivo* (Gavert et al., 2007). Importantly, no previous studies have investigated the link between colorectal cancer cellular proliferation and ADAM 10, indicating the data presented here are novel.

ADAM 10 inhibition with GI254023X did not demonstrate the same results, with a slight increase in HCT116 viability after treatment. However, when protein levels were examined it was found that GI254023X treatment increased ADAM 10 protein expression (**Appendix 1**). Therefore, further clarification on the effects of ADAM 10 inhibition on viability is required. It is possible that the increase in viability is as a result of ADAM 10 protein stimulation, or alternatively the result of an intra-cellular negative feedback mechanism. Nevertheless, the results presented here are in contrast to those reported by Mullooly et al. (2015), where a reduction in proliferation after ADAM 10 inhibition by GI254023X was seen. The variability in results with GI254023X treatment could have wide reaching implications, as ADAMs targeting small molecule inhibitors have been trialled in the treatment of cancer (as discussed in **Section 1.10**) (Zhou et al., 2006, Fridman et al., 2007, Witters et al., 2008, Duffy et al., 2011). Therefore, further characterisation of the true effects of GI25423X treatment on CRC cells must be determined before consideration of it for therapeutic use in CRC. Alternative SMIs are available for the inhibition of ADAM 10 however, GI254023X is one of the most specific, hence why it was chosen for study here (Ludwig et al., 2005, Hoettecke et al.,

2010). Testing of alternative SMIs could be undertaken, to determine whether similar effects on HCT116 cellular viability are seen. Additionally, to corroborate the findings here the experimental conditions used by Mullooly et al. (2015) could be tested, to determine whether results could be recreated. Thus, identifying problems with the inhibitor or differences between the methodologies used to assess proliferation. Furthermore, the proteolytic activity of ADAM 10 will be examined (Chapter 5), to determine whether the treatment of cells with GI254023X and subsequent protein upregulation translates to an alteration in activity.

One major limitation of MTS assays is their assessment of viability and whether this is a reliable measurement of a cells proliferative capacity. MTS assays measure the metabolic reduction of tetrazolium salts to formazan, and assumes that formazan production will be proportional to the number of exponentially growing cells (Riss et al., 2004, Berridge et al., 2005). As a result, MTS assays have long been used as a as a readout of proliferation, however, a metabolically active cell may not be an actively proliferating cell (Riss et al., 2004, van Tonder et al., 2015). As such, whilst the results in this chapter indicate a role of ADAM 10 in mediating the viability of HCT116 cells it cannot be definitively determined that this is indicative of cellular proliferation. A reduction in viability can also be indicative of cell death and steps should be undertaken to determine whether ADAM 10 decreases cellular proliferation or induces cell death in HCT116 cells, thus affecting their viability. Appropriate methodologies for assessment of induced cell death/apoptosis include apoptosis detection assays, such as ApoTox-Glo, or measurement of Annexin V by flow cytometry (Cummings et al., 2004). Annexin V binds to phosphatidylserine (PS) on cell surfaces, and offers a quick and reliable measurement of apoptosis in cells (Cummings et al., 2004, Rieger et al., 2011). TUNEL (terminal deoxynucleotidyl transferase-dUTP nick end labelling) assays would also allow for identification of apoptosis through detection of DNA fragmentation

(Huerta et al., 2007). One limitation of the experiments here is the lack of evidence confirming successful siRNA knockdown of ADAM 10 during the MTS assays. Protein lysates prepared alongside the MTS assays would allow for the knockdown efficiency to be monitored by Western Blotting, however such blots are absent throughout these experiments. Protein lysates were in fact prepared for this purpose, however due to problems with protein stability during storage, when utilised, ADAM 10 protein was found to be largely degraded and thus the lysates un-usable for their intended purpose. The knockdown efficiency has been found to be consistent throughout other experiments in this study, and as such it can be presumed that siRNA knockdown was successful during this experiment.

To assess the long term effect of ADAM 10 knockdown on CRC viability clonogenic assays were used. Clonogenic assays assess the capability of cells to form colonies and their ability to undergo unlimited replication (Munshi et al., 2005, Franken et al., 2006, Rafehi et al., 2011). A cell that has retained its reproductive ability, and therefore is an actively proliferating and viable cell, will form a colony consisting of 50 plus cells (Munshi et al., 2005, Franken et al., 2006, Rafehi et al., 2011). ADAM 10 knockdown again resulted in reduced HCT116 viability, independently of hypoxia, which supports the earlier MTS results. No effect was seen on HT29 cells. RKO cells, in this experimental setup, resulted in a plating efficiency of over 100%. It is believed that their low adherent nature and the experimental design may explain the discrepancies. E-Cadherin expression is poor in RKO cells compared to the other CRC cell lines investigated, and previous research has shown them to be less adhesive as a result (Byers et al., 1995, Buck et al., 2007). Here, cells had to undergo transportation from the incubator to the hypoxia chamber, and vice versa after hypoxic exposure. It is feasible that this movement and the less adherent nature of RKO cells resulted in satellite colony formation and increased plating efficiency. It is widely acknowledged

that movement or disruption of colonies during clonogenic assays can result in satellite colony formation (Munshi et al., 2005). Furthermore, whilst dedicated incubators were used for clonogenic storage, increased usage of the incubators, coupled with RKOs low adherent nature, may be responsible for satellite colony production. The results here are in conjunction with previous studies, albeit with slightly different methodologies. In hepatocellular carcinoma, soft-agar colony formation assays previously showed that ADAM 10 silencing resulted in a significantly reduced colony number (Yuan et al., 2013). Similarly, in tongue cancer it was also shown that knockdown of ADAM 10 caused decreased colony formation, as assessed by soft-agar assays (Shao et al., 2015).

Here, a role for ADAM 10 in mediating the cellular viability of HCT116 cells has been identified. As a result, cell cycle analysis was undertaken to determine whether the alterations in viability seen were as a result of cell cycle arrest after ADAM 10 knockdown. PI staining and flow cytometry analysis was used, which allows for detection of cellular DNA content and subsequent identification of current cell cycle phase (Nunez, 2001, Riccardi and Nicoletti, 2006, Pozarowski and Darzynkiewicz, 2004). Results showed that ADAM 10 knockdown had no effect on cell cycle progression, thus indicating that the alteration to viability reported in this study is not as a result of cell cycle arrest. There was a degree of intra-experimental variation in this study; and therefore experiments could be repeated further to clarify the role of ADAM 10 on CRC cell cycle regulation. These findings are in conflict to previous research which has shown that ADAM 10 knockdown induces a G1 phase arrest in lymphoma (Armanious et al., 2011). Similar findings have also been reported in nasopharyngeal cancer (You et al., 2015). PI staining utilises stoichiometric staining of cellular DNA for analysis of the cell cycle, however alternative methodologies such as the use of bromodeoxyuridine (BrdU) staining may be considered more appropriate for cell cycle analysis (Nunez, 2001, Riccardi and Nicoletti, 2006, Pozarowski and Darzynkiewicz,

2004). BrdU is incorporated into cellular DNA at S phase of the cell cycle, in place of thymidine, so can be used as measurement of active cellular proliferation (Cecchini et al., 2012). BrdU allows for a more distinguishable separation of cell cycle phases than PI staining, and can also be used for cell cycle kinetic analysis (Nunez, 2001, Cecchini et al., 2012, Pozarowski and Darzynkiewicz, 2004). However, PI staining offers a more cost-effective, quick analysis of cell cycle stages than BrdU, and is considered less hazardous than BrdU due to the lack of incorporation into DNA (Nunez, 2001, Riccardi and Nicoletti, 2006).

One limitation of the experiments within this chapter is the lack of siRNA validation. It was shown that siADAM 10 transfection resulted in efficient knockdown of ADAM 10 at both protein and transcript level, however further siRNA validation could have been undertaken. The siRNA used within these experiments (and those in Chapter 5) are a pool of four individual siRNA oligos, which is a commonly utilised strategy (Smith, 2006). However, to determine the effectiveness and any off target effects, each of the four oligos could have been tested individually. This would have identified whether all oligos exert the same effects on cellular viability, as reported in this chapter, or whether this was caused by one specific siRNA oligo. Pool siRNA's are recognised to cause less off target effects than individual oligos, as the concentrations are lower in a pool format than they would be as individual oligos (Smith, 2006, Parsons et al., 2009, Hannus et al., 2014). Furthermore, research indicates that pool siRNA is more likely to generate a phenotypical knockdown model in comparison to individual oligos (Parsons et al., 2009). However, despite this, it is feasible that the effect on viability shown here could be as a result of an off target effect. Therefore, characterisation of individual oligos within the pool siRNA should be undertaken.

A further limitation of this chapter is the lack of confirmation of a hypoxic environment throughout the experiments. As described in Chapter 3 attempts were made to analyse

HIF-1α expression by Western Blotting, however the lysis buffer was not stringent enough to extract HIF-1α from its nuclear localisation. To definitely confirm that all experiments were undertaken in hypoxia such controls should have been implemented.

Here, a role of ADAM 10 in mediating CRC viability has been identified. Interestingly, this was independent of hypoxia, thus rejecting the hypothesis that 'hypoxia-induced ADAM 10 expression will promote cellular proliferation and migration in CRC cell lines'. As cell cycle analysis showed no alterations it's important to elucidate the mechanisms behind the role of ADAM 10 in CRC cell viability. As such, a variety of signalling pathways linked to cell survival and proliferation in CRC will be investigated. Furthermore, the proteolytic activity of ADAM 10 under hypoxic conditions, which may activate such pathways, will be examined.

Chapter 5 : Evaluation of ADAM 10 Activity in Hypoxia

5.1 Introduction

In Chapter 4 it was shown that knockdown of ADAM 10 resulted in a significant downregulation of cellular proliferation in HCT116 cells. However, no alterations to the cell cycle were seen, thus indicating that other mechanisms are responsible. Therefore, this chapter will aim to elucidate the underlying mechanisms involved in ADAM 10 modulated cellular proliferation.

5.1.1 ADAMs Activity and Signalling in Cancer

ADAMs family members have been shown to be responsible for cleavage of transmembrane proteins, converting them into soluble forms and triggering downstream signalling (Murphy, 2008, Duffy et al., 2011, Reiss and Saftig, 2009). ADAM 10 in particular has been shown to be responsible for the shedding of a number of cancer associated proteins (as discussed in **Section 1.8.1**) (Fahrenholz et al., 2000, Six et al., 2003, Sahin et al., 2004, Maretzky et al., 2005, Reiss et al., 2005, Sanderson et al., 2006, Maretzky et al., 2008, Guo et al., 2012, Woods and Padmanabhan, 2013, Groot et al., 2014, Zhuang et al., 2015). Protein shedding by ADAMs members activates a variety of cancer-associated signalling pathways in a range of cancer types (Hartmann et al., 2002, Borrell-Pages et al., 2003, Bozkulak and Weinmaster, 2009, Baumgart et al., 2010, Christian, 2012, Maretzky et al., 2011, Wang et al., 2013). Two of the main ADAMs activated pathways are EGFR (**Section 1.9.2**) and Notch (**Section 1.9.3**), both of which have been implicated in promoting cancer progression (Tol et al., 2010, Peignon et al., 2011, Sethi and Kang, 2011, Mann et al., 2012, Yabuuchi et al., 2013, Yuan et al., 2015b).

ADAM 10 is involved in the regulation of Notch signalling through cleavage of the Notch receptor, resulting in promotion of cellular proliferation, survival and EMT (Hartmann et al., 2002, Borggrefe and Oswald, 2009, Bozkulak and Weinmaster, 2009,

Baumgart et al., 2010, Guo et al., 2013, Ishida et al., 2013, Hassan et al., 2014, Qiu et al., 2015). Crucially, Notch signalling is one of the key pathways associated with colon development, and it has been shown that ADAM 10 knockout models are embryonic lethal, due to the poor development as a result of Notch signalling disruption (**Section 1.11**) (Hartmann et al., 2002). Furthermore, Notch signalling has been implicated in CRC progression as Notch signalling is essential for evasion of apoptosis in CICCs (Sikandar et al., 2010, Gopalakrishnan et al., 2014, Fender et al., 2015). Similarly, it has been shown that increased Notch signalling within CRC results in increased EMT (Fender et al., 2015). Cleavage of ligands by ADAMs family members contribute to the activation of the EGFR signalling pathway resulting in altered cellular proliferation, survival and angiogenesis, in a variety of cancer types (Banck and Grothey, 2009, Tol et al., 2010, Ji et al., 2015, Song et al., 2015, Lim et al., 2016). EGFR signalling is of particular importance in CRC as EGFR is upregulated in approximately 60-80% of CRC tumours (Banck and Grothey, 2009, Li et al., 2011, Tan and Du, 2012, Hong et al., 2015, Pabla et al., 2015).

Hypoxia has been linked to both pathways, with results showing that EGFR targeted therapies result in a reduction of hypoxic related genes and proteins, along with reduced hypoxic CRC tumour volume post treatment (Greening et al., 2015). Notch1 has previously been found to be significantly upregulated in hypoxic tumour cells compared to normoxic controls (Chen et al., 2007). Notably, studies have previously linked Notch, EGFR and hypoxia together, showing that EGFR is linked to promotion of angiogenesis in tumours through activation of Notch1 and HIF-1α signalling (Baumgart et al., 2010, Wang et al., 2015b). It has previously been shown that the expression of ADAM 17 is correlated to increased Notch1 signalling and EGFR expression, and that Notch1 was responsible for modulating EGFR expression (Baumgart et al., 2010).

5.1.2 Rationale, Aims and Objectives of this Chapter

ADAMs family members have been linked to promotion of cancer progression through modulation of signalling pathways such as EGFR and Notch. Previous findings have shown a reduction in cellular proliferation after ADAM 10 knockdown, without effect on the cell cycle (Chapter 4). Therefore, this chapter aims to elucidate the underlying signalling mechanisms that may be involved in the modulation of cellular proliferation by ADAM 10. Furthermore, this chapter aims to identify what effects the hypoxia-mediated ADAM 10 upregulation (Chapter 3) has upon ADAM 10 activity.

The experimental work within this chapter was designed to test the hypothesis that 'Exposure to severe hypoxia will increase ADAM 10 proteolytic activity and subsequently activate downstream signalling mechanisms linked to CRC progression' and specifically answer the following questions:

- Is ADAM 10 activity modulated by exposure to severe hypoxia (0.5% O_2)?
- Does ADAM 10 regulate cancer associated signalling pathways such as Notch, EMT or EGFR, and does exposure to severe hypoxia (0.5% O_2) mediate this?

5.2 Methods

5.2.1 ADAM 10 Activity Assay

HCT116 cells underwent either ADAM 10 silencing by siRNA transfection (**Section 2.10**) or ADAM 10/generalised ADAMs family inhibition by GI254023X or GM6001, respectively (**Section 2.31.1**). Cells were then exposed to either normoxia or hypoxia (**Section 2.9**) for 16 hours before ADAM 10 activity was assessed through use of ADAM 10 fluorogenic substrates, as described in **Section 2.31**.

5.2.2 Western Blotting

HCT116 cells were transfected with either ADAM 10 targeting or non-targeting control siRNA (**Section 2.10**) before being exposed to hypoxia for a range of time points (0 – 48 hours). Cells were then lysed and quantified (**Sections 2.11** & **2.12** respectively) and 30 μg protein separated by SDS-PAGE (**Section 2.15**). Expression of a number of proteins was then assessed by Western Blotting (**Section 2.16**). Proteins analysed include E-Cadherin, β-Catenin, Slug, Snail, Vimentin, pEGFR, pGAB1, pStat5, pAKT, pERK 1/2, c-MYC, Cyclin D1 and p21. β-Actin was used as the loading control to which all resulted were normalised. All antibodies were used according to details specified in **Table 2.2**.

5.2.3 qPCR

HCT116 cells underwent siRNA transfection with either ADAM 10 targeting or non-targeting control siRNA before being exposed to either normoxia or hypoxia for 24 hours (**Section 2.9**). mRNA was then extracted and quantified (**Sections 2.23 & 2.24** respectively). 1 μg of extracted RNA then underwent cDNA synthesis (**Section 2.25**) before qPCR was undertaken as specified in **Section 2.26** and **Table 2.5**. Expression of *Notch1*, *Hes1*, *Hes5*, *Hey1*, *Hey2*, *c-MYC* and *CCND1* at transcript level was undertaken

using the custom designed primers specified in **Table 2.4**. *SLC2A1* expression was analysed to serve as a control for a hypoxic environment and *B2M* was used as the housekeeping control, to which all results were normalised. Details of both *SLC2A1* and *B2M* QuantiTECT primers can be found in **Table 2.3**.

5.3 Results

5.3.1 Effect of ADAM 10 Knockdown on ADAM 10 Activity in Severe Hypoxia

To determine the sheddase activity of ADAM 10 under hypoxic conditions two fluorogenic peptide substrates were used, in conjunction with ADAM 10 siRNA (to establish ADAM 10 specific activity). Results using the peptides are somewhat obscure and indeterminable at times, with large variability amongst the results, a finding which is consistent between both peptides. Nonetheless, use of peptide A suggests a downregulation in ADAM 10 activity in control cells after exposure to severe hypoxia (0.5% O_2, **Figure 5.1 A**). The results after ADAM 10 siRNA transfection show no alteration in ADAM 10 activity, with large error bars and negative values present (**Figure 5.1 B**). Usage of peptide B indicates no alteration in ADAM 10 activity post-hypoxic exposure (**Figure 5.2 A**). It can be seen that no alteration in activity was present after ADAM 10 knockdown, when peptide B was used (**Figure 5.2 B**). All results were deemed non-significant when statistically analysed.

5.3.2 Effect of ADAM 10 Inhibition on ADAM 10 Activity in Severe Hypoxia

To determine the effect of exposure to severe hypoxia (0.5% O_2) and the effectiveness of ADAM 10 inhibition using small molecule inhibitors, ADAM 10 activity was assessed through the use of two fluorogenic peptide substrates, Peptide A and Peptide B. The results are somewhat inconclusive and illustrate that large deviation between repeats was present, along with generation of negative values post-background fluorescence correction. It can be observed that in untreated cells there was no alteration in ADAM 10 activity after exposure to severe hypoxia (0.5% O_2), with either peptide (**Figure 5.3 A** & **Figure 5.4 A**). Peptide A usage shows that there is a reduction in

A)

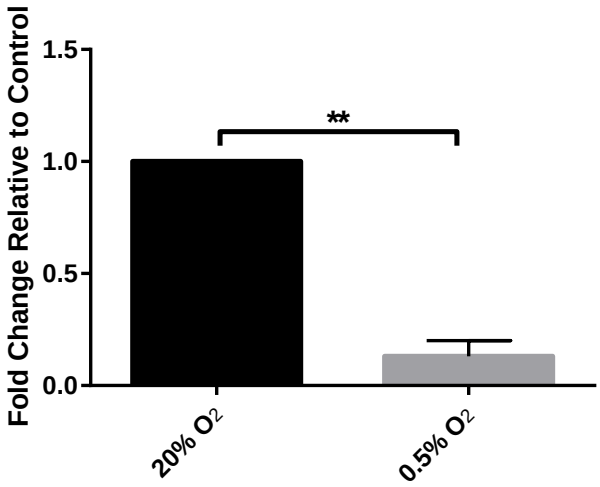

B)

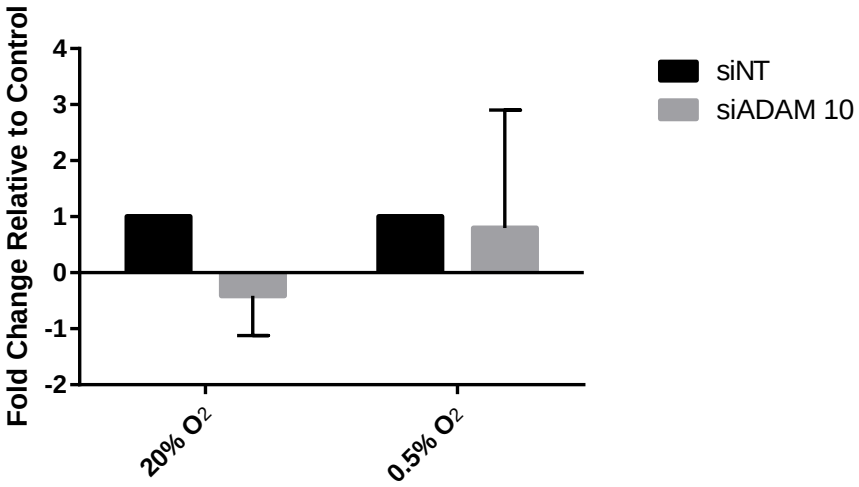

Figure 5.1: Effect of Severe Hypoxia (0.5% O_2) and ADAM 10 Knockdown on ADAM 10 Activity (Peptide A)

HCT116 cells were transfected with ADAM 10 targeting siRNA (siADAM 10) or a non-targeting siRNA (siNT), prior to being re-seeded and left to adhere (B). None transfected cells went through the same experimental process (A). Cells were then exposed to normoxia (20% O_2) or severe hypoxia (0.5% O_2) for 16 hours. 20 μM Peptide A was then added and incubated at 37°C for 1 hour. Fluorescence was then measured (Section 2.31.2). A) Results expressed as fold change in fluorescence relative to normoxic control, n=3. Error bars represent +/- SEM. Statistical analysis by unpaired, two-tailed T-test, with Welch's correction. ** = $p<0.01$. B) All results normalised to relative siNT control, n=3. Error bars represent +/- SEM. Statistical analysis by two-way ANOVA with Tukey's post-hoc correction. All results deemed non-significant.

A)

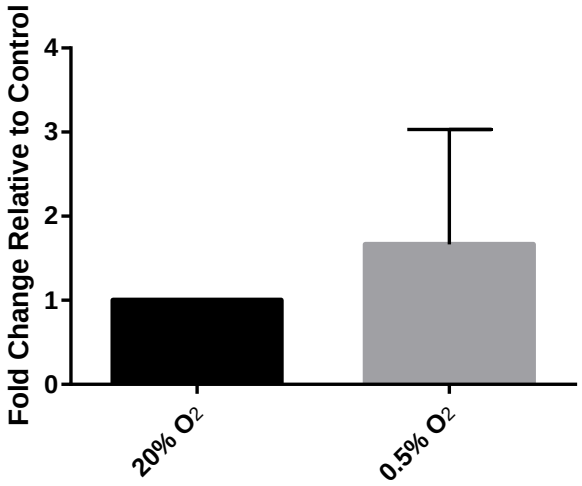

B)

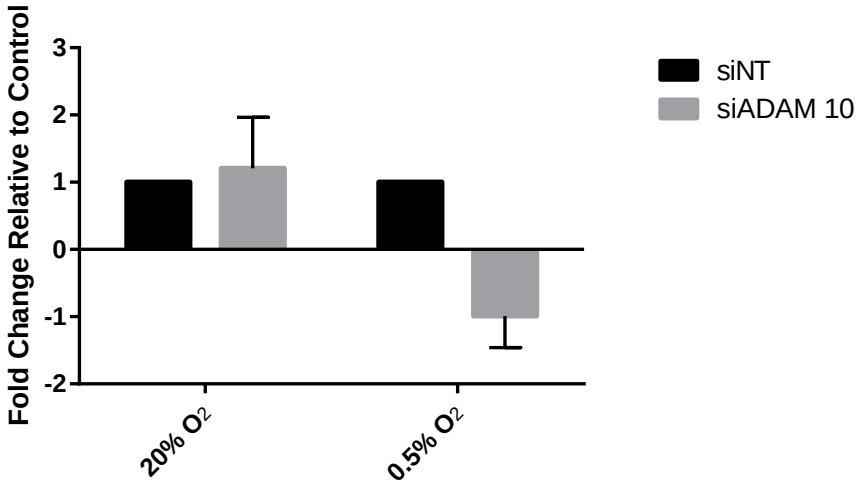

Figure 5.2: Effect of Severe Hypoxia (0.5% O_2) and ADAM 10 Knockdown on ADAM 10 Activity (Peptide B)

HCT116 cells were transfected with ADAM 10 targeting siRNA (siADAM 10) or a non-targeting siRNA (siNT), prior to being re-seeded and left to adhere (B). None transfected cells went through the same experimental process (A). Cells were then exposed to normoxia (20% O_2) or severe hypoxia (0.5% O_2) for 16 hours. 20 μM Peptide B was then added and incubated at 37°C for 1 hour. Fluorescence was then measured (Section 2.31.2). A) Results expressed as fold change in fluorescence relative to normoxic control, n=3. Error bars represent +/- SEM. Statistical analysis by unpaired, two-tailed T-test, with Welch's correction. ** = $p<0.01$. B) All results normalised to relative siNT control, n=3. Error bars represent +/- SEM. Statistical analysis by two-way ANOVA with Tukey's post-hoc correction. All results deemed non-significant.

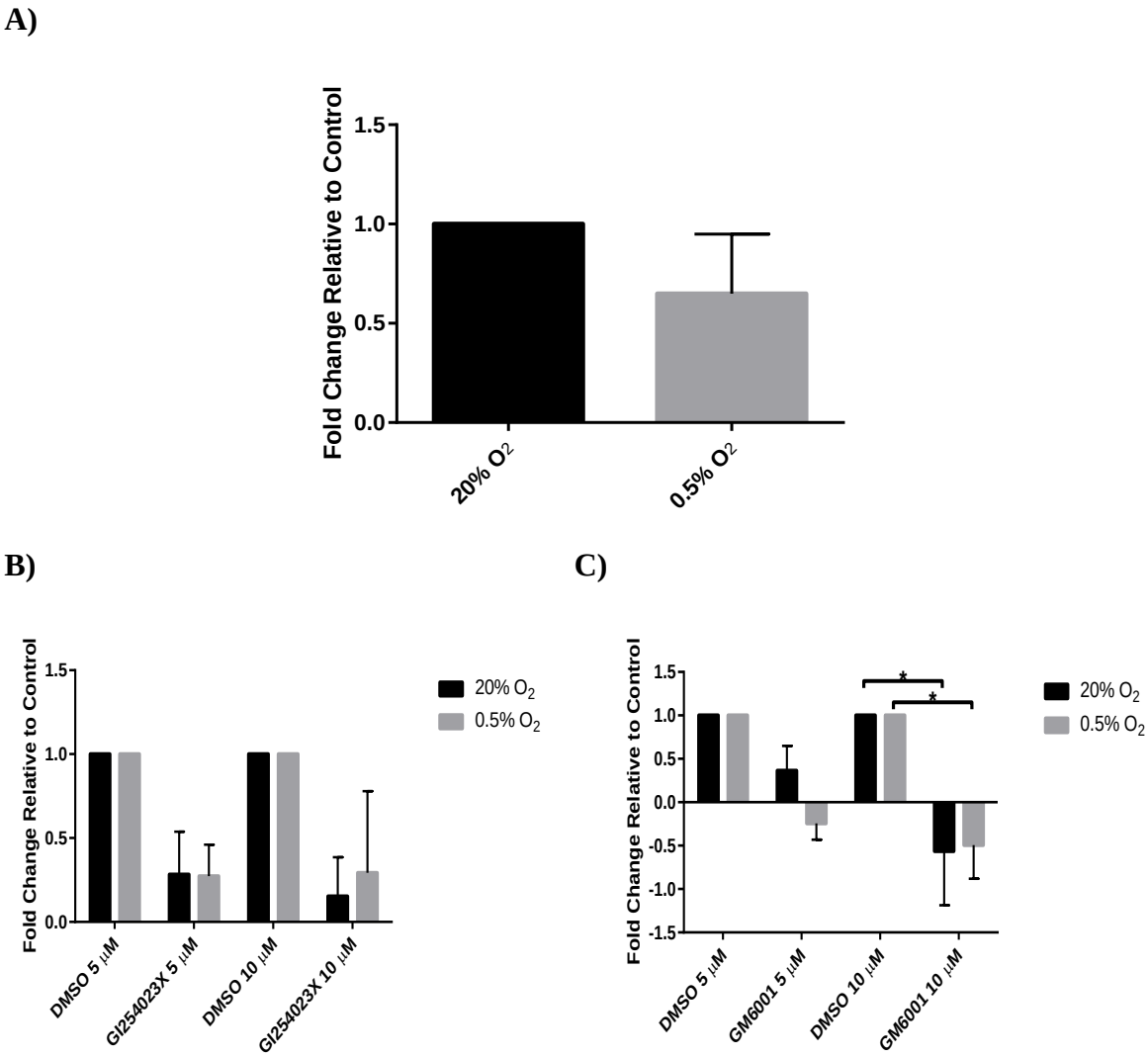

Figure 5.3: Effect of Severe Hypoxia and ADAM 10 Inhibition on ADAM 10 Activity (Peptide A)

HCT116 cells were seeded and left to adhere, they were then either left untreated (A) or treated with GI254023X (B) or GM6001 (C). Cells were then incubated in either normoxia (20% O_2) or severe hypoxia (0.5% O_2) for 16 hours. 20 μM Peptide A, alongside fresh treatment, was added before fluorescence was measured (as described in Section 2.31.1). A) Results expressed as fold change in fluorescence relative to normoxic control, n=3. Error bars represent +/- SEM. Statistical analysis by unpaired, two-tailed T-test, with Welch's correction. B & C) Results expressed as fold change relative to corresponding vehicle control, DMSO. Error bars represent +/- SEM, n=3. Statistical analysis by two-way ANOVA, with Tukey's post-hoc correction. * = $p<0.05$.

A)

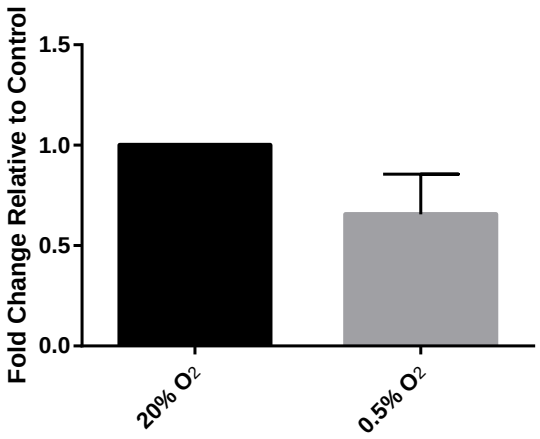

B)

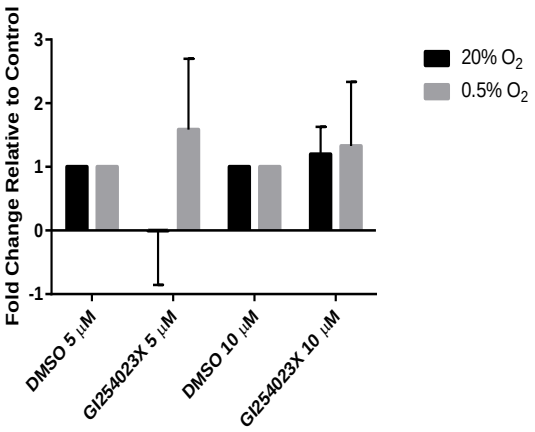

C)

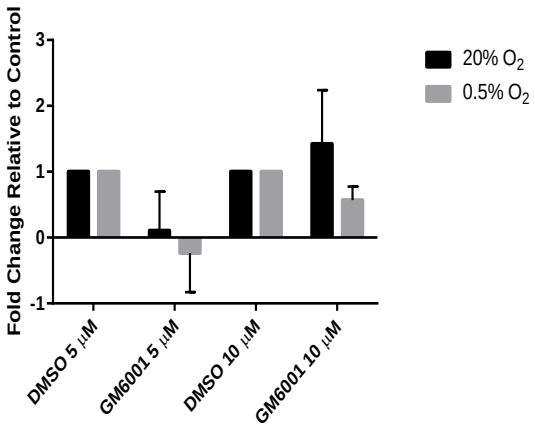

Figure 5.4: Effect of Severe Hypoxia and ADAM 10 Inhibition on ADAM 10 Activity (Peptide B)

HCT116 cells were seeded and left to adhere, they were then either left untreated (A) or treated with GI254023X (B) or GM6001 (C). Cells were then incubated in either normoxia (20% O_2) or severe hypoxia (0.5% O_2) for 16 hours. 20 μM Peptide B, alongside fresh treatment, was added before fluorescence was measured (as described in Section 2.31.1). A) Results expressed as fold change in fluorescence relative to normoxic control, n=3. Error bars represent +/- SEM. Statistical analysis by unpaired, two-tailed T-test, with Welch's correction. B & C) Results expressed as fold change relative to corresponding vehicle control, DMSO. Error bars represent +/- SEM, n=3. Statistical analysis by two-way ANOVA, with Tukey's post-hoc correction. All results deemed non-significant by analysis.

ADAM 10 activity after usage of either ADAM 10 inhibitor, albeit not significant (**Figure 5.3 B** & **C**). Significant reductions in ADAM 10 activity were seen at higher concentrations of GM6001 compared to vehicle controls (DMSO, **Figure 5.3 C**). It can be observed that there are no alterations in ADAM 10 activity after inhibition with either small molecule inhibitor, when using Peptide B as a substrate (**Figure 5.4 B** & **C**). Large margins of error can be seen throughout, as illustrated by the error bars. All results were deemed non-significant by statistical analysis.

5.3.3 Effects of ADAM 10 Knockdown on Associated Signalling Pathways in Severe Hypoxia

To determine the role of ADAM 10 in regulating cell signalling pathways associated with cancer progression, CRC cell lines models, particularly HCT116 cells, underwent ADAM 10 knockdown and were exposed to severe hypoxia (0.5% O_2) for a variety of time points. The expression of a number of molecules associated with ADAMs signalling were then examined by Western Blotting or qPCR.

5.3.3.1 ADAM 10 Knockdown has no Effect on EMT Markers in Severe Hypoxia

Known markers of EMT, as discussed in **Section 1.9.4**, were selected for examination at protein level to determine the role of ADAM 10 in mediating EMT in CRC. It can be observed that there is a slight increase in E-Cadherin expression across the hypoxic time course, however no effect of ADAM 10 knockdown can be observed (**Figure 5.5)**. A doublet band of E-Cadherin can be seen after 24 hours in hypoxia, which increases after 48 hours. β-Catenin expression is altered after exposure to severe hypoxia, however ADAM 10 knockdown has no effect on β-Catenin expression (**Figure 5.5**). It can be observed that after hypoxic exposure a laddering of bands is present, which increases in number and intensity in correlation with the length of hypoxic exposure. However, this pattern is not altered after ADAM 10 knockdown (**Figure 5.5**).

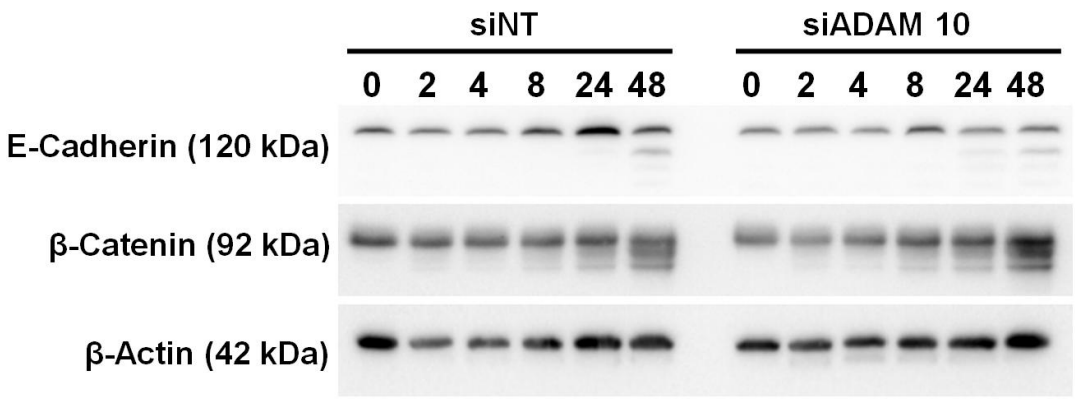

Figure 5.5: Effect of ADAM 10 Knockdown on EMT Markers in Severe Hypoxia (0.5% O_2)

HCT116 cells were transfected with ADAM 10 targeting siRNA (siADAM 10) or non-targeting siRNA (siNT) and exposed to severe hypoxia (0.5% O_2) for a range of time points. Cells were lysed, 30 μg of each protein sample were separated by SDS-PAGE and expression of various EMT associated proteins were analysed by Western Blotting. β-Actin was used as the loading control. Blots shown are representative of three independent experiments.

5.3.3.2 ADAM 10 Knockdown has no Effect on EGFR Signalling in Severe Hypoxia

ADAMs family members have been shown to activate EGFR signalling, although less is known about the involvement of ADAM 10 in this pathway. EGFR signalling is known to mediate cellular proliferation, and as alterations in proliferation were reported in Chapter 4, EGFR signalling molecules that may be involved were examined. Analysis of expression of EGFR signalling molecules after ADAM 10 knockdown in severe hypoxia (0.5% O_2) can be seen in **Figure 5.6**. The levels of pAKT phosphorylation increase during exposure to severe hypoxia (0.5% O_2) (**Figure 5.6**). However, ADAM 10 knockdown has no visible effect on the phosphorylation intensity of pAKT. Similarly, levels of pERK 1/2 phosphorylation increased after exposure to severe hypoxia (0.5% O_2), with consistent increases observed across the time course (**Figure 5.6**). Particularly, the bottom band of pERK 1/2, which corresponds to pERK 1, with a molecular weight of 42 kDa, is noticeably increased. ADAM 10 knockdown had no effect on the intensity of pERK 1/2 phosphorylation (**Figure 5.6**).

5.3.3.3 Neither Severe Hypoxia or ADAM 10 Knockdown have an Effect on *Notch1* Signalling

ADAM 10 is strongly implicated in Notch signalling, and downstream molecules of this pathway have been shown to mediate cancer progression and cell proliferation. Therefore, a number of downstream Notch signalling targets were examined. The effects of ADAM 10 knockdown and severe hypoxia (0.5% O_2) on *Notch1* expression were examined by qPCR. HCT116, HT29 and RKO cells were transfected with ADAM 10 targeting siRNA (siADAM 10) or scrambled control siRNA (siNT) and exposed to severe hypoxia (0.5% O_2) for 24 hours. It can be seen in **Figure 5.7** that there was no significant effect of either exposure to severe hypoxia or ADAM 10 knockdown in any of the CRC cell lines investigated.

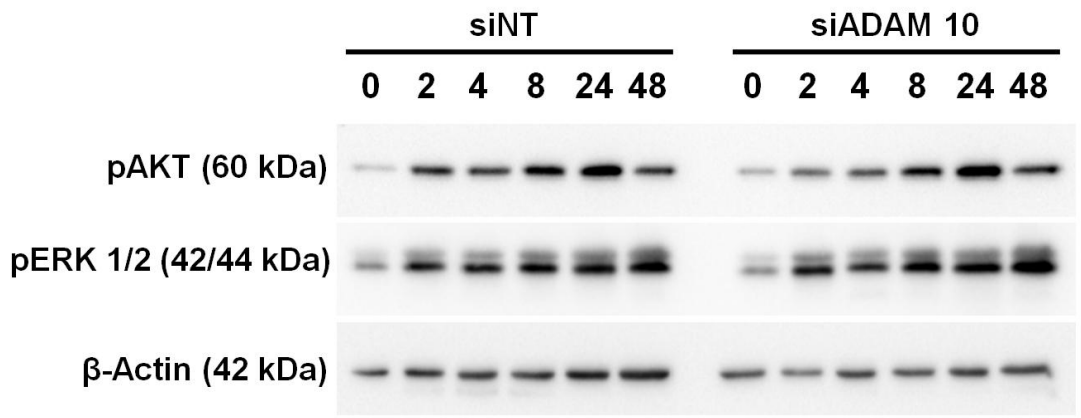

Figure 5.6: Effect of ADAM 10 Knockdown on EGFR Signalling in Severe Hypoxia (0.5% O_2)

HCT116 cells were transfected with ADAM 10 targeting siRNA (siADAM 10) or non-targeting siRNA (siNT) and exposed to severe hypoxia (0.5% O_2) for a range of time points. Cells were lysed, 30 μg of each protein sample were separated by SDS-PAGE and the phosphorylation status of various EGFR associated proteins were analysed by Western Blotting. β-Actin was used as the loading control. Blots shown are representative of three independent experiments.

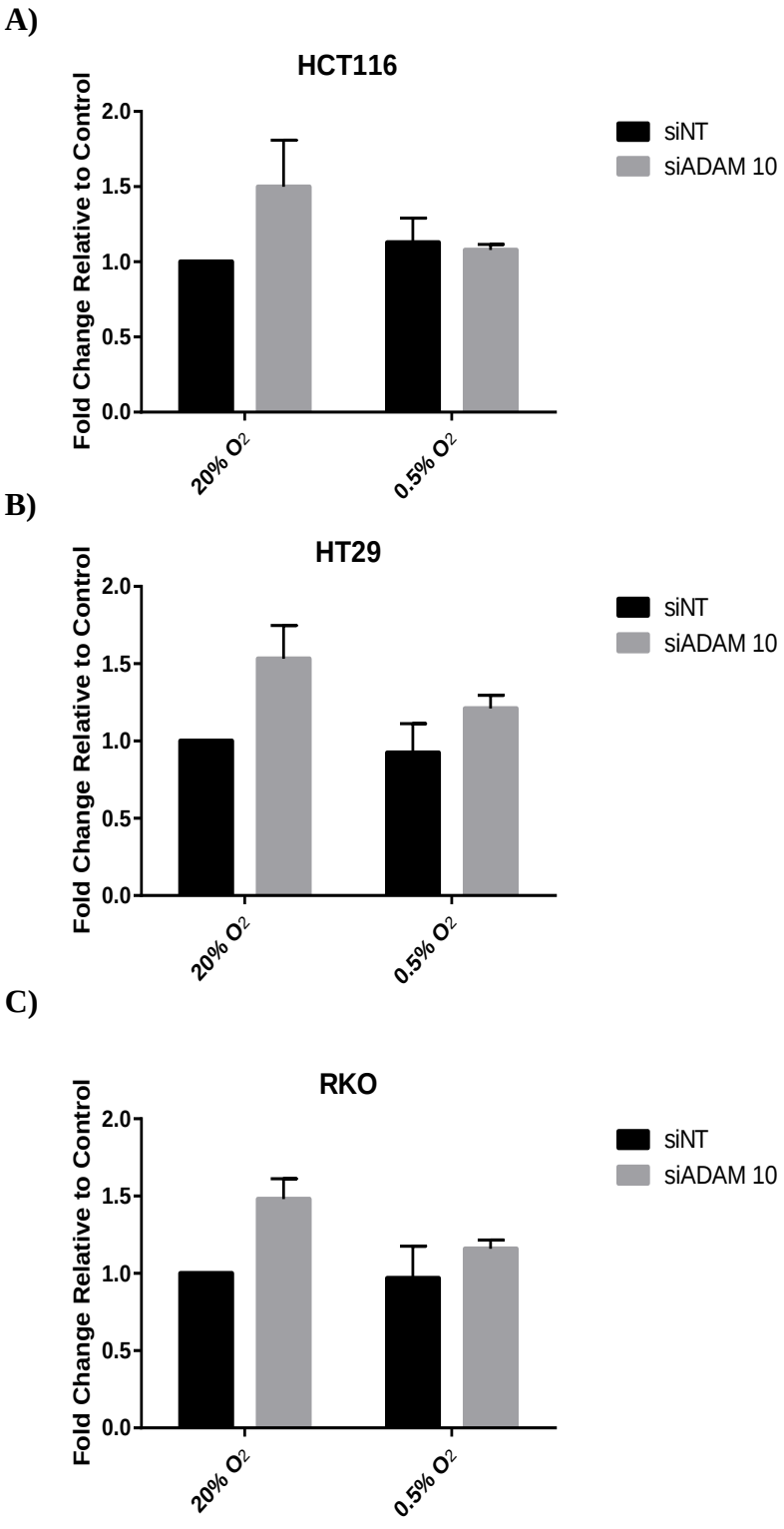

Figure 5.7: *Notch1* Expression in CRC Cells Lines after ADAM 10 Knockdown in Severe Hypoxia

CRC cell lines were transfected with ADAM 10 targeting siRNA (siADAM 10) or non-targeting siRNA (siNT), and exposed to hypoxia (0.5% O_2) for 24 hours. mRNA was extracted and *Notch1* expression analysed by qPCR. All results were normalised to the housekeeping gene, *B2M*. Results are expressed as fold change in expression relative to the 0h control (normoxia, 20% O_2), of n=3 experiments. Error bars represent +/- SEM. Statistical analysis by two-way ANOVA, with Tukey's post-hoc correction. All results deemed non-significant.

The same trend in *Notch1* expression is consistent amongst the CRC cell lines investigated, with a small increase in *Notch1* after ADAM 10 knockdown in normoxia, which is then reduced in hypoxia (**Figure 5.7**). However, no significance was determined by two-way ANOVA analysis.

The effect of ADAM 10 knockdown on *Hes1* expression was also evaluated in a panel of CRC cell lines. A small increase in *Hes1* expression in hypoxia can be observed for HCT116 cells, albeit non-significant (**Figure 5.8 A**). A similar trend was also observed for HT29 cells, albeit to a lesser extent. Again this was found to not be statistically significant (**Figure 5.8 B**). It can also be observed that a non-significant, marginal increase in *Hes1* expression after ADAM 10 knockdown was present in HT29 cells, consistent between both normoxia and hypoxia. A significant increase (2.14 ± 1.3-fold, $p<0.01$) in *Hes1* expression was observed for RKO cells, after exposure to severe hypoxia, which was then significantly reduced (1.03 ± 0.2) upon ADAM 10 knockdown (**Figure 5.8 C**, $p<0.01$). A small, non-significant reduction after ADAM 10 knockdown was observed in normoxia (0.58 ± 0.1), in RKO cells.

5.3.3.4 ADAM 10 Knockdown Increases *c-MYC* Expression in HCT116 Cells

Expression of *c-MYC* was examined as it strongly implicated in the progression of cancer. It is a downstream target of a number of cancer associated signalling pathways, including Notch signalling. Therefore, expression of *c-MYC* was examined by qPCR to determine the effects of ADAM 10 knockdown and exposure to severe hypoxia (0.5% O_2) in CRC cell lines. It can be observed that in HCT116 cells there was a significant upregulation ($p<0.01$) in *c-MYC* after ADAM 10 knockdown (**Figure 5.9 A**). This finding was consistent between both normoxia (1.67 ± 0.2-fold increase) and hypoxia (1.55 ± 0.0-fold increase). An upregulation of *c-MYC* in normoxia (1.73 ± 0.3-fold) after ADAM 10 knockdown, albeit non-significant, was also observed for HT29 cells

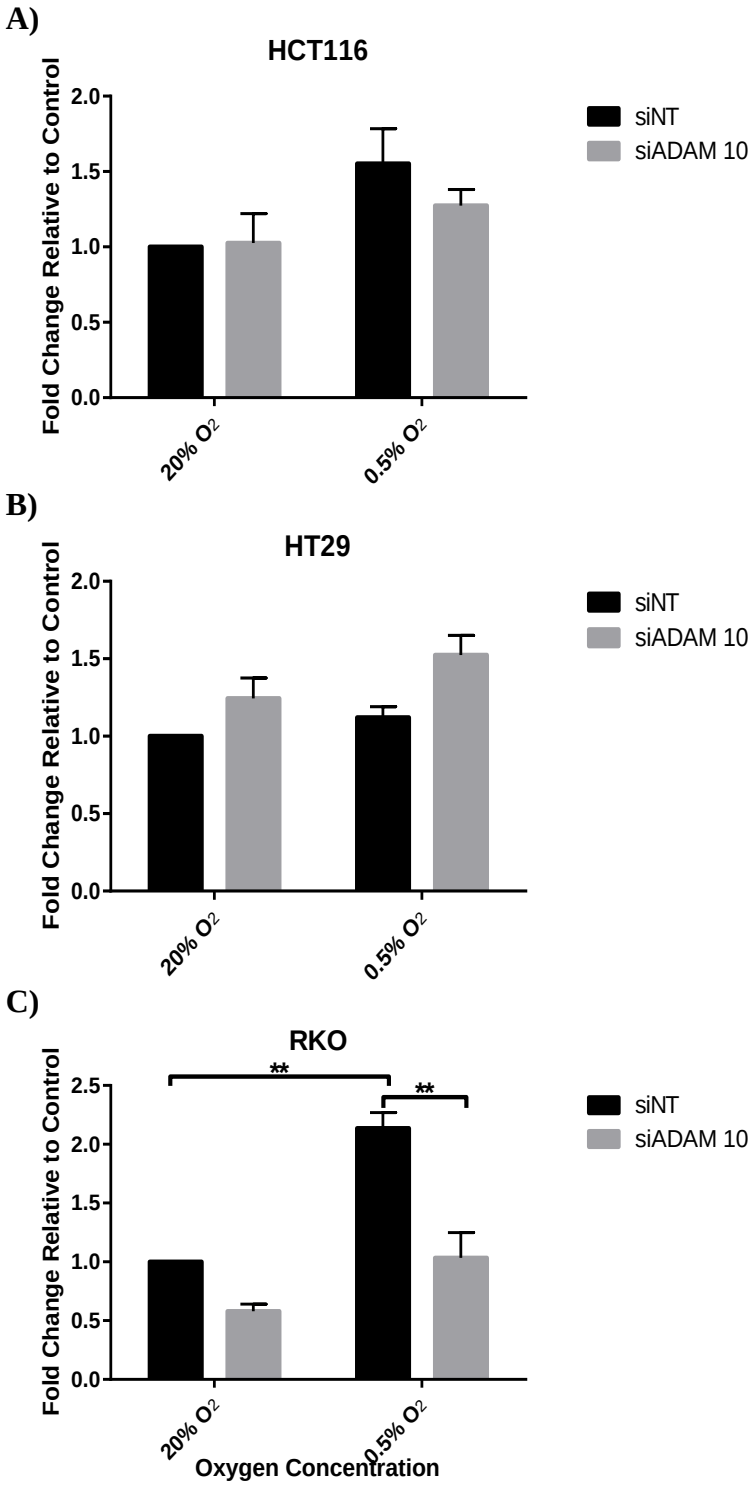

Figure 5.8: *Hes1* Expression in CRC Cells Lines after ADAM 10 Knockdown in Severe Hypoxia

CRC cell lines were transfected with ADAM 10 targeting siRNA (siADAM 10) or non-targeting siRNA (siNT), and exposed to hypoxia (0.5% O_2) for 24 hours. mRNA was extracted and *Hes1* expression analysed by qPCR. All results were normalised to the housekeeping gene, *B2M*. Results expressed as fold change in expression relative to the 0h control (normoxia, 20% O2), of n=3 experiments. Error bars represent +/- SEM. Statistical analysis by two-way ANOVA, with Tukey's post-hoc correction. ** = $p<0.01$.

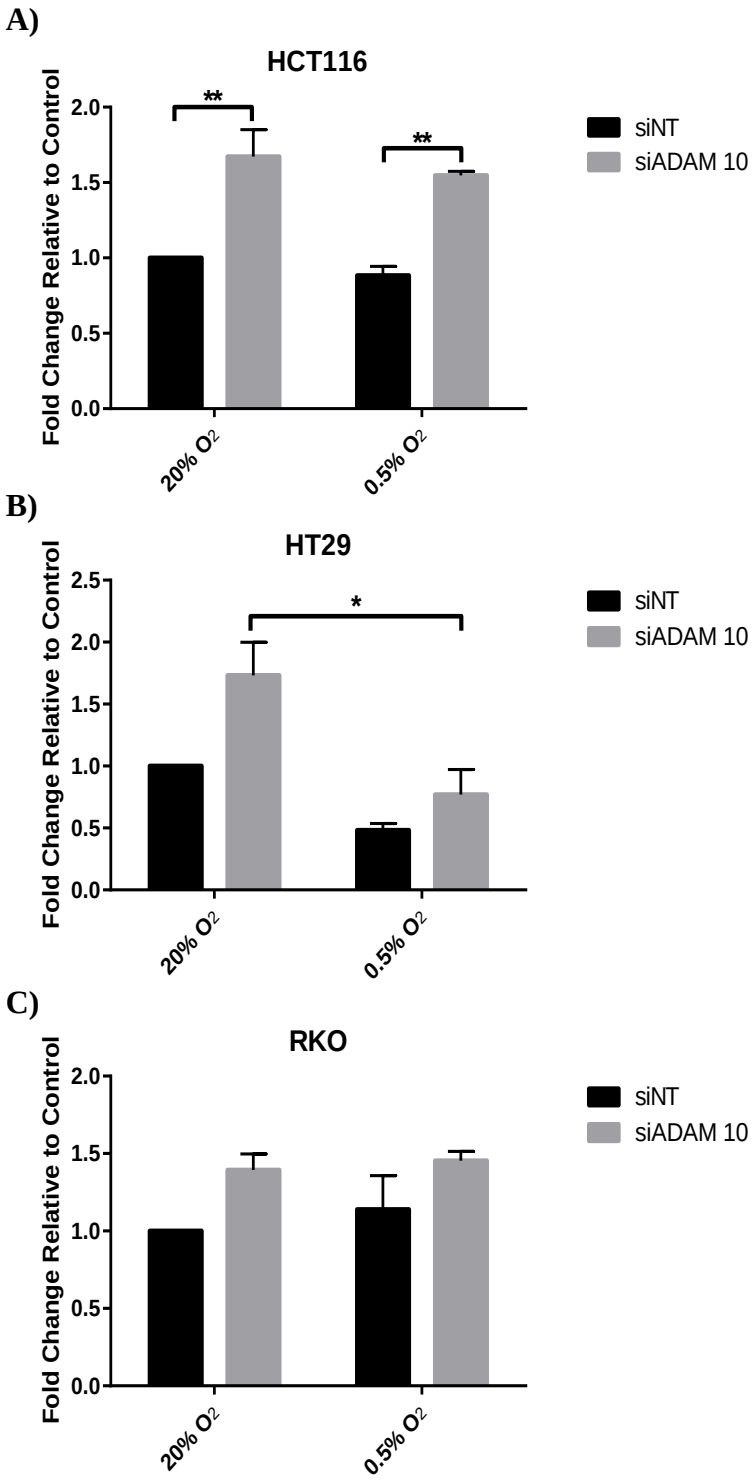

Figure 5.9: *c-MYC* Expression in CRC Cells Lines after ADAM 10 Knockdown in Severe Hypoxia

CRC cell lines were transfected with ADAM 10 targeting siRNA (siADAM 10) or non-targeting siRNA (siNT) and exposed to hypoxia (0.5% O_2) for 24 hours. mRNA was extracted and *c-MYC* expression analysed by qPCR. All results were normalised to the housekeeping gene, *B2M*. Results are expressed as fold change in expression relative to the 0h control (normoxia, 20% O_2), of n=3 experiments. Error bars represent +/- SEM. Statistical analysis by two-way ANOVA, with Tukey's post-hoc correction. * = $p<0.05$, ** = $p<0.01$.

Interestingly, a significant downregulation (0.96 ± 0.2-fold decrease) in *c-MYC* expression between normoxia and hypoxia, after ADAM 10 knockdown, was also observed for these cells (**Figure 5.9 B**) Finally, an increase in *c-MYC* expression after ADAM 10 knockdown was also observed for RKO cells, albeit non-significant (**Figure 5.9 C**).

5.3.3.5 ADAM 10 Knockdown and Severe Hypoxia Reduce *CCND1* Expression in CRC Cells

CCND1, the gene encoding Cyclin D1, was examined as a result of the downregulation in proliferation reported in Chapter 4, after ADAM 10 knockdown. As a regulator of the cell cycle *CCND1* is a target of a number of cancer associated signalling pathways, including Notch signalling, in which ADAM 10 is known to be involved. *CCND1* expression was found to be altered in HCT116 cells after both ADAM 10 knockdown and exposure to severe hypoxia (0.5% O_2; **Figure 5.10 A**). Specifically, it was shown that exposure to severe hypoxia led to a highly significant downregulation of *CCND1* expression in the scrambled control cells (siNT) (0.30 ± 0.0-fold decrease, $p<0.0001$). A significant decrease in the expression levels of *CCND1*, after ADAM 10 knockdown was observed in normoxia and hypoxia (**Figure 5.10 A**, 0.26 ± 0.0-fold and 0.41 ± 0.0-fold decreases, respectively). A highly significant downregulation ($p<0.0001$, normoxia = 0.62 ± 0.0-fold decrease, hypoxia = 0.66 ± 0.1-fold decrease) in *CCND1* expression after exposure to severe hypoxia was observed for HT29 cells (**Figure 5.10 B**). However, ADAM 10 knockdown had no effect on *CCND1* levels (**Figure 5.10 B**). No alteration in *CCND1* after exposure to severe hypoxia or ADAM 10 knockdown was observed for RKO cells (**Figure 5.10 C**).

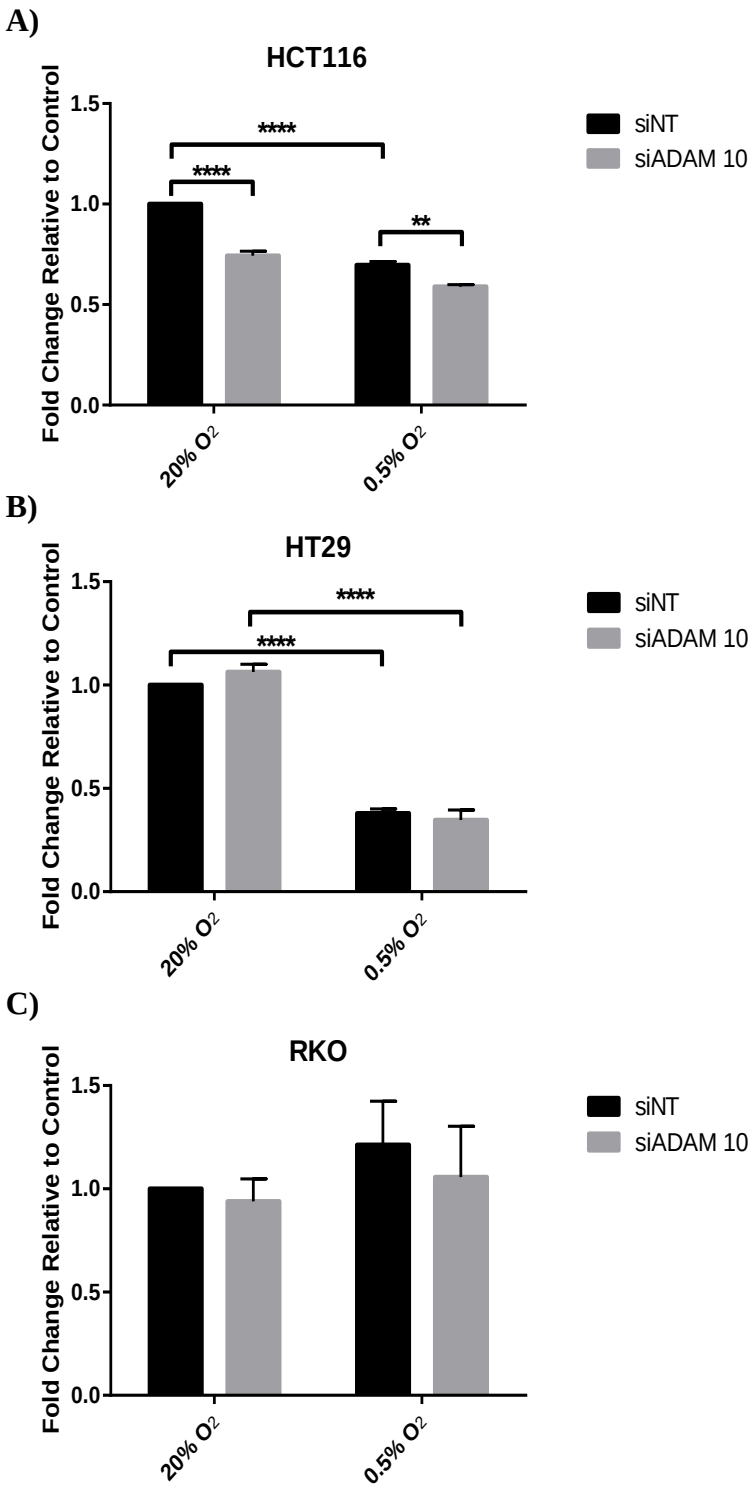

Figure 5.10: *CCND1* Expression in CRC Cells Lines after ADAM 10 Knockdown in Severe Hypoxia

CRC cell lines were transfected with ADAM 10 targeting siRNA (siADAM 10) or non-targeting siRNA (siNT) and exposed to hypoxia (0.5% O_2) for 24 hours. mRNA was extracted and *CCND1* expression analysed by qPCR. All results were normalised to the housekeeping gene, *B2M*. Results are expressed as fold change in expression relative to the 0h control (normoxia, 20% O_2), of n=3 experiments. Error bars represent +/- SEM. Statistical analysis by two-way ANOVA, with Tukey's post-hoc correction.** = $p<0.01$, **** = $p<0.0001$.

5.3.3.6 ADAM 10 Knockdown has no Effect on Oncogenic Markers at Protein Level

After examining *c-MYC* and *CCND1* at transcript level and observing highly significant alterations after ADAM 10 knockdown, these molecules were examined at protein level by Western Blotting, in HCT116 cells across a hypoxic time course.

Exposure to severe hypoxia has an effect on the pattern of c-MYC protein expression **Figure 5.11**. Specifically, a doublet band is visible after 2 hours exposure, which remains present throughout the hypoxia time course. After 48 hours the doublet shifts to lower molecular weight band, with evidence of possible PTM, degradation or processing below. These changes in protein expression are consistent between both siNT and siADAM 10 samples, indicating ADAM 10 knockdown does not contribute to it. Exposure to severe hypoxia also appears to modulate Cyclin D1 protein expression (**Figure 5.11**). It can be observed that protein expression appears reduced after a short hypoxic exposure (2-8 hours), however after 24 hours the levels increase again (**Figure 5.11**). No alterations in expression pattern of Cyclin D1 can be observed after ADAM 10 knockdown, indicating no effect is present. Similarly, p21 expression also appears un-altered by hypoxic exposure. However, there is a small increase in p21 expression after ADAM 10 knockdown, particularly after a short hypoxic exposure (2-8 hours) (**Figure 5.11**). However, when quantitatively analysed by densitometry a significant difference was only seen at 2 hours, due to intra-experimental variability.

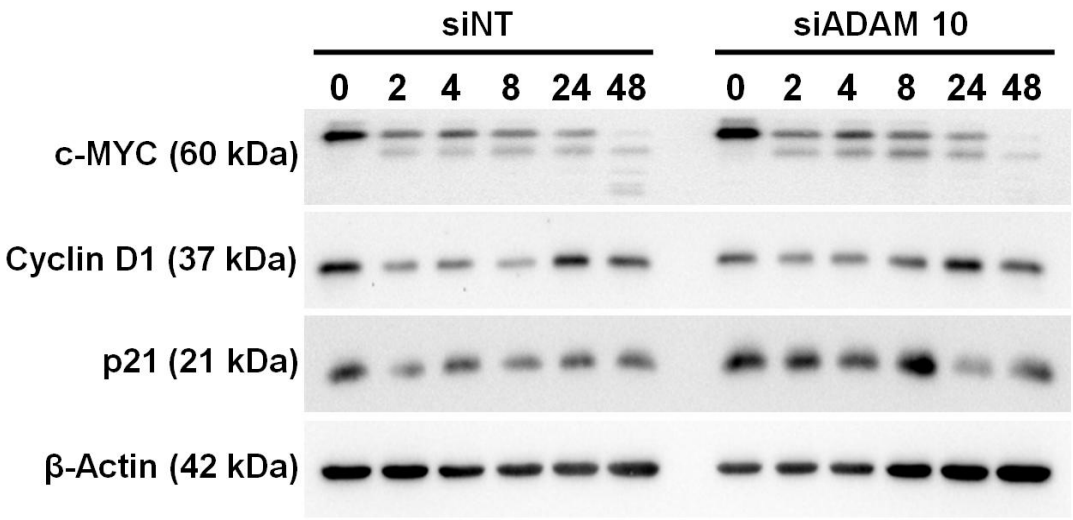

Figure 5.11: Effect of ADAM 10 Knockdown on Cell Proliferation Markers in Severe Hypoxia (0.5% O_2)

HCT116 cells were transfected with ADAM 10 targeting siRNA (siADAM 10) or non-targeting siRNA (siNT) and exposed to severe hypoxia (0.5% O_2) for a range of time points. Cells were lysed, 30 μg of each protein sample were separated by SDS-PAGE and expression of various proteins associated with oncogenesis were analysed by Western Blotting. β-Actin was used as the loading control. Blots shown are representative of three independent experiments.

5.4 Discussion

In the previous chapter the role of ADAM 10 in mediating the tumourigenic phenotype of CRC cell lines was examined. A role in regulating cellular viability was identified however this was not as a result of cell cycles arrest. As such, the potential underlying mechanisms behind such a role were examined, as it was hypothesised that ADAM 10 may play a role in regulating cellular signalling cascades involved in cellular viability, via its proteolytic activity.

Results for ADAM 10 activity under hypoxic conditions were inconclusive, as a result of methodological problems. Hypoxia-mediated effects were identified on a number of cellular signalling molecules, however only a few ADAM 10 mediated effects were seen. Importantly, a role for ADAM 10 in regulating *c-MYC* and *CCND1* expression was identified, independently of hypoxia.

Chapter 3 showed an upregulation of ADAM 10 at protein level after exposure to hypoxia, therefore it was hypothesised that this would coincide with an increase in proteolytic activity. Assessment of ADAM 10 proteolytic activity was undertaken using two fluorogenic peptides that mimic the sequence of known ADAMs substrates, and is a previously used strategy for evaluating ADAM 10 activity (Jin et al., 2002, Neumann et al., 2004, Escrevente et al., 2008). MOCAc-Lys-Pro-Leu-Gly-Leu-Dap(Dnp)-Ala-Arg-NH_2 (Peptide A) is based on the sequence of collagens, a known substrate of MMPs and metalloproteinases, which emits a fluorogenic signal when cleaved at the scissile bond, Gly-Leu (Neumann et al., 2004). Abz-Leu-Ala-Gln-Ala-Val-Arg-Ser-Ser-Ser-Arg-Dap(Dnp)-NH_2 (Peptide B) is based upon the sequence of TNF-α, a known substrate of ADAMs family members, and is cleaved at the scissile bond Ala-Val, thus emitting a fluorogenic signal (Jin et al., 2002). Usage of these peptides produced inconclusive data, with large margins of error, from which limited conclusions could be drawn. Some

results were suggestive of a potential downregulation in ADAM 10 activity in hypoxia, however further clarification is required due to the poor reproducibility. Such a finding would potentially be indicative that the ADAM 10 doublet, seen in Chapter 3, may be as a result of a hypoxia-mediated cleavage of ADAM 10, which subsequently inhibits its proteolytic activity. Previous usage of both peptides has been reported to be successful, thereby indicating that the inconclusiveness of the data presented here is not due to the individual peptides (Jin et al., 2002, Neumann et al., 2004, Escrevente et al., 2008, Zhu et al., 2011). It is possible that as the sequence of neither peptide is specific for cleavage by ADAM 10 the results may be masked by other ADAMs activity, such as ADAM 17, which is known to be altered in hypoxic conditions (Zheng et al., 2007, Rzymski et al., 2012, Wang et al., 2013). Also, knockdown or inhibition of ADAM 10 may lead to a compensatory upregulation of the activity of similar ADAMs, such as ADAM 17, which may mask any subtle ADAM 10 dependent effects. It was also noted that background readings were higher than the experimental readings for several samples, which may be due to the presence of Phenol red in the media. This is known to potentially cause interferences with fluorescent measurement, albeit not at the wavelengths used here (Ettinger and Wittmann, 2014). Further optimisation of this methodology is required before any conclusions can be drawn and alternative techniques for measuring ADAM 10 activity should be investigated. A number have studies have used alternative peptide substrates for readout of ADAM 10 activity, and it is feasible that these may produce less variable results (Moss et al., 2007, Moss et al., 2011). Alternative methodologies could include the measurement of ADAM 10 substrates (**Section 1.8**) in conditioned media by Western Blotting or ELISA, in conjunction with ADAM 10 knockdown/inhibition (Ebsen et al., 2013, Isozaki et al., 2015). Previously, shedding of ADAM 10 substrates was characterised through transfection of alkaline phosphatase tagged ADAM 10 substrates into cells, the

shedding of which was then stimulated with phorbol-12-myristate-13-acetate (PMA) and resultant change in alkaline phosphatase activity determined (Sahin et al., 2004).

It was hypothesised that ADAM 10 may play a role in mediating CRC cellular migration and EMT, therefore, a number of proteins associated with the EMT process were examined. Whilst a hypoxia-mediated effect was seen on both E-Cadherin and β-Catenin expression, there was no role for ADAM 10 in the regulation of these proteins identified. An element of degradation or PTM was seen to the expression of both proteins after exposure to hypoxia, again independent of ADAM 10 expression. Previous research has shown downregulated E-Cadherin expression in hypoxia, which is characteristic of cells undergoing EMT, a finding which is in contrast to data presented here (Chen et al., 2010, Cheng et al., 2013, Yu et al., 2013, Zhang et al., 2013b, Zhang et al., 2015b, Zuo et al., 2016). Chen et al. (2010) showed E-Cadherin expression was upregulated at both protein and transcript level in breast cancer, after exposure to hypoxia (1% O_2). Similar findings were reported in hepatocellular carcinoma by Yu et al. (2013) (3% O_2; 48 hours). Importantly, in CRC cell lines, overexpression of HIF-1α resulted in decreased E-Cadherin at protein level *in vitro* (Zhang et al., 2015b). Notably, high presence of HIF-1α was observed in both CRC primary and metastatic tissue, whereas expression of E-Cadherin was low (Zhang et al., 2015b). E-Cadherin is a known substrate of ADAM 10, which cleaves the full-length form, leaving a smaller C-terminal fragment which can also be detected (Gaida et al., 2010). Previously, it has been shown that ADAM 10 overexpression in keratinocytes resulted in reduced total E-Cadherin and increased cleaved form (Maretzky et al., 2008). Similarly, ADAM 10 knockdown in fibroblasts caused a reduction in cleaved E-Cadherin, although total levels remained unchanged (Maretzky et al., 2005). However in prostate cells, both the levels of total and cleaved E-Cadherin remained unchanged (Gaida et al., 2010). As only total E-Cadherin was examined here it can only be

concluded that ADAM 10 knockdown in CRC cell lines had no effect on full-length E-Cadherin expression.

It has previously been shown that hypoxia has no effect on β-Catenin expression at protein level after exposure to hypoxia (1% O_2) in HCT116 cells, and no protein degradation was observed (Kaidi et al., 2007). However, the oxygen tension is more moderate than that used here which may protect against protein degradation. Notably, β-Catenin has been shown to correlate with HIF-1α expression in colon cancer tumours (Wincewicz et al., 2010). Conflictingly, in CRC RKO cells, it was shown that exposure of severe hypoxia (<0.01% O_2) resulted in a significant downregulation of β-Catenin protein expression, which conflicts the findings here (Verras et al., 2008). In gastric cancer a hypoxia-mediated upregulation of β-Catenin, at protein and transcript level, was previously been reported (Liu et al., 2015a), which suggests the effect of hypoxia on β-Catenin expression is cell type and possibly oxygen tension dependent. Less research has been undertaken on the effects of ADAM 10 on β-Catenin expression, with one study showing inhibition of ADAM 10 decreased β-Catenin expression, which conflicts the data presented here (Woods et al., 2015). However, in non-small cell lung cancer, silencing of ADAM 10 had no effect on β-Catenin expression (Guo et al., 2012). The mesenchymal markers Slug and Snail were also investigated, however neither was detected at protein level in HCT116 cells, in either hypoxia or normoxia. This was unexpected due to previous confirmation of protein expression for both Slug and Snail in HCT116 cells (Fan et al., 2012, Qian et al., 2013). Therefore, it is reasonable to assume that the lack of detection here is as a result of antibody problems, suggesting further optimisation is required. Previous research has shown that hypoxia causes an upregulation of Slug and Snail expression (Chen et al., 2010, Yu et al., 2013, Zhang et al., 2013a). Little research has investigated the role of ADAM 10 in mediating Slug or

Snail expression in cancer cells, however one study has shown that ADAM 10 silencing resulted in increased Slug expression (Doberstein et al., 2011).

EGFR signalling has been shown to regulate cellular proliferation and survival, and ADAM 10 is known to shed a number of ligands which bind to ErbB receptors, phosphorylating them and activating downstream signalling (Sahin et al., 2004, Blobel, 2005, Kataoka, 2009). Therefore, it was hypothesised that ADAM 10 may play a role in regulating the activation of EGFR signalling molecules which may be involved in controlling cellular viability. PI3K-AKT and Ras-Raf-MEK-ERK pathways are strongly implicated in CRC progression, which made them key targets for investigation within this study (Roberts and Der, 2007, Engelman, 2009). Phosphorylation of GAB1 acts as a mediator between PI3K-AKT and Ras-Raf-MEK-ERK signalling after receptor activation (Mattoon et al., 2004) and phosphorylation of STAT5 has been reported to be upregulated in CRC and is known to promote cellular proliferation (Xiong et al., 2009). No expression of phosphorylated EGFR, GAB1 or Stat5 was detected in HCT116 cells, which was unexpected as studies have previously reported their expression in HCT116 cells (van Houdt et al., 2010, Weber et al., 2013, Bai et al., 2015). It is feasible that the lack of detection here is due to antibody problems requiring further optimisation, or a need to stimulate the pathway with a known substrate, such as EGF, to enable activation of the signalling cascade. A hypoxia-mediated increase in the phosphorylation of both AKT and ERK 1/2 was identified, however ADAM 10 knockdown had no effect. Suggesting that ADAM 10 plays no role in regulating the phosphorylation and activation of these proteins. Therefore, it is unlikely that ADAM 10 regulates HCT116 cell viability through these channels. It has previously been shown that ADAM 10 knockdown prevented the phosphorylation of AKT and ERK 1/2, which conflicts the data presented here (Grabowska et al., 2012, Zhang et al., 2014a, Liu et al., 2015b). The regulation of both AKT and ERK 1/2 phosphorylation in hypoxia appears to be

somewhat conflicting (Beitner-Johnson et al., 2001, Kwon et al., 2006, Liu et al., 2010, Du et al., 2011, Grabowska et al., 2012, Stegeman et al., 2012, Kilic-Eren et al., 2013, He et al., 2016). However, the hypoxia-mediated upregulation of AKT phosphorylation seen here is consistent with previous reports (Beitner-Johnson et al., 2001, Stegeman et al., 2012). Further in agreement with data presented here, previous studies have shown an upregulation of ERK 1/2 phosphorylation under hypoxic conditions (Liu et al., 2010, Du et al., 2011, He et al., 2016). However, conflicting data for both proteins has been shown (Kilic-Eren et al., 2013, Kwon et al., 2006, Grabowska et al., 2012). One limitation of the experiments investigating the phosphorylation of various cancer associated proteins, in this study, is the lack of normalisation to total protein levels. Examination of total protein levels would identify any experimentally induced alterations. Normalisation of phosphorylated proteins to total proteins allows for such changes to be taken into account, thus allowing for changes solely in phosphorylation to be identified. As such, further work should be undertaken to investigate the total protein counterparts of the phosphorylated proteins examined in this chapter.

Notch signalling is strongly implicated in cancer progression and it was hypothesised that the hypoxia-mediated upregulation of ADAM 10 in CRC may result in increased Notch signalling and downstream gene activation. The pathway is responsible for the activation of genes including Hes and Hey transcription factors, along with p21, Cyclin-D1 and c-MYC (Yuan et al., 2015b). *Notch1* has previously been implicated in CRC progression and therefore was the focus of investigation into Notch signalling in this study (Sikandar et al., 2010, Fender et al., 2015, Vinson et al., 2015). However, *Notch1* expression was unaltered in CRC cell lines after either hypoxic exposure or ADAM 10 knockdown. This is in disagreement to previous findings in various cancer types, where *Notch1* is significantly upregulated post hypoxic exposure (Chen et al., 2007, Yu et al., 2013, Villa et al., 2014). Similarly, it has previously been shown that ADAM 10 is

required for cleavage of Notch receptors and that knockdown of ADAM 10 inhibits Notch signalling (Hartmann et al., 2002, van Tetering et al., 2009). Conversely, previous reports have shown that ADAM 10 deficient mouse models displayed no alteration in *Notch1* expression in the intestinal compartments (Tsai et al., 2014). However, a more representative image of ADAM 10 involvement would be gained by looking downstream at cleaved NICD, this would show whether the hypoxia-mediated upregulation of ADAM 10 results in increased Notch cleavage and subsequent NICD generation by γ-secretase. Hes and Hey family genes are responsible for the transcriptional regulation of cell proliferation, apoptosis, differentiation and cell cycle regulation (Borggrefe and Oswald, 2009, Vinson et al., 2015). Expression of *Hes5*, *Hey1* and *Hey2* was found in low abundance within the CRC cell lines investigated, and thus were not further investigated. A hypoxia-mediated increase in *Hes1* was reduced upon ADAM 10 knockdown in RKO cells only, and this increase in *Hes1* expression in hypoxia is consistent with previous findings, in other cancer types (Asnaghi et al., 2014, Moriyama et al., 2014, Irshad et al., 2015). Notably, the downregulation of *Hes1* expression after ADAM 10 knockdown in RKO cells is supported by previous research that has shown that ADAM 10 knockout mice displayed impaired *Hes1* expression compared to counterparts (Zhuang et al., 2015). Similar results have also been evidenced in endothelial cells after ADAM 10 inhibition (Pabois et al., 2014). The results here indicate that the role of ADAM 10 or hypoxia in regulating *Hes1* expression may be specific to individual CRC cell lines, a difference that may be explained by epigenetic mutational differences amongst cell lines (**Section 6.1**).

Oncogenes are well reputed to promote cancer development through the dysregulation of cellular processes, such as cell cycle controls and proliferative capabilities. c-MYC and Cyclin D1 are known proto-oncogenes and are downstream targets of a number of signalling cascades, including Notch signalling (Casimiro et al., 2012, Dang, 2012,

Yuan et al., 2015b). It was hypothesised that the hypoxia-mediated upregulation of ADAM 10 (shown in Chapter 3) was responsible for c-MYC activation, and a downregulation would be seen after ADAM 10 knockdown. However, a suppressive effect of ADAM 10 on *c-MYC* expression was seen in HCT116 cells, independently of hypoxia, but this did not translate to protein level. At protein level hypoxia-mediated alterations were seen but ADAM 10 had no effect, which corroborates previous results showing that *c-MYC* expression in HCT116 cells does not alter under hypoxic conditions, however changes are seen at protein level (Okuyama et al., 2010, Wong et al., 2013). Few studies have investigated the role of ADAM 10 in c-MYC regulation, however one study showed that ADAM 10 silencing in pancreatic cancer resulted in downregulated c-MYC at protein level, a finding that is conflict to the data presented here (Woods et al., 2015). Here, the CRC cells investigated displayed different trends to one another, indicating that the effects of ADAM 10 on c-MYC regulation are cell type specific.

Cyclin D1 is also a proto-oncogene that is strongly implicated in cell cycle checkpoint dysregulation in cancer and subsequent promotion of cellular proliferation (Yang et al., 2006). It was hypothesised that hypoxia-upregulated ADAM 10 may play a role in modulating cellular viability through promotion of Cyclin D1. A hypoxia-mediated downregulation of *CCND1* was identified in CRC cell lines. Furthermore, in HCT116 cells ADAM 10 knockdown resulted in *CCND1* downregulation, independently of hypoxia. However, such results did not translate to protein level, where only a hypoxia-dependent effect was seen. Such results indicate that ADAM 10 may promote *CCND1* expression, which may affect cellular viability, as seen in Chapter 4, however further investigation is required to clarify why only transcript mediated effects are seen. Previously studies have identified a hypoxia-mediated upregulation of Cyclin D1 at protein level (Joung et al., 2005, Joung et al., 2008, Lim et al., 2010). Previous research

has indicated that hypoxia mediates a downregulation of *CCND1*, corroborating data presented here, as a result of HIF-1 binding to the promoter region within Cyclin D1 (Wen et al., 2010). The cyclic pattern of Cyclin D1 expression, seen here at protein level, may be due to the cell-cycle dependent regulatory mechanism behind Cyclin D1 expression, which is raised or lowered at different stages of the cell cycle (Yang et al., 2006). Similar protein expression patterns after hypoxic exposure have previously been shown in breast cancer (Joung et al., 2005). In lymphoma, it was shown that silencing of ADAM 10 reduced *CCND1* expression, which corroborates the findings in HCT116 cells in this study (Armanious et al., 2011). However, in pancreatic cancer ADAM 10 silencing leads to a downregulation of Cyclin D1 protein expression, which conflicts the data presented here (Woods et al., 2015).

p21 is another key regulator of cell cycle, which is a member of the cyclin-dependent kinase (cdk) inhibitor family shown to promote tumour suppression (Gartel, 2006, Abbas and Dutta, 2009, Xia et al., 2011, Benson et al., 2014). Its expression is upregulated by p53, which leads to a promotion of cell cycle arrest (Xia et al., 2011, Benson et al., 2014). Here, a possible role for ADAM 10 in the regulation of p21 in HCT116 cells was shown, however little significance was seen when quantitatively analysed (Appendix 1) due to inter-experimental variability. Therefore, further clarification is required to be able to definitively identify a role for ADAM 10 in p21 regulation. These results are in agreement with previous findings by Aramanious et al., 2011, which showed ADAM 10 silencing resulted in increased p21 protein expression in lymphoma. Little effect of hypoxia on p21 expression in CRC cells was shown here and previous data is conflicting in this area. In mesenchymal stem cells expression of p21 was downregulated in response to hypoxic exposure (1% O_2), thus inhibiting its tumour suppressor capabilities (Tsai et al., 2011). Furthermore, overexpression of HIF-1α was shown to result in decreased p21 expression at protein level (Hu et al., 2015),

and notably, high HIF-1α expression and low p21 expression correlated to poor prognosis in patients with gastric cancer (Mizokami et al., 2006). However, conversely it has been shown that hypoxia does not downregulate p21 expression, which is attributed to the slowing of the cell cycle under hypoxic conditions (Cho et al., 2008, Leontieva et al., 2012).

One limitation of the experiments in this chapter is the lack of confirmation of hypoxic response at protein level, via analysis of HIF-1α expression. As previously discussed extracting HIF-1α with the ADAMs lysis buffer was problematic and therefore no confirmation was achieved for these experiments. However, confirmation of hypoxia was undertaken for all mRNA experiments through analysis of *SLC2A1* expression, results of which can be seen in **Appendix 1**. This subsequently confirms that mRNA experiments were undertaken in a hypoxic environment.

Here, a role for ADAM 10 in the regulation of *c-MYC*, *CCND1* and p21 expression has been identified, however these were primarily independent of hypoxia. Thus meaning the hypothesis of 'exposure to severe hypoxia will increase ADAM 10 proteolytic activity and subsequently activate downstream signalling mechanisms linked to CRC progression' can be rejected. Such results may, in part, explain the effects of ADAM 10 seen on CRC cellular viability, however further clarification as to the implication of these effects are required before such conclusions can be drawn.

Chapter 6 : Concluding Discussion

6.1 Discussion

Colorectal cancer is one of the most prevalent and deadliest cancers in the UK, affecting over 40 000 patients every year (Massat et al., 2013). A number of risk factors are associated with the development of CRC, with the disease predominantly affecting the over 50s (Ballinger and Anggiansah, 2007). Environmental factors such as dietary and lifestyle choices are believed to contribute to 54% of CRC and as a result of such choices within the western world CRC incidence has risen in recent years (Parkin et al., 2011, Ferlay et al., 2015). Typically CRC tumours are adenocarcinomas and are highly metastatic in nature (Brenner et al., 2014). As some symptoms of CRC are somewhat generalised in nature late diagnosis is a particular problem affecting CRC patients, and as a result a comprehensive screening programme has been implemented throughout the UK (Ballinger and Anggiansah, 2007, Cunningham et al., 2010, Brenner et al., 2014). Predominantly, CRC is sporadic in onset as a result of epigenetic mutations and tumours are extremely heterogeneous in nature, resulting in problems associated with therapeutic targeting (Tan and Du, 2012, Lupini et al., 2015, Kocoglu et al., 2016). Epigenetic mediated aberration of EGFR expression is particularly prevalent amongst CRC tumours, with approximately 60 – 80% of CRC seeing an overexpression (Pabla et al., 2015, Kocoglu et al., 2016). Whilst this mutation is well characterised in the context of CRC, and targeted therapies have been developed, the heterogeneity of CRC tumours can render such therapies ineffective (Tan and Du, 2012, Lupini et al., 2015, Kocoglu et al., 2016). For example, *KRAS* mutations, which occur in approximately 35 – 45% of CRC tumours, will render tumours less susceptible to EGFR targeted therapies (Tan and Du, 2012, Lupini et al., 2015, Kocoglu et al., 2016). The heterogenic epigenetic mutations with CRC tumours activate a vast range of downstream signalling pathways associated with cancer progression and a tumourigenic phenotype (Banck and Grothey, 2009, Li et al., 2011, Tan and Du, 2012, Hong et al., 2015, Pabla et al., 2015, Kocoglu

et al., 2016). Two pathways affected by attenuated EGFR expression in CRC are the Ras-Raf-MAPK and PI3K-PTEN-AKT pathways, which promote cellular survival, growth, proliferation and differentiation (Pabla et al., 2015, Kocoglu et al., 2016). As solid tumours, hypoxic regions are present in CRC tumours, which further complicate therapeutic approaches and also contribute to the high metastatic potential of the disease (Cao et al., 2009). Although survival rates for CRC are increasing, currently 59%, a greater understanding of the molecular basis for this disease is required for further improvement in disease management and patient survival (Ferlay et al., 2015, Holleczek et al., 2015).

ADAMs family members are strongly implicated in the progression of a variety of cancer types, and as such research has shown their involvement in mediating cellular proliferation and inducing a more migratory and invasive phenotype in cells (Edwards et al., 2008, Duffy et al., 2011). As sheddases of a number of cancer associated molecules ADAMs family members have increasingly become important targets of research in recent years. Furthermore, there is increasing evidence for their involvement in facilitating cancer progression within the hypoxic tumour microenvironment, particularly ADAM 17 (Zheng et al., 2007, Rzymski et al., 2012). However, despite some ADAMs being well characterised there are some family members that remain somewhat understudied, particularly in the context of their involvement in hypoxia-mediated cancer progression. ADAM 10 in particular is one of the lesser studied family members, with very little hypoxia-focussed research carried out thus far, and what research there exists is somewhat conflicting in nature (Webster et al., 2002, Marshall et al., 2006, Barsoum et al., 2011). The inconsistency of current research highlights the lack of thorough understanding of ADAM 10 under hypoxic conditions and the effects this may have on cancer progression. Importantly, ADAM 10 has been shown to be essential in normal colon biology, due to its involvement in Notch signalling, and is

expressed within all intestinal cell types (Jones et al., 2016). Intestinal cells heavily utilise Notch signalling for the regulation cellular function, proliferation and differentiation, and as a result ADAM 10 knockout mouse models have been shown to be embryonic lethal (Hartmann et al., 2002, Zeki et al., 2011, Tsai et al., 2014, Carulli et al., 2015, Jones et al., 2016). Severe defects were identified in ADAM 10 knockout mice, thus highlighting its importance in the regulation of cellular processes (Hartmann et al., 2002, Tsai et al., 2014, Jones et al., 2016).

This project aimed to characterise ADAM 10 within severe hypoxia (0.5% O_2) in CRC cell lines, in the context of hypoxia-mediated CRC progression. Three CRC cell lines were used to determine the effects of severe hypoxia on ADAM 10 itself, in terms of expression levels (Chapter 3), and what subsequent downstream effects this may have (Chapter 4 and 5). It was hypothesised that hypoxia-induced ADAM 10 expression and activity would mediate the progression of CRC through promotion of a tumourigenic phenotype. It is known that cancer progression is partly driven by uncontrollable cellular proliferation and an increased migratory and invasive phenotype, as described by Hanahan and Weinberg (2011). As such, this project was designed to characterise the effects of hypoxia-mediated ADAM 10 on cellular proliferation and migration in three CRC cell lines (Chapter 4). Furthermore, it aimed to elucidate the ADAM 10 related signalling pathways that may drive such characteristics of CRC cancer progression under hypoxic conditions (Chapter 5).

It was hypothesised that ADAM 10 would be upregulated in response to hypoxia in CRC cell lines. This study identified an upregulation at both protein and transcript level in ADAM 10 expression. Importantly, a hypoxia-mediated doublet band for mature ADAM 10 was identified. This was hypothesised to be a hypoxia-regulated PTM or cleavage of mature ADAM 10 protein, due to knowledge of a number of PTMs affecting ADAM 10 (Anders et al., 2001, Moss et al., 2007, Parkin and Harris, 2009,

Tousseyn et al., 2009). However, attempts to characterise the nature of the doublet band were unsuccessful. An alteration in the glycosylation of ADAM 10 was identified under hypoxic conditions, which may be indicative of either reduced glycosylation of ADAM 10 or availability of glycosylated ADAM 10 due to PTMs. Dysregulated protein glycosylation is a key characteristic of cancer, and a hypoxia-mediated PTM of ADAM 10 could greatly affect the functionality of the protein, particularly in the context of hypoxia-mediated CRC progression (Shirato et al., 2011, Roth et al., 2012, Tian and Zhang, 2013). Therefore, it is important that the underlying mechanisms behind the doublet band are identified.

ADAM 10 is known to be responsible for the shedding of a variety of molecules that activate downstream signalling mechanisms (Hartmann et al., 2002, Borrell-Pages et al., 2003, Bozkulak and Weinmaster, 2009, Baumgart et al., 2010, Christian, 2012, Maretzky et al., 2011, Wang et al., 2013). It was hypothesised that the hypoxia-mediated upregulation in ADAM 10 expression seen in this study could potentially correlate with an increase in ADAM 10 proteolytic activity in hypoxic conditions (Chapter 5). Methodological problems prevented clear conclusions from being drawn, however the data indicates ADAM 10 activity may be reduced in hypoxia. Downregulation of ADAM 10 activity in hypoxia would see reduced ligand shedding and subsequent activation of signalling pathways, a finding which would be unexpected in the context of CRC. A number of CRC implicated signalling pathways are activated by ligands known to be substrates of ADAM 10 (Fahrenholz et al., 2000, Six et al., 2003, Sahin et al., 2004, Maretzky et al., 2005, Reiss et al., 2005, Sanderson et al., 2006, Maretzky et al., 2008, Guo et al., 2012, Woods and Padmanabhan, 2013, Groot et al., 2014, Zhuang et al., 2015). Therefore it would be expected that increased ADAM 10 activity would be seen, to coincide with the increased activation of such pathways and subsequent progression of CRC in the hypoxic tumour microenvironment. The effect of

hypoxia on ADAM 10 activity has not previously been investigated, therefore it is important further investigation is undertaken to clarify the regulation of ADAM 10 activity under hypoxic conditions.

ADAM 10 has previously been implicated in the promotion of cellular proliferation, believed to be through the activation of associated signalling pathways (Maretzky et al., 2005, Arima et al., 2007, Xu et al., 2010, Bulstrode et al., 2012, Yuan et al., 2013, Fu et al., 2014, Shao et al., 2015, You et al., 2015). It was hypothesised that the hypoxia-mediated upregulation of ADAM 10 would promote CRC cellular proliferation, which is a key characteristic of the disease (Jones et al., 2016). A hypoxia-independent role for ADAM 10 in regulating the cellular viability of HCT116 cells was identified, which may be indicative of altered proliferation or cell death. However, alternative methodologies are required to identify which is applicable in CRC cells after ADAM 10 knockdown. Cell cycle analysis determined that the alteration to viability is not as a result of cell cycle arrest, so further clarification is required. Nevertheless, it can be concluded that ADAM 10 plays a crucial role in the regulation of HCT116 cellular viability, which may promote the progression and growth of CRC tumours. If similar results were seen after stable knockdown of ADAM 10, *in vivo* studies would identify whether such results were translatable and if CRC tumour growth was affected. If corroborated, ADAM 10 could be identified as a new therapeutic target for CRC.

Both Notch and EGFR signalling are known to be attenuated in CRC, and therefore contribute to the progression of the disease. ADAM 10 is known to be involved in both pathways, particularly Notch signalling and previous data has linked such pathways to the promotion of proliferation (Phipps et al., 2013, Joseph et al., 2010, Bolos et al., 2013, Suman et al., 2013). ErbB receptors are activated by binding of ADAM 10 shed ligands, subsequently activating EGFR downstream pathways, whereas in Notch signalling ADAM 10 cleaves the Notch receptor as part of the pathway (Tol et al., 2010,

Peignon et al., 2011, Sethi and Kang, 2011, Mann et al., 2012, Yabuuchi et al., 2013, Yuan et al., 2015b). As such it was hypothesised that ADAM 10 would modulate the expression of molecules involved in these pathways and regulate CRC cellular proliferation. However, no alteration to molecules involved in either EGFR or Notch was identified after ADAM 10 knockdown, thus rejecting the hypothesis. Therefore, alternative mechanisms through which ADAM 10 may be regulating the cellular viability of HCT116 cells were investigated. Proto-oncogenes c-MYC and Cyclin D1, which are known to be associated with cancer progression and cellular proliferation, were investigated to determine the role of ADAM 10 in mediating their expression in CRC (Cappellen et al., 2007, Wang et al., 2008, Dang, 2012, Marampon et al., 2015). A surprising suppressive effect of ADAM 10 on *c-MYC* expression was identified in HCT116 cells, independently of hypoxia. Based on the knowledge that c-MYC is widely upregulated in CRC it was hypothesised that hypoxia-induced ADAM 10 would promote *c-MYC* expression, however this was not the case (Sikora et al., 1987, Rochlitz et al., 1996, Smith and Goh, 1996, Toon et al., 2014, Boudjadi et al., 2015, Lee et al., 2015a). Further investigation is required to elucidate the implications of this suppression in the context of CRC progression, however as a result it cannot be definitively concluded that ADAM 10 is modulating HCT116 viability through attenuation of *c-MYC* expression. Cyclin D1 is a key regulator of the cell cycle and is known to be overexpressed in CRC tumours, and furthermore this is often associated with a more aggressive tumour phenotype (Kong et al., 2001, Bahnassy et al., 2004, Wangefjord et al., 2011, Li et al., 2014b, Al-Maghrabi et al., 2015). Therefore, it was hypothesised that hypoxia-mediated ADAM 10 would promote *CCND1* expression in CRC cell lines, which was shown to be the case in HCT116 cells. Previous research has shown downregulation of Cyclin D1 results in decreased CRC cell proliferation, and it is feasible that ADAM 10 may be modulating HCT116 cellular viability through

attenuating *CCND1* expression (Tsukahara et al., 2015, Al-Qasem et al., 2016). PI staining however showed no role of ADAM 10 in regulating cell cycle progression, however, without more detailed profiling through the use of BrdU it cannot be definitively concluded that ADAM 10 has no effect on the cell cycle in HCT116 cells. Further clarification could be taken from examining other cell cycle molecules, such as CDK 4/6 and RB, which also display upregulation in CRC (Ali et al., 1993, Yamamoto et al., 1999, Collard et al., 2012, Li et al., 2014a, Yoshida and Diehl, 2015, O'Leary et al., 2016). RB protein is typically inactive in many tumour types, however in CRC it is overexpressed and notably, in HCT116 cells, levels of phosphorylated RB are high, thus promoting cell cycle progression (Yamamoto et al., 1999). The conflicting nature of the results of *c-MYC* and *CCND1* would indicate that ADAM 10 expression may influence a number of different pathways that are targeting c-MYC and Cyclin D1 separately from one another.

Another key facilitator of CRC progression is the induction of EMT, which is associated with a switch to a more mobile and aggressive phenotype. ADAM 10 has previously been shown to mediate migration and invasion in cancer, and thus it was hypothesised that the hypoxia-mediated upregulation of ADAM 10 shown in this study may be responsible for the induction of EMT in CRC cells (Maretzky et al., 2005, Liu et al., 2015b, Shao et al., 2015). However, no such role was identified, with ADAM 10 having no effect on CRC migration or expression of EMT markers. Alternative methodologies should be used to definitively rule out ADAM 10 in the modulation of CRC cell migration, however, it is feasible that ADAM 10 may induce invasion and not migration, as such this should also be a target for further investigation.

The use of SMIs within some experiments in this project was for the purpose of assessing their suitability in the context of potential therapeutic agents in the treatment of CRC. The hypothesis was that as an ADAM 10 specific agent GI254023X may be

able to prevent the ADAM 10 driven effects on cell viability within CRC, however no such evidence was found (Ludwig et al., 2005, Hoettecke et al., 2010, Pruessmeyer et al., 2014). Thus, there is insufficient evidence presented in this study to suggest that they may be suitable for further development in the prevention of ADAM 10 driven CRC proliferation for a translational therapeutic perspective.

The positive and coherent evidence presented within this study was primarily identified within HCT116 cells, as a lack of positive and consistent data was achieved in the other CRC cell lines investigated. As such qualitative investigations were undertaken to characterise the differences between the cell lines used in this study. To do this the Cancer Cell Line Encyclopaedia (CCLE) was used, which details the molecular mutations within cancer cell lines, thus allowing identification of alterations between CRC cell lines within this study, which may in part explain the differences between experimental results (**Table 6.1**) (Barretina et al., 2012, CCLE, 2013).

Table 6.1: Cancer Associated Mutations within CRC Cell Lines (Information gathered from CCLE (2013))

	HCT116	**HT29**	**RKO**
Cell origin	Carcinoma, colon	Adenocarcinoma, colon	Carcinoma, colon
ADAM 10	SNP in 3'UTR	Wild type	Wild type
HES-1	Wild type	Wild type	Wild type
MYC	Wild type	Wild type	Missense mutation (SNP)
CCND1	Wild type	Wild type	Wild type
CTNNB1	Frameshift deletion	Wild type	Wild type
EGFR	Wild type	Wild type	Wild type
KRAS	Missense mutation	Wild type	Wild type
TP53	Wild type	Wild type	Wild type
PTEN	Deletion in 3'UTR	Wild type	Wild type
APC	Wild type	Nonsense mutation & frameshift insertion	Wild type
GSK3	Wild type	Wild type	Wild type
EP300	Frameshift deletion	Deletion in 3'UTR	Frameshift deletion x2
CREBBP	Wild type	Wild type	Splice site SNP
TGF-β	Wild type	Wild type	Wild type
FOXO3	Wild type	Wild type	Missense mutation (SNP)
STAT3	Wild type	Wild type	In frame deletion
JAK	Wild type	Wild type	Wild type

The cell lines were analysed for known mutations within a number of oncogenes, tumour suppressors, transcription factors and signalling mechanisms involved in cellular viability/proliferation, relevant to CRC and/or ADAM 10 biology (Jones et al., 2016). The hypothesis was that mutational differences, in such molecules, between the cell lines may account for the experimental result differences shown in this study. A number of CRC specific mutations were examined, including *KRAS*, *APC* and *EGFR*, as these are known to impact upon CRC progression (Phipps et al., 2013, Pabla et al., 2015, Kocoglu et al., 2016). Whilst a number of mutations that may influence the molecular response of the CRC cell lines were present, there were no consistent indications separating HCT116 cells from the other two CRC cell lines. For example, alteration in *KRAS* is common within CRC and is known to promote cellular proliferation through downstream activation of AKT, and here it was shown that HCT116 cells possess this mutation (Phipps et al., 2013, Pabla et al., 2015, Kocoglu et al., 2016). However we reported no ADAM 10-mediated effect on AKT phosphorylation (and therefore potentially, activity) in HCT116 cells, thus suggesting that although *KRAS* is mutated ADAM 10 mediation of downstream effects is not related. Notably, a SNP mutation of ADAM 10 was identified in HCT116 cells, which was not present in the other two CRC cell lines examined, however as this is within the UTR (untranslated region) it is unknown as to whether has any effects on the functionality of ADAM 10 in this cell line. However, it is possible that this may affect microRNA binding, as these modulators of gene expression bind within the 3'UTR region (Zhang et al., 2015a). Such effects have previously been seen in the context of ADAMs in CRC, with miR-30c being shown to suppress CRC progression through direct interaction with ADAM 19 (Zhang et al., 2015a). However, no such studies have been undertaken on ADAM 10 in HCT116 cells. Additionally, both *MYC* and *CCND1* were found to be non-mutated within HCT116 cells. Notably, previous research has

shown that the frameshift mutation of *CTNNB1* (β-Catenin) present in HCT116 cells, stabilises β-Catenin and activates Wnt signalling (Morin et al., 1997, Sparks et al., 1998, Kaler et al., 2012). Furthermore, it was shown that HCT116 cells with this mutation could be protected from apoptosis by Wnt signalling activation, which is known to promote cell growth (Kaler et al., 2012). Based on the evidence presented in **Table 6.1** it can be concluded that without further investigation there is insufficient evidence to definitively identify a mutational difference between CRC cell lines as being responsible for all experimental differences seen. However, based on findings by Kaler et al. (2012) further investigation into Wnt signalling in HCT116 cells should be undertaken. It is important to determine whether ADAM 10 mediates cellular proliferation through Wnt signalling in HCT116 cells, as a result of the *CTNNB1* mutation (**Figure 6.1**) (Sparks et al., 1998, Kaler et al., 2012, CCLE, 2013).

In summary, a hypoxia-mediated upregulation was reported in the three CRC cell lines investigated. Furthermore, a previously unidentified doublet band was identified, however attempts to characterise its nature were unsuccessful. There is insufficient evidence to suggest that the hypoxia-mediated upregulation of ADAM 10 seen promotes CRC progression. However, there was a clear role of ADAM 10 in regulation of cellular viability identified in HCT116 cells. Furthermore, a role of ADAM 10 in the regulation of *c-MYC* and *CCND1* expression was identified within these cells. In conclusion, it can be determined that hypoxia-driven ADAM 10 has little effect on CRC cells and the characteristics of cancer progression, however there is scope for further investigating the role of ADAM 10 (independently of hypoxia) in CRC viability and progression (**Figure 6.1**).

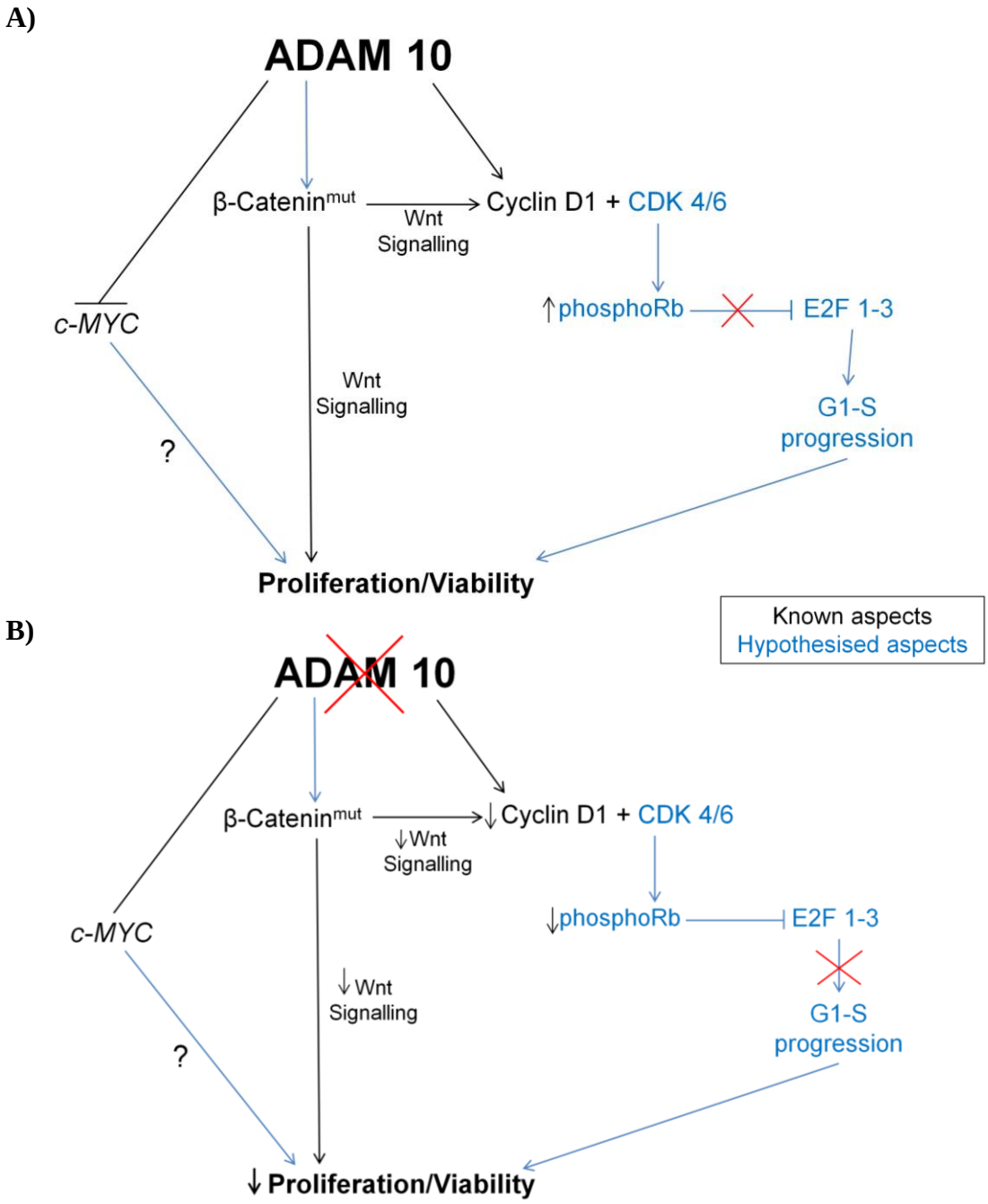

Figure 6.1: Hypothesised Mechanisms of Action of ADAM 10 on CRC Cellular Proliferation

This project has shown a role for ADAM 10 in mediating the viability of HCT116 cells and this figure illustrates the proposed underlying mechanisms (A). HCT116 cells are known to possess mutated β-Catenin, which results in its stabilization and activation of Wnt signalling. This activation is known to promote proliferation through a number of downstream targets, and these should be investigated. It is hypothesised that activation of Wnt signalling results in the promotion of *CCND1* expression, which leads to complex formation with CDK 4/6. As a result phosphorylation of RB is increased (a known characteristic of this cell line), resulting in its inactivation. E2F family transcription factors are then able to promote gene expression and GI/S phase transition, thus promoting cellular proliferation. In the absence of ADAM 10 (B) we have reported a downregulation in *CCND1* expression, thus reducing the complex formation with CDK 4/6. Phosphorylation of RB is reduced, which prevents E2F transcriptional activity and subsequent prevention of G1/S progression, resulting in decrease cellular proliferation.

6.2 Future Work

- Further characterisation into the nature of the ADAM 10 doublet band is needed, and the mechanisms behind the doublet formation need to be clarified, with focus on a hypoxia-mediated cleavage of the ADAM 10 protein. Furthermore, the implications of such a modification on the protein should be examined in terms of its functionality and possible role in CRC progression.
- Alternative methodology for examining the effect of hypoxia on ADAM 10 activity in CRC is required. The technology employed within this study did not produce any conclusive data and therefore alternative methodologies need to be tested. Clarification is important to identify the ramifications of altered ADAM 10 protein on its activity.
- Further clarification should be undertaken in the remit of the implications of *c-MYC* and *CCND1* modulation by ADAM 10 in CRC. No alteration to cell cycle was observed however other downstream effects as a result of *c-MYC* or *CCND1* modulation by ADAM 10 should be investigated. Furthermore, additional investigation into longer term effects of ADAM 10 on cell cycle regulation should be investigated.
- Investigation should be undertaken into Wnt signalling and the role ADAM 10 may play in its regulation of proliferation in CRC. Based on previous evidence of Wnt involvement in CRC progression and that presented here, of ADAM 10 mediated CRC proliferation, links between the two should be elucidated.

References

ABBAS, T. & DUTTA, A. 2009. p21 in cancer: intricate networks and multiple activities. *Nat Rev Cancer,* 9**,** 400-14.

AEBERSOLD, R. & MANN, M. 2003. Mass spectrometry-based proteomics. *Nature,* 422**,** 198-207.

AL-MAGHRABI, J., MUFTI, S., GOMAA, W., BUHMEIDA, A., AL-QAHTANI, M. & AL-AHWAL, M. 2015. Immunoexpression of cyclin D1 in colorectal carcinomas is not correlated with survival outcome. *Journal of Microscopy and Ultrastructure,* 3**,** 62-67.

AL-QASEM, A., AL-HOWAIL, H. A., AL-SWAILEM, M., AL-MAZROU, A., AL-OTAIBI, B., AL-JAMMAZ, I., AL-KHALAF, H. H. & ABOUSSEKHRA, A. 2016. PAC exhibits potent anti-colon cancer properties through targeting cyclin D1 and suppressing epithelial-to-mesenchymal transition. *Mol Carcinog,* 55**,** 233-244.

ALI, A. A., MARCUS, J. N., HARVEY, J. P., ROLL, R., HODGSON, C. P., WILDRICK, D. M., CHAKRABORTY, A. & BOMAN, B. M. 1993. RB1 protein in normal and malignant human colorectal tissue and colon cancer cell lines. *FASEB J,* 7**,** 931-7.

ALMEIDA, P. R., FERREIRA, V. A., SANTOS, C. C., ROCHA-FILHO, F. D., FEITOSA, R. R., FALCAO, E. A., CAVADA, B. K. & RIBEIRO, R. A. 2010. E-cadherin immunoexpression patterns in the characterisation of gastric carcinoma histotypes. *J Clin Pathol,* 63**,** 635-9.

ANDEREGG, U., EICHENBERG, T., PARTHAUNE, T., HAIDUK, C., SAALBACH, A., MILKOVA, L., LUDWIG, A., GROSCHE, J., AVERBECK, M., GEBHARDT, C., VOELCKER, V., SLEEMAN, J. P. & SIMON, J. C. 2009. ADAM10 is the constitutive functional sheddase of CD44 in human melanoma cells. *J Invest Dermatol,* 129**,** 1471-82.

ANDERS, A., GILBERT, S., GARTEN, W., POSTINA, R. & FAHRENHOLZ, F. 2001. Regulation of the alpha-secretase ADAM10 by its prodomain and proprotein convertases. *FASEB J,* 15**,** 1837-9.

ARIMA, T., ENOKIDA, H., KUBO, H., KAGARA, I., MATSUDA, R., TOKI, K., NISHIMURA, H., CHIYOMARU, T., TATARANO, S., IDESAKO, T., NISHIYAMA, K. & NAKAGAWA, M. 2007. Nuclear translocation of ADAM-10 contributes to the pathogenesis and progression of human prostate cancer. *Cancer Sci,* 98**,** 1720-6.

ARMANIOUS, H., GELEBART, P., ANAND, M., BELCH, A. & LAI, R. 2011. Constitutive activation of metalloproteinase ADAM10 in mantle cell lymphoma promotes cell growth and activates the TNFalpha/NFkappaB pathway. *Blood,* 117**,** 6237-46.

ASNAGHI, L., LIN, M. H., LIM, K. S., LIM, K. J., TRIPATHY, A., WENDEBORN, M., MERBS, S. L., HANDA, J. T., SODHI, A., BAR, E. E. & EBERHART, C. G. 2014. Hypoxia promotes uveal melanoma invasion through enhanced Notch and MAPK activation. *PLoS One,* 9**,** e105372.

BAHNASSY, A. A., ZEKRI, A.-R. N., EL-HOUSSINI, S., EL-SHEHABY, A. M. R., MAHMOUD, M. R., ABDALLAH, S. & EL-SERAFI, M. 2004. Cyclin A and cyclin D1 as significant prognostic markers in colorectal cancer patients. *BMC Gastroenterology,* 4**,** 22-22.

BAI, R., WENG, C., DONG, H., LI, S., CHEN, G. & XU, Z. 2015. MicroRNA-409-3p suppresses colorectal cancer invasion and metastasis partly by targeting GAB1 expression. *Int J Cancer,* 137**,** 2310-22.

BALLINGER, A. B. & ANGGIANSAH, C. 2007. Colorectal cancer. *BMJ,* 335**,** 715-8.

BANCK, M. S. & GROTHEY, A. 2009. Biomarkers of Resistance to Epidermal Growth Factor Receptor Monoclonal Antibodies in Patients with Metastatic Colorectal Cancer. *Clin Cancer Res,* 15**,** 7492-7501.

BARRETINA, J., CAPONIGRO, G., STRANSKY, N., VENKATESAN, K., MARGOLIN, A. A., KIM, S., WILSON, C. J., LEHAR, J., KRYUKOV, G. V., SONKIN, D., REDDY, A., LIU, M., MURRAY, L., BERGER, M. F., MONAHAN, J. E., MORAIS, P., MELTZER, J., KOREJWA, A., JANE-VALBUENA, J., MAPA, F. A., THIBAULT, J., BRIC-FURLONG, E., RAMAN, P., SHIPWAY, A., ENGELS, I. H., CHENG, J., YU, G. K., YU, J., ASPESI, P., DE SILVA, M., JAGTAP, K., JONES, M. D., WANG, L.,

HATTON, C., PALESCANDOLO, E., GUPTA, S., MAHAN, S., SOUGNEZ, C., ONOFRIO, R. C., LIEFELD, T., MACCONAILL, L., WINCKLER, W., REICH, M., LI, N., MESIROV, J. P., GABRIEL, S. B., GETZ, G., ARDLIE, K., CHAN, V., MYER, V. E., WEBER, B. L., PORTER, J., WARMUTH, M., FINAN, P., HARRIS, J. L., MEYERSON, M., GOLUB, T. R., MORRISSEY, M. P., SELLERS, W. R., SCHLEGEL, R. & GARRAWAY, L. A. 2012. The Cancer Cell Line Encyclopedia enables predictive modelling of anticancer drug sensitivity. *Nature,* 483**,** 603-307.

BARSOUM, I. B., HAMILTON, T. K., LI, X., COTECHINI, T., MILES, E. A., SIEMENS, D. R. & GRAHAM, C. H. 2011. Hypoxia induces escape from innate immunity in cancer cells via increased expression of ADAM10: role of nitric oxide. *Cancer Res,* 71**,** 7433-41.

BARTELS, K. M., FUNKEN, H., KNAPP, A., BROCKER, M., BOTT, M., WILHELM, S., JAEGER, K. E. & ROSENAU, F. 2011. Glycosylation is required for outer membrane localization of the lectin LecB in Pseudomonas aeruginosa. *J Bacteriol,* 193**,** 1107-13.

BAUMGART, A., SEIDL, S., VLACHOU, P., MICHEL, L., MITOVA, N., SCHATZ, N., SPECHT, K., KOCH, I., SCHUSTER, T., GRUNDLER, R., KREMER, M., FEND, F., SIVEKE, J. T., PESCHEL, C., DUYSTER, J. & DECHOW, T. 2010. ADAM17 regulates epidermal growth factor receptor expression through the activation of Notch1 in non-small cell lung cancer. *Cancer Res,* 70**,** 5368-78.

BEHROOZ, A. & ISMAIL-BEIGI, F. 1997. Dual control of glut1 glucose transporter gene expression by hypoxia and by inhibition of oxidative phosphorylation. *J Biol Chem,* 272**,** 5555-62.

BEITNER-JOHNSON, D., RUST, R. T., HSIEH, T. C. & MILLHORN, D. E. 2001. Hypoxia activates Akt and induces phosphorylation of GSK-3 in PC12 cells. *Cell Signal,* 13**,** 23-7.

BENNEWITH, K. L. & DEDHAR, S. 2011. Targeting hypoxic tumour cells to overcome metastasis. *BMC cancer,* 11**,** 504.

BENSON, E. K., MUNGAMURI, S. K., ATTIE, O., KRACIKOVA, M., SACHIDANANDAM, R., MANFREDI, J. J. & AARONSON, S. A. 2014. p53-dependent gene repression through p21 is mediated by recruitment of E2F4 repression complexes. *Oncogene,* 33**,** 3959-3969.

BERRIDGE, M. V., HERST, P. M. & TAN, A. S. 2005. Tetrazolium dyes as tools in cell biology: new insights into their cellular reduction. *Biotechnol Annu Rev,* 11**,** 127-52.

BERTOUT, J. A., PATEL, S. A. & SIMON, M. C. 2008. The impact of O(2) availability on human cancer. *Nature reviews. Cancer,* 8**,** 967-975.

BLACK, R. A., RAUCH, C. T., KOZLOSKY, C. J., PESCHON, J. J., SLACK, J. L., WOLFSON, M. F., CASTNER, B. J., STOCKING, K. L., REDDY, P., SRINIVASAN, S., NELSON, N., BOIANI, N., SCHOOLEY, K. A., GERHART, M., DAVIS, R., FITZNER, J. N., JOHNSON, R. S., PAXTON, R. J., MARCH, C. J. & CERRETTI, D. P. 1997. A metalloproteinase disintegrin that releases tumour-necrosis factor-alpha from cells. *Nature,* 385**,** 729-33.

BLANCHOT-JOSSIC, F., JARRY, A., MASSON, D., BACH-NGOHOU, K., PAINEAU, J., DENIS, M. G., LABOISSE, C. L. & MOSNIER, J. F. 2005. Up-regulated expression of ADAM17 in human colon carcinoma: co-expression with EGFR in neoplastic and endothelial cells. *J Pathol,* 207**,** 156-63.

BLOBEL, C. P. 2005. ADAMs: key components in EGFR signalling and development. *Nat Rev Mol Cell Biol,* 6**,** 32-43.

BODNAR, L., STANCZAK, A., CIERNIAK, S., SMOTER, M., CICHOWICZ, M., KOZLOWSKI, W., SZCZYLIK, C., WIECZOREK, M. & LAMPARSKA-PRZYBYSZ, M. 2014. Wnt/β-catenin pathway as a potential prognostic and predictive marker in patients with advanced ovarian cancer. *Journal of Ovarian Research,* 7**,** 16-16.

BOLOS, V., MIRA, E., MARTINEZ-POVEDA, B., LUXAN, G., CANAMERO, M., MARTINEZ, A. C., MANES, S. & DE LA POMPA, J. L. 2013. Notch activation stimulates migration of breast cancer cells and promotes tumor growth. *Breast Cancer Res,* 15**,** R54.

BORGGREFE, T. & OSWALD, F. 2009. The Notch signaling pathway: transcriptional regulation at Notch target genes. *Cell Mol Life Sci,* 66**,** 1631-46.

BORRELL-PAGES, M., ROJO, F., ALBANELL, J., BASELGA, J. & ARRIBAS, J. 2003. TACE is required for the activation of the EGFR by TGF-alpha in tumors. *EMBO J,* 22**,** 1114-24.

BOUDJADI, S., CARRIER, J. C., GROULX, J. F. & BEAULIEU, J. F. 2015. Integrin [alpha]1[beta]1 expression is controlled by c-MYC in colorectal cancer cells. *Oncogene*.

BOZKULAK, E. C. & WEINMASTER, G. 2009. Selective use of ADAM10 and ADAM17 in activation of Notch1 signaling. *Mol Cell Biol,* 29**,** 5679-95.

BRADEN, B. C. & POLJAK, R. J. 1995. Structural features of the reactions between antibodies and protein antigens. *FASEB J,* 9**,** 9-16.

BRENNER, H., KLOOR, M. & POX, C. P. 2014. Colorectal cancer. *Lancet,* 383**,** 1490-502.

BROGNARD, J., CLARK, A. S., NI, Y. & DENNIS, P. A. 2001. Akt/Protein Kinase B Is Constitutively Active in Non-Small Cell Lung Cancer Cells and Promotes Cellular Survival and Resistance to Chemotherapy and Radiation. *Cancer Research,* 61**,** 3986-3997.

BROWN, J. M. & GIACCIA, A. J. 1998. The unique physiology of solid tumors: opportunities (and problems) for cancer therapy. *Cancer Res,* 58**,** 1408-16.

BROWN, J. M. & WILSON, W. R. 2004. Exploiting tumour hypoxia in cancer treatment. *Nature reviews. Cancer,* 4**,** 437-47.

BUCK, E., EYZAGUIRRE, A., BARR, S., THOMPSON, S., SENNELLO, R., YOUNG, D., IWATA, K. K., GIBSON, N. W., CAGNONI, P. & HALEY, J. D. 2007. Loss of homotypic cell adhesion by epithelial-mesenchymal transition or mutation limits sensitivity to epidermal growth factor receptor inhibition. *Mol Cancer Ther,* 6.

BULSTRODE, H., JONES, L. M., SINEY, E. J., SAMPSON, J. M., LUDWIG, A., GRAY, W. P. & WILLAIME-MORAWEK, S. 2012. A-Disintegrin and Metalloprotease (ADAM) 10 and 17 promote self-renewal of brain tumor sphere forming cells. *Cancer Lett,* 326**,** 79-87.

BYERS, S. W., SOMMERS, C. L., HOXTER, B., MERCURIO, A. M. & TOZEREN, A. 1995. Role of E-cadherin in the response of tumor cell aggregates to lymphatic, venous and arterial flow: measurement of cell-cell adhesion strength. *J Cell Sci,* 108 (Pt 5)**,** 2053-64.

CAI, C. & ZHU, X. 2012. The Wnt/beta-catenin pathway regulates self-renewal of cancer stem-like cells in human gastric cancer. *Mol Med Rep,* 5**,** 1191-6.

CAIAZZA, F., MCGOWAN, P. M., MULLOOLY, M., MURRAY, A., SYNNOTT, N., O'DONOVAN, N., FLANAGAN, L., TAPE, C. J., MURPHY, G., CROWN, J. & DUFFY, M. J. 2015. Targeting ADAM-17 with an inhibitory monoclonal antibody has antitumour effects in triple-negative breast cancer cells. *Br J Cancer,* 112**,** 1895-1903.

CAMMAROTA, R., BERTOLINI, V., PENNESI, G., BUCCI, E. O., GOTTARDI, O., GARLANDA, C., LAGHI, L., BARBERIS, M. C., SESSA, F., NOONAN, D. M. & ALBINI, A. 2010. The tumor microenvironment of colorectal cancer: stromal TLR-4 expression as a potential prognostic marker. *J Transl Med,* 8**,** 112.

CANNITO, S., NOVO, E., COMPAGNONE, A., VALFRE DI BONZO, L., BUSLETTA, C., ZAMARA, E., PATERNOSTRO, C., POVERO, D., BANDINO, A., BOZZO, F., CRAVANZOLA, C., BRAVOCO, V., COLOMBATTO, S. & PAROLA, M. 2008. Redox mechanisms switch on hypoxia-dependent epithelial-mesenchymal transition in cancer cells. *Carcinogenesis,* 29**,** 2267-78.

CAO, D., HOU, M., GUAN, Y. S., JIANG, M., YANG, Y. & GOU, H. F. 2009. Expression of HIF-1alpha and VEGF in colorectal cancer: association with clinical outcomes and prognostic implications. *BMC Cancer,* 9**,** 432.

CAO, H., XU, E., LIU, H., WAN, L. & LAI, M. 2015. Epithelial-mesenchymal transition in colorectal cancer metastasis: A system review. *Pathol Res Pract,* 211**,** 557-69.

CAPPELLEN, D., SCHLANGE, T., BAUER, M., MAURER, F. & HYNES, N. E. 2007. Novel c-MYC target genes mediate differential effects on cell proliferation and migration. *EMBO Reports,* 8**,** 70-76.

CARULLI, A. J., KEELEY, T. M., DEMITRACK, E. S., CHUNG, J., MAILLARD, I. & SAMUELSON, L. C. 2015. Notch receptor regulation of intestinal stem cell homeostasis and crypt regeneration. *Developmental Biology,* 402**,** 98-108.

CASIMIRO, M. C., CROSARIOL, M., LORO, E., LI, Z. & PESTELL, R. G. 2012. Cyclins and Cell Cycle Control in Cancer and Disease. *Genes & Cancer,* 3**,** 649-657.

CATALANO, V., TURDO, A., DI FRANCO, S., DIELI, F., TODARO, M. & STASSI, G. 2013. Tumor and its microenvironment: a synergistic interplay. *Semin Cancer Biol,* 23**,** 522-32.

CCLE 2013. Broad-Norvartis Cancer Cell Line Encyclopedia. Broad-Norvartis.

CECCHINI, M. J., AMIRI, M. & DICK, F. A. 2012. Analysis of Cell Cycle Position in Mammalian Cells. *Journal of Visualized Experiments : JoVE***,** 3491.

CHARBONNEAU, M., HARPER, K., GRONDIN, F., PELMUS, M., MCDONALD, P. P. & DUBOIS, C. M. 2007. Hypoxia-inducible factor mediates hypoxic and tumor necrosis factor alpha-induced increases in tumor necrosis factor-alpha converting enzyme/ADAM17 expression by synovial cells. *J Biol Chem,* 282**,** 33714-24.

CHEN, G. & PRAMANIK, B. N. 2009. Application of LC/MS to proteomics studies: current status and future prospects. *Drug Discov Today,* 14**,** 465-71.

CHEN, J.-L., LIN, H. H., KIM, K.-J., LIN, A., OU, J. H. J. & ANN, D. K. 2009. PKCδ Signaling: A Dual Role in Regulating Hypoxic Stress-induced Autophagy and Apoptosis. *Autophagy,* 5**,** 244-246.

CHEN, J., IMANAKA, N., CHEN, J. & GRIFFIN, J. D. 2010. Hypoxia potentiates Notch signaling in breast cancer leading to decreased E-cadherin expression and increased cell migration and invasion. *Br J Cancer,* 102**,** 351-60.

CHEN, J., ZHAO, J., MA, R., LIN, H., LIANG, X. & CAI, X. 2014. Prognostic Significance of E-Cadherin Expression in Hepatocellular Carcinoma: A Meta-Analysis. *PLoS ONE,* 9**,** e103952.

CHEN, X., CHEN, L., CHEN, J., HU, W., GAO, H., XIE, B., WANG, X., YIN, Z., LI, S. & WANG, X. 2013. ADAM17 promotes U87 glioblastoma stem cell migration and invasion. *Brain Res,* 1538**,** 151-8.

CHEN, Y., DE MARCO, M. A., GRAZIANI, I., GAZDAR, A. F., STRACK, P. R., MIELE, L. & BOCCHETTA, M. 2007. Oxygen concentration determines the biological effects of NOTCH-1 signaling in adenocarcinoma of the lung. *Cancer Res,* 67**,** 7954-9.

CHENG, J. C., KLAUSEN, C. & LEUNG, P. C. 2013. Hypoxia-inducible factor 1 alpha mediates epidermal growth factor-induced down-regulation of E-cadherin expression and cell invasion in human ovarian cancer cells. *Cancer Lett,* 329**,** 197-206.

CHENG, J. Q., GODWIN, A. K., BELLACOSA, A., TAGUCHI, T., FRANKE, T. F., HAMILTON, T. C., TSICHLIS, P. N. & TESTA, J. R. 1992. AKT2, a putative oncogene encoding a member of a subfamily of protein-serine/threonine kinases, is amplified in human ovarian carcinomas. *Proceedings of the National Academy of Sciences of the United States of America,* 89**,** 9267-9271.

CHO, Y.-S., BAE, J.-M., CHUN, Y.-S., CHUNG, J.-H., JEON, Y.-K., KIM, I.-S., KIM, M.-S. & PARK, J.-W. 2008. HIF-1α controls keratinocyte proliferation by up-regulating p21(WAF1/Cip1). *Biochimica et Biophysica Acta (BBA) - Molecular Cell Research,* 1783**,** 323-333.

CHRISTIAN, L. M. 2012. The ADAM family: Insights into Notch proteolysis. *Fly (Austin),* 6**,** 30-4.

CIARDIELLO, F. & TORTORA, G. 2008. EGFR antagonists in cancer treatment. *N Engl J Med,* 358**,** 1160-74.

COHEN, P. 2002. The origins of protein phosphorylation. *Nat Cell Biol,* 4**,** E127-E130.

COLLARD, T. J., URBAN, B. C., PATSOS, H. A., HAGUE, A., TOWNSEND, P. A., PARASKEVA, C. & WILLIAMS, A. C. 2012. The retinoblastoma protein (Rb) as an anti-apoptotic factor: expression of Rb is required for the anti-apoptotic function of BAG-1 protein in colorectal tumour cells. *Cell Death Dis,* 3**,** e408.

CRIPPS, C., WINQUIST, E., DEVRIES, M. C., STYS-NORMAN, D. & GILBERT, R. 2010. Epidermal growth factor receptor targeted therapy in stages III and IV head and neck cancer. *Curr Oncol,* 17**,** 37-48.

CUMMINGS, B. S., WILLS, L. P. & SCHNELLMANN, R. G. 2004. Measurement of Cell Death in Mammalian Cells. *Current protocols in pharmacology / editorial board, S.J. Enna (editor-in-chief) ... [et al.],* 0 12**,** 10.1002/0471141755.ph1208s25.

CUNNINGHAM, D., ATKIN, W., LENZ, H.-J., LYNCH, H. T., MINSKY, B., NORDLINGER, B. & STARLING, N. 2010. Colorectal cancer. *The Lancet,* 375**,** 1030-1047.

DAI, Y., WILSON, G., HUANG, B., PENG, M., TENG, G., ZHANG, D., ZHANG, R., EBERT, M. P., CHEN, J., WONG, B. C., CHAN, K. W., GEORGE, J. & QIAO, L. 2014. Silencing of Jagged1 inhibits cell growth and invasion in colorectal cancer. *Cell Death Dis,* 5**,** e1170.

DANG, C. V. 2012. MYC on the path to cancer. *Cell,* 149**,** 22-35.

DANIELSEN, S. A., EIDE, P. W., NESBAKKEN, A., GUREN, T., LEITHE, E. & LOTHE, R. A. 2015. Portrait of the PI3K/AKT pathway in colorectal cancer. *Biochim Biophys Acta,* 1855**,** 104-21.

DAVIES, D. R. & COHEN, G. H. 1996. Interactions of protein antigens with antibodies. *Proc Natl Acad Sci U S A,* 93**,** 7-12.

DE FREITAS JUNIOR, J. C., SILVA BDU, R., DE SOUZA, W. F., DE ARAUJO, W. M., ABDELHAY, E. S. & MORGADO-DIAZ, J. A. 2011. Inhibition of N-linked glycosylation by tunicamycin induces E-cadherin-mediated cell-cell adhesion and inhibits cell proliferation in undifferentiated human colon cancer cells. *Cancer Chemother Pharmacol,* 68**,** 227-38.

DEMICHELE, A., CLARK, A. S., TAN, K. S., HEITJAN, D. F., GRAMLICH, K., GALLAGHER, M., LAL, P., FELDMAN, M., ZHANG, P., COLAMECO, C., LEWIS, D., LANGER, M., GOODMAN, N., DOMCHEK, S., GOGINENI, K., ROSEN, M., FOX, K. & O'DWYER, P. 2015. CDK 4/6 inhibitor palbociclib (PD0332991) in Rb+ advanced breast cancer: phase II activity, safety, and predictive biomarker assessment. *Clin Cancer Res,* 21**,** 995-1001.

DEPAULIS, F., BRAZIER, L. & VEUILLE, M. 1999. Selective sweep at the Drosophila melanogaster Suppressor of Hairless locus and its association with the In(2L)t inversion polymorphism. *Genetics,* 152**,** 1017-24.

DEWHIRST, M. W. 1998. Concepts of oxygen transport at the microcirculatory level. *Seminars in radiation oncology,* 8**,** 143-50.

DHILLON, A. S., HAGAN, S., RATH, O. & KOLCH, W. 2007. MAP kinase signalling pathways in cancer. *Oncogene,* 26.

DIAZ-RODRIGUEZ, E., MONTERO, J. C., ESPARIS-OGANDO, A., YUSTE, L. & PANDIELLA, A. 2002. Extracellular signal-regulated kinase phosphorylates tumor necrosis factor alpha-converting enzyme at threonine 735: a potential role in regulated shedding. *Mol Biol Cell,* 13**,** 2031-44.

DOBERSTEIN, K., PFEILSCHIFTER, J. & GUTWEIN, P. 2011. The transcription factor PAX2 regulates ADAM10 expression in renal cell carcinoma. *Carcinogenesis,* 32**,** 1713-1723.

DOLDO, E., COSTANZA, G., FERLOSIO, A., POMPEO, E., AGOSTINELLI, S., BELLEZZA, G., MAZZAGLIA, D., GIUNTA, A., SIDONI, A. & ORLANDI, A. 2015. High expression of cellular retinol binding protein-1 in lung adenocarcinoma is associated with poor prognosis. *Genes & Cancer,* 6**,** 490-502.

DORUDI, S., SHEFFIELD, J. P., POULSOM, R., NORTHOVER, J. M. & HART, I. R. 1993. E-cadherin expression in colorectal cancer. An immunocytochemical and in situ hybridization study. *Am J Pathol,* 142**,** 981-6.

DU, J., XU, R., HU, Z., TIAN, Y., ZHU, Y., GU, L. & ZHOU, L. 2011. PI3K and ERK-Induced Rac1 Activation Mediates Hypoxia-Induced HIF-1α Expression in MCF-7 Breast Cancer Cells. *PLoS ONE,* 6**,** e25213.

DUAN, G. & WALTHER, D. 2015. The Roles of Post-translational Modifications in the Context of Protein Interaction Networks. *PLoS Comput Biol,* 11**,** e1004049.

DUFFY, M. J., MULLOOLY, M., O'DONOVAN, N., SUKOR, S., CROWN, J., PIERCE, A. & MCGOWAN, P. M. 2011. The ADAMs family of proteases: new biomarkers and therapeutic targets for cancer? *Clinical proteomics,* 8**,** 9.

EBBING, E. A., MEDEMA, J. P., DAMHOFER, H., MEIJER, S. L., KRISHNADATH, K. K., VAN BERGE HENEGOUWEN, M. I., BIJLSMA, M. F. & VAN LAARHOVEN, H. W. 2016. ADAM10-mediated release of heregulin confers resistance to trastuzumab by activating HER3. *Oncotarget*.

EBSEN, H., SCHRODER, A., KABELITZ, D. & JANSSEN, O. 2013. Differential surface expression of ADAM10 and ADAM17 on human T lymphocytes and tumor cells. *PLoS One,* 8**,** e76853.

EDWARDS, D. R., HANDSLEY, M. M. & PENNINGTON, C. J. 2008. The ADAM metalloproteinases. *Molecular aspects of medicine,* 29**,** 258-89.

ENGELMAN, J. A. 2009. Targeting PI3K signalling in cancer: opportunities, challenges and limitations. *Nat Rev Cancer,* 9**,** 550-562.

ESCREVENTE, C., MORAIS, V. A., KELLER, S., SOARES, C. M., ALTEVOGT, P. & COSTA, J. 2008. Functional role of N-glycosylation from ADAM10 in processing, localization and activity of the enzyme. *Biochim Biophys Acta,* 1780**,** 905-13.

ETTINGER, A. & WITTMANN, T. 2014. Fluorescence Live Cell Imaging. *Methods in cell biology,* 123**,** 77-94.

EVAN, G. I. & VOUSDEN, K. H. 2001. Proliferation, cell cycle and apoptosis in cancer. *Nature,* 411**,** 342-348.

FAHRENHOLZ, F., GILBERT, S., KOJRO, E., LAMMICH, S. & POSTINA, R. 2000. Alpha-secretase activity of the disintegrin metalloprotease ADAM 10. Influences of domain structure. *Ann N Y Acad Sci,* 920**,** 215-22.

FAN, F., SAMUEL, S., EVANS, K. W., LU, J., XIA, L., ZHOU, Y., SCEUSI, E., TOZZI, F., YE, X. C., MANI, S. A. & ELLIS, L. M. 2012. Overexpression of snail induces epithelial-mesenchymal transition and a cancer stem cell-like phenotype in human colorectal cancer cells. *Cancer Med,* 1**,** 5-16.

FANG, J. Y. & RICHARDSON, B. C. 2005. The MAPK signalling pathways and colorectal cancer. *Lancet Oncol,* 6.

FANG, Y.-J., PAN, Z.-Z., LI, L.-R., LU, Z.-H., ZHANG, L.-Y. & WAN, D.-S. 2009. MMP7 expression regulated by endocrine therapy in ERβ-positive colon cancer cells. *Journal of Experimental & Clinical Cancer Research,* 28**,** 1-8.

FEITELSON, M. A., ARZUMANYAN, A., KULATHINAL, R. J., BLAIN, S. W., HOLCOMBE, R. F., MAHAJNA, J., MARINO, M., MARTINEZ-CHANTAR, M. L., NAWROTH, R., SANCHEZ-GARCIA, I., SHARMA, D., SAXENA, N. K., SINGH, N., VLACHOSTERGIOS, P. J., GUO, S., HONOKI, K., FUJII, H., GEORGAKILAS, A. G., BILSLAND, A., AMEDEI, A., NICCOLAI, E., AMIN, A., ASHRAF, S. S., BOOSANI, C. S., GUHA, G., CIRIOLO, M. R., AQUILANO, K., CHEN, S., MOHAMMED, S. I., AZMI, A. S., BHAKTA, D., HALICKA, D., KEITH, W. N. & NOWSHEEN, S. 2015. Sustained proliferation in cancer: Mechanisms and novel therapeutic targets. *Semin Cancer Biol,* 35 Suppl**,** S25-54.

FENDER, A. W., NUTTER, J. M., FITZGERALD, T. L., BERTRAND, F. E. & SIGOUNAS, G. 2015. Notch-1 Promotes Stemness and Epithelial to Mesenchymal Transition in Colorectal Cancer. *Journal of Cellular Biochemistry,* 116**,** 2517-2527.

FENG, Y., XU, X., ZHANG, Y., DING, J., WANG, Y., ZHANG, X., WU, Z., KANG, L., LIANG, Y., ZHOU, L., SONG, S., ZHAO, K. & YE, Q. 2015. HPIP is upregulated in colorectal cancer and regulates colorectal cancer cell proliferation, apoptosis and invasion. *Sci Rep,* 5**,** 9429.

FERENBACH, D. A. & BONVENTRE, J. V. 2015. Mechanisms of maladaptive repair after AKI leading to accelerated kidney ageing and CKD. *Nat Rev Nephrol,* 11**,** 264-276.

FERLAY, J., SOERJOMATARAM, I., DIKSHIT, R., ESER, S., MATHERS, C., REBELO, M., PARKIN, D. M., FORMAN, D. & BRAY, F. 2015. Cancer incidence and mortality worldwide: sources, methods and major patterns in GLOBOCAN 2012. *Int J Cancer,* 136**,** E359-86.

FESTUCCIA, C., GRAVINA, G. L., MUZI, P., MILLIMAGGI, D., DOLO, V., VICENTINI, C. & BOLOGNA, M. 2008. Akt down-modulation induces apoptosis of human prostate cancer cells and synergizes with EGFR tyrosine kinase inhibitors. *Prostate,* 68**,** 965-74.

FINN, R. S., DERING, J., CONKLIN, D., KALOUS, O., COHEN, D. J., DESAI, A. J., GINTHER, C., ATEFI, M., CHEN, I., FOWST, C., LOS, G. & SLAMON, D. J. 2009.

PD 0332991, a selective cyclin D kinase 4/6 inhibitor, preferentially inhibits proliferation of luminal estrogen receptor-positive human breast cancer cell lines in vitro. *Breast Cancer Res,* 11**,** R77.

FRANKEN, N. A., RODERMOND, H. M., STAP, J., HAVEMAN, J. & VAN BREE, C. 2006. Clonogenic assay of cells in vitro. *Nat Protoc,* 1**,** 2315-9.

FRANZKE, C. W., BRUCKNER-TUDERMAN, L. & BLOBEL, C. P. 2009. Shedding of collagen XVII/BP180 in skin depends on both ADAM10 and ADAM9. *J Biol Chem,* 284**,** 23386-96.

FREIRE-DE-LIMA, L. 2014. Sweet and Sour: The Impact of Differential Glycosylation in Cancer Cells Undergoing Epithelial-Mesenchymal Transition. *Frontiers in Oncology,* 4.

FRIDMAN, J. S., CAULDER, E., HANSBURY, M., LIU, X., YANG, G., WANG, Q., LO, Y., ZHOU, B. B., PAN, M., THOMAS, S. M., GRANDIS, J. R., ZHUO, J., YAO, W., NEWTON, R. C., FRIEDMAN, S. M., SCHERLE, P. A. & VADDI, K. 2007. Selective inhibition of ADAM metalloproteases as a novel approach for modulating ErbB pathways in cancer. *Clin Cancer Res,* 13**,** 1892-902.

FROHLICH, C., ALBRECHTSEN, R., DYRSKJOT, L., RUDKJAER, L., ORNTOFT, T. F. & WEWER, U. M. 2006. Molecular profiling of ADAM12 in human bladder cancer. *Clin Cancer Res,* 12**,** 7359-68.

FRY, D. W., HARVEY, P. J., KELLER, P. R., ELLIOTT, W. L., MEADE, M., TRACHET, E., ALBASSAM, M., ZHENG, X., LEOPOLD, W. R., PRYER, N. K. & TOOGOOD, P. L. 2004. Specific inhibition of cyclin-dependent kinase 4/6 by PD 0332991 and associated antitumor activity in human tumor xenografts. *Mol Cancer Ther,* 3**,** 1427-38.

FU, L., LIU, N., HAN, Y., XIE, C., LI, Q. & WANG, E. 2014. ADAM10 regulates proliferation, invasion, and chemoresistance of bladder cancer cells. *Tumor Biology,* 35**,** 9263-9268.

GAIDA, M. M., HAAG, N., GUNTHER, F., TSCHAHARGANEH, D. F., SCHIRMACHER, P., FRIESS, H., GIESE, N. A., SCHMIDT, J. & WENTE, M. N. 2010. Expression of A disintegrin and metalloprotease 10 in pancreatic carcinoma. *Int J Mol Med,* 26**,** 281-8.

GAMMON, L. & MACKENZIE, I. C. 2015. Roles of hypoxia, stem cells and epithelial–mesenchymal transition in the spread and treatment resistance of head and neck cancer. *Journal of Oral Pathology & Medicine***,** n/a-n/a.

GANGEMI, R., AMARO, A., GINO, A., BARISIONE, G., FABBI, M., PFEFFER, U., BRIZZOLARA, A., QUEIROLO, P., SALVI, S., BOCCARDO, S., GUALCO, M., SPAGNOLO, F., JAGER, M. J., MOSCI, C., ROSSELLO, A. & FERRINI, S. 2014. ADAM10 correlates with uveal melanoma metastasis and promotes in vitro invasion. *Pigment Cell Melanoma Res,* 27**,** 1138-48.

GARTEL, A. L. 2006. Is p21 an oncogene? *Mol Cancer Ther,* 5**,** 1385-6.

GASSMANN, M., GRENACHER, B., ROHDE, B. & VOGEL, J. 2009. Quantifying Western blots: pitfalls of densitometry. *Electrophoresis,* 30**,** 1845-55.

GAVERT, N., SHEFFER, M., RAVEH, S., SPADERNA, S., SHTUTMAN, M., BRABLETZ, T., BARANY, F., PATY, P., NOTTERMAN, D., DOMANY, E. & BEN-ZE'EV, A. 2007. Expression of L1-CAM and ADAM10 in human colon cancer cells induces metastasis. *Cancer Res,* 67**,** 7703-12.

GEDALY, R., GALUPPO, R., DAILY, M. F., SHAH, M., MAYNARD, E., CHEN, C., ZHANG, X., ESSER, K. A., COHEN, D. A., EVERS, B. M., JIANG, J. & SPEAR, B. T. 2014. Targeting the Wnt/β-Catenin Signaling Pathway in Liver Cancer Stem Cells and Hepatocellular Carcinoma Cell Lines with FH535. *PLoS ONE,* 9**,** e99272.

GEE, J. M. & KNOWLDEN, J. M. 2003. ADAM metalloproteases and EGFR signalling. *Breast Cancer Res,* 5**,** 223-4.

GONNET, F., LEMAITRE, G., WAKSMAN, G. & TORTAJADA, J. 2003. MALDI/MS peptide mass fingerprinting for proteome analysis: identification of hydrophobic proteins attached to eucaryote keratinocyte cytoplasmic membrane using different matrices in concert. *Proteome Sci,* 1**,** 2.

GOODEN, M. J., WIERSMA, V. R., BOERMA, A., LEFFERS, N., BOEZEN, H. M., TEN HOOR, K. A., HOLLEMA, H., WALENKAMP, A. M., DAEMEN, T., NIJMAN, H. W. & BREMER, E. 2014. Elevated serum CXCL16 is an independent predictor of poor

survival in ovarian cancer and may reflect pro-metastatic ADAM protease activity. *Br J Cancer,* 110**,** 1535-44.
GOOZ, M. 2010. ADAM-17: the enzyme that does it all. *Crit Rev Biochem Mol Biol,* 45**,** 146-69.
GÖŐZ, P., GÖŐZ, M., BALDYS, A. & HOFFMAN, S. 2009. ADAM-17 Regulates Endothelial Cell Morphology, Proliferation, and In Vitro Angiogenesis. *Biochemical and biophysical research communications,* 380**,** 33-38.
GOPALAKRISHNAN, N., SARAVANAKUMAR, M., MADANKUMAR, P., THIYAGU, M. & DEVARAJ, H. 2014. Colocalization of beta-catenin with Notch intracellular domain in colon cancer: a possible role of Notch1 signaling in activation of CyclinD1-mediated cell proliferation. *Mol Cell Biochem,* 396**,** 281-93.
GRABOWSKA, M. M., SANDHU, B. & DAY, M. L. 2012. EGF promotes the shedding of soluble E-cadherin in an ADAM10-dependent manner in prostate epithelial cells. *Cellular Signalling,* 24**,** 532-538.
GREENING, D. W., LEE, S. T., JI, H., SIMPSON, R. J., RIGOPOULOS, A., MURONE, C., FANG, C., GONG, S., O'KEEFE, G. & SCOTT, A. M. 2015. Molecular profiling of cetuximab and bevacizumab treatment of colorectal tumours reveals perturbations in metabolic and hypoxic response pathways. *Oncotarget,* 6**,** 38166-80.
GROOT, A. J., HABETS, R., YAHYANEJAD, S., HODIN, C. M., REISS, K., SAFTIG, P., THEYS, J. & VOOIJS, M. 2014. Regulated proteolysis of NOTCH2 and NOTCH3 receptors by ADAM10 and presenilins. *Mol Cell Biol,* 34**,** 2822-32.
GROTH, C., ALVORD, W. G., QUIÑONES, O. A. & FORTINI, M. E. 2010. Pharmacological Analysis of Drosophila melanogaster γ-Secretase with Respect to Differential Proteolysis of Notch and APP. *Molecular Pharmacology,* 77**,** 567-574.
GUO, J., HE, L., YUAN, P., WANG, P., LU, Y., TONG, F., WANG, Y., YIN, Y., TIAN, J. & SUN, J. 2012. ADAM10 overexpression in human non-small cell lung cancer correlates with cell migration and invasion through the activation of the Notch1 signaling pathway. *Oncol Rep,* 28**,** 1709-18.
GUO, Z., JIN, X. & JIA, H. 2013. Inhibition of ADAM-17 more effectively down-regulates the Notch pathway than that of gamma-secretase in renal carcinoma. *J Exp Clin Cancer Res,* 32**,** 26.
HAMMOND, E. M., DENKO, N. C., DORIE, M. J., ABRAHAM, R. T. & GIACCIA, A. J. 2002. Hypoxia Links ATR and p53 through Replication Arrest. *Molecular and Cellular Biology,* 22**,** 1834-1843.
HAMMOND, E. M., GREEN, S. L. & GIACCIA, A. J. 2003. Comparison of hypoxia-induced replication arrest with hydroxyurea and aphidicolin-induced arrest. *Mutat Res,* 532**,** 205-13.
HANAHAN, D. & WEINBERG, R. A. 2000. The hallmarks of cancer. *Cell,* 100**,** 57-70.
HANAHAN, D. & WEINBERG, R. A. 2011. Hallmarks of cancer: the next generation. *Cell,* 144**,** 646-74.
HANCOCK, R. L., DUNNE, K., WALPORT, L. J., FLASHMAN, E. & KAWAMURA, A. 2015. Epigenetic regulation by histone demethylases in hypoxia. *Epigenomics,* 7**,** 791-811.
HANNUS, M., BEITZINGER, M., ENGELMANN, J. C., WEICKERT, M.-T., SPANG, R., HANNUS, S. & MEISTER, G. 2014. siPools: highly complex but accurately defined siRNA pools eliminate off-target effects. *Nucleic Acids Research*.
HARTMANN, D., DE STROOPER, B., SERNEELS, L., CRAESSAERTS, K., HERREMAN, A., ANNAERT, W., UMANS, L., LUBKE, T., LENA ILLERT, A., VON FIGURA, K. & SAFTIG, P. 2002. The disintegrin/metalloprotease ADAM 10 is essential for Notch signalling but not for alpha-secretase activity in fibroblasts. *Hum Mol Genet,* 11**,** 2615-24.
HASSAN, W. A., YOSHIDA, R., KUDOH, S., HASEGAWA, K., NIIMORI-KITA, K. & ITO, T. 2014. Notch1 controls cell invasion and metastasis in small cell lung carcinoma cell lines. *Lung Cancer,* 86**,** 304-10.
HE, X., WANG, J., WEI, W., SHI, M., XIN, B., ZHANG, T. & SHEN, X. 2016. Hypoxia regulates ABCG activity through the activivation of ERK1/2/HIF-1alpha and contributes to chemoresistance in pancreatic cancer cells. *Cancer Biol Ther***,** 0.

HERBST, A., JURINOVIC, V., KREBS, S., THIEME, S. E., BLUM, H., GÖKE, B. & KOLLIGS, F. T. 2014. Comprehensive analysis of β-catenin target genes in colorectal carcinoma cell lines with deregulated Wnt/β-catenin signaling. *BMC Genomics,* 15**,** 1-15.

HIGGINS, D. F., KIMURA, K., BERNHARDT, W. M., SHRIMANKER, N., AKAI, Y., HOHENSTEIN, B., SAITO, Y., JOHNSON, R. S., KRETZLER, M., COHEN, C. D., ECKARDT, K.-U., IWANO, M. & HAASE, V. H. 2007. Hypoxia promotes fibrogenesis in vivo via HIF-1 stimulation of epithelial-to-mesenchymal transition. *The Journal of Clinical Investigation,* 117**,** 3810-3820.

HIKITA, A., YANA, I., WAKEYAMA, H., NAKAMURA, M., KADONO, Y., OSHIMA, Y., NAKAMURA, K., SEIKI, M. & TANAKA, S. 2006. Negative regulation of osteoclastogenesis by ectodomain shedding of receptor activator of NF-kappaB ligand. *J Biol Chem,* 281**,** 36846-55.

HO, C. S., LAM, C. W. K., CHAN, M. H. M., CHEUNG, R. C. K., LAW, L. K., LIT, L. C. W., NG, K. F., SUEN, M. W. M. & TAI, H. L. 2003. Electrospray Ionisation Mass Spectrometry: Principles and Clinical Applications. *The Clinical Biochemist Reviews,* 24**,** 3-12.

HOETTECKE, N., LUDWIG, A., FORO, S. & SCHMIDT, B. 2010. Improved synthesis of ADAM10 inhibitor GI254023X. *Neurodegener Dis,* 7**,** 232-8.

HOFBAUER, K. H., GESS, B., LOHAUS, C., MEYER, H. E., KATSCHINSKI, D. & KURTZ, A. 2003. Oxygen tension regulates the expression of a group of procollagen hydroxylases. *Eur J Biochem,* 270**,** 4515-22.

HOLLAND, W. S., CHINN, D. C., LARA, P. N., JR., GANDARA, D. R. & MACK, P. C. 2015. Effects of AKT inhibition on HGF-mediated erlotinib resistance in non-small cell lung cancer cell lines. *J Cancer Res Clin Oncol,* 141**,** 615-26.

HOLLECZEK, B., ROSSI, S., DOMENIC, A., INNOS, K., MINICOZZI, P., FRANCISCI, S., HACKL, M., EISEMANN, N. & BRENNER, H. 2015. On-going improvement and persistent differences in the survival for patients with colon and rectum cancer across Europe 1999–2007 – Results from the EUROCARE-5 study. *European Journal of Cancer,* 51**,** 2158-2168.

HONG, S., KIM, S., KIM, H. Y., KANG, M., JANG, H. H. & LEE, W. S. 2015. Targeting the PI3K signaling pathway in KRAS mutant colon cancer. *Cancer Med.*

HONGO, K., TSUNO, N. H., KAWAI, K., SASAKI, K., KANEKO, M., HIYOSHI, M., MURONO, K., TADA, N., NIREI, T., SUNAMI, E., TAKAHASHI, K., NAGAWA, H., KITAYAMA, J. & WATANABE, T. 2013. Hypoxia enhances colon cancer migration and invasion through promotion of epithelial-mesenchymal transition. *J Surg Res,* 182**,** 75-84.

HU, Y.-L., DELAY, M., JAHANGIRI, A., MOLINARO, A. M., ROSE, S. D., CARBONELL, W. S. & AGHI, M. K. 2012. Hypoxia-induced autophagy promotes tumor cell survival and adaptation to anti-angiogenic treatment in glioblastoma. *Cancer Research,* 72**,** 1773-1783.

HU, Y., BAI, J., HOU, S. X., TANG, J. S., SHI, X. X., QIN, J. & REN, N. 2015. Hypoxia-Inducible Factor 1-Alpha Regulates Cancer-Inhibitory Effect of Human Mesenchymal Stem Cells. *Cell Biochem Biophys.*

HUANG, R. Y.-J., GUILFORD, P. & THIERY, J. P. 2012. Early events in cell adhesion and polarity during epithelial-mesenchymal transition. *Journal of Cell Science,* 125**,** 4417-4422.

HUERTA, S., GOULET, E. J., HUERTA-YEPEZ, S. & LIVINGSTON, E. H. 2007. Screening and Detection of Apoptosis. *Journal of Surgical Research,* 139**,** 143-156.

HULKOWER, K. I. & HERBER, R. L. 2011. Cell Migration and Invasion Assays as Tools for Drug Discovery. *Pharmaceutics,* 3**,** 107-124.

HUMPHREY, S. J., JAMES, D. E. & MANN, M. 2015. Protein Phosphorylation: A Major Switch Mechanism for Metabolic Regulation. *Trends in Endocrinology & Metabolism,* 26**,** 676-687.

HUYNH, N., BEUTLER, J. A., SHULKES, A., BALDWIN, G. S. & HE, H. 2015. Glaucarubinone inhibits colorectal cancer growth by suppression of hypoxia-inducible

factor 1alpha and beta-catenin via a p-21 activated kinase 1-dependent pathway. *Biochim Biophys Acta,* 1853**,** 157-65.

IRSHAD, K., MOHAPATRA, S. K., SRIVASTAVA, C., GARG, H., MISHRA, S., DIKSHIT, B., SARKAR, C., GUPTA, D., CHANDRA, P. S., CHATTOPADHYAY, P., SINHA, S. & CHOSDOL, K. 2015. A Combined Gene Signature of Hypoxia and Notch Pathway in Human Glioblastoma and Its Prognostic Relevance. *PLoS ONE,* 10**,** e0118201.

ISHIDA, T., HIJIOKA, H., KUME, K., MIYAWAKI, A. & NAKAMURA, N. 2013. Notch signaling induces EMT in OSCC cell lines in a hypoxic environment. *Oncol Lett,* 6**,** 1201-1206.

ISOZAKI, T., ISHII, S., NISHIMI, S., NISHIMI, A., OGURO, N., SEKI, S., MIURA, Y., MIWA, Y., OH, K., TOYOSHIMA, Y., NAKAMURA, M., INAGAKI, K. & KASAMA, T. 2015. A disintegrin and metalloprotease-10 is correlated with disease activity and mediates monocyte migration and adhesion in rheumatoid arthritis. *Translational Research,* 166**,** 244-253.

IVANOVIC, Z. 2009. Hypoxia or in situ normoxia: The stem cell paradigm. *J Cell Physiol,* 219**,** 271-5.

IZUMI, Y., HIRATA, M., HASUWA, H., IWAMOTO, R., UMATA, T., MIYADO, K., TAMAI, Y., KURISAKI, T., SEHARA-FUJISAWA, A., OHNO, S. & MEKADA, E. 1998. A metalloprotease-disintegrin, MDC9/meltrin-gamma/ADAM9 and PKCdelta are involved in TPA-induced ectodomain shedding of membrane-anchored heparin-binding EGF-like growth factor. *EMBO J,* 17**,** 7260-72.

JANES, P. W., SAHA, N., BARTON, W. A., KOLEV, M. V., WIMMER-KLEIKAMP, S. H., NIEVERGALL, E., BLOBEL, C. P., HIMANEN, J.-P., LACKMANN, M. & NIKOLOV, D. B. 2005. Adam Meets Eph: An ADAM Substrate Recognition Module Acts as a Molecular Switch for Ephrin Cleavage In trans. *Cell,* 123**,** 291-304.

JANG, G.-B., KIM, J.-Y., CHO, S.-D., PARK, K.-S., JUNG, J.-Y., LEE, H.-Y., HONG, I.-S. & NAM, J.-S. 2015a. Blockade of Wnt/β-catenin signaling suppresses breast cancer metastasis by inhibiting CSC-like phenotype. *Scientific Reports,* 5**,** 12465.

JANG, G. B., HONG, I. S., KIM, R. J., LEE, S. Y., PARK, S. J., LEE, E. S., PARK, J. H., YUN, C. H., CHUNG, J. U., LEE, K. J., LEE, H. Y. & NAM, J. S. 2015b. Wnt/beta-Catenin Small-Molecule Inhibitor CWP232228 Preferentially Inhibits the Growth of Breast Cancer Stem-like Cells. *Cancer Res,* 75**,** 1691-702.

JASPERSON, K. W., TUOHY, T. M., NEKLASON, D. W. & BURT, R. W. 2010. Hereditary and Familial Colon Cancer. *Gastroenterology,* 138**,** 2044-2058.

JI, H., LEE, J. H., WANG, Y., PANG, Y., ZHANG, T., XIA, Y., ZHONG, L., LYU, J. & LU, Z. 2015. EGFR phosphorylates FAM129B to promote Ras activation. *Proc Natl Acad Sci U S A*.

JIN, G., HUANG, X., BLACK, R., WOLFSON, M., RAUCH, C., MCGREGOR, H., ELLESTAD, G. & COWLING, R. 2002. A continuous fluorimetric assay for tumor necrosis factor-alpha converting enzyme. *Anal Biochem,* 302**,** 269-75.

JONES, A. V., LAMBERT, D. W., SPEIGHT, P. M. & WHAWELL, S. A. 2013. ADAM 10 is over expressed in oral squamous cell carcinoma and contributes to invasive behaviour through a functional association with alphavbeta6 integrin. *FEBS Lett,* 587**,** 3529-34.

JONES, J. C., RUSTAGI, S. & DEMPSEY, P. J. 2016. ADAM Proteases and Gastrointestinal Function. *Annu Rev Physiol,* 78**,** 243-76.

JOO, Y. E., REW, J. S., CHOI, S. K., BOM, H. S., PARK, C. S. & KIM, S. J. 2002. Expression of e-cadherin and catenins in early gastric cancer. *J Clin Gastroenterol,* 35**,** 35-42.

JORISSEN, E., PROX, J., BERNREUTHER, C., WEBER, S., SCHWANBECK, R., SERNEELS, L., SNELLINX, A., CRAESSAERTS, K., THATHIAH, A., TESSEUR, I., BARTSCH, U., WESKAMP, G., BLOBEL, C. P., GLATZEL, M., DE STROOPER, B. & SAFTIG, P. 2010. The disintegrin/metalloproteinase ADAM10 is essential for the establishment of the brain cortex. *J Neurosci,* 30**,** 4833-44.

JOSEPH, E. W., PRATILAS, C. A., POULIKAKOS, P. I., TADI, M., WANG, W., TAYLOR, B. S., HALILOVIC, E., PERSAUD, Y., XING, F., VIALE, A., TSAI, J., CHAPMAN, P. B., BOLLAG, G., SOLIT, D. B. & ROSEN, N. 2010. The RAF inhibitor PLX4032 inhibits ERK signaling and tumor cell proliferation in a V600E BRAF-selective

manner. *Proceedings of the National Academy of Sciences of the United States of America,* 107**,** 14903-14908.

JOUNG, Y. H., LIM, E. J., KIM, M. S., LIM, S. D., YOON, S. Y., LIM, Y. C., YOO, Y. B., YE, S. K., PARK, T., CHUNG, I. M., BAE, K. Y. & YANG, Y. M. 2008. Enhancement of hypoxia-induced apoptosis of human breast cancer cells via STAT5b by momilactone B. *Int J Oncol,* 33**,** 477-84.

JOUNG, Y. H., LIM, E. J., LEE, M. Y., PARK, J. H., YE, S. K., PARK, E. U., KIM, S. Y., ZHANG, Z., LEE, K. J., PARK, D. K., PARK, T., MOON, W. K. & YANG, Y. M. 2005. Hypoxia activates the cyclin D1 promoter via the Jak2/STAT5b pathway in breast cancer cells. *Exp Mol Med,* 37**,** 353-64.

KAIDI, A., WILLIAMS, A. C. & PARASKEVA, C. 2007. Interaction between [beta]-catenin and HIF-1 promotes cellular adaptation to hypoxia. *Nat Cell Biol,* 9**,** 210-217.

KALER, P., AUGENLICHT, L. & KLAMPFER, L. 2012. Activating Mutations in ?-Catenin in Colon Cancer Cells Alter Their Interaction with Macrophages; the Role of Snail. *PLoS ONE,* 7**,** e45462.

KALLURI, R. & WEINBERG, R. A. 2009. The basics of epithelial-mesenchymal transition. *J Clin Invest,* 119**,** 1420-8.

KANNAN, A., KRISHNAN, A., ALI, M., SUBRAMANIAM, S., HALAGOWDER, D. & SIVASITHAMPARAM, N. D. 2013. Caveolin-1 promotes gastric cancer progression by up-regulating epithelial to mesenchymal transition by crosstalk of signalling mechanisms under hypoxic condition. *Eur J Cancer*.

KARPIEVITCH, Y. V., POLPITIYA, A. D., ANDERSON, G. A., SMITH, R. D. & DABNEY, A. R. 2010. Liquid Chromatography Mass Spectrometry-Based Proteomics: Biological and Technological Aspects. *Ann Appl Stat,* 4**,** 1797-1823.

KATAOKA, H. 2009. EGFR ligands and their signaling scissors, ADAMs, as new molecular targets for anticancer treatments. *Journal of Dermatological Science,* 56**,** 148-153.

KE, Q. & COSTA, M. 2006. Hypoxia-inducible factor-1 (HIF-1). *Molecular pharmacology,* 70**,** 1469-80.

KESKIN, O. 2007. Binding induced conformational changes of proteins correlate with their intrinsic fluctuations: a case study of antibodies. *BMC Structural Biology,* 7**,** 1-11.

KILIC-EREN, M., BOYLU, T. & TABOR, V. 2013. Targeting PI3K/Akt represses Hypoxia inducible factor-1α activation and sensitizes Rhabdomyosarcoma and Ewing's sarcoma cells for apoptosis. *Cancer Cell International,* 13**,** 1-8.

KIM, T., VERONESE, A., PICHIORRI, F., LEE, T. J., JEON, Y.-J., VOLINIA, S., PINEAU, P., MARCHIO, A., PALATINI, J., SUH, S.-S., ALDER, H., LIU, C. G., DEJEAN, A. & CROCE, C. M. 2011. p53 regulates epithelial–mesenchymal transition through microRNAs targeting ZEB1 and ZEB2. *The Journal of Experimental Medicine,* 208**,** 875-883.

KIM, Y. & MARUKI, T. 2011. Hitchhiking effect of a beneficial mutation spreading in a subdivided population. *Genetics,* 189**,** 213-26.

KIRKIN, V., CAHUZAC, N., GUARDIOLA-SERRANO, F., HUAULT, S., LUCKERATH, K., FRIEDMANN, E., NOVAC, N., WELS, W. S., MARTOGLIO, B., HUEBER, A. O. & ZORNIG, M. 2007. The Fas ligand intracellular domain is released by ADAM10 and SPPL2a cleavage in T-cells. *Cell Death Differ,* 14**,** 1678-87.

KLEIN, T. & BISCHOFF, R. 2011. Active metalloproteases of the A Disintegrin and Metalloprotease (ADAM) family: biological function and structure. *J Proteome Res,* 10**,** 17-33.

KNÖSEL, T., EMDE, A., SCHLÜNS, K., CHEN, Y., JÜRCHOTT, K., KRAUSE, M., DIETEL, M. & PETERSEN, I. 2005. Immunoprofiles of 11 Biomarkers Using Tissue Microarrays Identify Prognostic Subgroups in Colorectal Cancer. *Neoplasia (New York, N.Y.),* 7**,** 741-747.

KOCOGLU, H., VELIBEYOGLU, F. M., KARACA, M. & TURAL, D. 2016. Clinical efficacy and drug resistance of anti-epidermal growth factor receptor therapy in colorectal cancer. *World J Gastrointest Oncol,* 8**,** 1-7.

KONG, S., WEI, Q., AMOS, C. I., LYNCH, P. M., LEVIN, B., ZONG, J. & FRAZIER, M. L. 2001. Cyclin D1 Polymorphism and Increased Risk of Colorectal Cancer at Young Age. *Journal of the National Cancer Institute,* 93**,** 1106-1108.

KOONG, A. C., MEHTA, V. K., LE, Q. T., FISHER, G. A., TERRIS, D. J., BROWN, J. M., BASTIDAS, A. J. & VIERRA, M. 2000. Pancreatic tumors show high levels of hypoxia. *Int J Radiat Oncol Biol Phys,* 48**,** 919-22.

KOPITZ, C., GERG, M., BANDAPALLI, O. R., ISTER, D., PENNINGTON, C. J., HAUSER, S., FLECHSIG, C., KRELL, H. W., ANTOLOVIC, D., BREW, K., NAGASE, H., STANGL, M., VON WEYHERN, C. W., BRUCHER, B. L., BRAND, K., COUSSENS, L. M., EDWARDS, D. R. & KRUGER, A. 2007. Tissue inhibitor of metalloproteinases-1 promotes liver metastasis by induction of hepatocyte growth factor signaling. *Cancer Res,* 67**,** 8615-23.

KORNFELD, J. W., MEDER, S., WOHLBERG, M., FRIEDRICH, R. E., RAU, T., RIETHDORF, L., LONING, T., PANTEL, K. & RIETHDORF, S. 2011. Overexpression of TACE and TIMP3 mRNA in head and neck cancer: association with tumour development and progression. *Br J Cancer,* 104**,** 138-45.

KOWALSKI, P. J., RUBIN, M. A. & KLEER, C. G. 2003. E-cadherin expression in primary carcinomas of the breast and its distant metastases. *Breast Cancer Research,* 5**,** R217-R222.

KRAMER, N., WALZL, A., UNGER, C., ROSNER, M., KRUPITZA, G., HENGSTSCHLÄGER, M. & DOLZNIG, H. 2013. In vitro cell migration and invasion assays. *Mutation Research/Reviews in Mutation Research,* 752**,** 10-24.

KRESS, T. R., RAABE, T. & FELLER, S. M. 2010. High Erk activity suppresses expression of the cell cycle inhibitor p27Kip1 in colorectal cancer cells. *Cell Communication and Signaling,* 8**,** 1-7.

KROEPIL, F., FLUEGEN, G., VALLBÖHMER, D., BALDUS, S. E., DIZDAR, L., RAFFEL, A. M., HAFNER, D., STOECKLEIN, N. H. & KNOEFEL, W. T. 2013. Snail1 expression in colorectal cancer and its correlation with clinical and pathological parameters. *BMC Cancer,* 13**,** 1-9.

KUNZ, M. & IBRAHIM, S. M. 2003. Molecular responses to hypoxia in tumor cells. *Mol Cancer,* 2**,** 23.

KWON, D. S., KWON, C. H., KIM, J. H., WOO, J. S., JUNG, J. S. & KIM, Y. K. 2006. Signal transduction of MEK/ERK and PI3K/Akt activation by hypoxia/reoxygenation in renal epithelial cells. *European Journal of Cell Biology,* 85**,** 1189-1199.

LAMOUILLE, S., XU, J. & DERYNCK, R. 2014. Molecular mechanisms of epithelial-mesenchymal transition. *Nat Rev Mol Cell Biol,* 15**,** 178-96.

LAO, V. V. & GRADY, W. M. 2011. Epigenetics and colorectal cancer. *Nat Rev Gastroenterol Hepatol,* 8**,** 686-700.

LE GALL, S. M., MARETZKY, T., ISSUREE, P. D., NIU, X. D., REISS, K., SAFTIG, P., KHOKHA, R., LUNDELL, D. & BLOBEL, C. P. 2010. ADAM17 is regulated by a rapid and reversible mechanism that controls access to its catalytic site. *J Cell Sci,* 123**,** 3913-22.

LEE, J. G. & WU, R. 2015. Erlotinib-cisplatin combination inhibits growth and angiogenesis through c-MYC and HIF-1alpha in EGFR-mutated lung cancer in vitro and in vivo. *Neoplasia,* 17**,** 190-200.

LEE, K. S., KWAK, Y., NAM, K. H., KIM, D.-W., KANG, S.-B., CHOE, G., KIM, W. H. & LEE, H. S. 2015a. <italic>c-MYC</italic> Copy-Number Gain Is an Independent Prognostic Factor in Patients with Colorectal Cancer. *PLoS ONE,* 10**,** e0139727.

LEE, S. C., KIM, O.-H., LEE, S. K. & KIM, S.-J. 2015b. IWR-1 inhibits epithelial-mesenchymal transition of colorectal cancer cells through suppressing Wnt/β-catenin signaling as well as survivin expression. *Oncotarget,* 6**,** 27146-27159.

LEFLOCH, R., POUYSSEGUR, J. & LENORMAND, P. 2008. Single and combined silencing of ERK1 and ERK2 reveals their positive contribution to growth signaling depending on their expression levels. *Mol Cell Biol,* 28**,** 511-27.

LEMIEUX, E., CAGNOL, S., BEAUDRY, K., CARRIER, J. & RIVARD, N. 2015. Oncogenic KRAS signalling promotes the Wnt/beta-catenin pathway through LRP6 in colorectal cancer. *Oncogene,* 34**,** 4914-27.

LENDECKEL, U., KOHL, J., ARNDT, M., CARL-MCGRATH, S., DONAT, H. & ROCKEN, C. 2005. Increased expression of ADAM family members in human breast cancer and breast cancer cell lines. *J Cancer Res Clin Oncol,* 131**,** 41-8.

LEONARD, JENNIFER D., LIN, F. & MILLA, MARCOS E. 2005. Chaperone-like properties of the prodomain of TNFα-converting enzyme (TACE) and the functional role of its cysteine switch. *Biochemical Journal,* 387**,** 797-805.

LEONTIEVA, O. V., NATARAJAN, V., DEMIDENKO, Z. N., BURDELYA, L. G., GUDKOV, A. V. & BLAGOSKLONNY, M. V. 2012. Hypoxia suppresses conversion from proliferative arrest to cellular senescence. *Proc Natl Acad Sci U S A,* 109**,** 13314-8.

LI, C., QI, L., BELLAIL, A. C., HAO, C. & LIU, T. 2014a. PD-0332991 induces G1 arrest of colorectal carcinoma cells through inhibition of the cyclin-dependent kinase-6 and retinoblastoma protein axis. *Oncology Letters,* 7**,** 1673-1678.

LI, H. T., LU, Y. Y., AN, Y. X., WANG, X. & ZHAO, Q. C. 2011. KRAS, BRAF and PIK3CA mutations in human colorectal cancer: relationship with metastatic colorectal cancer. *Oncol Rep,* 25**,** 1691-7.

LI, J., TENG, Y., LIU, S., WANG, Z., CHEN, Y., ZHANG, Y., XI, S., XU, S., WANG, R. & ZOU, X. 2015a. Cinnamaldehyde affects the biological behavior of human colorectal cancer cells and induces apoptosis via inhibition of the PI3K/Akt signaling pathway. *Oncol Rep*.

LI, M., TAN, J., MIAO, Y., LEI, P. & ZHANG, Q. 2015b. The dual role of autophagy under hypoxia-involvement of interaction between autophagy and apoptosis. *Apoptosis,* 20**,** 769-77.

LI, Y., WEI, J., XU, C., ZHAO, Z. & YOU, T. 2014b. Prognostic Significance of Cyclin D1 Expression in Colorectal Cancer: A Meta-Analysis of Observational Studies. *PLoS ONE,* 9**,** e94508.

LI, Z., WANG, H., WANG, Z. & CAI, H. 2015c. MiR-195 inhibits the proliferation of human cervical cancer cells by directly targeting cyclin D1. *Tumour Biol*.

LIANG, C.-C., PARK, A. Y. & GUAN, J.-L. 2007. In vitro scratch assay: a convenient and inexpensive method for analysis of cell migration in vitro. *Nat. Protocols,* 2**,** 329-333.

LIANG, H., YANG, C. X., ZHANG, B., WANG, H. B., LIU, H. Z., LAI, X. H., LIAO, M. J. & ZHANG, T. 2015. Sevoflurane suppresses hypoxia-induced growth and metastasis of lung cancer cells via inhibiting hypoxia-inducible factor-1alpha. *J Anesth,* 29**,** 821-30.

LIM, E. J., JOUNG, Y. H., JUNG, S. M., PARK, S. H., PARK, J. H., KIM, S. Y., HWANG, T. S., HONG, D. Y., CHUNG, S. C., YE, S. K., MOON, E. S., PARK, E. U., PARK, T., CHUNG, I. M. & YANG, Y. M. 2010. Hemin inhibits cyclin D1 and IGF-1 expression via STAT5b under hypoxia in ERalpha-negative MDA-MB 231 breast cancer cells. *Int J Oncol,* 36**,** 1243-51.

LIM, J. H., CHUN, Y. S. & PARK, J. W. 2008. Hypoxia-inducible factor-1alpha obstructs a Wnt signaling pathway by inhibiting the hARD1-mediated activation of beta-catenin. *Cancer Res,* 68**,** 5177-84.

LIM, S. O., LI, C. W., XIA, W., LEE, H. H., CHANG, S. S., SHEN, J., HSU, J. L., RAFTERY, D., DJUKOVIC, D., GU, H., CHANG, W. C., WANG, H. L., CHEN, M. L., HUO, L., CHEN, C. H., WU, Y., SAHIN, A., HANASH, S. M., HORTOBAGYI, G. N. & HUNG, M. C. 2016. EGFR signaling enhances aerobic glycolysis in triple negative breast cancer cells to promote tumor growth and immune escape. *Cancer Res*.

LIM, Y. P. 2005. Mining the tumor phosphoproteome for cancer markers. *Clin Cancer Res,* 11**,** 3163-9.

LIN, P., SUN, X., FENG, T., ZOU, H., JIANG, Y., LIU, Z., ZHAO, D. & YU, X. 2012. ADAM17 regulates prostate cancer cell proliferation through mediating cell cycle progression by EGFR/PI3K/AKT pathway. *Mol Cell Biochem,* 359**,** 235-43.

LIOTTA, L. A. & KOHN, E. C. 2001. The microenvironment of the tumour-host interface. *Nature,* 411**,** 375-9.

LIU, H.-L., LIU, D., DING, G.-R., LIAO, P.-F. & ZHANG, J.-W. 2015a. Hypoxia-inducible factor-1α and Wnt/β-catenin signaling pathways promote the invasion of hypoxic gastric cancer cells. *Molecular Medicine Reports,* 12**,** 3365-3373.

LIU, L., ZHANG, H., SUN, L., GAO, Y., JIN, H., LIANG, S., WANG, Y., DONG, M., SHI, Y., LI, Z. & FAN, D. 2010. ERK/MAPK activation involves hypoxia-induced MGr1-Ag/37LRP expression and contributes to apoptosis resistance in gastric cancer. *International Journal of Cancer,* 127**,** 820-829.

LIU, P. C., LIU, X., LI, Y., COVINGTON, M., WYNN, R., HUBER, R., HILLMAN, M., YANG, G., ELLIS, D., MARANDO, C., KATIYAR, K., BRADLEY, J., ABREMSKI, K., STOW, M., RUPAR, M., ZHUO, J., LI, Y. L., LIN, Q., BURNS, D., XU, M., ZHANG, C., QIAN, D. Q., HE, C., SHARIEF, V., WENG, L., AGRIOS, C., SHI, E., METCALF, B., NEWTON, R., FRIEDMAN, S., YAO, W., SCHERLE, P., HOLLIS, G. & BURN, T. C. 2006. Identification of ADAM10 as a major source of HER2 ectodomain sheddase activity in HER2 overexpressing breast cancer cells. *Cancer Biol Ther,* 5**,** 657-64.

LIU, S., ZHANG, W., LIU, K., JI, B. & WANG, G. 2015b. Silencing ADAM10 inhibits the in vitro and in vivo growth of hepatocellular carcinoma cancer cells. *Mol Med Rep,* 11**,** 597-602.

LIU, Y., WU, C., WANG, Y., WEN, S., WANG, J., CHEN, Z., HE, Q. & FENG, D. 2014. MicroRNA-145 inhibits cell proliferation by directly targeting ADAM17 in hepatocellular carcinoma. *Oncol Rep,* 32**,** 1923-30.

LIU, Z., ZHU, G., GETZENBERG, R. H. & VELTRI, R. W. 2015c. The Upregulation of PI3K/Akt and MAP Kinase Pathways is Associated with Resistance of Microtubule-Targeting Drugs in Prostate Cancer. *J Cell Biochem,* 116**,** 1341-9.

LOGAN, J. E., MOSTOFIZADEH, N., DESAI, A. J., E, V. O. N. E., CONKLIN, D., KONKANKIT, V., HAMIDI, H., ECKARDT, M., ANDERSON, L., CHEN, H. W., GINTHER, C., TASCHEREAU, E., BUI, P. H., CHRISTENSEN, J. G., BELLDEGRUN, A. S., SLAMON, D. J. & KABBINAVAR, F. F. 2013. PD-0332991, a potent and selective inhibitor of cyclin-dependent kinase 4/6, demonstrates inhibition of proliferation in renal cell carcinoma at nanomolar concentrations and molecular markers predict for sensitivity. *Anticancer Res,* 33**,** 2997-3004.

LOO, J. A. 2000. Electrospray ionization mass spectrometry: a technology for studying noncovalent macromolecular complexes. *International Journal of Mass Spectrometry,* 200**,** 175-186.

LORUSSO, G. & RUEGG, C. 2008. The tumor microenvironment and its contribution to tumor evolution toward metastasis. *Histochem Cell Biol,* 130**,** 1091-103.

LU, X. & KANG, Y. 2010. Hypoxia and hypoxia-inducible factors: master regulators of metastasis. *Clin Cancer Res,* 16**,** 5928-35.

LUDWIG, A., HUNDHAUSEN, C., LAMBERT, M. H., BROADWAY, N., ANDREWS, R. C., BICKETT, D. M., LEESNITZER, M. A. & BECHERER, J. D. 2005. Metalloproteinase inhibitors for the disintegrin-like metalloproteinases ADAM10 and ADAM17 that differentially block constitutive and phorbol ester-inducible shedding of cell surface molecules. *Comb Chem High Throughput Screen,* 8**,** 161-71.

LUNN, C. A., FAN, X., DALIE, B., MILLER, K., ZAVODNY, P. J., NARULA, S. K. & LUNDELL, D. 1997. Purification of ADAM 10 from bovine spleen as a TNFalpha convertase. *FEBS Lett,* 400**,** 333-5.

LUPINI, L., BASSI, C., MLCOCHOVA, J., MUSA, G., RUSSO, M., VYCHYTILOVA-FALTEJSKOVA, P., SVOBODA, M., SABBIONI, S., NEMECEK, R., SLABY, O. & NEGRINI, M. 2015. Prediction of response to anti-EGFR antibody-based therapies by multigene sequencing in colorectal cancer patients. *BMC Cancer,* 15**,** 808.

LV, X., LI, Y., QIAN, M., MA, C., JING, H., WEN, Z. & QIAN, D. 2014. ADAM17 silencing suppresses the migration and invasion of non-small cell lung cancer. *Mol Med Rep,* 9**,** 1935-40.

LV, X. J., ZHAO, L. J., HAO, Y. Q., SU, Z. Z., LI, J. Y., DU, Y. W. & ZHANG, J. 2015. Schisandrin B inhibits the proliferation of human lung adenocarcinoma A549 cells by inducing cycle arrest and apoptosis. *Int J Clin Exp Med,* 8**,** 6926-36.

LYNCH, J., KELLER, M., GUO, R.-J., YANG, D. & TRABER, P. 2015. Cdx1 inhibits the proliferation of human colon cancer cells by reducing cyclin D1 gene expression. *Oncogene,* 22**,** 6395-6407.

LYNCH, P. M., MORRIS, J. S., WEN, S., ADVANI, S. M., ROSS, W., CHANG, G. J., RODRIGUEZ-BIGAS, M., RAJU, G. S., RICCIARDIELLO, L., IWAMA, T., ROSSI, B. M., PELLISE, M., STOFFEL, E., WISE, P. E., BERTARIO, L., SAUNDERS, B., BURT, R., BELLUZZI, A., AHNEN, D., MATSUBARA, N., BÜLOW, S., JESPERSEN, N., CLARK, S. K., ERDMAN, S., MARKOWITZ, A. J., BERNSTEIN,

I., DE HAAS, N., SYNGAL, S. & MOESLEIN, G. 2016. A proposed staging system and stage-specific interventions for familial adenomatous polyposis. *Gastrointestinal Endoscopy*.

MA, Y., LIANG, D., LIU, J., AXCRONA, K., KVALHEIM, G., STOKKE, T., NESLAND, J. M. & SUO, Z. 2011. Prostate Cancer Cell Lines under Hypoxia Exhibit Greater Stem-Like Properties. *PLoS ONE,* 6**,** e29170.

MACDONALD, B. T., TAMAI, K. & HE, X. 2009. Wnt/beta-catenin signaling: components, mechanisms, and diseases. *Dev Cell,* 17**,** 9-26.

MAGALHAES, B., PELETEIRO, B. & LUNET, N. 2012. Dietary patterns and colorectal cancer: systematic review and meta-analysis. *Eur J Cancer Prev,* 21**,** 15-23.

MANDL, M., KAPELLER, B., LIEBER, R. & MACFELDA, K. 2013. Hypoxia-inducible factor-1beta (HIF-1beta) is upregulated in a HIF-1alpha-dependent manner in 518A2 human melanoma cells under hypoxic conditions. *Biochemical and biophysical research communications*.

MANN, C. D., BASTIANPILLAI, C., NEAL, C. P., MASOOD, M. M., JONES, D. J., TEICHERT, F., SINGH, R., KARPOVA, E., BERRY, D. P. & MANSON, M. M. 2012. Notch3 and HEY-1 as prognostic biomarkers in pancreatic adenocarcinoma. *PLoS One,* 7**,** e51119.

MARAMPON, F., GRAVINA, G. L., JU, X., VETUSCHI, A., SFERRA, R., CASIMIRO, M. C., POMPILI, S., FESTUCCIA, C., COLAPIETRO, A., GAUDIO, E., DI CESARE, E., TOMBOLINI, V. & PESTELL, R. G. 2015. Cyclin D1 silencing suppresses tumorigenicity, impairs DNA double strand break repair and thus radiosensitizes androgenindependent prostate cancer cells to DNA damage. *Oncotarget*.

MARCELLO, E., GARDONI, F., DI LUCA, M. & PEREZ-OTANO, I. 2010. An arginine stretch limits ADAM10 exit from the endoplasmic reticulum. *J Biol Chem,* 285**,** 10376-84.

MARETZKY, T., EVERS, A., LE GALL, S., ALABI, R. O., SPECK, N., REISS, K. & BLOBEL, C. P. 2015. The cytoplasmic domain of a disintegrin and metalloproteinase 10 (ADAM10) regulates its constitutive activity but is dispensable for stimulated ADAM10-dependent shedding. *J Biol Chem,* 290**,** 7416-25.

MARETZKY, T., EVERS, A., ZHOU, W., SWENDEMAN, S. L., WONG, P. M., RAFII, S., REISS, K. & BLOBEL, C. P. 2011. Migration of growth factor-stimulated epithelial and endothelial cells depends on EGFR transactivation by ADAM17. *Nat Commun,* 2**,** 229.

MARETZKY, T., REISS, K., LUDWIG, A., BUCHHOLZ, J., SCHOLZ, F., PROKSCH, E., DE STROOPER, B., HARTMANN, D. & SAFTIG, P. 2005. ADAM10 mediates E-cadherin shedding and regulates epithelial cell-cell adhesion, migration, and beta-catenin translocation. *Proc Natl Acad Sci U S A,* 102**,** 9182-7.

MARETZKY, T., SCHOLZ, F., KOTEN, B., PROKSCH, E., SAFTIG, P. & REISS, K. 2008. ADAM10-mediated E-cadherin release is regulated by proinflammatory cytokines and modulates keratinocyte cohesion in eczematous dermatitis. *J Invest Dermatol,* 128**,** 1737-46.

MARSHALL, A. J., RATTRAY, M. & VAUGHAN, P. F. 2006. Chronic hypoxia in the human neuroblastoma SH-SY5Y causes reduced expression of the putative alpha-secretases, ADAM10 and TACE, without altering their mRNA levels. *Brain Res,* 1099**,** 18-24.

MASSAT, N. J., MOSS, S. M., HALLORAN, S. P. & DUFFY, S. W. 2013. Screening and primary prevention of colorectal cancer: a review of sex-specific and site-specific differences. *J Med Screen,* 20**,** 125-48.

MATHEW, R., KARANTZA-WADSWORTH, V. & WHITE, E. 2007. Role of autophagy in cancer. *Nat Rev Cancer,* 7**,** 961-7.

MATHIAS, R. A., GOPAL, S. K. & SIMPSON, R. J. 2013. Contribution of cells undergoing epithelial-mesenchymal transition to the tumour microenvironment. *J Proteomics,* 78**,** 545-57.

MATTOON, D. R., LAMOTHE, B., LAX, I. & SCHLESSINGER, J. 2004. The docking protein Gab1 is the primary mediator of EGF-stimulated activation of the PI-3K/Akt cell survival pathway. *BMC Biology,* 2**,** 1-12.

MAZUMDAR, J., O'BRIEN, W. T., JOHNSON, R. S., LAMANNA, J. C., CHAVEZ, J. C., KLEIN, P. S. & SIMON, M. C. 2010. O2 regulates stem cells through Wnt/beta-catenin signalling. *Nat Cell Biol,* 12**,** 1007-13.

MBEUNKUI, F. & JOHANN, D. J., JR. 2009. Cancer and the tumor microenvironment: a review of an essential relationship. *Cancer Chemother Pharmacol,* 63**,** 571-82.

MCCUBREY, J. A., STEELMAN, L. S., CHAPPELL, W. H., ABRAMS, S. L., WONG, E. W. T., CHANG, F., LEHMANN, B., TERRIAN, D. M., MILELLA, M., TAFURI, A., STIVALA, F., LIBRA, M., BASECKE, J., EVANGELISTI, C., MARTELLI, A. M. & FRANKLIN, R. A. 2007. ROLES OF THE RAF/MEK/ERK PATHWAY IN CELL GROWTH, MALIGNANT TRANSFORMATION AND DRUG RESISTANCE. *Biochimica et biophysica acta,* 1773**,** 1263-1284.

MCCULLOCH, D. R., AKL, P., SAMARATUNGA, H., HERINGTON, A. C. & ODORICO, D. M. 2004. Expression of the disintegrin metalloprotease, ADAM-10, in prostate cancer and its regulation by dihydrotestosterone, insulin-like growth factor I, and epidermal growth factor in the prostate cancer cell model LNCaP. *Clin Cancer Res,* 10**,** 314-23.

MCGOWAN, P. M., MULLOOLY, M., CAIAZZA, F., SUKOR, S., MADDEN, S. F., MAGUIRE, A. A., PIERCE, A., MCDERMOTT, E. W., CROWN, J., O'DONOVAN, N. & DUFFY, M. J. 2013. ADAM-17: a novel therapeutic target for triple negative breast cancer. *Ann Oncol,* 24**,** 362-9.

MCGOWAN, P. M., RYAN, B. M., HILL, A. D., MCDERMOTT, E., O'HIGGINS, N. & DUFFY, M. J. 2007. ADAM-17 expression in breast cancer correlates with variables of tumor progression. *Clin Cancer Res,* 13**,** 2335-43.

MEDICI, D., HAY, E. D. & GOODENOUGH, D. A. 2006a. Cooperation between snail and LEF-1 transcription factors is essential for TGF-beta1-induced epithelial-mesenchymal transition. *Mol Biol Cell,* 17**,** 1871-9.

MEDICI, D., HAY, E. D. & GOODENOUGH, D. A. 2006b. Cooperation between Snail and LEF-1 Transcription Factors Is Essential for TGF-β1-induced Epithelial-Mesenchymal Transition. *Molecular Biology of the Cell,* 17**,** 1871-1879.

MEDICI, D., HAY, E. D. & OLSEN, B. R. 2008. Snail and Slug Promote Epithelial-Mesenchymal Transition through β-Catenin–T-Cell Factor-4-dependent Expression of Transforming Growth Factor-β3. *Molecular Biology of the Cell,* 19**,** 4875-4887.

MEHTA, M., KHAN, A., DANISH, S., HAFFTY, B. G. & SABAAWY, H. E. 2015. Radiosensitization of Primary Human Glioblastoma Stem-like Cells with Low-Dose AKT Inhibition. *Mol Cancer Ther,* 14**,** 1171-80.

MELLACHERUVU, D., WRIGHT, Z., COUZENS, A. L., LAMBERT, J. P., ST-DENIS, N. A., LI, T., MITEVA, Y. V., HAURI, S., SARDIU, M. E., LOW, T. Y., HALIM, V. A., BAGSHAW, R. D., HUBNER, N. C., AL-HAKIM, A., BOUCHARD, A., FAUBERT, D., FERMIN, D., DUNHAM, W. H., GOUDREAULT, M., LIN, Z. Y., BADILLO, B. G., PAWSON, T., DUROCHER, D., COULOMBE, B., AEBERSOLD, R., SUPERTI-FURGA, G., COLINGE, J., HECK, A. J., CHOI, H., GSTAIGER, M., MOHAMMED, S., CRISTEA, I. M., BENNETT, K. L., WASHBURN, M. P., RAUGHT, B., EWING, R. M., GINGRAS, A. C. & NESVIZHSKII, A. I. 2013. The CRAPome: a contaminant repository for affinity purification-mass spectrometry data. *Nat Methods,* 10**,** 730-6.

MERCHANT, N. B., VOSKRESENSKY, I., ROGERS, C. M., LAFLEUR, B., DEMPSEY, P. J., GRAVES-DEAL, R., REVETTA, F., FOUTCH, A. C., ROTHENBERG, M. L., WASHINGTON, M. K. & COFFEY, R. J. 2008. TACE/ADAM-17: a component of the epidermal growth factor receptor axis and a promising therapeutic target in colorectal cancer. *Clin Cancer Res,* 14**,** 1182-91.

MĘŻYK-KOPEĆ, R., BZOWSKA, M., STALIŃSKA, K., CHEŁMICKI, T., PODKALICKI, M., JUCHA, J., KOWALCZYK, K., MAK, P. & BERETA, J. 2009. Identification of ADAM10 as a major TNF sheddase in ADAM17-deficient fibroblasts. *Cytokine,* 46**,** 309-315.

MILLA, M. E., GONZALES, P. E. & LEONARD, J. D. 2006. The TACE zymogen: re-examining the role of the cysteine switch. *Cell Biochem Biophys,* 44**,** 342-8.

MILLER, D. M., THOMAS, S. D., ISLAM, A., MUENCH, D. & SEDORIS, K. 2012. c-Myc and cancer metabolism. *Clin Cancer Res,* 18**,** 5546-53.

MINDER, P., BAYHA, E., BECKER-PAULY, C. & STERCHI, E. E. 2012. Meprinalpha transactivates the epidermal growth factor receptor (EGFR) via ligand shedding, thereby enhancing colorectal cancer cell proliferation and migration. *J Biol Chem,* 287**,** 35201-11.

MIZOKAMI, K., KAKEJI, Y., ODA, S. & MAEHARA, Y. 2006. Relationship of hypoxia-inducible factor 1α and p21WAF1/CIP1 expression to cell apoptosis and clinical outcome in patients with gastric cancer. *World Journal of Surgical Oncology,* 4**,** 1-7.

MOCHIZUKI, S. & OKADA, Y. 2007. ADAMs in cancer cell proliferation and progression. *Cancer Sci,* 98**,** 621-8.

MOLLER, P., SEPPALA, T., BERNSTEIN, I., HOLINSKI-FEDER, E., SALA, P., EVANS, D. G., LINDBLOM, A., MACRAE, F., BLANCO, I., SIJMONS, R., JEFFRIES, J., VASEN, H., BURN, J., NAKKEN, S., HOVIG, E., RODLAND, E. A., THARMARATNAM, K., DE VOS TOT NEDERVEEN CAPPEL, W. H., HILL, J., WIJNEN, J., GREEN, K., LALLOO, F., SUNDE, L., MINTS, M., BERTARIO, L., PINEDA, M., NAVARRO, M., MORAK, M., RENKONEN-SINISALO, L., FRAYLING, I. M., PLAZZER, J. P., PYLVANAINEN, K., SAMPSON, J. R., CAPELLA, G., MECKLIN, J. P. & MOSLEIN, G. 2015. Cancer incidence and survival in Lynch syndrome patients receiving colonoscopic and gynaecological surveillance: first report from the prospective Lynch syndrome database. *Gut*.

MORIN, P. J., SPARKS, A. B., KORINEK, V., BARKER, N., CLEVERS, H., VOGELSTEIN, B. & KINZLER, K. W. 1997. Activation of beta-catenin-Tcf signaling in colon cancer by mutations in beta-catenin or APC. *Science,* 275**,** 1787-90.

MORIYAMA, H., MORIYAMA, M., ISSHI, H., ISHIHARA, S., OKURA, H., ICHINOSE, A., OZAWA, T., MATSUYAMA, A. & HAYAKAWA, T. 2014. Role of notch signaling in the maintenance of human mesenchymal stem cells under hypoxic conditions. *Stem Cells Dev,* 23**,** 2211-24.

MOSS, M. L., BOMAR, M., LIU, Q., SAGE, H., DEMPSEY, P., LENHART, P. M., GILLISPIE, P. A., STOECK, A., WILDEBOER, D., BARTSCH, J. W., PALMISANO, R. & ZHOU, P. 2007. The ADAM10 prodomain is a specific inhibitor of ADAM10 proteolytic activity and inhibits cellular shedding events. *J Biol Chem,* 282**,** 35712-21.

MOSS, M. L., JIN, S. L., MILLA, M. E., BICKETT, D. M., BURKHART, W., CARTER, H. L., CHEN, W. J., CLAY, W. C., DIDSBURY, J. R., HASSLER, D., HOFFMAN, C. R., KOST, T. A., LAMBERT, M. H., LEESNITZER, M. A., MCCAULEY, P., MCGEEHAN, G., MITCHELL, J., MOYER, M., PAHEL, G., ROCQUE, W., OVERTON, L. K., SCHOENEN, F., SEATON, T., SU, J. L., BECHERER, J. D. & ET AL. 1997. Cloning of a disintegrin metalloproteinase that processes precursor tumour-necrosis factor-alpha. *Nature,* 385**,** 733-6.

MOSS, M. L., POWELL, G., MILLER, M. A., EDWARDS, L., QI, B., SANG, Q.-X. A., DE STROOPER, B., TESSEUR, I., LICHTENTHALER, S. F., TAVERNA, M., ZHONG, J. L., DINGWALL, C., FERDOUS, T., SCHLOMANN, U., ZHOU, P., GRIFFITH, L. G., LAUFFENBURGER, D. A., PETROVICH, R. & BARTSCH, J. W. 2011. ADAM9 Inhibition Increases Membrane Activity of ADAM10 and Controls α-Secretase Processing of Amyloid Precursor Protein. *Journal of Biological Chemistry,* 286**,** 40443-40451.

MOVSAS, B., CHAPMAN, J. D., HANLON, A. L., HORWITZ, E. M., PINOVER, W. H., GREENBERG, R. E., STOBBE, C. & HANKS, G. E. 2001. Hypoxia in human prostate carcinoma: an Eppendorf PO2 study. *Am J Clin Oncol,* 24**,** 458-61.

MU, D. W., GUO, H. Q., ZHOU, G. B., LI, J. Y. & SU, B. 2015. Oleanolic acid suppresses the proliferation of human bladder cancer by Akt/mTOR/S6K and ERK1/2 signaling. *Int J Clin Exp Pathol,* 8**,** 13864-70.

MULLOOLY, M., MCGOWAN, P. M., KENNEDY, S. A., MADDEN, S. F., CROWN, J., N, O. D. & DUFFY, M. J. 2015. ADAM10: a new player in breast cancer progression? *Br J Cancer,* 113**,** 945-51.

MUNSHI, A., HOBBS, M. & MEYN, R. E. 2005. Clonogenic cell survival assay. *Methods Mol Med,* 110**,** 21-8.

MURPHY, G. 2008. The ADAMs: signalling scissors in the tumour microenvironment. *Nature reviews. Cancer,* 8**,** 929-41.

NAGANO, O., MURAKAMI, D., HARTMANN, D., DE STROOPER, B., SAFTIG, P., IWATSUBO, T., NAKAJIMA, M., SHINOHARA, M. & SAYA, H. 2004. Cell–matrix interaction via CD44 is independently regulated by different metalloproteinases activated in response to extracellular Ca(2+) influx and PKC activation. *The Journal of Cell Biology,* 165**,** 893-902.

NAGARAJU, G. P., BRAMHACHARI, P. V., RAGHU, G. & EL-RAYES, B. F. 2015. Hypoxia inducible factor-1alpha: Its role in colorectal carcinogenesis and metastasis. *Cancer Lett,* 366**,** 11-8.

NEUMANN, U., KUBOTA, H., FREI, K., GANU, V. & LEPPERT, D. 2004. Characterization of Mca-Lys-Pro-Leu-Gly-Leu-Dpa-Ala-Arg-NH2, a fluorogenic substrate with increased specificity constants for collagenases and tumor necrosis factor converting enzyme. *Anal Biochem,* 328**,** 166-73.

NICASTRI, A., GASPARI, M., SACCO, R., ELIA, L., GABRIELE, C., ROMANO, R., RIZZUTO, A. & CUDA, G. 2014. N-Glycoprotein Analysis Discovers New Up-Regulated Glycoproteins in Colorectal Cancer Tissue. *Journal of Proteome Research,* 13**,** 4932-4941.

NICE. 2011. *Colorectal cancer: diagnosis and management* [Online]. NICE. Available: http://www.nice.org.uk/guidance/cg131 [Accessed 26/01/2016.

NIEHRS, C. 2012. The complex world of WNT receptor signalling. *Nat Rev Mol Cell Biol,* 13**,** 767-79.

NISHIMURA, T., NAKAMURA, K., YAMASHITA, S., IKEDA, S., KIGURE, K. & MINEGISHI, T. 2015. Effect of the molecular targeted drug, erlotinib, against endometrial cancer expressing high levels of epidermal growth factor receptor. *BMC Cancer,* 15**,** 957.

NORDSMARK, M., LONCASTER, J., AQUINO-PARSONS, C., CHOU, S. C., LADEKARL, M., HAVSTEEN, H., LINDEGAARD, J. C., DAVIDSON, S. E., VARIA, M., WEST, C., HUNTER, R., OVERGAARD, J. & RALEIGH, J. A. 2003. Measurements of hypoxia using pimonidazole and polarographic oxygen-sensitive electrodes in human cervix carcinomas. *Radiother Oncol,* 67**,** 35-44.

NORMANNO, N., DE LUCA, A., BIANCO, C., STRIZZI, L., MANCINO, M., MAIELLO, M. R., CAROTENUTO, A., DE FEO, G., CAPONIGRO, F. & SALOMON, D. S. 2006. Epidermal growth factor receptor (EGFR) signaling in cancer. *Gene,* 366**,** 2-16.

NUNEZ, F., BRAVO, S., CRUZAT, F., MONTECINO, M. & DE FERRARI, G. V. 2011. Wnt/beta-catenin signaling enhances cyclooxygenase-2 (COX2) transcriptional activity in gastric cancer cells. *PLoS One,* 6**,** e18562.

NUNEZ, R. 2001. DNA measurement and cell cycle analysis by flow cytometry. *Curr Issues Mol Biol,* 3**,** 67-70.

O'LEARY, B., FINN, R. S. & TURNER, N. C. 2016. Treating cancer with selective CDK4/6 inhibitors. *Nat Rev Clin Oncol,* advance online publication.

OKUYAMA, H., ENDO, H., AKASHIKA, T., KATO, K. & INOUE, M. 2010. Downregulation of c-MYC protein levels contributes to cancer cell survival under dual deficiency of oxygen and glucose. *Cancer Res,* 70**,** 10213-23.

OLIVE, P. L., VIKSE, C. & TROTTER, M. J. 1992. Measurement of oxygen diffusion distance in tumor cubes using a fluorescent hypoxia probe. *International journal of radiation oncology, biology, physics,* 22**,** 397-402.

OUIDDIR, A., PLANES, C., FERNANDES, I., VANHESSE, A. & CLERICI, C. 1999. Hypoxia upregulates activity and expression of the glucose transporter GLUT1 in alveolar epithelial cells. *Am J Respir Cell Mol Biol,* 21**,** 710-8.

PABLA, B., BISSONNETTE, M. & KONDA, V. J. 2015. Colon cancer and the epidermal growth factor receptor: Current treatment paradigms, the importance of diet, and the role of chemoprevention. *World J Clin Oncol,* 6**,** 133-41.

PABOIS, A., DEVALLIÈRE, J., QUILLARD, T., COULON, F., GÉRARD, N., LABOISSE, C., TOQUET, C. & CHARREAU, B. 2014. The disintegrin and metalloproteinase ADAM10 mediates a canonical Notch-dependent regulation of IL-6 through Dll4 in human endothelial cells. *Biochemical Pharmacology,* 91**,** 510-521.

PAGE, C., HUANG, M., JIN, X., CHO, K., LILJA, J., REYNOLDS, R. K. & LIN, J. 2000. Elevated phosphorylation of AKT and Stat3 in prostate, breast, and cervical cancer cells. *Int J Oncol,* 17**,** 23-8.

PAN, Y., HAN, C., WANG, C., HU, G., LUO, C., GAN, X., ZHANG, F., LU, Y. & DING, X. 2012. ADAM10 promotes pituitary adenoma cell migration by regulating cleavage of CD44 and L1. *J Mol Endocrinol,* 49**,** 21-33.

PAPANDREOU, I., LIM, A. L., LADEROUTE, K. & DENKO, N. C. 2008. Hypoxia signals autophagy in tumor cells via AMPK activity, independent of HIF-1, BNIP3, and BNIP3L. *Cell Death Differ,* 15**,** 1572-81.

PARKIN, D. M. & BOYD, L. 2011. 8. Cancers attributable to overweight and obesity in the UK in 2010. *British Journal of Cancer,* 105**,** S34-S37.

PARKIN, D. M., BOYD, L. & WALKER, L. C. 2011. 16. The fraction of cancer attributable to lifestyle and environmental factors in the UK in 2010. *Br J Cancer,* 105**,** S77-S81.

PARKIN, E. & HARRIS, B. 2009. A disintegrin and metalloproteinase (ADAM)-mediated ectodomain shedding of ADAM10. *J Neurochem,* 108**,** 1464-79.

PARSONS, B. D., SCHINDLER, A., EVANS, D. H. & FOLEY, E. 2009. A Direct Phenotypic Comparison of siRNA Pools and Multiple Individual Duplexes in a Functional Assay. *PLoS ONE,* 4**,** e8471.

PASING, Y., SICKMANN, A. & LEWANDROWSKI, U. 2012. N-glycoproteomics: mass spectrometry-based glycosylation site annotation. *Biol Chem,* 393**,** 249-58.

PECINA-SLAUS, N. 2003. Tumor suppressor gene E-cadherin and its role in normal and malignant cells. *Cancer Cell Int,* 3**,** 17.

PEDDAREDDIGARI, V. G., WANG, D. & DUBOIS, R. N. 2010. The tumor microenvironment in colorectal carcinogenesis. *Cancer Microenviron,* 3**,** 149-66.

PEIGNON, G., DURAND, A., CACHEUX, W., AYRAULT, O., TERRIS, B., LAURENT-PUIG, P., SHROYER, N. F., VAN SEUNINGEN, I., HONJO, T., PERRET, C. & ROMAGNOLO, B. 2011. Complex interplay between beta-catenin signalling and Notch effectors in intestinal tumorigenesis. *Gut,* 60**,** 166-76.

PEIRETTI, F., CANAULT, M., DEPREZ-BEAUCLAIR, P., BERTHET, V., BONARDO, B., JUHAN-VAGUE, I. & NALBONE, G. 2003. Intracellular maturation and transport of tumor necrosis factor alpha converting enzyme. *Exp Cell Res,* 285**,** 278-85.

PESCHON, J. J., SLACK, J. L., REDDY, P., STOCKING, K. L., SUNNARBORG, S. W., LEE, D. C., RUSSELL, W. E., CASTNER, B. J., JOHNSON, R. S., FITZNER, J. N., BOYCE, R. W., NELSON, N., KOZLOSKY, C. J., WOLFSON, M. F., RAUCH, C. T., CERRETTI, D. P., PAXTON, R. J., MARCH, C. J. & BLACK, R. A. 1998. An Essential Role for Ectodomain Shedding in Mammalian Development. *Science,* 282**,** 1281-1284.

PHIPPS, A. I., BUCHANAN, D. D., MAKAR, K. W., WIN, A. K., BARON, J. A., LINDOR, N. M., POTTER, J. D. & NEWCOMB, P. A. 2013. KRAS-mutation status in relation to colorectal cancer survival: the joint impact of correlated tumour markers. *Br J Cancer,* 108**,** 1757-1764.

PINHO, S. S. & REIS, C. A. 2015. Glycosylation in cancer: mechanisms and clinical implications. *Nat Rev Cancer,* 15**,** 540-555.

PIRES, I. M., BENCOKOVA, Z., MILANI, M., FOLKES, L. K., LI, J.-L., STRATFORD, M. R., HARRIS, A. L. & HAMMOND, E. M. 2010. Effects of acute versus chronic hypoxia on DNA damage responses and genomic instability. *Cancer research,* 70**,** 925-935.

POZAROWSKI, P. & DARZYNKIEWICZ, Z. 2004. Analysis of cell cycle by flow cytometry. *Methods Mol Biol,* 281**,** 301-11.

PRINZEN, C., MULLER, U., ENDRES, K., FAHRENHOLZ, F. & POSTINA, R. 2005. Genomic structure and functional characterization of the human ADAM10 promoter. *FASEB J,* 19**,** 1522-4.

PRUESSMEYER, J., HESS, F. M., ALERT, H., GROTH, E., PASQUALON, T., SCHWARZ, N., NYAMOYA, S., KOLLERT, J., VAN DER VORST, E., DONNERS, M., MARTIN, C., UHLIG, S., SAFTIG, P., DREYMUELLER, D. & LUDWIG, A. 2014. Leukocytes require ADAM10 but not ADAM17 for their migration and inflammatory recruitment into the alveolar space. *Blood,* 123**,** 4077-88.

PRZEMYSLAW, L., BOGUSLAW, H. A., ELZBIETA, S. & MALGORZATA, S. M. 2013. ADAM and ADAMTS family proteins and their role in the colorectal cancer etiopathogenesis. *BMB Rep,* 46**,** 139-50.

PUGLISI, M., THAVASU, P., STEWART, A., DE BONO, J. S., O'BRIEN, M. E., POPAT, S., BHOSLE, J. & BANERJI, U. 2014. AKT inhibition synergistically enhances growth-inhibitory effects of gefitinib and increases apoptosis in non-small cell lung cancer cell lines. *Lung Cancer,* 85**,** 141-6.

QIAN, J., LIU, H., CHEN, W., WEN, K., LU, W., HUANG, C. & FU, Z. 2013. Knockdown of Slug by RNAi inhibits the proliferation and invasion of HCT116 colorectal cancer cells. *Mol Med Rep,* 8**,** 1055-9.

QIU, H., TANG, X., MA, J., SHAVERDASHVILI, K., ZHANG, K. & BEDOGNI, B. 2015. Notch1 Autoactivation via Transcriptional Regulation of Furin, Which Sustains Notch1 Signaling by Processing Notch1-Activating Proteases ADAM10 and Membrane Type 1 Matrix Metalloproteinase. *Mol Cell Biol,* 35**,** 3622-32.

RADEMAKERS, S. E., SPAN, P. N., KAANDERS, J. H., SWEEP, F. C., VAN DER KOGEL, A. J. & BUSSINK, J. 2008. Molecular aspects of tumour hypoxia. *Molecular oncology,* 2**,** 41-53.

RADIVOJAC, P., BAENZIGER, P. H., KANN, M. G., MORT, M. E., HAHN, M. W. & MOONEY, S. D. 2008. Gain and loss of phosphorylation sites in human cancer. *Bioinformatics,* 24**,** i241-i247.

RAFEHI, H., ORLOWSKI, C., GEORGIADIS, G. T., VERVERIS, K., EL-OSTA, A. & KARAGIANNIS, T. C. 2011. Clonogenic assay: adherent cells. *J Vis Exp*.

REIMAND, J., WAGIH, O. & BADER, G. D. 2013. The mutational landscape of phosphorylation signaling in cancer. *Sci Rep,* 3**,** 2651.

REISS, K., MARETZKY, T., LUDWIG, A., TOUSSEYN, T., DE STROOPER, B., HARTMANN, D. & SAFTIG, P. 2005. ADAM10 cleavage of N-cadherin and regulation of cell-cell adhesion and beta-catenin nuclear signalling. *EMBO J,* 24**,** 742-52.

REISS, K. & SAFTIG, P. 2009. The "a disintegrin and metalloprotease" (ADAM) family of sheddases: physiological and cellular functions. *Seminars in cell & developmental biology,* 20**,** 126-37.

REVERBERI, R. & REVERBERI, L. 2007. Factors affecting the antigen-antibody reaction. *Blood Transfusion,* 5**,** 227-240.

RICCARDI, C. & NICOLETTI, I. 2006. Analysis of apoptosis by propidium iodide staining and flow cytometry. *Nat Protoc,* 1**,** 1458-61.

RICHARDS, F. M., TAPE, C. J., JODRELL, D. I. & MURPHY, G. 2012. Anti-tumour effects of a specific anti-ADAM17 antibody in an ovarian cancer model in vivo. *PLoS One,* 7**,** e40597.

RIEGER, A. M., NELSON, K. L., KONOWALCHUK, J. D. & BARREDA, D. R. 2011. Modified Annexin V/Propidium Iodide Apoptosis Assay For Accurate Assessment of Cell Death. *Journal of Visualized Experiments : JoVE***,** 2597.

RISS, T. L., MORAVEC, R. A., NILES, A. L., BENINK, H. A., WORZELLA, T. J. & MINOR, L. 2004. Cell Viability Assays. *In:* SITTAMPALAM, G. S., COUSSENS, N. P., NELSON, H., ARKIN, M., AULD, D., AUSTIN, C., BEJCEK, B., GLICKSMAN, M., INGLESE, J., IVERSEN, P. W., LI, Z., MCGEE, J., MCMANUS, O., MINOR, L., NAPPER, A., PELTIER, J. M., RISS, T., TRASK, O. J., JR. & WEIDNER, J. (eds.) *Assay Guidance Manual*. Bethesda MD.

RIVADENEIRA, D. B., MAYHEW, C. N., THANGAVEL, C., SOTILLO, E., REED, C. A., GRANA, X. & KNUDSEN, E. S. 2010. Proliferative suppression by CDK4/6 inhibition: complex function of the retinoblastoma pathway in liver tissue and hepatoma cells. *Gastroenterology,* 138**,** 1920-30.

ROBERTS, P. J. & DER, C. J. 2007. Targeting the Raf-MEK-ERK mitogen-activated protein kinase cascade for the treatment of cancer. *Oncogene,* 26**,** 3291-3310.

ROCHLITZ, C. F., HERRMANN, R. & DE KANT, E. 1996. Overexpression and amplification of c-myc during progression of human colorectal cancer. *Oncology,* 53**,** 448-54.

ROCKS, N., ESTRELLA, C., PAULISSEN, G., QUESADA-CALVO, F., GILLES, C., GUEDERS, M. M., CRAHAY, C., FOIDART, J. M., GOSSET, P., NOEL, A. &

CATALDO, D. D. 2008a. The metalloproteinase ADAM-12 regulates bronchial epithelial cell proliferation and apoptosis. *Cell Prolif,* 41**,** 988-1001.
ROCKS, N., PAULISSEN, G., EL HOUR, M., QUESADA, F., CRAHAY, C., GUEDERS, M., FOIDART, J. M., NOEL, A. & CATALDO, D. 2008b. Emerging roles of ADAM and ADAMTS metalloproteinases in cancer. *Biochimie,* 90**,** 369-79.
ROSENDAHL, M. S., KO, S. C., LONG, D. L., BREWER, M. T., ROSENZWEIG, B., HEDL, E., ANDERSON, L., PYLE, S. M., MORELAND, J., MEYERS, M. A., KOHNO, T., LYONS, D. & LICHENSTEIN, H. S. 1997. Identification and characterization of a pro-tumor necrosis factor-alpha-processing enzyme from the ADAM family of zinc metalloproteases. *J Biol Chem,* 272**,** 24588-93.
ROTH, Z., YEHEZKEL, G. & KHALAILA, I. 2012. Identification and Quantification of Protein Glycosylation. *International Journal of Carbohydrate Chemistry,* 2012**,** 10.
ROUSSELET, E., BENJANNET, S., HAMELIN, J., CANUEL, M. & SEIDAH, N. G. 2011. The proprotein convertase PC7: unique zymogen activation and trafficking pathways. *J Biol Chem,* 286**,** 2728-38.
ROY, H. K., OLUSOLA, B. F., CLEMENS, D. L., KAROLSKI, W. J., RATASHAK, A., LYNCH, H. T. & SMYRK, T. C. 2002. AKT proto-oncogene overexpression is an early event during sporadic colon carcinogenesis. *Carcinogenesis,* 23**,** 201-205.
ROY, R. & MOSES, M. A. 2012. ADAM12 Induces Estrogen Independence in Breast Cancer Cells. *Breast Cancer Research and Treatment,* 131**,** 731-741.
RUBIN, M. A., MUCCI, N. R., FIGURSKI, J., FECKO, A., PIENTA, K. J. & DAY, M. L. 2001. E-cadherin expression in prostate cancer: A broad survey using high-density tissue microarray technology. *Human Pathology,* 32**,** 690-697.
RZYMSKI, T., PETRY, A., KRACUN, D., RIESS, F., PIKE, L., HARRIS, A. L. & GORLACH, A. 2012. The unfolded protein response controls induction and activation of ADAM17/TACE by severe hypoxia and ER stress. *Oncogene,* 31**,** 3621-34.
SAGI, D., KIENZ, P., DENECKE, J., MARQUARDT, T. & PETER-KATALINIC, J. 2005. Glycoproteomics of N-glycosylation by in-gel deglycosylation and matrix-assisted laser desorption/ionisation-time of flight mass spectrometry mapping: application to congenital disorders of glycosylation. *Proteomics,* 5**,** 2689-701.
SAHIN, U., WESKAMP, G., KELLY, K., ZHOU, H. M., HIGASHIYAMA, S., PESCHON, J., HARTMANN, D., SAFTIG, P. & BLOBEL, C. P. 2004. Distinct roles for ADAM10 and ADAM17 in ectodomain shedding of six EGFR ligands. *J Cell Biol,* 164**,** 769-79.
SANDERSON, M. P., ABBOTT, C. A., TADA, H., SENO, M., DEMPSEY, P. J. & DUNBAR, A. J. 2006. Hydrogen peroxide and endothelin-1 are novel activators of betacellulin ectodomain shedding. *J Cell Biochem,* 99**,** 609-23.
SANDERSON, M. P., ERICKSON, S. N., GOUGH, P. J., GARTON, K. J., WILLE, P. T., RAINES, E. W., DUNBAR, A. J. & DEMPSEY, P. J. 2005. ADAM10 mediates ectodomain shedding of the betacellulin precursor activated by p-aminophenylmercuric acetate and extracellular calcium influx. *J Biol Chem,* 280**,** 1826-37.
SANTO, L., SIU, K. T. & RAJE, N. 2015. Targeting Cyclin-Dependent Kinases and Cell Cycle Progression in Human Cancers. *Seminars in Oncology,* 42**,** 788-800.
SATO, Y., MATSUSAKA, S., SUENAGA, M., SHINOZAKI, E. & MIZUNUMA, N. 2015. Cetuximab could be more effective without prior bevacizumab treatment in metastatic colorectal cancer patients. *Onco Targets Ther,* 8**,** 3329-36.
SCHLAGE, P. & AUF DEM KELLER, U. 2015. Proteomic approaches to uncover MMP function. *Matrix Biology,* 44–46**,** 232-238.
SCHLONDORFF, J., BECHERER, J. D. & BLOBEL, C. P. 2000. Intracellular maturation and localization of the tumour necrosis factor alpha convertase (TACE). *Biochem J,* 347 Pt 1**,** 131-8.
SCHULTE, M., REISS, K., LETTAU, M., MARETZKY, T., LUDWIG, A., HARTMANN, D., DE STROOPER, B., JANSSEN, O. & SAFTIG, P. 2007. ADAM10 regulates FasL cell surface expression and modulates FasL-induced cytotoxicity and activation-induced cell death. *Cell Death Differ,* 14**,** 1040-1049.
SCHWARZ, J., BRODER, C., HELMSTETTER, A., SCHMIDT, S., YAN, I., MULLER, M., SCHMIDT-ARRAS, D., BECKER-PAULY, C., KOCH-NOLTE, F., MITTRUCKER, H. W., RABE, B., ROSE-JOHN, S. & CHALARIS, A. 2013. Short-term TNFalpha

shedding is independent of cytoplasmic phosphorylation or furin cleavage of ADAM17. *Biochim Biophys Acta,* 1833**,** 3355-67.
SESHACHARYULU, P., PONNUSAMY, M. P., HARIDAS, D., JAIN, M., GANTI, A. K. & BATRA, S. K. 2012. Targeting the EGFR signaling pathway in cancer therapy. *Expert Opinion on Therapeutic Targets,* 16**,** 15-31.
SETHI, N. & KANG, Y. 2011. Notch signalling in cancer progression and bone metastasis. *Br J Cancer,* 105**,** 1805-1810.
SETIA, S., NEHRU, B. & SANYAL, S. N. 2014. Upregulation of MAPK/Erk and PI3K/Akt pathways in ulcerative colitis-associated colon cancer. *Biomedicine & Pharmacotherapy,* 68**,** 1023-1029.
SHAO, S., LI, Z., GAO, W., YU, G., LIU, D. & PAN, F. 2014. ADAM-12 as a diagnostic marker for the proliferation, migration and invasion in patients with small cell lung cancer. *PLoS One,* 9**,** e85936.
SHAO, Y., SHA, X. Y., BAI, Y. X., QUAN, F. & WU, S. L. 2015. Effect of A disintegrin and metalloproteinase 10 gene silencing on the proliferation, invasion and migration of the human tongue squamous cell carcinoma cell line TCA8113. *Mol Med Rep,* 11**,** 212-8.
SHARGH, S. A., SAKIZLI, M., KHALAJ, V., MOVAFAGH, A., YAZDI, H., HAGIGATJOU, E., SAYAD, A., MANSOURI, N., MORTAZAVI-TABATABAEI, S. A. & KHORRAM KHORSHID, H. R. 2014. Downregulation of E-cadherin expression in breast cancer by promoter hypermethylation and its relation with progression and prognosis of tumor. *Med Oncol,* 31**,** 250.
SHIN, J. Y., KIM, J. O., LEE, S. K., CHAE, H. S. & KANG, J. H. 2010. LY294002 may overcome 5-FU resistance via down-regulation of activated p-AKT in Epstein-Barr virus-positive gastric cancer cells. *BMC Cancer,* 10**,** 425.
SHIRATO, K., NAKAJIMA, K., KOREKANE, H., TAKAMATSU, S., GAO, C., ANGATA, T., OHTSUBO, K. & TANIGUCHI, N. 2011. Hypoxic regulation of glycosylation via the N-acetylglucosamine cycle. *Journal of Clinical Biochemistry and Nutrition,* 48**,** 20-25.
SHOU, J., ROSS, S., KOEPPEN, H., DE SAUVAGE, F. J. & GAO, W. Q. 2001. Dynamics of notch expression during murine prostate development and tumorigenesis. *Cancer Res,* 61**,** 7291-7.
SIKANDAR, S. S., PATE, K. T., ANDERSON, S., DIZON, D., EDWARDS, R. A., WATERMAN, M. L. & LIPKIN, S. M. 2010. NOTCH signaling is required for formation and self-renewal of tumor-initiating cells and for repression of secretory cell differentiation in colon cancer. *Cancer Res,* 70**,** 1469-78.
SIKORA, K., CHAN, S., EVAN, G., GABRA, H., MARKHAM, N., STEWART, J. & WATSON, J. 1987. c-myc oncogene expression in colorectal cancer. *Cancer,* 59**,** 1289-95.
SIX, E., NDIAYE, D., LAABI, Y., BROU, C., GUPTA-ROSSI, N., ISRAEL, A. & LOGEAT, F. 2003. The Notch ligand Delta1 is sequentially cleaved by an ADAM protease and gamma-secretase. *Proc Natl Acad Sci U S A,* 100**,** 7638-43.
SMITH, C. 2006. Sharpening the tools of RNA interference. *Nat Meth,* 3**,** 475-486.
SMITH, D. R. & GOH, H. S. 1996. Overexpression of the c-myc proto-oncogene in colorectal carcinoma is associated with a reduced mortality that is abrogated by point mutation of the p53 tumor suppressor gene. *Clinical Cancer Research,* 2**,** 1049-1053.
SMITH, J. M. & HAIGH, J. 1974. The hitch-hiking effect of a favourable gene. *Genet Res,* 23**,** 23-35.
SONG, W., LIU, W., ZHAO, H., LI, S., GUAN, X., YING, J., ZHANG, Y., MIAO, F., ZHANG, M., REN, X., LI, X., WU, F., ZHAO, Y., TIAN, Y., WU, W., FU, J., LIANG, J., WU, W., LIU, C., YU, J., ZONG, S., MIAO, S., ZHANG, X. & WANG, L. 2015. Rhomboid domain containing 1 promotes colorectal cancer growth through activation of the EGFR signalling pathway. *Nat Commun,* 6**,** 8022.
SOTTORIVA, A., KANG, H., MA, Z., GRAHAM, T. A., SALOMON, M. P., ZHAO, J., MARJORAM, P., SIEGMUND, K., PRESS, M. F., SHIBATA, D. & CURTIS, C. 2015. A Big Bang model of human colorectal tumor growth. *Nat Genet,* 47**,** 209-16.
SPADERNA, S., SCHMALHOFER, O., WAHLBUHL, M., DIMMLER, A., BAUER, K., SULTAN, A., HLUBEK, F., JUNG, A., STRAND, D., EGER, A., KIRCHNER, T.,

BEHRENS, J. & BRABLETZ, T. 2008. The transcriptional repressor ZEB1 promotes metastasis and loss of cell polarity in cancer. *Cancer Res,* 68**,** 537-44.
SPARKS, A. B., MORIN, P. J., VOGELSTEIN, B. & KINZLER, K. W. 1998. Mutational analysis of the APC/beta-catenin/Tcf pathway in colorectal cancer. *Cancer Res,* 58**,** 1130-4.
STEGEMAN, H., KAANDERS, J. H., WHEELER, D. L., VAN DER KOGEL, A. J., VERHEIJEN, M. M., WAAIJER, S. J., IIDA, M., GRENMAN, R., SPAN, P. N. & BUSSINK, J. 2012. Activation of AKT by hypoxia: a potential target for hypoxic tumors of the head and neck. *BMC Cancer,* 12**,** 463.
STOWELL, S. R., JU, T. & CUMMINGS, R. D. 2015. Protein glycosylation in cancer. *Annu Rev Pathol,* 10**,** 473-510.
SUMAN, S., DAS, T. P. & DAMODARAN, C. 2013. Silencing NOTCH signaling causes growth arrest in both breast cancer stem cells and breast cancer cells. *Br J Cancer,* 109**,** 2587-96.
SUNNARBORG, S. W., HINKLE, C. L., STEVENSON, M., RUSSELL, W. E., RASKA, C. S., PESCHON, J. J., CASTNER, B. J., GERHART, M. J., PAXTON, R. J., BLACK, R. A. & LEE, D. C. 2002. Tumor Necrosis Factor-α Converting Enzyme (TACE) Regulates Epidermal Growth Factor Receptor Ligand Availability. *Journal of Biological Chemistry,* 277**,** 12838-12845.
SUSNEA, I., BERNEVIC, B., WICKE, M., MA, L., LIU, S., SCHELLANDER, K. & PRZYBYLSKI, M. 2013. Application of MALDI-TOF-mass spectrometry to proteome analysis using stain-free gel electrophoresis. *Top Curr Chem,* 331**,** 37-54.
SUZUKI, A., KADOTA, N., HARA, T., NAKAGAMI, Y., IZUMI, T., TAKENAWA, T., SABE, H. & ENDO, T. 2000. Meltrin alpha cytoplasmic domain interacts with SH3 domains of Src and Grb2 and is phosphorylated by v-Src. *Oncogene,* 19**,** 5842-50.
SZALAD, A., KATAKOWSKI, M., ZHENG, X., JIANG, F. & CHOPP, M. 2009. Transcription factor Sp1 induces ADAM17 and contributes to tumor cell invasiveness under hypoxia. *J Exp Clin Cancer Res,* 28**,** 129.
TAN, C. & DU, X. 2012. KRAS mutation testing in metastatic colorectal cancer. *World Journal of Gastroenterology : WJG,* 18**,** 5171-5180.
TANG, J., CHEN, Y., CUI, R., LI, D., XIAO, L., LIN, P., DU, Y., SUN, H., YU, X. & ZHENG, X. 2015. Upregulation of fractalkine contributes to the proliferative response of prostate cancer cells to hypoxia via promoting the G1/S phase transition. *Mol Med Rep,* 12**,** 7907-14.
TANJORE, H. & KALLURI, R. 2006. The role of type IV collagen and basement membranes in cancer progression and metastasis. *Am J Pathol,* 168**,** 715-7.
TAYLOR, S. C., BERKELMAN, T., YADAV, G. & HAMMOND, M. 2013. A defined methodology for reliable quantification of Western blot data. *Mol Biotechnol,* 55**,** 217-26.
TAYLOR, S. C. & POSCH, A. 2014. The Design of a Quantitative Western Blot Experiment. *BioMed Research International,* 2014**,** 8.
THOMAS, G. 2002. FURIN AT THE CUTTING EDGE: FROM PROTEIN TRAFFIC TO EMBRYOGENESIS AND DISEASE. *Nature reviews. Molecular cell biology,* 3**,** 753-766.
THORBURN, A., THAMM, D. H. & GUSTAFSON, D. L. 2014. Autophagy and Cancer Therapy. *Molecular Pharmacology,* 85**,** 830-838.
TIAN, Y. & ZHANG, H. 2013. Characterization of disease-associated N-linked glycoproteins. *Proteomics,* 13**,** 504-11.
TIEN, L. T., ITO, M., NAKAO, M., NIINO, D., SERIK, M., NAKASHIMA, M., WEN, C. Y., YATSUHASHI, H. & ISHIBASHI, H. 2005. Expression of beta-catenin in hepatocellular carcinoma. *World J Gastroenterol,* 11**,** 2398-401.
TOL, J., DIJKSTRA, J. R., KLOMP, M., TEERENSTRA, S., DOMMERHOLT, M., VINK-BORGER, M. E., VAN CLEEF, P. H., VAN KRIEKEN, J. H., PUNT, C. J. & NAGTEGAAL, I. D. 2010. Markers for EGFR pathway activation as predictor of outcome in metastatic colorectal cancer patients treated with or without cetuximab. *Eur J Cancer,* 46**,** 1997-2009.

TOON, C. W., CHOU, A., CLARKSON, A., DESILVA, K., HOUANG, M., CHAN, J. C., SIOSON, L. L., JANKOVA, L. & GILL, A. J. 2014. Immunohistochemistry for myc predicts survival in colorectal cancer. *PLoS One,* 9**,** e87456.

TOUSSEYN, T., JORISSEN, E., REISS, K. & HARTMANN, D. 2006. (Make) stick and cut loose--disintegrin metalloproteases in development and disease. *Birth Defects Res C Embryo Today,* 78**,** 24-46.

TOUSSEYN, T., THATHIAH, A., JORISSEN, E., RAEMAEKERS, T., KONIETZKO, U., REISS, K., MAES, E., SNELLINX, A., SERNEELS, L., NYABI, O., ANNAERT, W., SAFTIG, P., HARTMANN, D. & DE STROOPER, B. 2009. ADAM10, the Rate-limiting Protease of Regulated Intramembrane Proteolysis of Notch and Other Proteins, Is Processed by ADAMS-9, ADAMS-15, and the γ-Secretase. *The Journal of Biological Chemistry,* 284**,** 11738-11747.

TSAI, C.-C., CHEN, Y.-J., YEW, T.-L., CHEN, L.-L., WANG, J.-Y., CHIU, C.-H. & HUNG, S.-C. 2011. Hypoxia inhibits senescence and maintains mesenchymal stem cell properties through down-regulation of E2A-p21 by HIF-TWIST. *Blood,* 117**,** 459-469.

TSAI, Y. H., VANDUSSEN, K. L., SAWEY, E. T., WADE, A. W., KASPER, C., RAKSHIT, S., BHATT, R. G., STOECK, A., MAILLARD, I., CRAWFORD, H. C., SAMUELSON, L. C. & DEMPSEY, P. J. 2014. ADAM10 regulates Notch function in intestinal stem cells of mice. *Gastroenterology,* 147**,** 822-834 e13.

TSUKAHARA, T., HANIU, H. & MATSUDA, Y. 2015. Cyclic phosphatidic acid induces G0/G1 arrest, inhibits AKT phosphorylation, and downregulates cyclin D1 expression in colorectal cancer cells. *Cell Mol Biol Lett,* 20**,** 38-47.

UMBAS, R., SCHALKEN, J. A., AALDERS, T. W., CARTER, B. S., KARTHAUS, H. F., SCHAAFSMA, H. E., DEBRUYNE, F. M. & ISAACS, W. B. 1992. Expression of the cellular adhesion molecule E-cadherin is reduced or absent in high-grade prostate cancer. *Cancer Res,* 52**,** 5104-9.

VAIOPOULOS, A. G., ATHANASOULA, K. & PAPAVASSILIOU, A. G. 2014. Epigenetic modifications in colorectal cancer: molecular insights and therapeutic challenges. *Biochim Biophys Acta,* 1842**,** 971-80.

VALENTA, T., HAUSMANN, G. & BASLER, K. 2012. The many faces and functions of beta-catenin. *EMBO J,* 31**,** 2714-36.

VAN HOUDT, W. J., HOOGWATER, F. J. H., DE BRUIJN, M. T., EMMINK, B. L., NIJKAMP, M. W., RAATS, D. A. E., VAN DER GROEP, P., VAN DIEST, P., BOREL RINKES, I. H. M. & KRANENBURG, O. 2010. Oncogenic KRAS Desensitizes Colorectal Tumor Cells to Epidermal Growth Factor Receptor Inhibition and Activation. *Neoplasia (New York, N.Y.),* 12**,** 443-452.

VAN TETERING, G., VAN DIEST, P., VERLAAN, I., VAN DER WALL, E., KOPAN, R. & VOOIJS, M. 2009. Metalloprotease ADAM10 Is Required for Notch1 Site 2 Cleavage. *The Journal of Biological Chemistry,* 284**,** 31018-31027.

VAN TONDER, A., JOUBERT, A. M. & CROMARTY, A. D. 2015. Limitations of the 3-(4,5-dimethylthiazol-2-yl)-2,5-diphenyl-2H-tetrazolium bromide (MTT) assay when compared to three commonly used cell enumeration assays. *BMC Res Notes,* 8**,** 47.

VANARSDALE, T., BOSHOFF, C., ARNDT, K. T. & ABRAHAM, R. T. 2015. Molecular Pathways: Targeting the Cyclin D-CDK4/6 Axis for Cancer Treatment. *Clin Cancer Res,* 21**,** 2905-10.

VARELA-NALLAR, L., ROJAS-ABALOS, M., ABBOTT, A. C., MOYA, E. A., ITURRIAGA, R. & INESTROSA, N. C. 2014. Chronic hypoxia induces the activation of the Wnt/β-catenin signaling pathway and stimulates hippocampal neurogenesis in wild-type and APPswe-PS1ΔE9 transgenic mice in vivo. *Frontiers in Cellular Neuroscience,* 8**,** 17.

VAUPEL, P., BRIEST, S. & HOCKEL, M. 2002. Hypoxia in breast cancer: pathogenesis, characterization and biological/therapeutic implications. *Wien Med Wochenschr,* 152**,** 334-42.

VAUPEL, P. & HARRISON, L. 2004. Tumor hypoxia: causative factors, compensatory mechanisms, and cellular response. *The oncologist,* 9 Suppl 5**,** 4-9.

VERRAS, M., PAPANDREOU, I., LIM, A. L. & DENKO, N. C. 2008. Tumor Hypoxia Blocks Wnt Processing and Secretion through the Induction of Endoplasmic Reticulum Stress. *Molecular and Cellular Biology,* 28**,** 7212-7224.

VIDAL, F., DE ARAUJO, W. M., CRUZ, A. L., TANAKA, M. N., VIOLA, J. P. & MORGADO-DIAZ, J. A. 2011. Lithium reduces tumorigenic potential in response to EGF signaling in human colorectal cancer cells. *Int J Oncol,* 38**,** 1365-73.

VILLA, J. C., CHIU, D., BRANDES, A. H., ESCORCIA, F. E., VILLA, C. H., MAGUIRE, W. F., HU, C. J., DE STANCHINA, E., SIMON, M. C., SISODIA, S. S., SCHEINBERG, D. A. & LI, Y. M. 2014. Nontranscriptional role of Hif-1alpha in activation of gamma-secretase and notch signaling in breast cancer. *Cell Rep,* 8**,** 1077-92.

VINSON, K. E., GEORGE, D. C., FENDER, A. W., BERTRAND, F. E. & SIGOUNAS, G. 2015. The Notch pathway in colorectal cancer. *Int J Cancer*.

VLEMINCKX, K., VAKAET, L., JR., MAREEL, M., FIERS, W. & VAN ROY, F. 1991. Genetic manipulation of E-cadherin expression by epithelial tumor cells reveals an invasion suppressor role. *Cell,* 66**,** 107-19.

VORA, S. R., JURIC, D., KIM, N., MINO-KENUDSON, M., HUYNH, T., COSTA, C., LOCKERMAN, E. L., POLLACK, S. F., LIU, M., LI, X., LEHAR, J., WIESMANN, M., WARTMANN, M., CHEN, Y., CAO, Z. A., PINZON-ORTIZ, M., KIM, S., SCHLEGEL, R., HUANG, A. & ENGELMAN, J. A. 2014. CDK 4/6 inhibitors sensitize PIK3CA mutant breast cancer to PI3K inhibitors. *Cancer Cell,* 26**,** 136-49.

WAHLSTROM, T. & HENRIKSSON, M. A. 2015. Impact of MYC in regulation of tumor cell metabolism. *Biochim Biophys Acta,* 1849**,** 563-9.

WALSH, C. T., GARNEAU-TSODIKOVA, S. & GATTO, G. J., JR. 2005. Protein posttranslational modifications: the chemistry of proteome diversifications. *Angew Chem Int Ed Engl,* 44**,** 7342-72.

WANG, H., MANNAVA, S., GRACHTCHOUK, V., ZHUANG, D., SOENGAS, M. S., GUDKOV, A. V., PROCHOWNIK, E. V. & NIKIFOROV, M. A. 2008. c-Myc depletion inhibits proliferation of human tumor cells at various stages of the cell cycle. *Oncogene,* 27**,** 1905-1915.

WANG, P., ZHAO, J., YANG, X., GUAN, S., FENG, H., HAN, D., LU, J., OU, B., JIN, R., SUN, J., ZONG, Y., FENG, B., MA, J., LU, A. & ZHENG, M. 2015a. PFDN1, an indicator for colorectal cancer prognosis, enhances tumor cell proliferation and motility through cytoskeletal reorganization. *Med Oncol,* 32**,** 264.

WANG, W. M., ZHAO, Z. L., MA, S. R., YU, G. T., LIU, B., ZHANG, L., ZHANG, W. F., KULKARNI, A. B., SUN, Z. J. & ZHAO, Y. F. 2015b. Epidermal growth factor receptor inhibition reduces angiogenesis via hypoxia-inducible factor-1alpha and Notch1 in head neck squamous cell carcinoma. *PLoS One,* 10**,** e0119723.

WANG, W. M., ZHAO, Z. L., ZHANG, W. F., ZHAO, Y. F., ZHANG, L. & SUN, Z. J. 2015c. Role of hypoxia-inducible factor-1alpha and CD146 in epidermal growth factor receptor-mediated angiogenesis in salivary gland adenoid cystic carcinoma. *Mol Med Rep,* 12**,** 3432-8.

WANG, X. J., FENG, C. W. & LI, M. 2013. ADAM17 mediates hypoxia-induced drug resistance in hepatocellular carcinoma cells through activation of EGFR/PI3K/Akt pathway. *Mol Cell Biochem,* 380**,** 57-66.

WANG, Y.-C., PETERSON, S. E. & LORING, J. F. 2014. Protein post-translational modifications and regulation of pluripotency in human stem cells. *Cell Res,* 24**,** 143-160.

WANG, Y. Y., YE, Z. Y., LI, L., ZHAO, Z. S., SHAO, Q. S. & TAO, H. Q. 2011a. ADAM 10 is associated with gastric cancer progression and prognosis of patients. *J Surg Oncol,* 103**,** 116-23.

WANG, Z., LI, Y., AHMAD, A., BANERJEE, S., AZMI, A. S., KONG, D. & SARKAR, F. H. 2011b. Pancreatic cancer: understanding and overcoming chemoresistance. *Nat Rev Gastroenterol Hepatol,* 8**,** 27-33.

WANGEFJORD, S., MANJER, J., GABER, A., NODIN, B., EBERHARD, J. & JIRSTRÖM, K. 2011. Cyclin D1 expression in colorectal cancer is a favorable prognostic factor in men but not in women in a prospective, population-based cohort study. *Biology of Sex Differences,* 2**,** 1-10.

WEBER, A., BORGHOUTS, C., BRENDEL, C., MORIGGL, R., DELIS, N., BRILL, B., VAFAIZADEH, V. & GRONER, B. 2013. The Inhibition of Stat5 by a Peptide Aptamer Ligand Specific for the DNA Binding Domain Prevents Target Gene Transactivation and the Growth of Breast and Prostate Tumor Cells. *Pharmaceuticals,* 6**,** 960-987.

WEBSTER, N. J., GREEN, K. N., PEERS, C. & VAUGHAN, P. F. 2002. Altered processing of amyloid precursor protein in the human neuroblastoma SH-SY5Y by chronic hypoxia. *J Neurochem,* 83**,** 1262-71.

WEI, Y., VAN NHIEU, J. T., PRIGENT, S., SRIVATANAKUL, P., TIOLLAIS, P. & BUENDIA, M.-A. 2002. Altered expression of E-cadherin in hepatocellular carcinoma: Correlations with genetic alterations, β-catenin expression, and clinical features. *Hepatology,* 36**,** 692-701.

WEN, W., DING, J., SUN, W., WU, K., NING, B., GONG, W., HE, G., HUANG, S., DING, X., YIN, P., CHEN, L., LIU, Q., XIE, W. & WANG, H. 2010. Suppression of cyclin D1 by hypoxia-inducible factor-1 via direct mechanism inhibits the proliferation and 5-fluorouracil-induced apoptosis of A549 cells. *Cancer Res,* 70**,** 2010-9.

WESTWOOD, D. A., PATEL, O. & BALDWIN, G. S. 2014. Gastrin mediates resistance to hypoxia-induced cell death in xenografts of the human colorectal cancer cell line LoVo. *Biochim Biophys Acta,* 1843**,** 2471-80.

WHITE, E. 2015. The role for autophagy in cancer. *The Journal of Clinical Investigation,* 125**,** 42-46.

WIESENAUER, C. A., YIP-SCHNEIDER, M. T., WANG, Y. & SCHMIDT, C. M. 2004. Multiple anticancer effects of blocking MEK-ERK signaling in hepatocellular carcinoma. *J Am Coll Surg,* 198**,** 410-21.

WINCEWICZ, A., KODA, M., SULKOWSKI, S., KANCZUGA-KODA, L. & SULKOWSKA, M. 2010. Comparison of beta-catenin with TGF-beta1, HIF-1alpha and patients' disease-free survival in human colorectal cancer. *Pathol Oncol Res,* 16**,** 311-8.

WITTERS, L., SCHERLE, P., FRIEDMAN, S., FRIDMAN, J., CAULDER, E., NEWTON, R. & LIPTON, A. 2008. Synergistic inhibition with a dual epidermal growth factor receptor/HER-2/neu tyrosine kinase inhibitor and a disintegrin and metalloprotease inhibitor. *Cancer Res,* 68**,** 7083-9.

WOJTOWICZ, K., SZAFLARSKI, W., JANUCHOWSKI, R., ZAWIERUCHA, P., NOWICKI, M. & ZABEL, M. 2012. Inhibitors of N-glycosylation as a potential tool for analysis of the mechanism of action and cellular localisation of glycoprotein P. *Acta Biochim Pol,* 59**,** 445-50.

WONG, W. J., QIU, B., NAKAZAWA, M. S., QING, G. & SIMON, M. C. 2013. MYC degradation under low O2 tension promotes survival by evading hypoxia-induced cell death. *Mol Cell Biol,* 33**,** 3494-504.

WOODS, N., TREVINO, J., COPPOLA, D., CHELLAPPAN, S., YANG, S. & PADMANABHAN, J. 2015. Fendiline inhibits proliferation and invasion of pancreatic cancer cells by interfering with ADAM10 activation and beta-catenin signaling. *Oncotarget,* 6**,** 35931-48.

WOODS, N. K. & PADMANABHAN, J. 2013. Inhibition of amyloid precursor protein processing enhances gemcitabine-mediated cytotoxicity in pancreatic cancer cells. *J Biol Chem,* 288**,** 30114-24.

XIA, M., KNEZEVIC, D. & VASSILEV, L. T. 2011. p21 does not protect cancer cells from apoptosis induced by nongenotoxic p53 activation. *Oncogene,* 30**,** 346-55.

XIONG, H., SU, W. Y., LIANG, Q. C., ZHANG, Z. G., CHEN, H. M., DU, W., CHEN, Y. X. & FANG, J. Y. 2009. Inhibition of STAT5 induces G1 cell cycle arrest and reduces tumor cell invasion in human colorectal cancer cells. *Lab Invest,* 89**,** 717-25.

XU, J., PROSPERI, J. R., CHOUDHURY, N., OLOPADE, O. I. & GOSS, K. H. 2015. β-Catenin Is Required for the Tumorigenic Behavior of Triple-Negative Breast Cancer Cells. *PLoS ONE,* 10**,** e0117097.

XU, Q., LIU, X., CHEN, W. & ZHANG, Z. 2010. Inhibiting adenoid cystic carcinoma cells growth and metastasis by blocking the expression of ADAM 10 using RNA interference. *J Transl Med,* 8**,** 136.

YABUUCHI, S., PAI, S. G., CAMPBELL, N. R., DE WILDE, R. F., DE OLIVEIRA, E., KORANGATH, P., STREPPEL, M. M., RASHEED, Z. A., HIDALGO, M., MAITRA, A. & RAJESHKUMAR, N. V. 2013. Notch signaling pathway targeted therapy suppresses tumor progression and metastatic spread in pancreatic cancer. *Cancer Letters,* 335**,** 41-51.

YAMAMOTO, H., SOH, J.-W., MONDEN, T., KLEIN, M. G., ZHANG, L. M., SHIRIN, H., ARBER, N., TOMITA, N., SCHIEREN, I., STEIN, C. A. & WEINSTEIN, I. B. 1999. Paradoxical Increase in Retinoblastoma Protein in Colorectal Carcinomas May Protect Cells from Apoptosis. *Clinical Cancer Research,* 5**,** 1805-1815.

YANG, D., WANG, L. L., DONG, T. T., SHEN, Y. H., GUO, X. S., LIU, C. Y., LIU, J., ZHANG, P., LI, J. & SUN, Y. P. 2015. Progranulin promotes colorectal cancer proliferation and angiogenesis through TNFR2/Akt and ERK signaling pathways. *Am J Cancer Res,* 5**,** 3085-97.

YANG, K., HITOMI, M. & STACEY, D. W. 2006. Variations in cyclin D1 levels through the cell cycle determine the proliferative fate of a cell. *Cell Division,* 1**,** 32-32.

YANG, Z. J., CHEE, C. E., HUANG, S. & SINICROPE, F. A. 2011. The role of autophagy in cancer: therapeutic implications. *Mol Cancer Ther,* 10**,** 1533-41.

YAO, K., GIETEMA, J. A., SHIDA, S., SELVAKUMARAN, M., FONROSE, X., HAAS, N. B., TESTA, J. & O'DWYER, P. J. 2005a. In vitro hypoxia-conditioned colon cancer cell lines derived from HCT116 and HT29 exhibit altered apoptosis susceptibility and a more angiogenic profile in vivo. *Br J Cancer,* 93**,** 1356-63.

YAO, K., SHIDA, S., SELVAKUMARAN, M., ZIMMERMAN, R., SIMON, E., SCHICK, J., HAAS, N. B., BALKE, M., ROSS, H., JOHNSON, S. W. & O'DWYER, P. J. 2005b. Macrophage migration inhibitory factor is a determinant of hypoxia-induced apoptosis in colon cancer cell lines. *Clin Cancer Res,* 11**,** 7264-72.

YATES, J. R., RUSE, C. I. & NAKORCHEVSKY, A. 2009. Proteomics by mass spectrometry: approaches, advances, and applications. *Annu Rev Biomed Eng,* 11**,** 49-79.

YILMAZ, M. & CHRISTOFORI, G. 2009. EMT, the cytoskeleton, and cancer cell invasion. *Cancer and Metastasis Reviews,* 28**,** 15-33.

YIN, J. & YU, F. S. 2009. ERK1/2 mediate wounding- and G-protein-coupled receptor ligands-induced EGFR activation via regulating ADAM17 and HB-EGF shedding. *Invest Ophthalmol Vis Sci,* 50**,** 132-9.

YOSHIDA, A. & DIEHL, J. A. 2015. CDK4/6 inhibitor: from quiescence to senescence. *Oncoscience,* 2**,** 896-897.

YOSHIOKA, S., KING, M. L., RAN, S., OKUDA, H., MACLEAN, J. A., MCASEY, M. E., SUGINO, N., BRARD, L., WATABE, K. & HAYASHI, K. 2012. WNT7A Regulates Tumor Growth and Progression in Ovarian Cancer through the WNT/β-Catenin Pathway. *Molecular Cancer Research,* 10**,** 469-482.

YOU, B., SHAN, Y., SHI, S., LI, X. & YOU, Y. 2015. Effects of ADAM10 upregulation on progression, migration, and prognosis of nasopharyngeal carcinoma. *Cancer Sci*.

YU, L. & HALES, C. A. 2011. Long-term exposure to hypoxia inhibits tumor progression of lung cancer in rats and mice. *BMC Cancer,* 11**,** 331-331.

YU, L. X., ZHOU, L., LI, M., LI, Z. W., WANG, D. S. & ZHANG, S. G. 2013. The Notch1/cyclooxygenase-2/Snail/E-cadherin pathway is associated with hypoxia-induced hepatocellular carcinoma cell invasion and migration. *Oncol Rep,* 29**,** 362-70.

YUAN, R., KE, J., SUN, L., HE, Z., ZOU, Y., HE, X., CHEN, Y., WU, X., CAI, Z., WANG, L., WANG, J., FAN, X., WU, X. & LAN, P. 2015a. HES1 promotes metastasis and predicts poor survival in patients with colorectal cancer. *Clin Exp Metastasis,* 32**,** 169-79.

YUAN, S., LEI, S. & WU, S. 2013. ADAM10 is overexpressed in human hepatocellular carcinoma and contributes to the proliferation, invasion and migration of HepG2 cells. *Oncol Rep,* 30**,** 1715-22.

YUAN, X., WU, H., XU, H., XIONG, H., CHU, Q., YU, S., WU, G. S. & WU, K. 2015b. Notch signaling: An emerging therapeutic target for cancer treatment. *Cancer Letters,* 369**,** 20-27.

YUAN, X., ZHANG, M., WU, H., XU, H., HAN, N., CHU, Q., YU, S., CHEN, Y. & WU, K. 2015c. Expression of Notch1 Correlates with Breast Cancer Progression and Prognosis. *PLoS ONE,* 10**,** e0131689.

ZEKI, S. S., GRAHAM, T. A. & WRIGHT, N. A. 2011. Stem cells and their implications for colorectal cancer. *Nat Rev Gastroenterol Hepatol,* 8**,** 90-100.

ZHANG, J., CHENG, Q., ZHOU, Y., WANG, Y. & CHEN, X. 2013a. Slug is a key mediator of hypoxia induced cadherin switch in HNSCC: correlations with poor prognosis. *Oral Oncol,* 49**,** 1043-50.

ZHANG, J. Z., BEHROOZ, A. & ISMAIL-BEIGI, F. 1999. Regulation of glucose transport by hypoxia. *Am J Kidney Dis,* 34**,** 189-202.

ZHANG, L., HUANG, G., LI, X., ZHANG, Y., JIANG, Y., SHEN, J., LIU, J., WANG, Q., ZHU, J., FENG, X., DONG, J. & QIAN, C. 2013b. Hypoxia induces epithelial-mesenchymal transition via activation of SNAI1 by hypoxia-inducible factor -1alpha in hepatocellular carcinoma. *BMC Cancer,* 13**,** 108.

ZHANG, Q., BAI, X., CHEN, W., MA, T., HU, Q., LIANG, C., XIE, S., CHEN, C., HU, L., XU, S. & LIANG, T. 2013c. Wnt/beta-catenin signaling enhances hypoxia-induced epithelial-mesenchymal transition in hepatocellular carcinoma via crosstalk with hif-1alpha signaling. *Carcinogenesis,* 34**,** 962-73.

ZHANG, Q., THOMAS, S. M., LUI, V. W., XI, S., SIEGFRIED, J. M., FAN, H., SMITHGALL, T. E., MILLS, G. B. & GRANDIS, J. R. 2006. Phosphorylation of TNF-alpha converting enzyme by gastrin-releasing peptide induces amphiregulin release and EGF receptor activation. *Proc Natl Acad Sci U S A,* 103**,** 6901-6.

ZHANG, Q., YU, L., QIN, D., HUANG, R., JIANG, X., ZOU, C., TANG, Q., CHEN, Y., WANG, G., WANG, X. & GAO, X. 2015a. Role of microRNA-30c Targeting ADAM19 in Colorectal Cancer. *PLoS ONE,* 10**,** e0120698.

ZHANG, W., LIU, S., LIU, K., JI, B., WANG, Y. & LIU, Y. 2014a. Knockout of ADAM10 enhances sorafenib antitumor activity of hepatocellular carcinoma in vitro and in vivo. *Oncol Rep,* 32**,** 1913-22.

ZHANG, W., SHI, X., PENG, Y., WU, M., ZHANG, P., XIE, R., WU, Y., YAN, Q., LIU, S. & WANG, J. 2015b. HIF-1α Promotes Epithelial-Mesenchymal Transition and Metastasis through Direct Regulation of ZEB1 in Colorectal Cancer. *PLoS ONE,* 10**,** e0129603.

ZHANG, Y., JIAO, J., YANG, P. & LU, H. 2014b. Mass spectrometry-based N-glycoproteomics for cancer biomarker discovery. *Clin Proteomics,* 11**,** 18.

ZHENG, L., ZHOU, Z. & HE, Z. 2015. Knockdown of PFTK1 inhibits tumor cell proliferation, invasion and epithelial-to-mesenchymal transition in pancreatic cancer. *Int J Clin Exp Pathol,* 8**,** 14005-12.

ZHENG, X., JIANG, F., KATAKOWSKI, M., KALKANIS, S. N., HONG, X., ZHANG, X., ZHANG, Z. G., YANG, H. & CHOPP, M. 2007. Inhibition of ADAM17 reduces hypoxia-induced brain tumor cell invasiveness. *Cancer Sci,* 98**,** 674-84.

ZHENG, X., JIANG, F., KATAKOWSKI, M., LU, Y. & CHOPP, M. 2012. ADAM17 promotes glioma cell malignant phenotype. *Mol Carcinog,* 51**,** 150-64.

ZHENG, X., JIANG, F., KATAKOWSKI, M., ZHANG, Z. G., LU, Q. E. & CHOPP, M. 2009. ADAM17 promotes breast cancer cell malignant phenotype through EGFR-PI3K-AKT activation. *Cancer Biol Ther,* 8**,** 1045-54.

ZHOU, B. B., PEYTON, M., HE, B., LIU, C., GIRARD, L., CAUDLER, E., LO, Y., BARIBAUD, F., MIKAMI, I., REGUART, N., YANG, G., LI, Y., YAO, W., VADDI, K., GAZDAR, A. F., FRIEDMAN, S. M., JABLONS, D. M., NEWTON, R. C., FRIDMAN, J. S., MINNA, J. D. & SCHERLE, P. A. 2006. Targeting ADAM-mediated ligand cleavage to inhibit HER3 and EGFR pathways in non-small cell lung cancer. *Cancer Cell,* 10**,** 39-50.

ZHU, J. H., CHEN, C. L., FLAVAHAN, S., HARR, J., SU, B. & FLAVAHAN, N. A. 2011. Cyclic stretch stimulates vascular smooth muscle cell alignment by redox-dependent activation of Notch3. *Am J Physiol Heart Circ Physiol,* 300**,** H1770-80.

ZHU, P., NING, Y., YAO, L., CHEN, M. & XU, C. 2010. The proliferation, apoptosis, invasion of endothelial-like epithelial ovarian cancer cells induced by hypoxia. *J Exp Clin Cancer Res,* 29**,** 124.

ZHUANG, J., WEI, Q., LIN, Z. & ZHOU, C. 2015. Effects of ADAM10 deletion on Notch-1 signaling pathway and neuronal maintenance in adult mouse brain. *Gene,* 555**,** 150-8.
ZUO, J., WEN, J., LEI, M., WEN, M., LI, S., LV, X., LUO, Z. & WEN, G. 2016. Hypoxia promotes the invasion and metastasis of laryngeal cancer cells via EMT. *Med Oncol,* 33**,** 15.

Appendix 1

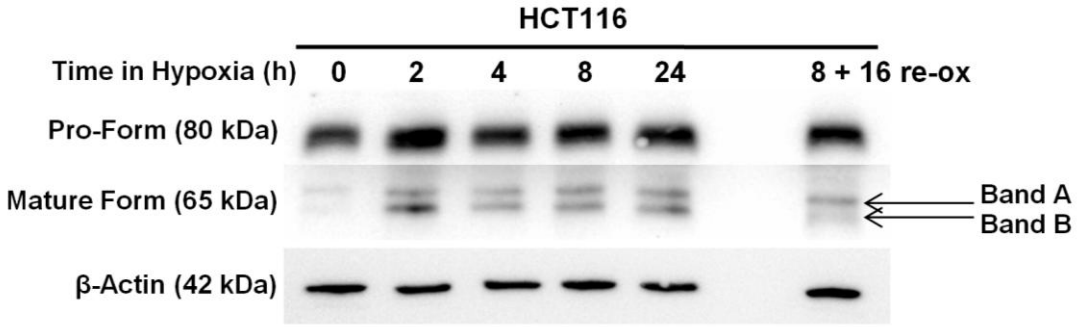

Figure A1.1: ADAM 10 Doublet Band is not Resolved upon Re-oxygenation

HCT116 cells were exposed to hypoxia (0.5% O_2) for a range of time points. Alongside these one sample was exposed to hypoxia (0.5% O_2) for 8 hours before being re-oxygenated in normoxia for 16 hours (20% O_2). Cells were lysed, 30 μg of each protein sample were separated by SDS-PAGE and expression of ADAM 10 was analysed by Western Blotting. The mature form of ADAM 10 is visible as a doublet, comprised of a higher (Band A) and lower (Band B) molecular weight bands, which does not appear to completely resolve upon re-oxygenation. β-Actin was used as a loading control. Blot is representative of one, preliminary experiment.

Table A1.1: LC-MS Methodology Settings

Equipment	Function	Setting
Loading pump	Reagents	2% acetonitrile, 98% H_2O with 0.1% trifluoroacetic acid
	Flow Rate	8.0 µL min^{-1}
Separation Nano Pumps	Solvent A	5% acetonitrile, 95% H_2O with 0.1% formic acid
	Solvent B	95% acetonitrile, 5% H_2O with 0.1% formic acid
	Flow Rate	300 nL min^{-1} throughout the run
Gradient Elution	Cleaning	98% Reagent A, 2% Reagent B for 5 minutes
	Sample Gradient	2% Reagent B to 40% Reagent B over 20 minutes. Increased to 98% Reagent B from 25 minutes to 27 minutes. Held at 98% Reagent B for 5 minutes then decreased back to 2% Reagent B
	Column Washing	95% Reagent B for 4 minutes, then decreased to 2% Reagent B for 1 minutes. Repeated 3 times
	Sample Gradient	2% Reagent B for 22 minutes to re-equilibrate
Mass Spectrometry	Capillary Voltage	1400 V
	Endplate Offset	-500 V
	Nebuliser	0.0 Bar
	Drying Gas Temperature	150 °C
	Dry Gas Flow	3.0 L min^{-1}

Table A1.2: Post-CRAPome Analysis Results for 0h Pro-Form

Protein	MW (kDa)	Rank	Found/Total	% of Studies
ADAM 10	84.1	3	1/411	0.2
GSN	85.6	19	26/411	6.3
TGM2	77.3	31	6/411	1.5
EPS8L1	80.2	32	2/411	0.5
ALDH16A1	85.1	33	12/411	2.9
STAT1	87.3	34	23/411	5.6
BCAM	97.4	37	2/411	0.5
NCBP1	91.8	38	38/411	9.3

Table A1.3: Post-CRAPome Analysis for 0h Mature Form

Protein	MW (kDa)	Rank	Found/Total	% of Studies
ADAM 10	84.1	4	1/411	0.2
DLAT	69	28	38/411	9.3
PCK2	70.7	29	5/411	1.2
LTA4H	69.2	30	14/411	3.4
TRIM29	65.8	32	5/411	1.2
POR	76.6	44	16/411	3.9
CAPN1	81.8	50	19/411	4.6
SRPR	69.8	51	25/411	6.1
UBN1	121.4	57	8/411	2
LGALS3BP	65.3	58	25/411	6.1
TGM2	77.3	59	6/411	1.5
APOB	515.3	62	11/411	2.7
GRIN3A	125.4	64	2/411	0.5
RNPEP	72.5	65	10/411	2.4

Table A1.4: Post-CRAPome Analysis for 2h Pro-Form

Protein	MW (kDa)	Rank	Found/Total	% of Studies
GSN	85.6	11	26/411	6.3
EPS8L1	80.2	12	2/411	0.5
ADAM 10	84.1	13	1/411	0.2
FAM129B	84.1	14	17/411	4.1
PYGB	96.6	19	19/411	4.6
RRM1	90	27	22/411	5.4
CTNNA1	100	32	34/411	8.3
UBA2	50.1	36	41/411	10
HEATR2	93.5	43	7/411	1.7
LGALS3BP	65.3	48	25/411	6.1
STAT1	87.3	54	23/411	5.6
MOGS	91.9	60	15/411	3.6
TNPO2	101.3	65	34/411	8.3

NPEPPS	103.2	67	34/411	8.3
PEPD	54.5	70	7/411	1.7
XRCC1	69.4	73	10/411	2.4
PKP3	87	78	6/411	1.5
NAA15	101.2	79	32/411	7.8
NOC2L	84.9	80	27/411	6.6
BCAM	67.4	82	2/411	0.5
MVP	99.3	86	8/411	2
TGM2	77.3	95	6/411	1.5
GIT1	84.3	98	9/411	2.2
COG5	92.7	101	2/411	0.5
GYS1	83.7	103	22/411	5.4
DNAJC10	91	104	26/411	6.3
OPA1	111.6	105	13/411	3.2
PARP9	96.3	105	1/411	0.2
SYNE1	1010.5	107	10/411	2.4
USP5	95.7	112	28/411	6.8
CARS	85.4	113	11/411	2.7
DPP9	98.2	115	10/411	2.4
FAM91A1	93.8	117	21/411	5.1
GSR	56.2	119	13/411	3.2
AGO2	97.1	120	22/411	5.4
DNM1	97.3	121	19/411	4.6
UFL1	89.5	122	11/411	2.7
CLPTM1	76	123	2/411	0.5
ACO2	85.4	124	27/411	6.6
EPS8L1	91.8	125	1/411	0.2
DTX3L	83.5	126	4/411	1
WASF2	54.3	127	21/411	5.1
SEC63	87.9	129	11/411	2.7
CAPN1	81.8	130	19/411	4.6
OSBP	89.4	131	4/411	1

Table A1.5: Post-CRAPome Analysis for 2h Mature Form

Protein	MW (kDa)	Rank	Found/Total	% of Studies
POR	76.6	11	16/411	3.89
RNPEP	72.5	24	10/411	2.43
SRPR	69.8	26	25/411	6.08
CAPN2	79.9	29	15/411	3.65
GPD2	80.8	31	3/411	0.73
ADAM 10	84.1	32	1/411	0.24
XPNPEP	69.9	33	6/411	1.46
TGM2	77.3	34	6/411	1.46
AGPS	72.9	35	11/411	2.68
CAPN1	81.8	36	19/411	4.62

TOMM70A	97.4	39	7/411	1.70
AACS	75.1	41	1/411	0.24
TRIM29	65.8	43	5/411	1.22
TXNRD1	70.9	45	4/411	0.97
PREP	80.6	48	7/411	1.70
COLGALT1	71.6	50	29/411	7.06
LRRC40	68.2	51	9/411	2.19
NSF	82.5	58	31/411	7.54
SNX1	59	61	31/411	7.54
CTNND1	108.1	62	32/411	7.79
DPP3	82.5	63	12/411	2.92
ERMP1	100.2	65	1/411	0.24
APEH	81.2	67	11/411	2.68
SNX2	58.4	68	30/411	7.30
MIPEP	80.6	70	1/411	0.24
GFPT1	78.8	74	15/411	3.65
VPS35	91.6	75	35/411	8.52
SCFD1	72.3	77	17/411	4.14
DNM1L	81.8	78	35/411	8.52
ACSL1	77.9	79	2/411	0.49
NT5E	63.3	80	2/411	0.49
PYGB	96.6	83	19/411	4.62
NXF1	70.1	87	38/411	9.25
PICALM	70.7	89	18/411	4.38
LGALS3BP	65.3	90	25/411	6.08
CTNNBL1	65.1	92	19/411	4.62
NF2	69.6	93	6/411	1.46
GNL1	68.6	95	2/411	0.49
LARP7	66.9	97	35/411	8.52
SAMHD1	72.2	98	18/411	4.38
RBM47	64.1	99	1/411	0.24
ZWILCH	67.2	100	3/411	0.73
ORC3	82.2	104	8/411	1.95
ATG7	77.9	106	2/411	0.49
SYNE1	1010.5	109	10/411	2.43
RANBP3	60.2	110	28/411	6.81
NDUFS1	79.4	111	19/411	4.62
GCLC	72.7	113	1/411	0.24
DLAT	69	114	38/411	9.25
PKP3	87	116	6/411	1.46
RELA	60.2	117	9/411	2.19
FAM129B	84.1	122	17/411	4.14
EPS8L1	80.2	124	2/411	0.49
OPA1	111.6	126	13/411	3.16
PGM2	68.2	127	3/411	0.73
EIF2AK2	62.1	128	14/411	3.41

MANBA	100.8	131	1/411	0.24
ACSL4	79.1	136	39/411	9.49
RNGTT	68.5	136	1/411	0.24
CD2AP	71.4	138	33/411	8.03
PRKCI	68.2	139	2/411	0.49
TXLNG	60.5	140	8/411	1.95
UBQLN1	62.5	140	10/411	2.43
YAP1	54.4	141	15/411	3.65
TNPO3	104.1	142	16/411	3.89
CEP152	195.5	143	6/411	1.46

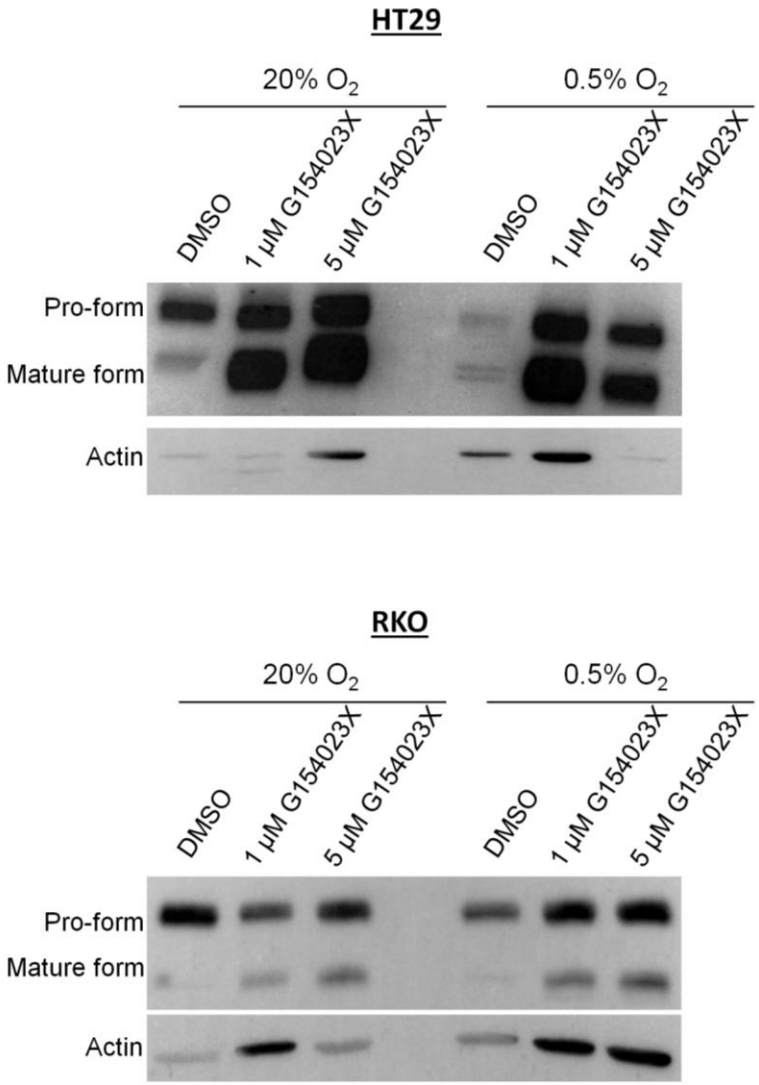

Figure A1.2: ADAM 10 is Upregulated at Protein Level after GI254023X Treatment

RKO and HT29 cells were treated with ADAM 10 inhibitor, GI254023X and after 6 hours were utilised for a scratch assay (as described in section 2.20.1). After completion of the scratch assay cells were then lysed and 30 µg of each protein sample were separated by SDS-PAGE and expression of ADAM 10 analysed by Western Blotting. β-Actin was used as a loading control, however this also appears to be affected by GI254023X treatment. Blots are representative of one experiment.

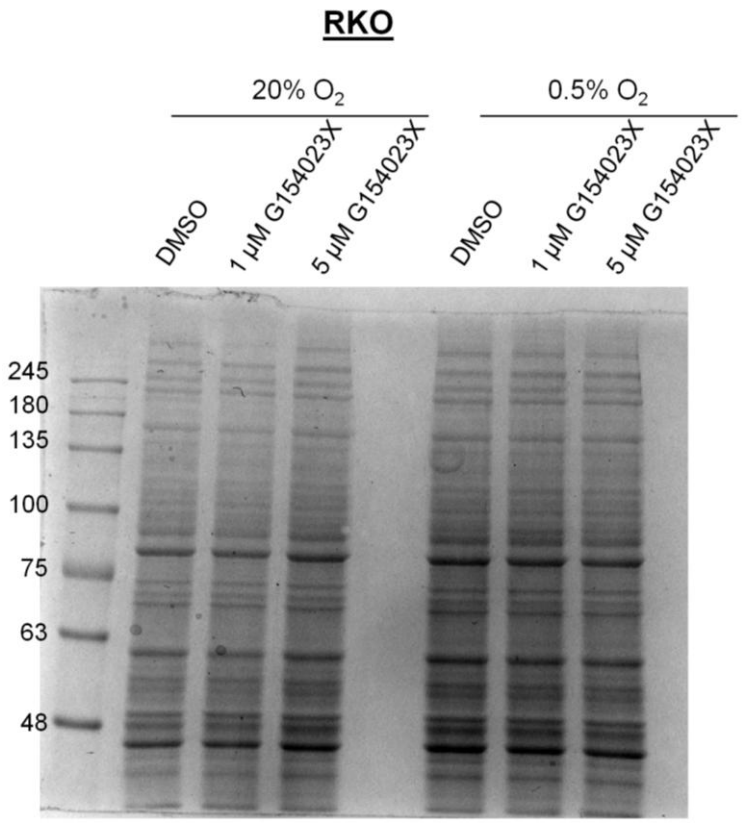

Figure A1.3: Coomassie Stained Gel to Confirm Equal Protein Content in GI254023X Stained Samples

As a result of abnormal β-Actin expression after GI254023X treatment (Figure A1.2) 30 µg of GI254023X treated RKO scratch assay samples were separated by SDS-PAGE and stained for total protein content with Coomassie Blue. Coomassie is representative of one experiment and demonstrates equal protein content within samples.

Table A1.6: CHARM Algorithm Settings for Clonogenic Assay Analysis

	Function	Setting
Pre-Processed	Smoothing	5
Edge Detection	Edge Detection Sensitivity	91.6/100
Centre Detection	Detection mode	Dark on light
	Centre Detection Sensitivity	50/100
	Soft Colony Diameter Range	Lower – 60 µm Upper – 3000 µm
	Min Centre to Centre Separation	60 µm (auto-select)
	Smoothing	3
Shape Controls	Circularity Factor	74/100
	Edge Distance Threshold	0.85/1.00
	Number of Spokes	32
	Shape Filtering	Fast Gaussian Filter Size 5
	Shape Processing	Best Fit Circle
Filtering Controls	Colony Diameter Filter	Min Diameter – 60 µm Max Diameter – 3000 µm
	Colony Intensity (OD)	Min Density – 0.10 Max Density – 2.00
	Good Edge Factor	0.90/1.00
	Borders from Centroids	Yes
Overlap Controls	Merge Overlapping Objects	Yes
	Overlap Threshold	60%
	Overlap Calculation	Area
	Retain the	Most Intense
	Calculate new Cluster Boundaries	Yes

Table A1.7: Average Colony Numbers and Plating Efficiencies for Clonogenic Assays

Cell Line	Normoxia or Hypoxia	siRNA	Cells Seeded	Average Colony Number	Average Plating Efficiency (%)
HCT116	Normoxia	siNT	250	146	58.5
		siADAM 10	250	104	41.6
	Hypoxia	siNT	250	128	51.2
		siADAM 10	250	97	38.8
HT29	Normoxia	siNT	500	359	71.8
		siADAM 10	500	404	80.7
	Hypoxia	siNT	500	339	67.8
		siADAM 10	500	379	75.6

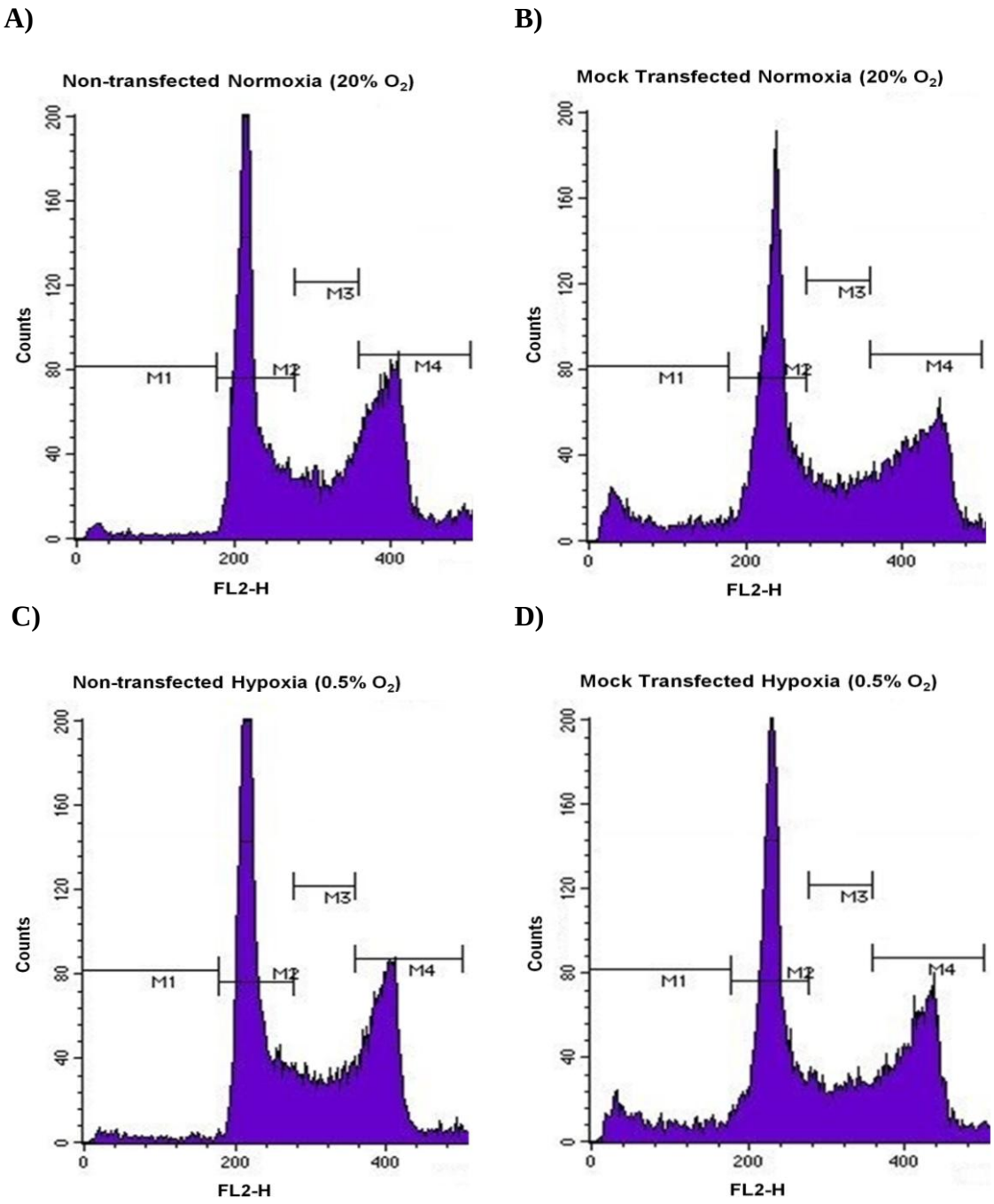

Figure A1.4: HCT116 Control Cell Cycle Profiles

HCT116 cells were left un-transfected or mock transfected for control purposes. Cells were then incubated in normoxia (20% O_2) or hypoxia (0.5% O_2) for 24 hours. Cells were fixed prior to staining with PI, before being analysed by flow cytometry (Section 2.30). Histograms are representative of three independent experiments. Gates represented by M1-M4 on histograms. Each gate represents different a cell cycle phase. M1 = sub-G1; M2 = G1; M3 = S and M4 = G2/M.

A)

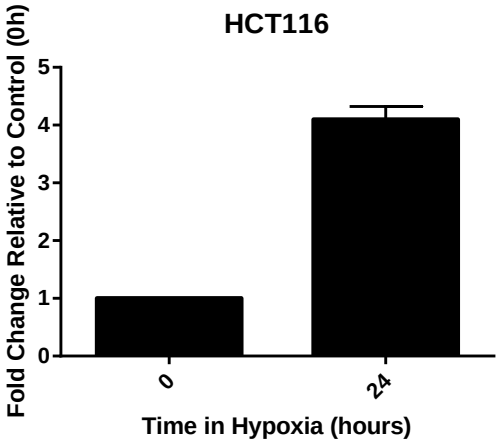

B)

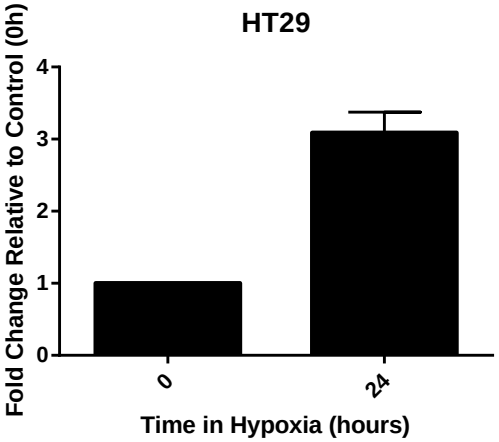

C)

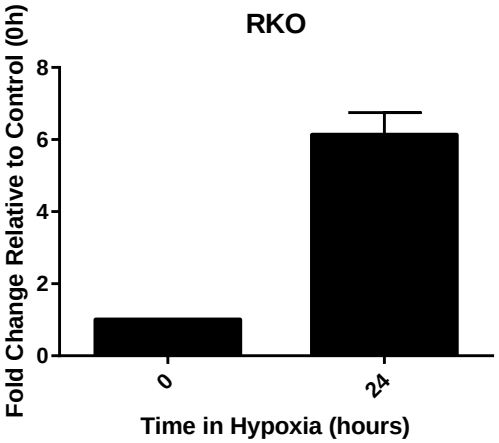

Figure A1.5: *SLC2A1* Induction in Response to Hypoxic Exposure

CRC cell lines were exposed to hypoxia (0.5% O_2) for 24 hours. mRNA was extracted (as described in Section 2.23), *SLC2A1* expression analysed by qPCR (as described in Section 2.26). All results are normalised to the housekeeping gene, *B2M*. *SLC2A1* expression used as a control for confirmation of hypoxic induction. Results are expressed as fold change relative to the 0 h control (normoxia). n=3 experiments; Error bars represent +/- SEM; Statistical analysis by one way ANOVA, with Tukey's post-hoc correction. * $p<0.05$. This figure acts as confirmation of hypoxic environment for Figures 5.7 – 5.10.

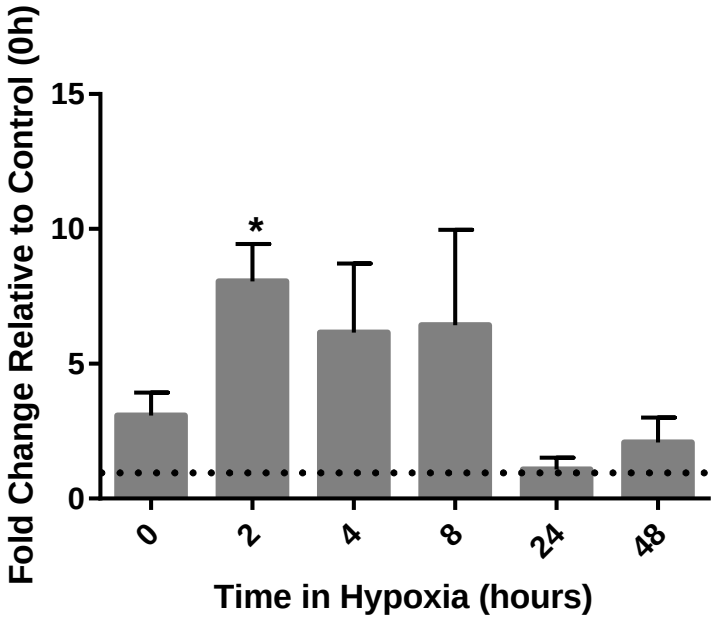

Figure A1.6: Densitometry Analysis of p21 Expression in HCT116 Cells

HCT116 cells were transfected with ADAM 10 targeting siRNA (siADAM 10) or non-targeting siRNA (siNT) and exposed to severe hypoxia (0.5% O_2) for a range of time points. Cells were lysed, 30 µg of each protein sample were separated by SDS-PAGE and expression of p21 analysed by Western Blotting. β-Actin was used as the loading control, to which all results were normalised. Fold change in expression relative to normoxic (0h) control. n=3 experiments; Error bars represent +/- SEM; Statistical analysis by two way ANOVA, with Tukey's post-hoc correction. * $p<0.05$. This figure corresponds to Figure 5.12.